Modelling impacts of climate change on water resources in the Volta Basin, West Africa

Dissertation

zur

Erlangung des Doktorgrades (Dr. rer. nat)

der

Mathematisch-Naturwissenschaftlichen Fakultät

der

Rheinischen Friedrich-Wilhelms-Universität Bonn

vorgelegt von

RAYMOND ABUDU KASEI

aus

TAMALE; GHANA

Bonn 2009

1. Referent: Prof. Dr. Bernd Diekkrüger

2. Referent: Prof. Dr. Paul Vlek

Tag der Promotion: 11.12.2009

Erscheinungsjahr: 2010

Diese Dissertation ist auf dem Hochschulschriftenserver der ULB Bonn
http://hss.ulb.uni-bonn.de/diss_online elektronisch publiziert

ABSTRACT

The Volta River Basin is one of the largest river systems in Africa covering an area of approximately 400,000 km^2 and shared by six riparian states of West Africa. The semi-arid to sub-humid regions of the basin are climate sensitive. The population is mainly dependent on rainfed agriculture and therefore highly vulnerable to the spatial and temporal variability to rainfall and climate change. Even though the per capita water availability of the basin may be perceived as normal, deforestation, land degradation, and high population growth rate coupled with global climate change promises to exacerbate the growing scarcity on water resources due to climate change, as water supplies are unreliable and insufficient to meet the water demands of the growing population. The basin has experienced prolonged dry seasons when many rivers and streams dried up, and lately flooding due to excessive rainfall.

To assess the impact of plausible global climate change to regional climate as well as land surface and as to sub-surface hydrology in the region of the Volta Basin, hydrology simulations were performed with the use of calibrated regional climate models.

The WaSiM-ETH hydrological model was calibrated and validated at Pwalugu (north of basin) and Bui (south of basin). Using the WaSiM-simulated water balance for the period 1961-2000 as the basis for comparison, the simulated future (2001-2050) water balance in the Volta Basin shows increases in the mean annual discharge and surface runoff with the regional model MM5 and decreases with the regional model REMO.

The results of the MM5 and WaSiM simulations show an annual mean temperature increase of 1.2 ^oC over the basin. Mean annual precipitation increases for both the north and the south of the basin are projected. The averaged increase over the basin is about 15 %. The simulated mean change in discharge at the subsurface is about 40 % of total rainfall between the periods 1991-2000 and 2030-2039. Consequently, interflow and base flows are expected to increase in the range of 0 and 20 %, respectively.

The results of two ensemble runs of the IPCC scenarios A1B and B1 by REMO applied to WaSiM show an annual mean increase in temperature of 1^oC. Precipitation over the basin is expected to reduce between 3 % and 6 % in the period 2001-2050 compared to 1961-2000. An average decrease of 5 % is projected for total discharge with corresponding decreases in surface, lateral and base flows.

KURZFASSUNG

Modellierung der Auswirkung des Klimawandels auf die Wasserressourcen des Volta Einzugsgebiet, Westafrika

Das Voltabecken ist eines der größten Flusssysteme in Afrika und erstreckt sich über eine Fläche von circa 400.000 km^2 mit sechs westafrikanischen Anrainerstaaten. Die semi-ariden bis sub-humiden Regionen desVoltaeinzugsgebieest gehören zu den klimasensitiven Gebieten Afrikas. Die Bevölkerung ist überwiegend vom Regenfeldbau abhängig und daher sehr stark durch die räumliche und zeitliche Variabilität von Niederschlag und deren Änderung aufgrund des Klimawandels beeinflusst.

Obwohl die mittlere Wasserverfügbarkeit pro Kopf der Bevölkerung im Einzugsgebiet nicht auf einen hohen Wasserstress hinweist, gibt es einen großen Gradienten zwischen dem Süden Ghanas und dem Norden Burkina Fasos. Es ist zu erwarten, dass Abholzung, Landdegradation und ein hohes Bevölkerungswachstum zusammen mit dem globalen Klimawandel zu einer Abnahme der verfügbaren Wasserressourcen führen wird, so dass der Wasserbedarf der zunehmenden Bevölkerung nicht befriedigt werden kann.

In der Vergangenheit gab es im Einzugsgebiet einerseits lange Trockenzeiten, in denen Flüsse und Bäche austrockneten, sowie andererseits, wie in den letzten Jahren, extreme Überschwemmungen aufgrund von sehr starken Niederschlägen. Es ist zu erwarten, dass sich diese Extreme verstärken werden.

Um die Auswirkungen des zu erwartenden globalen Klimawandels auf das regionale Klima und die Landoberfläche sowie auf die Wasserressourcen des Voltabeckens zu quantifizieren, wurden hydrologische Simulationen durchgeführt. Dafür wurde das hydrologische Modell WaSiM-ETH anhand der Abflüsse in Pwalugu (im Norden des Einzugsgebietes) und Bui (im Süden des Einzugsgebietes) kalibriert und validiert. Mit dem kalibrierten Modell wurden verschiedene Klimaszenarien berechnet, die mit zwei regionalen Klimamodellen erzeugt wurden.

Die Klimaszenarien des MM5 Modells zeigen eine Zunahme der Niederschläge für den Zeitraum 2030-2039 was zu einer Zunahme der Wasserverfügbarkeit und der Abflüsse führt. Im Gegensatz dazu berechnet das Modell REMO für den Zeitraum 2001-2050 eine Abnahme der Niederschläge und somit eine Abnahme des verfügbaren Wassers.

Die Ergebnisse der MM5-WaSiM-Simulationen zeigen eine jährliche mittlere Temperaturzunahme von 1,2 ^oC und eine Zunahme des Niederschlags sowohl im Norden als auch im Süden des Einzugsgebietes von ca. 15 %. Die simulierte mittlere Zunahme des Gesamtabflusses beträgt ca. 40 % für den Zeitraum 2030-2039 verglichen mit 1991-2000. Als Folge der Änderung im Niederschlag wird eine Zunahme des Zwischenabflusses und des Basisabflusses von 0 bis 20 % erwartet.

Die REMO-WASIM Ergebnisse der Ensembleläufe der beiden IPCC-Szenarien A1B und B1 zeigen eine jährliche mittlere Temperaturzunahme von 1^oC. Die Niederschläge nehmen zwischen 3 % und 6 % im Zeitraum 2001-2050 im Vergleich zum Zeitraum 1961-2000 ab. Eine durchschnittliche Abnahme des Gesamtabflusses von 5 % wird durch entsprechende Abnahmen des Oberflächen-, Zwischen- und Basisabflusses erfolgen.

TABLE OF CONTENTS

List of Abbreviations

AGCMs	Atmospheric global circulation models
AMO	Atlantic Multidecadal Oscillation
CRU	Climate Research Unit
CV	Correlation Variance
DEM	Digital Elevation Model
ENSO	El Nino Southern Oscillation
ET	Evapotranspiration
ETP	Potential Evapotranspiration
FAO	Food and Agriculture Organization
FDCs	Frequency Distribution Curves
GDP	Gross Domestic Product
GHG	Green House Gas
GMA	Ghana Meteorological Agency
HSD	Hydrological Services Department
HSPF	Hydrologic Simulation Program FORTRAN
IDW	Inverse Distance Weighting
IIED	International Institute of Environment and Development
IPCC	Intergovernmental Panel on Climate Change
ITCZ	Inter-Tropical Convergence Zone
IUCN	International Union for Conservation of Nature
LAI	Leaf Area Index
MM5	Meteorological Model version 5
MOS	model output statistics
MPI	Max-Planck-Institute for Meteorology
NCAR	National Center for Atmospheric Research
PMCC	Pearson product-moment correlation coefficient
PSU	Pennsylvania State University
RCMs	Regional Climate Models
SHE	Hydrological system model
SPI	Standardized Precipitation Index
SRTM	Shuttle Radar Topography Mission

SSTs	Sea Surface Temperatures
UNFCCC	United Nations Convention on Climate Change
WaSiM-ETH	Water Balance Simulation model –ETH
WPI	Water Poverty Index

1 GENERAL INTRODUCTION

1.1 Introduction

While still debated amongst politicians and economists, most of the natural science community agrees that global warming is occurring as a result of anthropogenic activities and is causing climate change. The United Nations Convention on Climate Change (UNFCCC) is the foremost governmental body with global authority and the intent to understand and address the effects of global warming. The UNFCCC addresses climate change in terms of two basic premises: mitigation, reducing the causes of anthropogenic activities on the natural environment, and adaptation, preparing for the effects of a changed environment on human beings. The UNFCCC has observed that those who are least responsible for climate change are also the most vulnerable to its projected impacts. In no place is this more evident than in Sub-Saharan Africa, where greenhouse gas (GHG) emissions are negligible. It is also important to note however that considering the landcover changes mostly due to deforestation, GHG emissions of sub-Sahara Africa may not be negligible. Extreme climate variability is expected to impact on the inhabitants significantly. Interestingly, due to the sheer scale of African sub-climates, the effects are also being perceived in terms of global dimensions, one example being the relationship of the western winds from the Sahara desert and hurricanes impacting the United States' eastern seaboard. Such elements as changes in vegetation, hydrology and dust export from land surface to atmosphere also have the potential to modify large-scale atmospheric properties regionally and globally (CLIVAR, 2004). In the not too far past, adaptation issues have largely been overlooked, partly because the United Nations has focused its attention on the reduction of GHG emissions and enhancing " carbon sink" options. It is now evident that irrespective of the measures and policies aimed at mitigating the impacts of climate change there is an urgent need to build adaptive capacity to reduce vulnerability to climate variability and change. Only recently the UNFCCC has begun to address adaptation issues more directly through conferences and meetings of the involved parties.

The Intergovernmental Panel on Climate Change (IPCC) has defined adaptation as the "adjustment in natural or human systems in response to actual or

expected climatic stimuli or their effects, in order to moderate harm." While mitigation represents activities to protect nature from society, in contrast, Stehr and Storch (2005) describe adaptation to constitute ways of protecting society from nature. Adaptation has always been an activity African societies have developed to prepare for changing climatic conditions (Diamond, 2005); At present however, due to the global scale of climate change causal relationships, locally derived knowledge, either intuitive or historical, is often rendered irrelevant. It is this lack of ability for societal adjustment to occur within a given timeframe that determines the magnitude of impacts as well as their secondary consequences (Adger et al. 2004). Adaptation can be either reactive or anticipatory according to UNEP (2008). UNEP found that in integrating adaptation to climate change, usually happens only after initial impacts of climate change have become manifest, then reactive adaptation occurs thereafter; whereas in anticipatory or proactive approaches, adaptation takes place before the impacts are evident. The latter type of adaptation is best seen as a process entailing more than merely the implementation of a policy or the application of a technology. It is essentially a multi-stage and reiterative process, involving four basic steps: 1) information development and awareness raising, 2) planning and design, 3) implementation, and 4) monitoring and evaluation. Inherently linked to the causes of global warming and climate change are rapid population increases. Most African nations are witnessing exponential population increases. As populations increase, government structures subdivide and delegate authority to address local needs. The decentralization of government structures presents opportunities and challenges to the development of adaptation frameworks. With local governments taking on new and increasingly important roles, advantages are presented, but these added benefits require more intergovernmental coordination and cooperation as well as stakeholder engagement and consensus building.

The African continent is a vast land, and known to experience a wide variety of climate regimes with varied magnitudes. Within the chapter on impacts, adaptation and vulnerability in Africa the IPCC report on climate change (2001) states that location, size, and shape of this continent play key roles in determining changes in climate that is being observed. The pole-ward extremes of the continent example South Africa are known to experience winter rainfall that are said to be associated with the passage of mid-latitude air masses.

According to the IPCC report on Climate Change (2001), precipitation has been inhibited due to subsidence in areas like Kalahari and Sahara deserts almost throughout the year. In equatorial and tropical areas however, moderate to heavy precipitation known to be associated with the Inter-Tropical Convergence Zone (ITCZ) is experienced. The position of maximum surface heating is at the equator which is linked with meridional displacement of the overhead cast of the sun causes the movement of the ITCZ, resulting in these parts to experience two rain seasons. Only one rainy season is observed in areas further from the equatorial regions towards the poles (IPCC, 2001). Semazzi and Sun (1995) found that the mean climate of the continent is further modified by the presence of large distinctions in topography and the existence of large lakes in many parts of the continent. Significantly, climatic variations and the persistent decline in rainfall have been evident in most parts of Africa especially in the Sahel since the late 1960s. In 1994, the West African Sahel experienced one of the wettest years since the early 1960s as reported in LeCompte et al. (1994); and Nicholson et al. (1996). With excess late rains of 1994 came some optimism that the dry conditions, which had prevailed for nearly three decades, had finally ended. However, rainfall barely exceeded the long-term mean. The observed persistent drying trend will ultimately result in loss of water resources, losses in food production, displacement of people and a major constraints on hydropower generation. These concerns are shared by governments and development planners across African continent. The interannual variability of rainfall over Africa, especially sub-Sahara, has been extensively analyzed by various authors in numerous publications (e.g., Nicholson, 1979, 1983, 1985, 1993, 1994; Nicholson and Palao, 1993; Nicholson et al. 1996; Nicholson et al. 2007) emphasizing the need to address the rapid loss in water resources in the changing climate.

The Volta basin, which is the major focus of this research, generates the major surface and ground water resources for the riparian countries Ghana, Burkina Faso and Togo. Analyses of rainfall data from various stations within the Volta River system indicate that the months in which precipitation exceeds the evapotranspiration to generate runoff and direct recharge are usually June, July, August, and September. Martin (2005) found out that the annual recharge for the Volta River system ranges from 13 % to 16 % of the mean annual precipitation.

Throughout the Volta Basin, reservoirs and dams have been constructed to mobilize water for agricultural, hydro-electricity generation and industrial use. The number of large and small dams continues to increase in line with increasing settlements and increasing population growth.

Van Edig et al. (2001) state that, major conflict potential exists between the two main users of the basin; Ghana and Burkina Faso. Ghana is known to rely heavily on the flow of the Volta primarily for hydro-power whose water heads originate in Burkina Faso. Burkina Faso on the other hand, dam most of its tributaries for the purposes of irrigated agriculture. The tension arises from Ghana wanting Burkina Faso to keep the water flowing. In recent decades, most especially from the severe droughts that hit the region from the 1980s, the fresh water needs and demands of Burkina Faso have increased, thus pushing the country to increase the number of dams in the Volta River Basin to meet the growing demand. This has further compounded the already tensed relation with Ghana. Impacts of climate change with the anticipated increase in potential evaporation and a reduction in precipitation threaten to exacerbate the problems related to lack of adequate water resources in the basin.

1.2 Motivation

Water and food are becoming the critical factors after wars in the development of the sub-humid and semi-arid countries of West Africa. Millions of people in the developing countries die every year of water-related diseases. Modern developments, changing life styles and population growth have greatly increased water demand. As water crises are forecasted for the future, and meeting the water demands of the increasing population in the Volta basin is closely tied to understanding and the development of groundwater, surface and coastal water resources in order to prevent their depletion. The Regional model REMO, a climatic model downscaled from Global models was applied by the GLOWA Impetus project to access the changes in climate for part of the region.

Until the year 2050, Paeth et al. (2007) project a decrease in rainfall of around 25-30 %, which is comparable to the observed decline after the 1960s. Other regional climate simulations for the Volta Basin predict an overall slight increase of the total yearly rainfall, exhibiting strong spatial (-20 % to + 50 %) and temporal heterogeneity (-20 % to +20 %) (Kunstmann and Jung, 2005). Over the last decade, a number of

climatic models have conflicting predictions over the sign of the variation for the continent of Africa and especially at large regional scales such as for West Africa. Although individual models may disagree on the signs, but there is a consensus on the increase of the frequency of extreme events for the future (Hewitson, and Crane (2006), IPCC-AR4 (2005)).

Water resources systems in the Volta Basin are very sensitive to climatic variations. During the 1980s and 1990s, there were several drought events that affected water resources (International Institute of Environment and Development - IIED, 1992), exacerbated by an enhanced hydrologic seasonality. The aggravation of seasonal rainfall coupled with a changing climate may have profound effects on water resources systems in areas that are known to be already vulnerable, such as the northern part of the Volta Basin. The geology of many areas results in a low groundwater storage potential and groundwater recharge, resulting in an over reliance on surface water resources. These resources are depleted rapidly during a dry period in most areas and water quality is decreasing with decreased quantity.

The rapid growth of about 3 % per annum in the basin's population will put constraints on the quantity and quality of water with time. Climate change may put further constraints on the water resources because of changes in spatial and temporal distribution of the resources which several studies such as the Green Cross International report (2001) have shown that unless proactive measures are employed the resources will not be able to stand-up to such constraints. Therefore, there is a need to modify or design methods and/or programs to evaluate risk and uncertainty under the present understood climate-generating mechanisms. This is critical in evaluating future risks of droughts, floods, threats to food security, and the reliability of hydropower generation.

Until very recently, there was little or no hydro-meteorological information on the Volta Basin of West Africa contributing to the challenges faced in sustainable water-management programmes (FAO, 2005). This drives the core of the objectives of this research, which are to determine if a mainly model-based water balance monitoring system can be used to provide a scientific and reliable quantification of the spatial and temporal changes of water fluxes in the Volta catchment for predicting extreme events such as droughts. This information is of immense importance for decision and policy makers in water resources management in the Volta Basin.

1.3 Objectives

1. Assess changes in precipitation and runoff over the recent past using historical meteorological and hydrological data.
2. Assess the impact of projected climate change using MM5 and REMO climate inputs on surface runoff of the Volta Basin.

1.4 Questions

- How can we characterize statistically the variations in climate or weather within the Volta Basin over the recent historical period?
- Are model-generated simulations of climate and hydrologic conditions capable of depicting such variation realistically? How can the probabilities of adverse climate events (droughts) and associated water scarcity be modeled?
- What risks apply to water availability and modeled soil moisture for improving farming in the Volta Basin

1.5 Thesis structure

This thesis is organized in eight chapters. The first chapter gives a general introduction to climate and the changes that have been observed within the region in various studies. This includes objectives and research questions that this research seeks to answer. The Volta Basin is described in relation to noticeable climate variability in Chapter 2. Climate and hydrological data availability and data quality assessments are discussed in Chapter 3; Chapter 4 describes the methodology used for this research. Chapters 5 through 7 focuses on the Water Balance Simulation model WaSiM-ETH model (Jasper and Schulla, 1999) and some of the results obtained from the modules which are the independent processes on which the WaSiM model runs. Chapter 5 concentrates on concepts of WaSiM-ETH and the adaptation of the model to the study site. This involves the calibration, validation and predictive analysis of the model. Chapter 6, which is one of the major results chapters, seeks to assess drought occurrences against precipitation and stream flow at selected stations within the catchments. From the 40 year simulation beginning 1961, Chapter 7, a key synthesis chapter, discusses the changing hydrological time series of the Volta basin and accompanying risk for water resources with emphasis on future prediction by a regional downscaled climatic model-

MM5 done by Jung (2006) and REMO by Paeth (2005). The key results are summarized and discussed in Chapter 8, which includes the general conclusions and recommendations.

2 STUDY AREA

2.1 Location and overview

The Volta River Basin is located between latitudes 5°N and 14°N and longitudes 2°E and 5°W. It has a surface area of about 414,000 km^2 covering areas in six riparian West African countries (Benin to the east, Burkina Faso to the north, Côte d'Ivoire to the west, Mali, Togo and Ghana to the south). (Table 2.1) The total basin population is estimated at a little over 14 million inhabitants, with an annual growth rate estimated at 2.9 % (Green Cross International, 2001). The hydrographical network of the basin is delineated into three main sub-catchments: the Mouhoun (Black Volta), the Nakambé (White Volta) and the Oti River.

According to Andreini (2000), the Volta Basin covers about 28 % of West Africa. The Sourou River is one of the trans-boundary rivers that crosses the border from Mali to Burkina Faso, but lately records little or zero flow. Almost 66 % of the land surface of Burkina Faso is within the Volta Basin where the Black Volta (Monhoun) and White Volta (Nakambé) originate. The Black Volta stems from the southwest of Burkina Faso. In the south, it serves as the borders between Ghana and Burkina Faso and then further south between Ghana and Côte d'Ivoire. The White Volta originates from the northern part of Burkina Faso and also flows south-eastwards to Ghana. The Oti River flows along the border of Benin and Burkina Faso, crosses the northern part of Togo and passes along the border of Ghana and Togo before it reaches Lake Volta (Figure 2.1).

Table 2.1: Coverage of the Volta Basin in bordering riparian states

Country	**Area of Volta Basin (km^2)**	**Percentage of Volta Basin (%)**
Burkina Faso	171,105	42.9
Ghana	165,830	41.6
Togo	25,545	6.4
Benin	13,590	3.4
Mali	12,430	3.2
Cote d'Ivoire	9, 890	2.5

Source: Andreini (2000)

Table 2.2: Major river system of the Volta Basin

Volta Basin System	**Area (km^2)**
Black Volta	149,015
White Volta	104,752
Oti River	72,778
Lower Volta	62,651
Total	**389,196**

Source: Barry et al. (2005)

Figure 2.1: Volta River Basin of West Africa, between latitudes 5°N and 14°N and longitudes 2°E and 5°W (Source: GLOWA Volta project)

Many other small tributaries have their source within Ghana, especially in the northern savannah, but are dry after the rainy seasons. The groundwater in most parts of the basin yield is little and cannot be depended on for extensive irrigation. In Akosombo to the south of Ghana a dam was constructed for hydroelectric power. Behind this dam is one of the world's largest artificial lakes,the Volta Lake, with a surface area of 8.500 km^2 and a capacity of 148 km^3. According to Andreini (2000), significant run-off occurs only when the basin has received about 340 km^3 of rainfall, and once this threshold is reached, about 50 % of the total precipitation thereafter is as run-off. This implies that small changes in rainfall could dramatically affect run-off rates. It is noted that, although rainfall decreased by only 5 % from 1936 to 1998, run-off decreased by 14 %. The average discharge flowing into the sea from this lake per annum is estimated at about 38 km^3.

2.1.1 White Volta Basin

The White Volta Basin, the second largest catchment of the Volta Basin, covers about 104,752 km^2 and represents 46 % of the total Volta catchment area. It is located within the Interior Savannah Ecological Zone and is underlaid by the Voltarian and granite geologic formations (Opoku-Ankomah, 1998).

The main tributaries of the White Volta are the Morago and Tamne rivers. The total surface area of the Morago is 1,608 km^2 with 596 km^2 in Ghana, 912 km^2 in Togo and 100 km^2 in Burkina Faso. The Tamne tributary, however, lies entirely in Ghana with a total area of 855 km^2. The White Volta covers mainly the north-central parts of Ghana (Barry et al., 2005).

Annual rainfall in this sub-basin (Opoku-Ankomah, 1998) ranges between 685 mm in the north (Mali) and 1,300 mm in the south (Ghana). Pan evaporation is estimated to range between 1,400 mm to 3000 mm per annum with an average rainfall runoff about 96.5 mm. The average annual runoff from the White Volta catchment is estimated at 272m^3/s. Barry et al. (2005) found a maximum annual flow of 1,216 m^3/s runoff at the peak of the rainy season and a minimum of about 0.11m^3/s during the dry season. Potential sites have been identified for storage within the basin totaling nearly 8,180 x 10^6 m^3 found to be capable of regulating the basin yield at a minimum flow of about 209m^3/s. The total annual flow contribution to the Volta Lake is about

20 %. Current surface water uses in the basin are estimated at about 0.11m^3/s for domestic and about 2m^3/s for many small irrigation projects in the watersheds (Barry et al., 2005). The construction of the Bagre dam covering a total area of 33,120 km^2 in 1993 has changed the flow of the White Volta significantly, most especially the stable base flow during the years. The annual average flow from the dam within the last decade is estimated at 29.7m^3/s. At the bottom and of the White Volta, an annual mean discharge of 1,180 m^3/s is observed at Akosombo (Rodier, 1964).

2.1.2 Black Volta Basin

The Black Volta Basin, the largest of the catchments in the Volta Basin has a total area of 142,056 km^2 of which 33,302 km^2 (23.5 %) is located in Ghana. The tributaries are the Aruba, Bekpong, Benchi, Chridi, Chuco Gbalon, Kamba, Kule Dagare, Kuon, Laboni, Oyoko, Pale, and rivers San . The basin is mainly located in the north-western part of Ghana and the south-western part of Burkina Faso. The basin includes northern and central parts of Ghana, southern Burkina Faso and northern Cote D'Ivoire.

Annual rainfall in this sub-basin is between about 1,150 mm in the north and 1,380 mm in the south, with pan evaporation estimated at 2,540 mm per year, and an average annual rainfall runoff of about 88.9 mm. The sub-catchment produces about 243m^3/s runoff per year. The mean monthly runoff from the sub-basin varies on average from about 623 m^3/s at the peak of the rainy season to about 2m^3/s in the dry season (Opoku-Ankomah, 1998). Its contribution to the annual total flow of the LakeVolta is about 18 %. The potential storage at Bui south of the basin, a site being constructed for hydropower generation, has a volume in excess of 12.3 x$10^9 m^3$ and yields a minimum of 200 m^3/s and is capable of regulating the basin. Current surface water use from this sub-basin for domestic use is estimated to be only 0.03m^3/s.

The inflow downstream into Ghana measured at the Lawra station is the estimated discharge between Ghana and Cote D'Ivoire. Similarly, the total discharge in this sub-basin can be estimated from Bamboi station (Table 2.3).

Table 2.3: Surface water flows of the Black Volta in Ghana

Station	**Catchment area (km^2)**	**Annual discharge (m^3/s)**	**Annual dry season discharge (m^3/s)**	**Annual wet season discharge (m^3/s)**
Lawra (inflow)	90,658	103.75	34.75	172.13
Bamboi	128,759	218.97	62.83	373.79
Catchment outlet outflow		243.30	69.81	415.32
Flow from within Ghana		139.55	35.06	243.19
% contribution to Lake Volta		42.64	49.7	41.45

Source: Barry et al. (2005)

2.1.3 Lower Volta Basin

The Lower Volta Basin is located below the two big sub-catchments of the Volta, the Black Volta and the White Volta rivers, and is largely in Ghana. The surface water resources in this sub-basin consist of flows from Togo and Ghana.

The basin covers a total area of about 68,588 km^2 and almost 70 % is located in the east-central part of Ghana. This sub-basin is located in the Northern, Brong Ahafo, Ashanti, Eastern and Volta Regions of Ghana and parts of Togo.

Annual rainfall in the Black Volta ranges from about 1,100 mm in the northern part of the basin to about 1,500 mm in the central. In the southern part, annual rainfall is about 900 mm. Pan evaporation is estimated at about 1,800 mm per year and precipitation runoff about 89 mm per year. The total mean runoff from this sub-catchment of the Volta is estimated to be about 1,160m^3/s (Table 2.4). Current water withdrawals from the total flow are estimated at 1.86m^3/s for domestic and 0.71m^3/s for irrigation, and over 566m^3/s for power (Nathan Consortium, 1970).

Table 2.4**:** Surface Water flows of the Lower Volta in Ghana

Station	**River**	**Catchment area**	**Annual discharge (m^3/s)**	**Annual dry season discharge (m^3/s)**	**Annual wet season discharge (m^3/s)**
Nangodi Yarugu	Red Volta White Volta	10,974 41,619	30.72 80.00	0.34 2.17	61.12 157.00
Total inflow			110.72	2.51	218.12
Nawuni Lankatere	White Volta Mole	96,957	229.98 73.31	18.95 15.78	440.05 131.33
Total flow	White Volta		303.29	34.73	571.38
Total flow from catchment			192.57	32.22	353.26

Source: Barry et al. (2005)

2.1.4 Oti Basin

The Oti River Basin is among the smallest of the catchments and has a surface area of about 72000 km^3 and is mainly located in north-eastern Ghana. The basin comprises parts of the Northern and Volta Regions of Ghana. It also covers more than 40 % of the land in Togo. Annual rainfall in this sub-basin varies from 1,010 mm in the north to 1,400 mm in the south with a pan evaporation of 2,540 mm per year and runoff of about 254 mm per year.

The Nathan Consortium (1970) estimated the average annual runoff within the basin from the Oti Basin between 849m^3/s at peak of the rainy season and 1.1m^3/s during the dry season, and the mean annual flow 12.6 km^3. The topography of this catchment is steep with relatively high rainfall, thus facilitating surface runoff and leading to about 25 % of the annual total flow contributions into the Volta Lake.

2.2 Vegetation

The natural vegetation in the Volta Basin ranges from tropical humid forests, dry forests and savannah spanning from short grass at the desert border to humid rain forests at the south near the Atlantic coast. For map see (chapter 5).

The Volta Basin lies almost at the centre of the West African region. Due to its location, it covers parts of the equatorial forest zone, mainly the Guinea and Sudan savannah, and a small fraction of the Sahel zone (Figure 2.2).

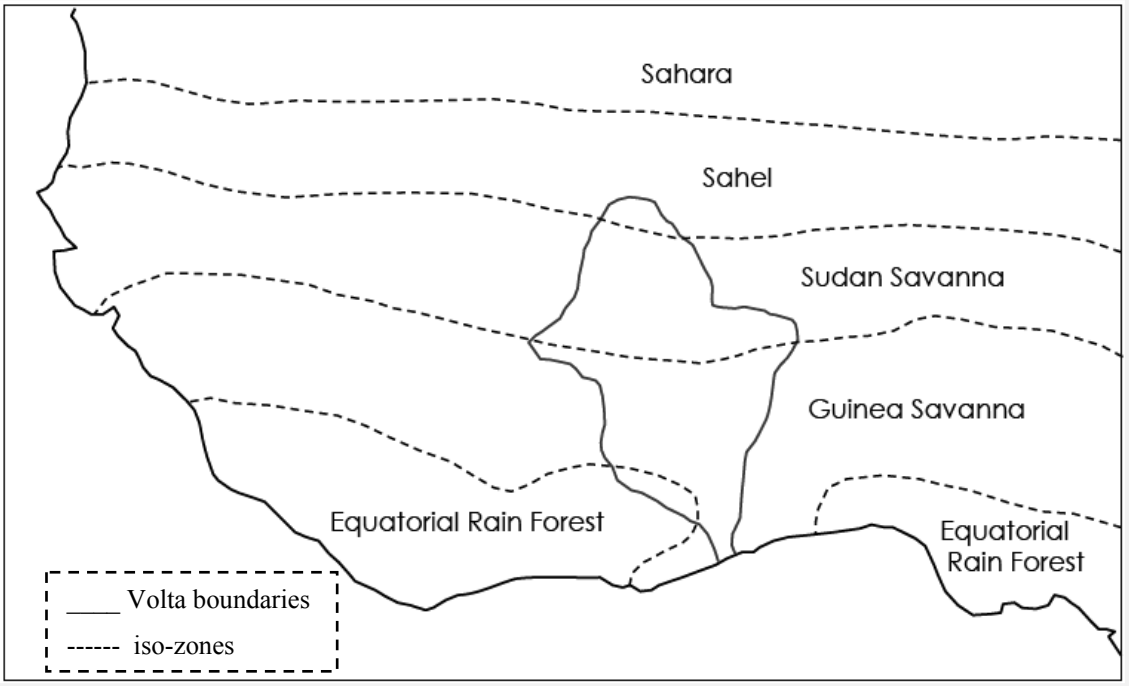

Figure 2.2: Tropical zone of the Volta Basin (Barry et al. 2005)

2.3 Climate

The climate of the Volta Basin is predominately semi-arid to sub-humid. The potential evaporation in this semi-arid climate exceeds precipitation for 6-9 months. In the sharply contrasting sub-humid climate precipitation exceeding potential evaporation in 6-9 months of a year (Hayward and Oguntoyinbo, 1987). The rainfall regime is divided into a dry and rainy season and is largely influenced by the West African Monsoon (WAM).

2.3.1 Temperature

The mean annual temperature in the Volta Basin lies between 27^{o}C in the south and 36^{o}C in the northern part (Figure 2.4), with an annual range of 9^{o}C (Oguntunde, 2004). The daily temperature range in the north lies between 8 and14^{o}C, and in the south an annual temperature range of around 6^{o}C is observed. In March, the hottest month of the

year in the basin, temperatures in the southern parts may rise from a mean of 24°C to 30°C in August (Figure 2.3). The daily temperature range in this area is about 3-5°C (Hayward and Oguntoyinbo, 1987).

2.3.2 Precipitation

The three climatic zones in the Volta Basin are1) the tropical climate covering over 50 % of the basin (north of latitude 9° N), with one rainfall season peaking in August, 2) the humid south with two distinct rainy seasons, and3) the tropical transition zone with two rainfall seasons very close to each other (south of Latitude 9°N). The high average annual rainfall variation of 1,600 mm in the south-eastern section of the basin (Ghana), to about 360 mm in the northern part (Burkina Faso) shows a strong north-south gradient, with higher rainfall amounts in the tropical South and smaller amounts in the semi-arid north (Figure 2.3 and 2.4). In the south-western corner of Ghana at the edge of the Volta Basin annual precipitation exceeding 2,100 mm, whereas in the south-eastern areas it is less than 800 mm. This is an indication that not only a North-South gradient is apparent, but also a strong west-east gradient (Figure 2.3). According to Opoku-Ankomah (2000), since the 1970s there have been a number of changes in the precipitation patterns in some sub-catchments in the basin, with corresponding rainfall and run-off reduction. Some areas now have only one rainfall season compared to the bi-modal system of the past, with the second minor season becoming very weak or non-existent. Agriculture practiced in the basin, which is rainfed is also shifting from two-season cropping to single season cropping is evidence of this process.

Around 80 % of annual rainfall occurs from July to September with the monsoonal rains.

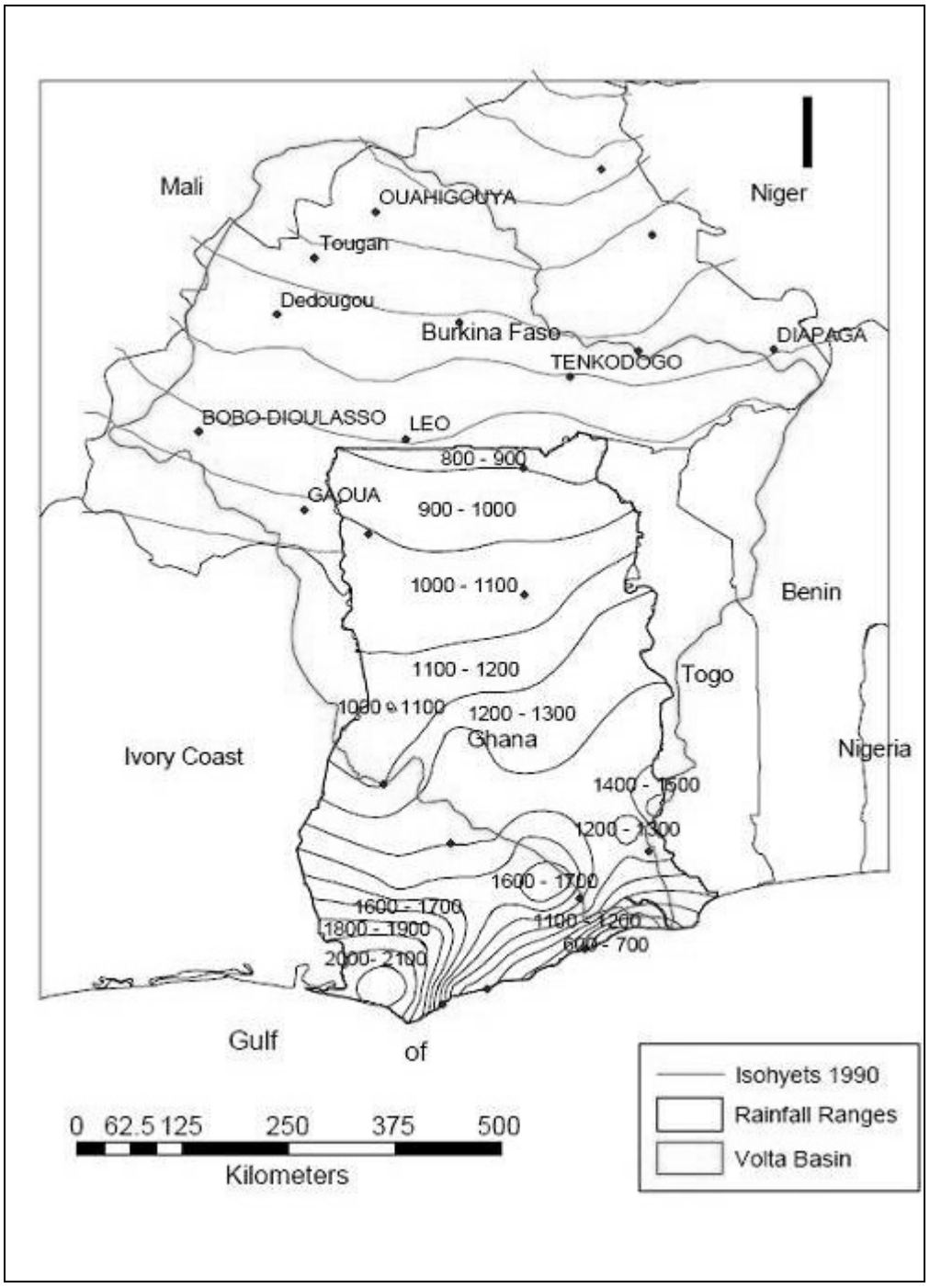

Figure 2.3: Rainfall distribution in the Volta Basin 1990 – 2000, between latitudes 5°N and 14°N and longitudes 2°E and 5°W (Opoku-Ankomah, 2000).

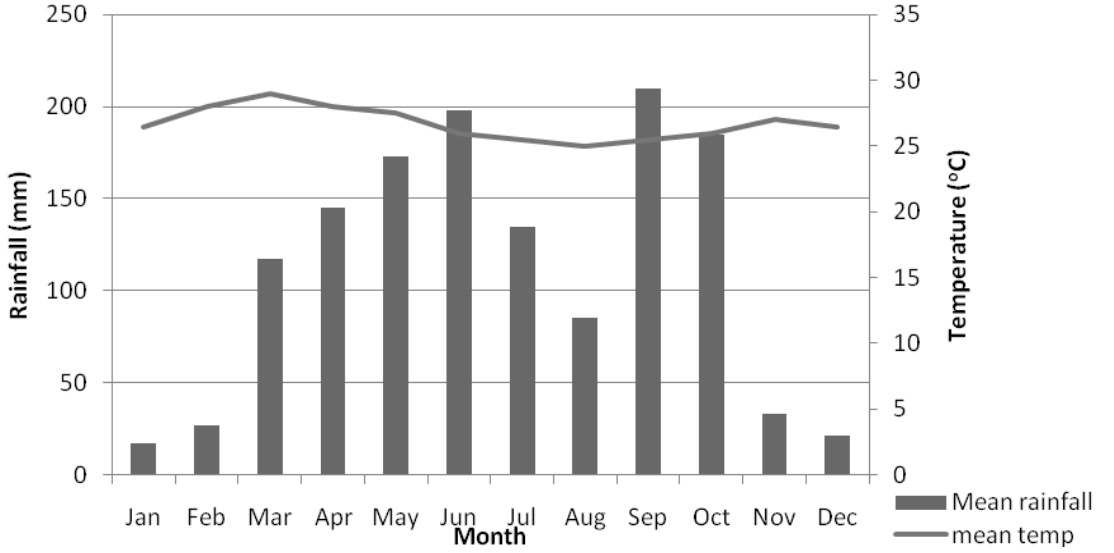

Figure 2.4: Average monthly rainfall and temperature in the south of the Volta Basin measured at Ejura (1970-2000) [Data source; Ghana Meteorological Services]

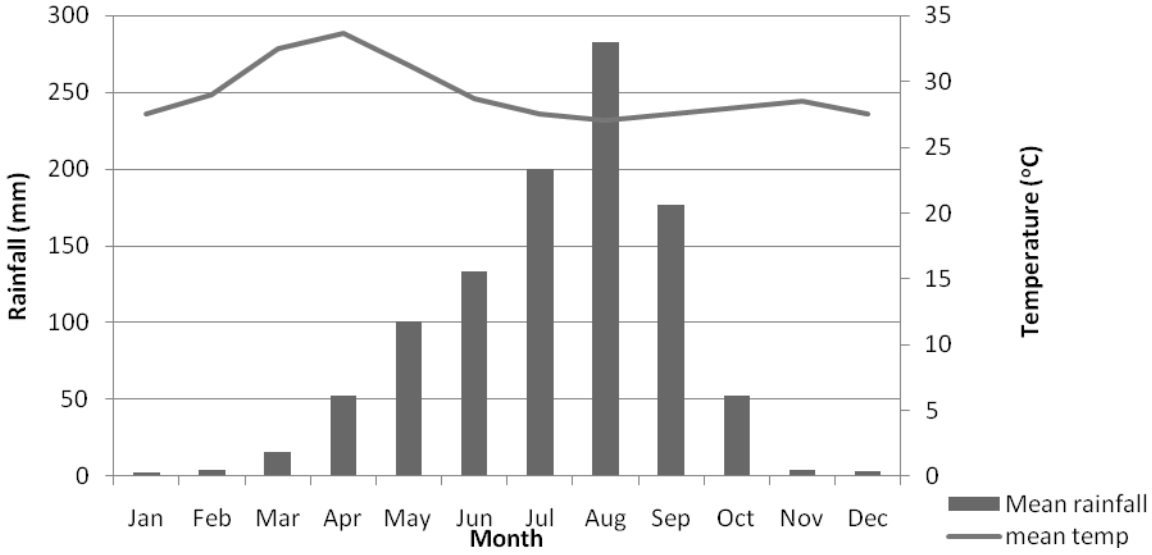

Figure 2.5: Average monthly rainfall and temperature in the north of the Volta Basin measured at Tamale (1970-2000) [Data source; Ghana Meteorological Services]

2.3.3 Evaporation

Mean annual potential evaporation is estimated to be lowest in the south (1,500 mm) while it exceeds 2,500 mm in the northern part of the basin. It is estimated that nearly 80 % of the rainfall is lost to evapotranspiration during the rainy season (Oguntunde, 2004). Real evapotranspiration in most parts of the basin depending on soil properties is

between 10 mm/day in the rainy season and 2 mm/day in the dry season (Martin, 2005). The annual average potential evapotranspiration varies between 2,500 mm and 1,800 mm from the north of the basin to the coastal zone (Green Cross International, 2001).

2.4 Geology and soils

The geological formation that dominates the Volta is Voltaian system. Recent formations include the Buem formation, Dahomeyan formation, and Togo series. In the report of the Volta basin by Barry et al. (2005), the Voltaian system consists of Precambrian to Paleozoic sandstones, shale and conglomerates. The Buem series lie between the Togo series in the east and the Voltaian system in the west. The Buem series comprise calcareous, argillaceous, sandy and ferruginous shale, sandstones, arkose, greywacke and agglomerates, tuffs, and jaspers. The Togo series lie toward the eastern and southern parts of the main Volta Basin and consist of alternating erinaceous and argillaceous sediments. The Dahomeyan system occurs at the southern part of the main Volta Basin and consists of mainly metamorphic rocks, including hornblende, biotite, gneisses, migmatites, granulites, and schist (Barry et al. 2005).

The Man Shield consists of Birimian rocks which are the oldest rock, comprising mainly Siluro-Devonian sandstone and shale and some igneous and granitic material and covers much of Ghana, Burkina Faso and a small part Cote d'Ivoire (Figure 2.4). The largest fraction of this Paleoproterozoic domain according to Castaing et al. (2003) cited in Martin (2005) consists of granitoids, which are said to have intruded into the Birimian metasediments during the Eburnian event over 2 billion years ago (Leube and Hirdes, 1986). These cover over 66 % of the Volta Basin.

The soils of the basin are derived from rocks of the mid-Paleozoic age due to the high precipitation events in the southern forest zone and are between 1m and 2 m thick. They are characterized by an accumulation of organic matter in the surface horizon. Forest ochrosols are the most extensive and important of these soils. The rest, mainly in the wetter areas, are Forest Oxysol intergrades. Unlike soils in the south, the soils of the northern savannah contain much less organic matter and are lower in nutrient than the forest soils. The groundwater laterites formed over granite, Voltaian shale and ochrosols form the main part of the savannah soils. In the coastal savannah, soils are younger and closely related to the underlying rocks. They are mainly a mixture of savannah ochrosols, regosolic groundwater laterites, tropical black earths, sodium

vleisols, tropical grey earths and acid gleisols and are generally poor largely because of inadequate moisture.

The soils of the northern part (Burkina Faso) are largely lateritic compared to the southern part of the Basin (Ghana), where they are of the lixisol type. According to Adams et al. (1996), the weathered soils are usually a composition of kaolinite clays and have high contents of iron, aluminium and titanium oxide. The aggregate stability at the surfaces is usually low, and soils with low vegetation cover are prone to erosion.

The other main group of soils in the Volta Basin consists of arenosols, mainly found in the arid north of the basin. They are basically sandy and coated with iron oxides, which gives the soil its specific reddish color. These soils are characterized by high infiltration rates. A study on soil properties conducted by Agyare (2004) revealed high discrepancies between subsoil and topsoil due to less soil disturbance in the subsoils. The computed saturated hydraulic conductivity (Ksat) is a high variability in space for the soil layers considered. Another study by Giertz (2004) cited in Jung (2006) supports these findings.

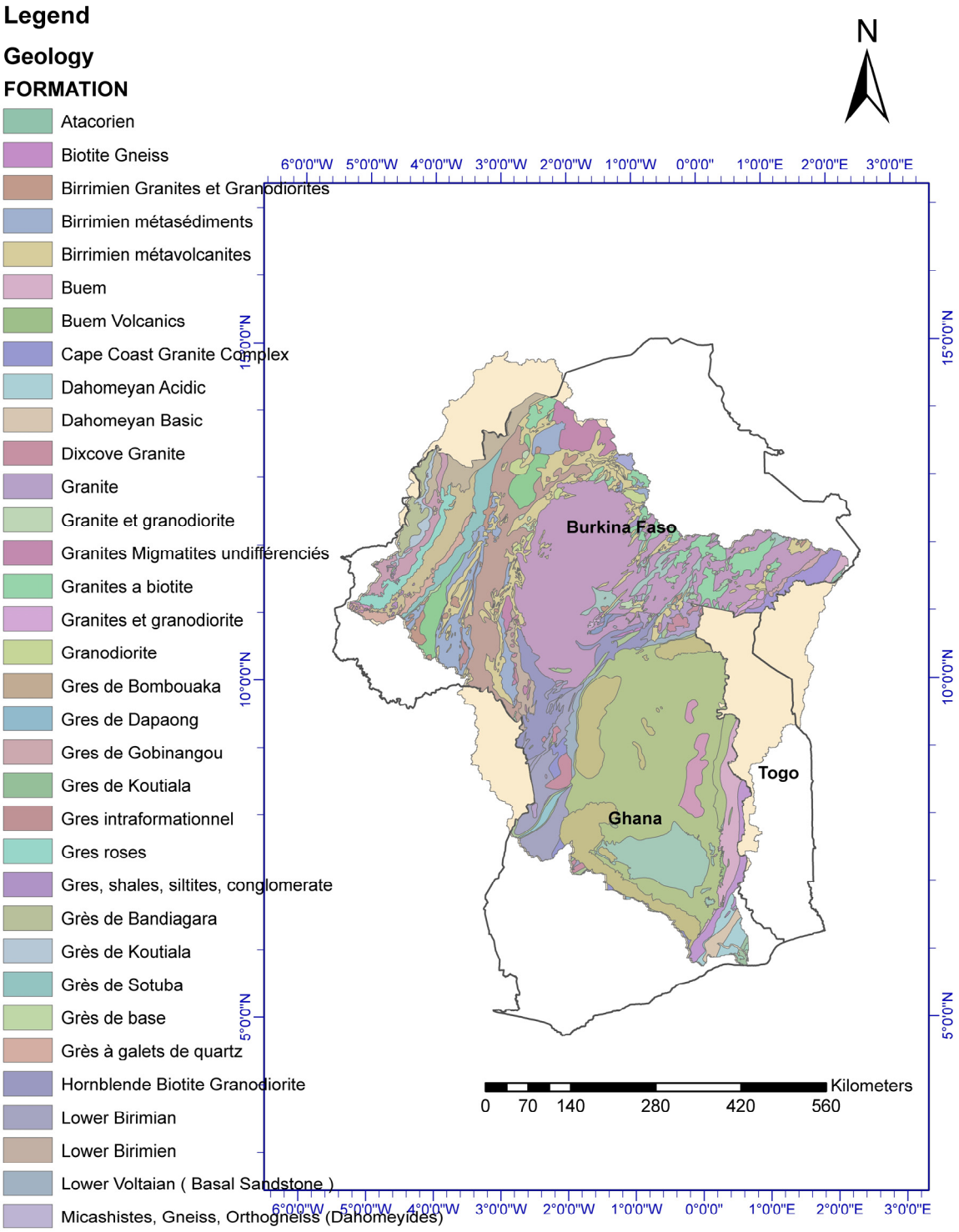

Figure 2.6*:* Geological map of the Volta Basin (Source: EPA)[1]

[1] The EPA contracted the RSAU for digitising the information from the available 1:1 000 000-scale geological survey map. This map contains a description of major geological formations concerning their type and origin.

2.5 Land use and agriculture

Increasing population growth all over the Volta Basin is leading to an increasing pressure on agricultural land for food production. Most Farmers have therefore abandoned the original farming practice of shifting cultivation with long fallow periods because it is viewed to be less viable and unpractical. Some of the crops cultivated on uplands are maize (*Zea mays*), sorghum (*Sorghum bicolor*), groundnut (*Arachis hypogaea*), cowpea (*Vigna unguiculata*), with rice (*Oryza spp.*) grown in valley bottoms. The majority of the farms are small-scale subsistence farms and these are only a few commercial farms. Traditional shifting cultivation with land rotation is practiced to some extent across the basin.

Livestock production on a small and large scale is important for the livelihood of the people in the basin. Mostly, the family owns cattle with the family head having the direct responsibility for the animals in the north, while poultry and farming on pig on a commercial scale are practiced in the south. The livestock mostly owned by household are sheep, goat, and birds.

2.6 Hydrology and water resources

Apart from the huge network of rivers, the basin is dotted with a number reservoirs, ponds and dugouts. In areas where surface water is inadequate, groundwater resources are used by the small communities for domestic and irrigation purposes. According to the World Bank report (1992), groundwater resources are of relatively good quality and usually only need minimum treatment. Many communities within the basin depend largely on groundwater for their water needs. Data is scanty on groundwater level fluctuation and recharge, but in some areas a high recharge is observed.

Runoff is essential for hydropower generation, which is a major source of energy for the countries within the basin. Reduction in flows has rendered the hydropower systems vulnerable, and this shows no sign of ending soon. Since the Akosombo hydro-electric dam was constructed, discharge has barely reached 1000 m^3/s, and recent records show a further decline (Figure 2.5).

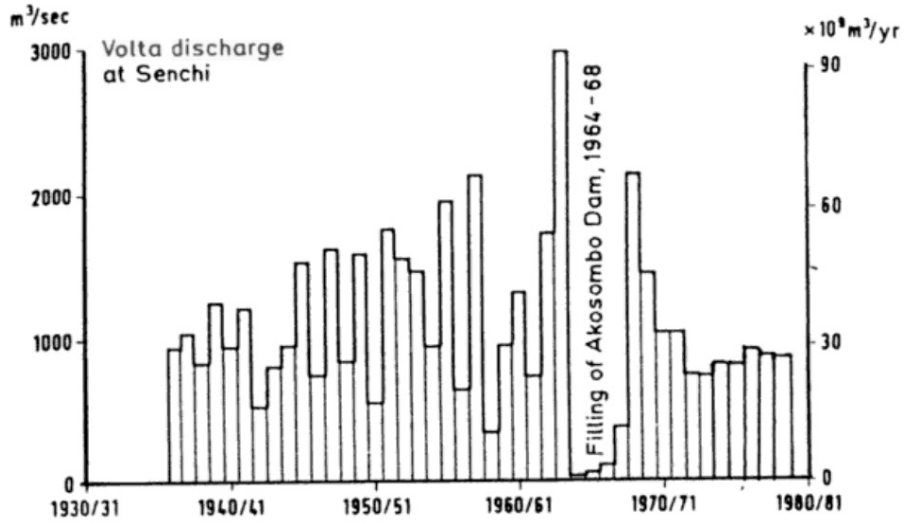

Figure 2.7: Annual discharge series of the Volta River at Senchi before and after the construction of the Akosombo Dam (Mamdouh, 2002)

3 CLIMATOLOGICAL AND HYDROLOGICAL DATA

3.1 Data availability

Until the beginning of the last decade, little was known about what data exist for the Volta Basin with regards to Meteorological and hydrological, and what time periods they represent. In the GLOWA-Volta project; the analysis of the physical and socio-economic determinants of the hydrological cycle of the Volta Basin created the umbrella under which a number of PhD scientific researchers were conducted. For example, within the framework of the Volta Project, Martin (2005) studied on a watershed within the White Volta, Jung (2006) in the "Regional Climate Change and the Impact on Hydrology in the Volta Basin of West Africa" considered the entire basin and focused more on the Burkina Faso and the northern parts of the Volta Basin while Wagner (2008) used data from the Ghana part of White Volta. Recent reports and publications based on archived data highlight the availability of some collected and archived data in the countries within the basin. At the beginning of this research, the data base of GLOWA Volta had scant information for areas outside previous research sites. Little was known about what may have been achieved in these areas for the desired periods of 1961-2007 to synchronize with the already cleaned data of pervious work. This time series is essential for this research because for any useful comparison of conditions of the past and the future, a good presentation of the meteorological and hydrological data is needed. Although some models are sometimes able to generate data, they have often failed to simulate most extremes (e.g. temperature, rainfall etc) correctly, hence archived gauged data is preferred for this study. Initial assessment of the data archived by national agencies showed that continuous meteorological data for the basin for long periods was lacking, and where data existed, the quality was questionable with large gaps of missing data. After the initial sorting of the available data for the basin, data from gauges that could be used were widely spaced. Available monthly and daily data from meteorological stations monitored solely by the metrological services of both Ghana and Burkina Faso needed some verification and quality checks. Information from the hydrological services also revealed that most of the rivers were previously ungauged; hence no run-off data exist for such rivers. On the whole, continuous stream discharge measurements data at daily intervals were available

for some stations in Ghana and Burkina Faso, also with some gaps and questionable values that needed attention.

3.1.1 Data quality assessment

The quality of the data determines to a great extent the hydrological model efficiency and hence the conclusions that can be drawn from the modeling results.

Data which many human hands have handled in different locations and spanning many years are bound to have some problems with quality. This is more so the case when the data are influenced by human activities in almost all the stages of production. In situations like these, Beven (2002) cautioned that models will not be able to simulate accurate predictions if the areal precipitation is not adequately represented. In developing countries such as those in West Africa, hydro- meteorology data are collected and recorded manually. Digitizing these large amounts of data by poorly trained people also leads to quality problems.

The quality of any measured parameter depends on precision and accuracy, where the former is associated with how close and reproducible the measured value is from a repeated measurement if there were to be one, whereas the latter is focused on how good the measured value agrees with the true value. However, natural irregularities or differences in what is being measured must not be considered as errors. This thus demands a careful approach in error analysis of large amounts of data of a cast area that has high variation in hydrology and climate (Bevington, 1992). This renders most statistical methods that are based on normal distributions useless in this analysis.

Errors may occur because of gauge management, human errors in reading and/or recording or typing errors in digitizing data from data sheets. The latter causes by far the greatest error and is usually the case. Underestimation of the gauge catch compared to the ground catch may be as high as 100 % and more (UNESCO, 1978 referred to in Herschy, 1999).

Errors limited to gauges management are those where gauges malfunction due to poor maintenance such as cleaning, and recalibration among others. Other uncertainties may be due to poor reading of the equipment. Since data were collected manually, an error in reading measurement automatically introduced an error. In situations where data was correctly read, a different value could be recorded, such as

placing a decimal point in the wrong place. Human error in entering the data into a spreadsheet brought along some errors as typing errors. As these uncertainties usually do not show regular patterns, correcting such errors becomes more difficult when comparing data with other neighboring station data, where different conditions apply, data values might differ immensely.

Three steps were taken for verifying the data used in this research: visualization, comparison to nearby stations within the same zone, and regression. Base knowledge of the area was essential for visually picking out doubtful data. Personnel from the respective organization of the countries were contacted on data that were abnormal with respect to the long term data set of the stations. The data was accepted when adequate reasons were given for such data sets to differ that much from the normal values.

Comparing neighboring stations for data verification required that squall lines of rainfall were considered to enable the assessment of these data to be related and compared. Rainfall amounts from neighboring stations during a rainy event from the same squall line would not necessarily be equal but would show some relative magnitudes.

Station data was always regressed with the long-term data of the same station, and though season change and seasonal averages change, outliers offer some ideas regarding unusual occurrences to stations.

3.2 Climate data

This research demanded a variety of input data most especially climate information. Data used heavily relied on collected historical data that were available and accessible to the GLOWA Volta project (GVP). A memorandum of agreement signed between GLOWA Volta project and the national agencies allowed access and use of the data for this research. Priority was put on stations across the regions where data was lacking in the data base of GLOWA Volta project but required for this research. Some of the historical data from some stations existed in handwritten papers and had to be entered into a spreadsheet to facilitate processing. From the large pool of stations with data, stations were selected according to the criteria that the location of the station was not in the catalogue of station of GVP and in a region that did not have a good concentration

or distribution of gauged stations within the catchment in the catalogue. A considerable part of the research area is covered by protected national parks in Ghana (Mole) and Burkina Faso; hence data does not come from these parts of the research area. The nearest stations to these parks were used for interpolation.

3.2.1 Meteorological agencies

The Ghana Meteorological Department; now called Ghana Meteorological Agency (GMA) is the major source of the meteorological data used in this research. Most of the historical daily data covered from 1961 to 2004. The GMA operated two types of stations: 1) the synoptic stations; record data for temperature, relative humidity, sunshine duration, pan evaporation and wind speed (Figure 3.1) and 2) rain gauge stations that were dotted around synoptic stations mainly to monitor rainfall amount over an area. Additional meteorological data was obtained from the meteorological agency in Burkina Faso for stations that were needed from the Burkina Faso part of the basin. The list of stations selected for this research (table 3.1) shows locations at a range of different distances and elevations.

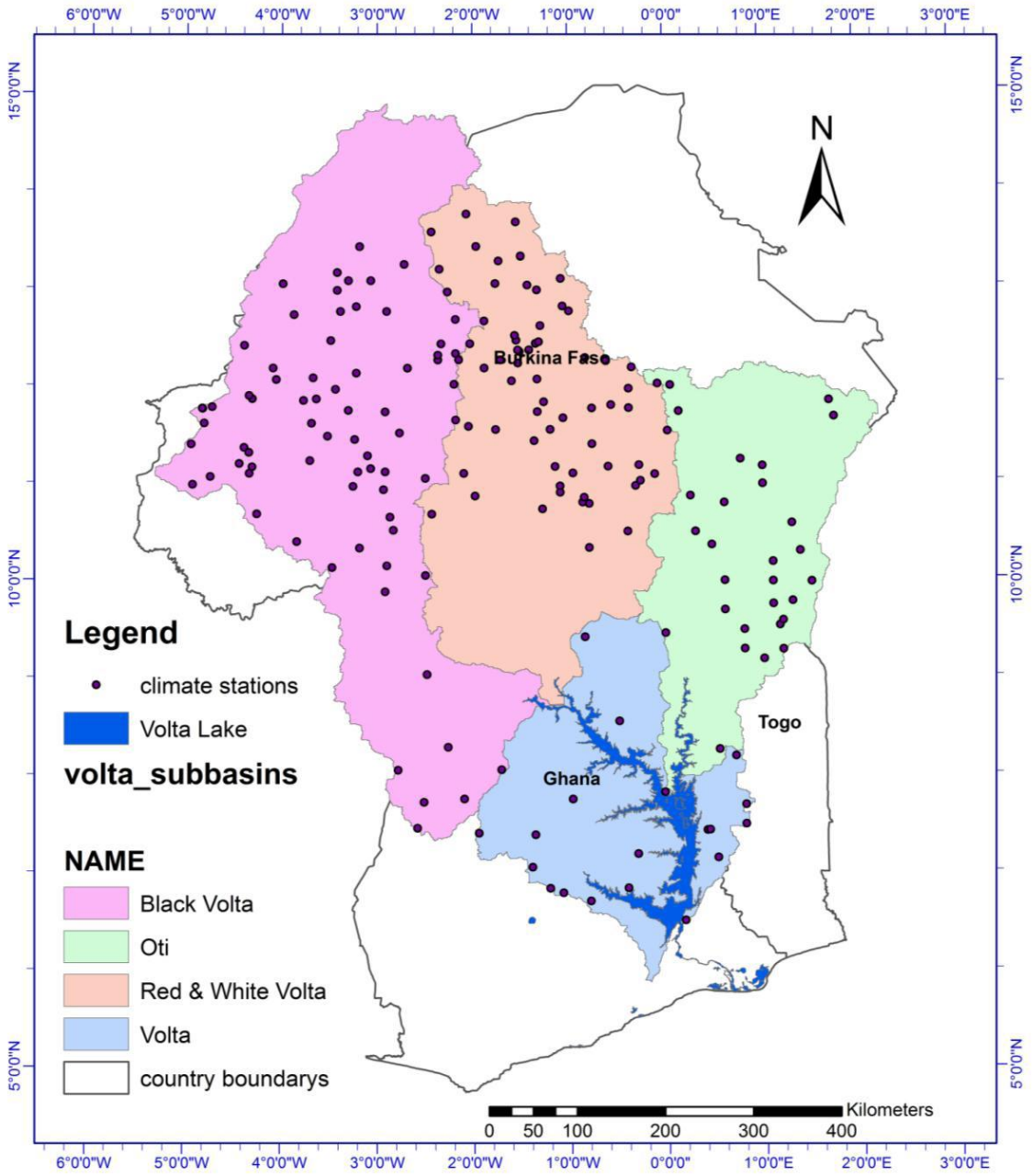

Figure 3.1: Climate stations within the Volta Basin

Table 3.1: Meteorology stations in the Volta Basin used in the study[2]

Station	Elevation (m)	Latitude (°)	Longitude (°)	Station	Elevation (m)	Latitude (°)	Longitude (°)
Bole (GH)	299.5	9.03	-2.48	Kintampo (GH)	372.6	8.07	-1.73
Ho(GH)	158.0	6.60	0.46	Kpandu (GH)	213.3	7.00	0.28
Kete-Krachi(GH)	122.0	7.81	-0.03	Aribinda(BF)	370.0	14.23	-0.87
Navrongo (GH)	201.3	10.90	-1.10	Bagassi (BF)	280.0	11.75	-3.30
Sunyani (GH)	308.8	7.33	-2.33	Baguéra (BF)	315.0	10.53	-5.42
Tamale (GH)	183.3	9.50	-0.85	Bam (Tourcoing) (BF)	264.0	13.33	-1.50
Wa (GH)	322.7	10.05	-2.50	Banfora (BF)	284.0	10.63	-4.77
Wenchi (GH)	338.9	7.75	-2.10	Banfora Agri (BF)	270.0	10.62	-4.77
Yendi (GH)	195.2	9.45	-0.01	Bani (BF)	310.0	13.72	-0.17
Tumu (GH)	313.2	10.87	-1.98	Baraboulé (BF)	308.0	14.22	-1.85
Adidome (GH)	8.8	6.10	0.50	Barsalogho (BF)	330.0	13.42	-1.07
Agogo (GH)	426.5	6.78	-1.08	Batié (BF)	298.0	9.88	-2.92
Ahunda-Adaklu (GH)	76.2	6.28	0.55	Bilanga (BF)	281.0	12.55	-0.02
AKUSE (GH)	17.4	6.10	0.11	Bobo-Dioulasso (BF)	432.0	11.17	-4.30
Ash_Bekwai (GH)	228.6	6.45	-1.58	Bogandé (BF)	250.0	12.98	-0.13
Babile (GH)	304.7	10.52	-2.83	Bomborokuy (BF)	279.0	13.05	-3.98
Bechem (GH)	289.4	7.08	-2.03	Bondoukuy (BF)	359.0	11.85	-3.77
Berekum (GH)	304.7	7.45	-2.58	Boromo (BF)	264.0	11.73	-2.92
Bolgatanga (Gh)	213.0	10.80	-0.87	Boulbi (BF)	315.0	12.23	-1.53
Bui (GH)	106.6	8.25	-2.27	Boulsa (BF)	313.0	12.65	-0.57
Hohoe (GH)	169.1	7.15	0.48	Boura (BF)	281.0	11.05	-2.50
Kpeve (GH)	130.7	6.68	0.33	Boussé (BF)	345.0	12.67	-1.88
Lawra (GH)	4.8	10.87	-1.48	Dakiri (BF)	280.0	13.28	-0.23
Bobiri (GH)	228.7	6.67	-1.37	Dano (BF)	290.0	11.15	-3.07
Ejura (GH)	228.5	7.40	-1.35	Diébougou (BF)	294.0	10.97	-3.25
Garu (GH)	237.7	10.85	-0.18	Djibo (BF)	274.0	14.10	-1.62

(GH): Station in Ghana, (BF): Station in Burkina Faso

3.2.2 GLOWA Volta Project (GVP)

Many of the researches conducted within the framework of the projected required climate data for some specific watersheds and varied resolutions. The GLOWA Volta

[2] Complete inventory of station available in Appendix I

project setup automated observation stations in three locations in the Ghana part of the basin: Ejura in the transition zone, Tamale in the guinea savannah zone and Navrongo in the Sudan savannah zone. In a 10mim interval, a Campbell automated data loggers monitored and recorded temperature, relative humidity, net and global radiation, wind speed and direction, soil heat at 5cm and 10cm, atmospheric pressure and precipitation. Additional rain gauges were installed at 5 km radius to the automated stations to monitor rainfall intensities and squall lines (Friesen, 2002; Kasei, 2006). These rain gauges consist of a 263cm² diameter funnel over a rocker with a small compartment at each end (Figure 3.2). When one compartment is full, the rocker tips to the other side emptying the full compartment and exposing the other compartment. The tipping is transformed into an electric signal, which is recorded as one click in a Hobo data logger. The outlet of the rain gauge was connected to a container, and the collected amount was measured manually again every morning. Information from these gauges were sometimes used in the validation of some the neighboring data that were in question.

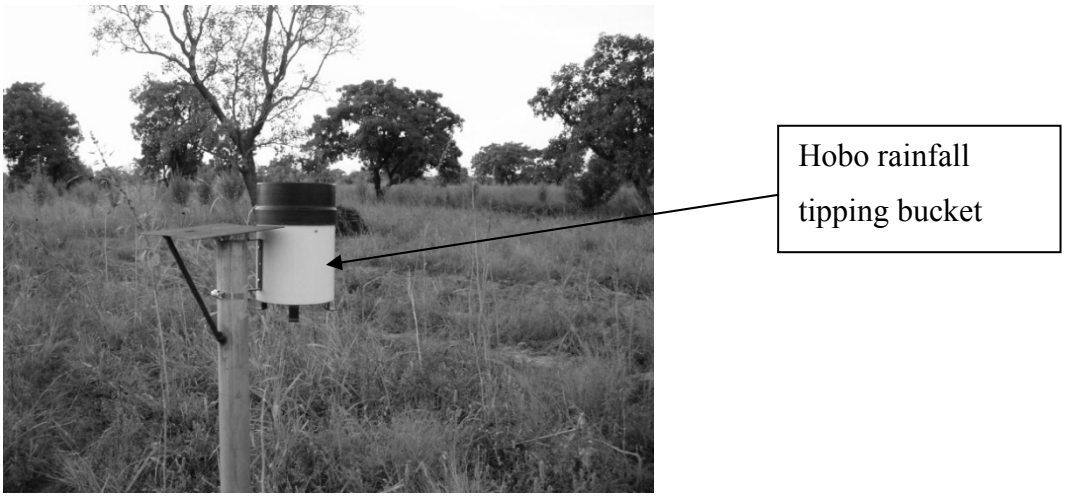

Figure 3.2: Tipping bucket rain gauge

3.3 Hydrological data

In the quest to understand the hydrological cycle of basin as large as the Volta Basin and to calibrate and validate a hydrological model for the Basin, historical hydrological data is essential. One of the primary goals of this research is to assess if any; the changes in the hydrology of the basin, and the potential risk of climate change might

have impact on the water resources of the Volta Basin. Flow data is required to calibrate and validate models that are expected to mimic the water balance of the basin.

3.3.1 Hydrological Service Department

The Hydrological Services Department (HSD) of Ghana is the only source of the hydrological data used in this research since data required to compare with model outputs were mainly within Ghana. GVP catalogued all hydrological stations within the basin (Figure 3.3) and sorted historical data with most spanning from 1961 till 2006; a few dating far back as 1951. The HSD installed staff gauges in streams and manually measured the water level daily. Calculating discharge for any water level; the HSD developed a stage discharge relationship which is expressed in an exponential rating curve. (The rating equations vary slightly from one station to another (Table 3.2).

Data used in this research had gaps for most of the stations that had been retrieved. Attempts to fill some of the gaps with mathematical algorithms developed by Amisigo (2005) was successful for some catchments but were not used in this research.

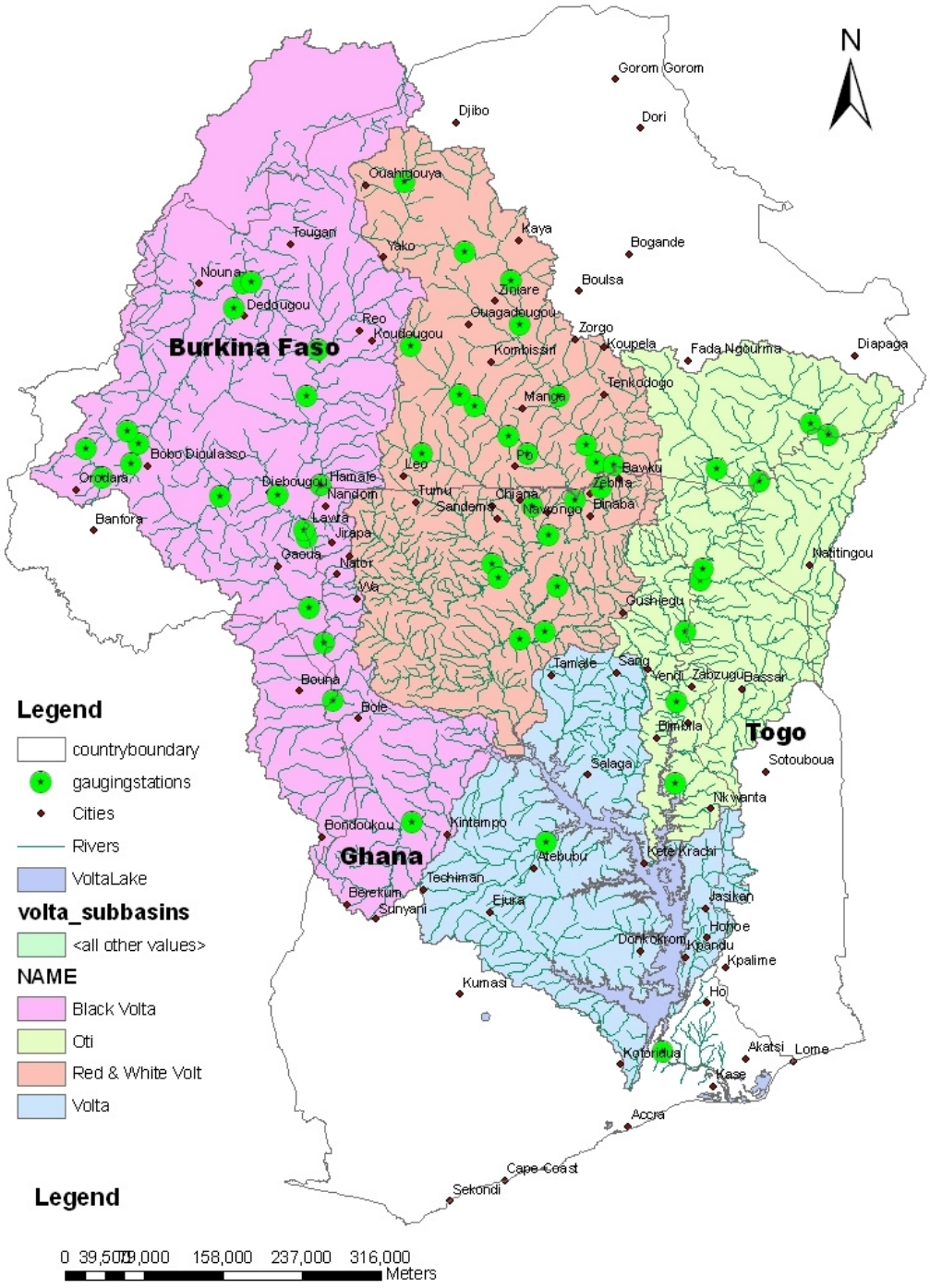

Figure 3.3: Hydrologic gauging stations in the Volta Basin

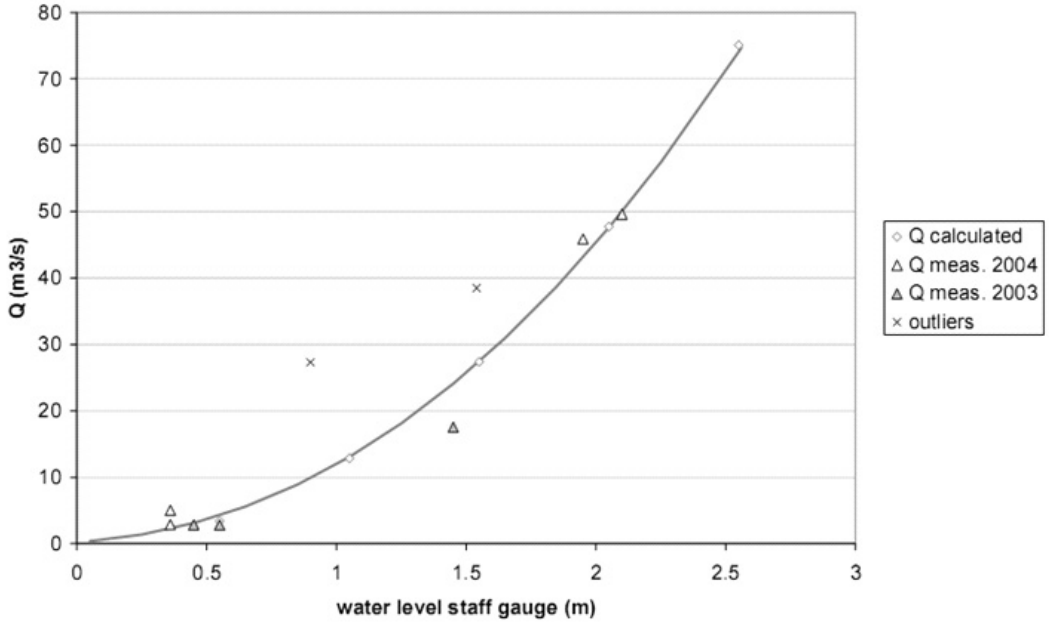

Figure 3.4: Rating curve to calculate river discharge from observed water levels at Pwalugu (56,760 km^2) by HSD[3]

Table 3.2: Rating equation for gauging stations (Data source: HSD)

Station name	Date established	Current gauge zero	Rating equation
Kpasinkpe on White Volta	30 April 2004	89.69 m	$Q = 22.52(h - 1.786)^{1.566}$
Pwalugu on White Volta	1 May 1951	123.77 m	$Q = 35.252(h - 1.193)^{1.593}$
Yarugu (Kobore) on White Volta	24 June 1995	24.69 m	$Q = 53.248(h + 0.115)^{2.030}$
Nangodi on Red Volta	6 November 1957	184.12 m	$Q = 22.291(h - 0.004)^{1.774}$

[3] Outliers are determined by the HSD

3.3.2 GLOWA Volta Project

Wagner (2008) installed two gauges in Pwalugu and Yarugu both in the White Volta to obtain additional discharge data for hydrological modeling of the White Volta. Hydro Argos systems were also installed in cooperation with the HSD in Ghana in order to contribute to the Volta Hycos System. Additionally Martin (2005) instrumented the Atankwidi (White Volta) catchment with water level recording. This data is available in the data base of the GVP but were not used in this research.

4 METHODOLOGY

Hydrological modeling usually is a physically-based distributed-parameter system, developed in an attempt to simulate the hydrologic processes such as the transformation of precipitation to runoff, and response of watershed and river basins to those processes. Flow simulations over the years have ranged from very simple antecedent precipitation and tank models to very complex nested and distributed parameter models such as the European Hydrological system model (SHE) and the Hydrologic Simulation Program Fortran (HSPF) (Maidment, 1992). Hydrological simulation models are often used to provide information on the interaction between water and land resources to aid in decision making, usually regarding the development and management of the scarce resources. Traditionally, hydrologic models have considered the watersheds as homogeneous against the complex terrain in which they are applied (Kilgore, 1997). These processes are sometimes described by differential equations based on simplified hydraulic laws with other processes, which may be expressed by empirical algebraic equations (Arnold et al. 1998). Hydrological simulation modeling systems are usually classified in three main groups namely: empirical black box, lumped conceptual, and the distributed physically-based systems. The great majority of the modeling systems used in practice today belongs to the empirical black box and lumped conceptual systems, which are known to be relatively simple and require a small number of parameters (approximately 5-10) to calibrate. Despite their simplicity, many models have proven to be quite successful in representing the hydraulics of watersheds (Refsgaard et al. 1996).

Hydrological models have been developed in recent times to incorporate the heterogeneity of the watershed such as the spatial distribution of various boundary conditions of topography, vegetation, land use, soil characteristics, rainfall, and temperature among others. The results have been detailed spatial outputs such as soil moisture grids, groundwater fluxes and many more (Troch et al. 2003). According to Schulla (1999), the WaSiM used in this study is capable of incorporating spatial heterogeneity in its analyses and is also built to be sensitive to the grid size of large watersheds of varied topography and with used success in the investigation of mountainous basins such as the Thur Basin with an area of 1700 km². The Water balance- Simulation-Model WaSiM-ETH is regarded as one of the models that

adequately describe the major processes of evaporation, canopy interception, transpiration, snowmelts, saturated and unsaturated sub flows, and channel/routed flow. One major bottleneck for many hydrological models according to Jain et al. (1992) and Troch et al. (2003) is the substantial data requirement for the various processes by these models.

For an effective modeling for management of the ecology of a watershed such as one of the goals of this research, thorough understanding of the hydrologic processes is essential. The complexity of the spatial and temporal variations in soils, vegetation and land-use practices of the large Volta Basin make it even more difficult. As suggested by Singh and Woolhiser (2002), mathematical models such as WaSiM and geospatial analysis tools are needed to comprehensively study the various processes.

4.1 Model selection

A thorough literature review on models used on large watersheds that incorporated land-use changes, runoff and soil characteristics of watersheds and basins was carried out. According to Brown and Heuvelink (2005), hydrological models are inherently imperfect in many ways because they abstract and simplify “real” hydrological patterns and processes. This imperfection is partly due to the scale of the catchment against the backdrop that most hydrological modeling is based on regionalization of hydrologic variables, with constituent process and theories essentially derived at the laboratory or other small scales (Blöschel, 1996). The underpinned assumption of catchment homogeneity and uniformity and time invariance of various flow paths over watersheds and through soils and vegetation underscores the embedded processes such as channel hydraulics, soil physics and chemistry, groundwater flow, crop micrometeorology, plant physiology, boundary layer meteorology, etc.(Brown and Heuvelink, 2005). All the flaws of hydrological modeling notwithstanding, process-based distributed models have proven to simulate fairly well the spatial variability of the water balance among other processes when the main hydrological parameters and processes are known (Schellekens, 2000). Until now, there has not been an alternative to hydrological simulation of watersheds that incorporate spatial scenarios such as land use changes.

Previous application of the process-based distributed model WaSiM-ETH for various environments and the proven capabilities were essential for the selection of this

model for this study. One major successful use of the model in a challenging topographic terrain was by Schulla (1997) in the assessment of the impact of climate change on the hydrological regimes and water of the Thur Basin located in north-east part of Switzerland. Furthermore, Niehoff (2001) cited in Leemhuis (2005), Jasper et al. (2002), Gurtz et al. (2003), Verbunt et al. (2003), and Leemhuis (2005) among others have successfully applied WaSiM-ETH to watersheds of different sizes and structures. For the arid region of the Volta, WaSiM-ETH was successfully applied by Martin (2005), Jung (2006) and Wagner (2008).

For this study, the Model WaSiM-ETH after Schulla and Jasper (1999) was selected, because it has the ability to characterize complex watershed representations to explicitly account for spatial variability of the soil profiles at the desired resolution amidst water balance and rainfall distribution in the assessment of changes in precipitation and runoff over the recent past using historical data.

4.2 Basic concept

The basic concept for the modeling in this study is to provide the spatial and temporal data over time that reflect and adequately represent the specific physio-geographical variability and heterogeneity of the Volta River system.

The use of the model WaSiM-ETH focuses on mimicking the hydrology of the Volta Basin through the reproduction of gauged station hydrographs and subsequently investigates the impact of changes in climate and/or rainfall anomalies on water resources over time (Figure 4.1) for the large watershed of the Volta Basin. For a detailed description of WaSiM-ETH see Chapter 5.

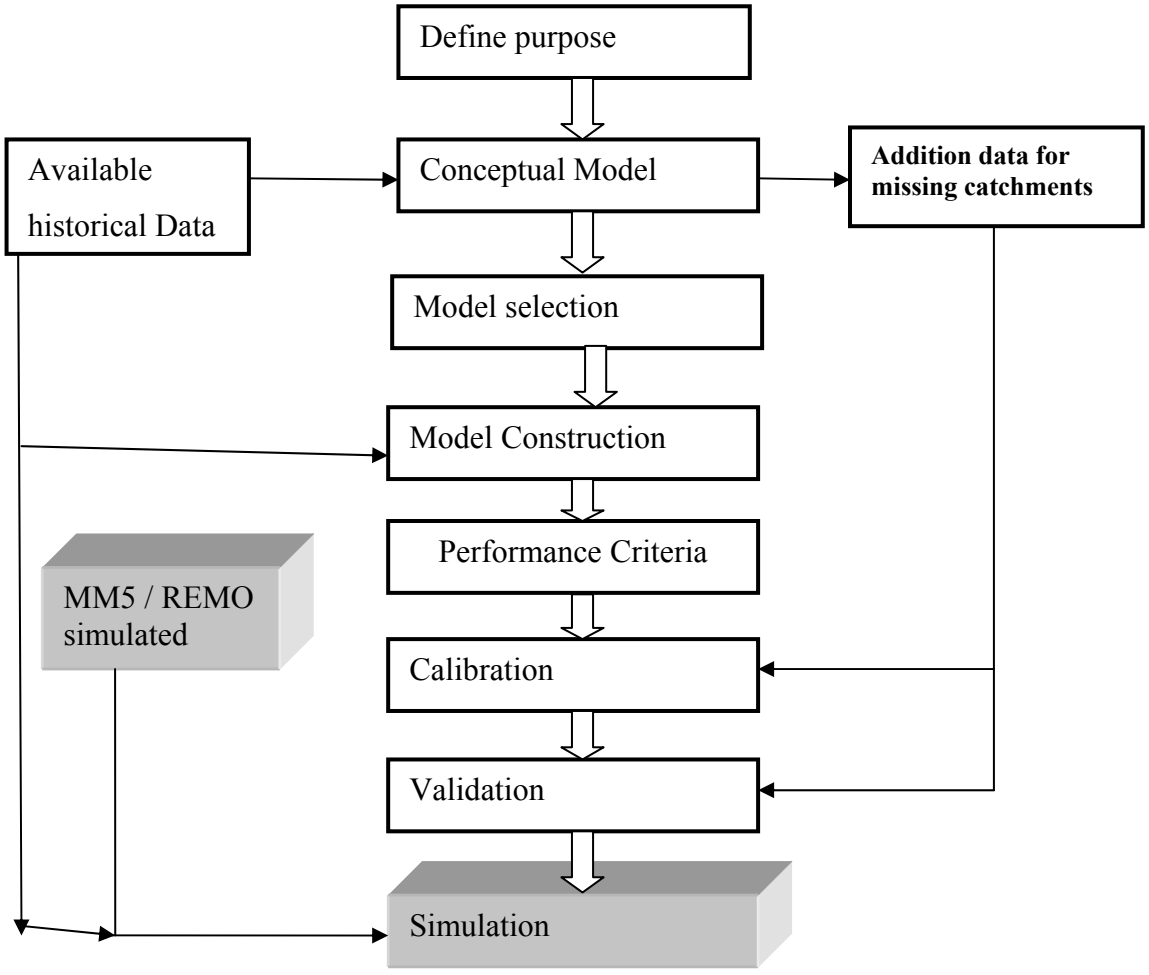

Figure 4.1**:** Modeling protocol for the analysis of risk applied to water resources management in the Volta Basin under climate change. (Modified after Anderson and Woessner, 1992; cited in Leemhuis 2005)

4.3 Running WaSiM-ETH for the Volta Basin

After selecting the area of interest where WaSiM was to be applied (Volta Basin) and delineating it to reflect routed gauged points, the various gridded spatial distributed data (e.g., DEM, land-use, soil maps, etc.), time series of meteorological data (temperature, precipitation, radiation etc.), hydrological (runoff) data and catchment details were assigned to the input folder of the model (Figure 4.2).

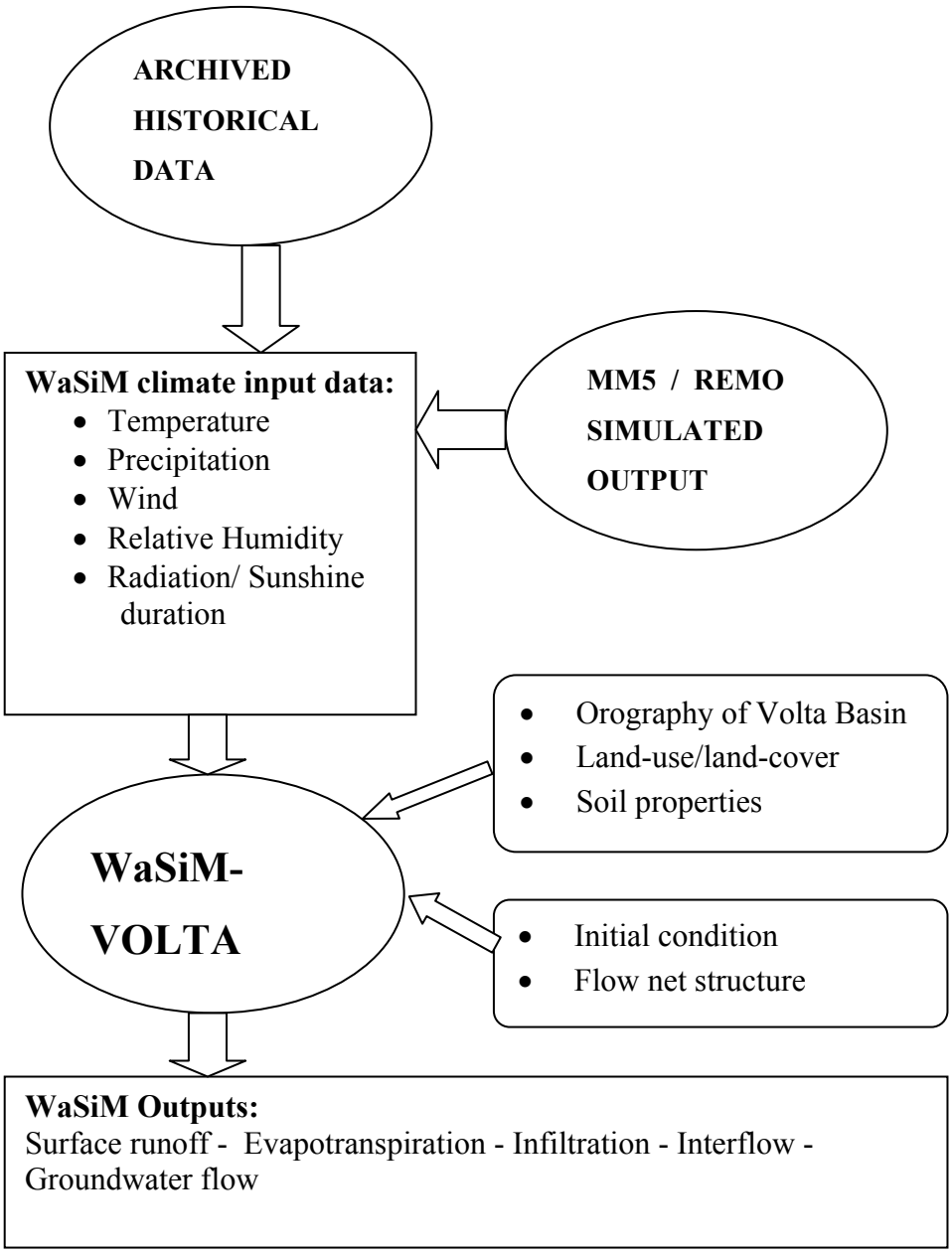

Figure 4.2: Running WaSiM with MM5 and REMO output (modified after Jung, 2006)

Other inputs were the DEM derived from the Shuttle Radar Topography Mission (SRTM) subset at 90m resolution and the land-use/ land-cover data provided by the GVP which were found to be relatively exact and of high resolution. The soil types with their related soil properties and the aquifer data (e.g., conductivities, thicknesses, storage coefficients, etc.) were obtained from literature and some rough

estimates. A control file designed to contain all the information required for the model run was modified to include initial conditions and parameterization. These mainly consisted of parameters controlling the model run (e.g., grid write codes, statistic file write codes, output lists etc.); formats for file names, path names for the input and output streams, and the hydrologic model parameters and property tables for the land use and soil types.

Schulla and Jasper (1999) suggest that a suitable spatial resolution to balance between model efficiency and a reasonable computer run time is important. The LINUX version 7.10.3 of the WaSiM model was run on faster computers processors of the Department of Computer Science III (University of Bonn), which offered the computer resources required to handle the volume of the processes.

The configuration of the model therefore depended largely on the amount and quality of the input data for this study; most of the available data were used to give a fair distribution of data over the area for optimum interpolation (see Chapter 5).

4.4 Model construction

The flow chart (Figure 4.3) shows the stepwise processes within WaSiM, comprising the different modules that are regarded as independent mathematical computations. There are further extensions, which are not shown in this chart; further details are available in Schulla and Jasper (1999).

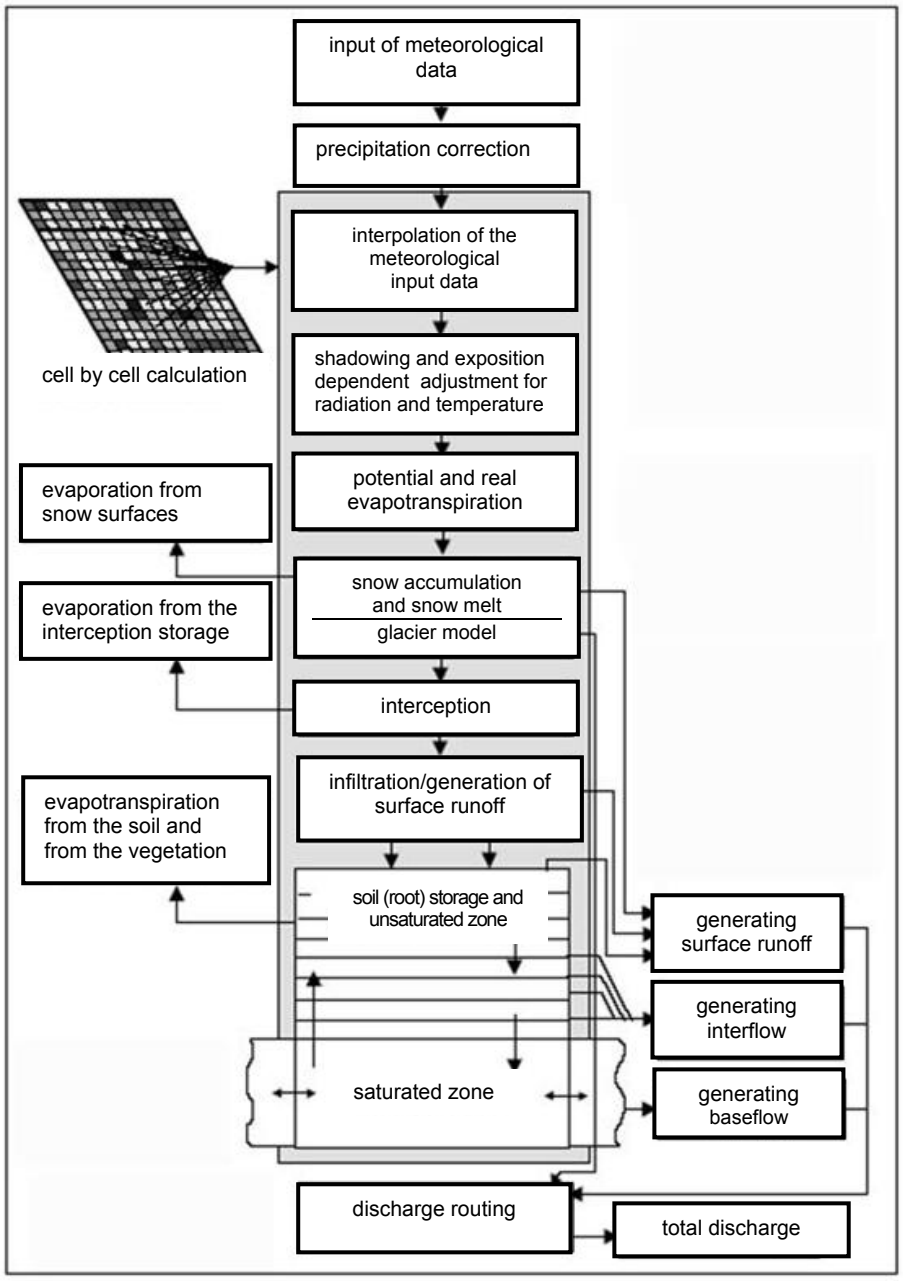

Figure 4.3: Schematic structure of WaSiM-ETH Model after Schulla and Jasper (2000)

4.5 Calibration and validation

Model calibration and validation is the process of evaluating and testing the different aspects of a model for the purpose of refining, enhancing, and building confidence in the model predictions in such a way that allows for sound decision-making (Hassan, 2005).

The validation process adopted to sufficiently predict with a satisfactory accuracy was the split sample test method (see also Xu, 1999). The time series of the period under investigation is split into a period of model warming, calibration and validation. The warm-up period is usually at the beginning of the time series and is used by the model to set up initial conditions for subsequent runs. The calibration procedure is applying optimum values to the sensitive parameters in order to optimize the predictive ability of the model. The validation procedure involves applying the calibrated model without changing any parameter value for another period. Again the model's performance is evaluated and is expected to correspond with the accuracy achieved during the calibration period (Figure 4.4). The model is then regarded as validated and can be used for predictive analysis thereafter.

The accuracy of the model is mainly assessed by comparing observed hydrograph versus simulated ones. This comparison is possible either with objective functions (e.g. Willmott (1981), Nash and Sutcliffe (1970)) or graphically. In general, the two most common methods of calibration are: the trial-and-error adjustment and automatic parameter estimation method or a combination of the two methods.

The iteration calibration process (Figure 4.2) followed to successfully reach the attained values of the calibrated parameter for this study under the set acceptable statistics.

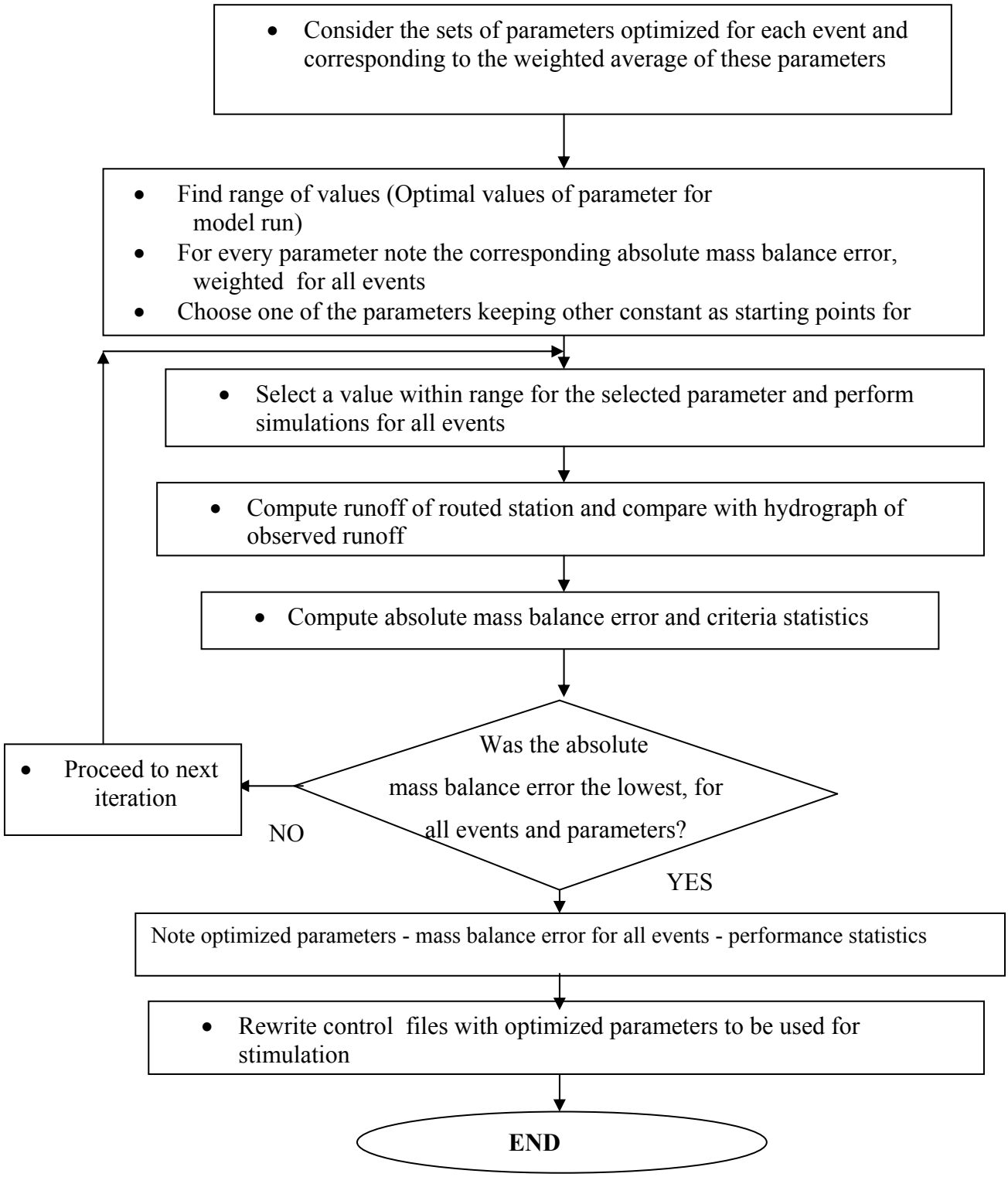

Figure 4.4: Iteration calibration flow chart used in this study

4.6 Predictive validity

Assessments of predictive validity are generally conducted on longitudinal datasets, where the measurement under assessment is tested for association with an outcome after a number of follow-ups has been conducted. The ideal assessment of predictive validity for the model-based estimates would therefore be to test for association between the model-based estimates for runoff and the gauged or estimated discharge of the various stations for various seasons. This evaluates the performance of the model and level of accuracy of simulated outputs. The following are the applied performance assessments conducted during the calibration and validation steps of the model building.

4.6.1 Pearson's r and R^2

Pearson's statistic and the deviance are used as overall goodness-of-fit tests. A small *r* is desirable, since a large value is usually interpreted as indicating poor goodness-of-fit of the model. According to Pierce and Schafer (1986), the Pearson statistic is often found to be almost chi-squared distributed rather than just the deviance.

The Pearson product-moment correlation coefficient (PMCC) typically denoted by *r* is referred to as a measure of the correlation between two variables *X* and *Y,* which are linearly dependent, ranging between +1 and −1.

From paired data (X_i, Y_i), the sample Pearson correlation coefficient is calculated as:

$$r = \frac{\sum_{i=1}^{n}(X_i-\overline{X})(Y_i-\overline{Y})}{\sqrt{\sum_{i=1}^{n}(X_i-\overline{X})^2}\sqrt{\sum_{i=1}^{n}(Y_i-\overline{Y})^2}} \quad (4.1)$$

Where $\overline{X}$ *and* $\overline{Y}$ are representing the sample means of X and Y respectively.

Altman (1991) observed that if a set of model-based estimates showed a significant positive correlation with the survey-based estimates it achieved convergent validity. The R^2 statistic from the fit measures the fraction of the total variability in response to that which is accounted for by the model and ranges from 1 (perfect fit) to 0.

The r and R^2 statistics were closely monitored in the calibration and validation of WaSiM Volta.

4.6.2 Nash-Sutcliffe efficiency index

The Nash-Sutcliffe efficiency index *Ef* is a reliable statistic widely used for assessing the goodness-of-fit of hydrologic models. *Ef* ranges from 1 to -∞, where *Ef* =1 indicates a perfect match of simulated to measured data; *Ef* = 0 corresponds to the model predictions matching the mean of the measured data; a negative *Ef* shows that the measured mean is a better predictor than the model. Moussa (2008) notes that *Ef* is a common criteria index used by hydro-geologists for model performance assessment.

The success of the use of this index in many reports shows how useful a tool it is in assessing the efficiency of a model, e.g., Erpul et al. (2003) used the index to assess nonlinear regression models of sediment transport. Merz and Bloschl (2004) used the index in the calibration and verification of catchment model parameters, while Kalin et al. (2003) used the index as a goodness-of-fit indicator for a storm event model. E*f* has also been used in a wide range of continuous moisture accounting models as reflected in Birikundavyi et al. (2002), Johnson et al. (2003), and Downer and Ogden (2004). The ASCE Task Committee on Definition of Criteria for Evaluation of Watershed Models of the Watershed Management (ASCE 1993) recommends the Nash-Sutcliffe index for evaluation of continuous moisture accounting models.

The use of this index for a wide variety of model types indicates its flexibility as a goodness-of-fit statistic and it is the reason for its use in this study.

E*f* is calculated as:

$$E_f = 1 - \frac{\sum_{i=1}^{n}(\hat{Y}_i - Y_i)^2}{\sum(Y_i - \hat{Y}_i)^2} \tag{4.2}$$

Where $\hat{Y}_i$ and *Yi* are predicted and measured values of the dependent variable *Y*,
$\hat{Y}_i$ is the mean of the measured values of *Y*; and *n* sample size.
Essentially, the closer E_f is to 1, the more accurate the model is.

4.6.3 Index of Agreement (d)

The Index of Agreement (d) is the evaluation of the agreement between the estimated and observed runoff (Legates and McCabe, 1999; Willmott, 1984; and Willmott, 1981). Recent successes in the use of (d) in hydrological modeling include Obuobie (2008), Hiepe and Diekkrüger (2007), Chekol (2006) among others.

Willmott developed the index of agreement to overcome the insensitivity of correlation-based measurements that were based on differences in sampled means and variances of the observed and model-simulated outputs (Willmott, 1981 and 1984):

$$d = 1.0 - \frac{\sum_{i=1}^{n}(O_i - P_i)^2}{\sum_{i=1}^{n}(|P_i - \overline{O}| + |O_i - \overline{O}|_i)^2} \quad (4.3)$$

where O_i is the observed data; P_i is the model-simulated values of O_i, $\overline{O}$ is the mean of O; and n *is* the number of data O.

4.6.4 Mass balance error

The minimization of the errors in the mass balance is considered the most important objective in calibration after the water balance is fairly correct. This is derived from the fact that the processes within the unsaturated zone and evapotranspiration are considered the core of the model, and the processes are responsible for keeping the mass balance as realistic as possible. If good estimates are obtained for the parameters of infiltration process (unsaturated zone), it is very likely that good estimates for runoff starting time and good matches between simulated and observed surface discharge may also be obtained (David et al., 1991).

4.7 Drought analysis in the Volta Basin

Evaluating future watershed changes is more difficult than the evaluation of changes that have already taken place because of the non-stationary nature of some input data such as land use/land cover. Satisfactory simulation of the water resources of the Volta

meteorological, soil-moisture, and hydrological droughts. The different types of droughts are linked (Figure 4.5) to each other with each type of drought referring to a specific type of water deficit in a specific part of the hydrological cycle. A meteorological drought is said to occur when precipitation is less than normal. Soil moisture droughts and hydrological droughts are usually characterized by low soil water content and low stream flows and usually occur after a meteorological drought. For the development of soil moisture droughts, precipitation deficit coupled with high evapotranspiration are the two most important factors. Low stream flows usually linked to hydrological drought are common in the Volta Basin and can be linked to the development of other types of droughts.

For this study, meteorological inputs for the past were obtained from the GVP. For the simulations, the calibrated model generated inputs using the Mesoscale Meteorological Model version 5 (MM5) adopted for the Volta Basin by the GVP, based on the IS92a–f greenhouse gas emissions scenarios (IPCC 2001). The used REMO model outputs were adopted by GLOWA IMPETUS project based on the IPCC climate assemble models A1B and B1. The future time slice of 2030 to 2039 was compared with time slices of the past and present climates of 1961-1970 and 1991-2000, respectively, for the evaluation of changes with MM5 and 1961-2000 and 2001-2050 with REMO.

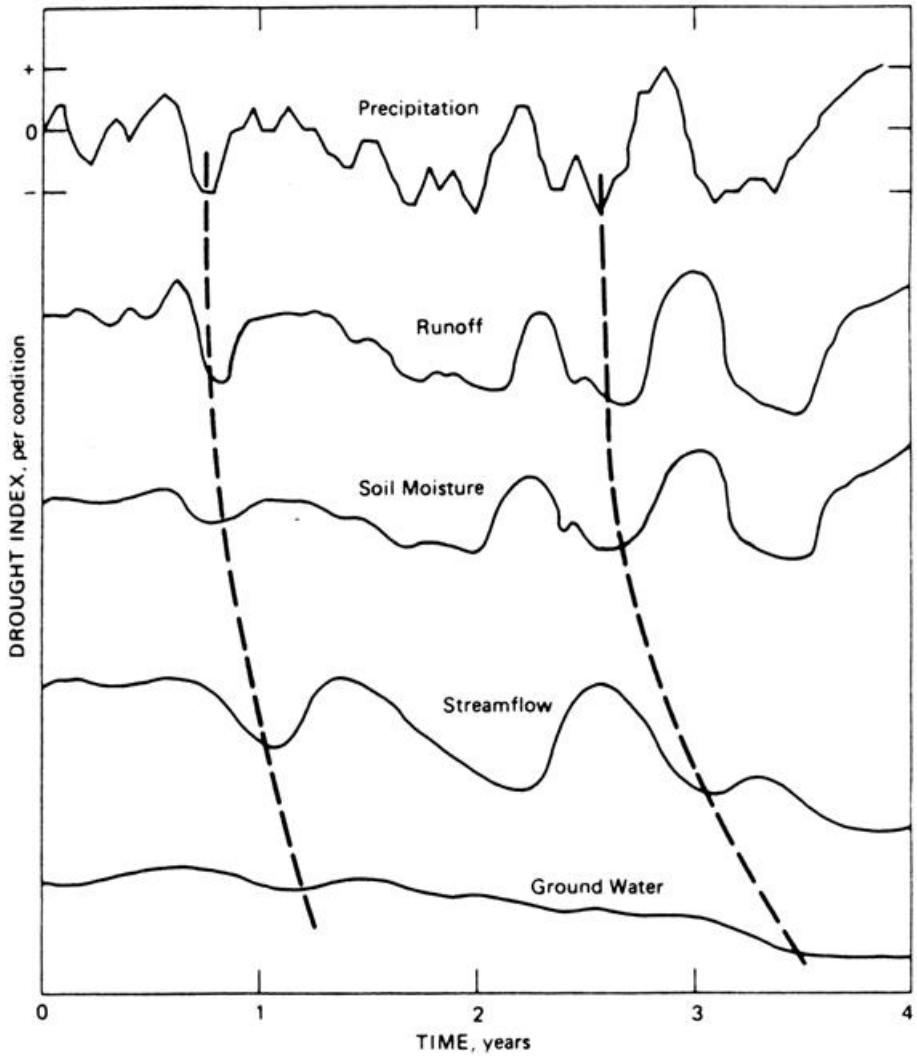

Figure 4.5 Schematic illustration of hypothetical precipitation deficits transcending throughout the hydrological cycle over time (Rasmusson et al. 1993).

4.8 Historical drought events in the Volts Basin

Meteorological droughts are the most sensitive as compared to all other forms of droughts and usually occur after a meteorological drought has occurred. Meteorological droughts are usually expressions of precipitation's departure from normal over some period of time and hence reflects one of the primary causes of a drought (Hisdal, 2000).

In the analysis of historical droughts that have occurred in the basin the Standardized Precipitation Index (SPI) method developed by McKee et al., (1993) is utilized. The method was simple and straightforward, since precipitation was the only meteorological variable used. An advantage of this method is the use of various time periods in drought assessments.

The Standardized precipitation series is calculated using the arithmetic average and the standard deviation of precipitation series. For a given X_1, X_2, X_n series, the standardized precipitation series, SPI_i, is calculated from the following equation:

$$SPI_i = \frac{X_i - \bar{X}}{S_x} \quad (4.4)$$

where $\bar{X}$ is the average and S_x is the standard deviation of the precipitation series. Negative values obtained from this equation indicate precipitation deficit (drought events), while positive values stand for precipitation excess (wet events).

Table 4.1: Classification and evaluation of different standardized precipitation indices (SPI) according to McKee et al. (1993)

SPI Value	**Category**
(0.0) – (-0.99)	Normal year
(-1.0) – (-1.49)	Moderately dry
(-1.5) – (-1.99)	Severely dry
≤ -2	Extremely dry

4.9 Regional drought analysis

Henrique and Santos (1999) proposed a method used in recent times for regional drought analysis was verified by Yildiz (2007). The method characterizes both the temporal and spatial extent of regional droughts by computing an intensity-areal extent-frequency curve. This curve applies the polygons to determine the area of influence of each individual station and utilizes synthetic precipitation series in the study area. However, the polygons method does not take into account the stochastic characteristics of precipitation data. As an alternative, Schulla (1999) proposed techniques to obtain regional distribution of precipitation data. Schulla and Jasper (2000) later developed the Water balance Simulation Model ETH (WaSiM-ETH), which uses the inverse distance weighting (IDW) technique to obtain regional precipitation distributions. The method

used in this study was used by Jung (2006) to evaluate runoff, evapotranspiration and soil moisture dependency to climate change for the total catchment of the Volta River basin. With the use of drought intensity-areal extent-frequency curves for a region Henrique and Santos (1999) determined intensity, areal extent and return periods of severe drought events. Similarly, in this study, a regional drought analysis was performed for the Volta Basin using drought intensity, areal extent and frequency with the method proposed by McKee et al. (1993) and Jung (2006).Annual drought intensity values at each station were first obtained from the annual SPI time series over the whole period of 1961-2005.

For this purpose, in a given year, SPI values of evenly spaced stations over the basin were added together to obtain the total SPI intensities. Then the regional distributions of annual drought intensities from 52 stations (Appendix I) were obtained using the IDW method. Finally, percent areal distributions of drought intensities for selected threshold levels (e.g., -1.0, -1.5, etc.) were calculated and a frequency analysis of percent areal distributions was performed to determine return periods of drought intensities.

5 HYDROLOGICAL MODEL WASIM-ETH

5.1 Introduction

WaSiM-ETH is a water balance simulation model and was first developed at the Technical University of Zürich (ETH) (Schulla, 1997). It was later extended to combine a 1-D unsaturated zone model based on the Richards equation with a watershed run-off model by Schulla and Jasper (2000). Until recently, the hydrological model WaSiM has not been used in a catchment of the size of the Volta Basin, or in a semi-arid environment such as West Africa. WaSiM-ETH is popular in Europe and has been applied in Germany and Switzerland in several researches, often to mountainous watersheds (e.g., Schulla, (1997); Krause, (2003); Stadler, (2002) cited in Jung (2006)). Within the GLOWA-Volta research project, WaSiM has been applied on three different scales within the Volta Basin. the Atankwidi Basin covering an area of 275 km², the White Volta catchment of 34,000 km², and the entire Volta Basin of 400,000 km² (Martin, 2005; Wagner, 2008; Jung, 2006).

5.2 WaSiM Concept

WaSiM is a deterministic hydrological model with a modular structure. The open source code is written in C+ consisting of three major components 1) the pre-processor TANALYS (Topographical ANALYSis), which calculates basin boundaries, stream network and flow times using the topographical information. This is used for processing spatial raster data into the required input format for WaSiM model runs 2) The spatial interpolation of meteorological input data and calculation of potential evapotranspiration, and 3) flow dynamics in relation to water budget modeling.

The water budget simulation section of WaSiM comprises a chain of modules that combine both the physical and empirical descriptions of water flow. Depending on desired outputs and conditions of the area of interest, modules can be activated or deactivated to reduce model run time and computer resources, The glacier and snow modules were deactivated for this research because the area of interest (Volta Basin) is in the tropics and has neither snow nor glaciers.

5.3 Data requirements and processing in WaSiM

The meteorological input data required are precipitation, temperature, relative humidity, wind velocity, global radiation, and sunshine duration. Radiation and sunshine duration are used alternatively. Of these input variables, temperature and precipitation are most sensitive (Jung, 2006). However, to run WaSiM needs all these required parameters. WaSiM employs a variety of methods of interpolation from gauged stationed data to a regular grid. The methods available for interpolation are:

1) Inverse Distance Weighting (IDW): This interpolation method uses all available station data within a specified search radius and performs a distance weighting based on an assigned weighting.
2) Regression: In mountainous catchments, e.g., the mountainous landscape of Switzerland, this mode of interpolation could be very important for variables such as temperature and wind speed, which generally have a stronger dependence on altitude than on horizontal positioning for such topography.
3) Regression and IDW: This method combines both altitude dependant regression and IDW. Where using input variables from areas that are horizontally and vertically correlated this method is useful for improving the temporal and spatial resolutions of the interpolation.
4) Thiessen: This method is similar to IDW, but only considers the influence of the station nearest to a certain grid point by drawing polygons around neighboring stations and interpolating using the midpoint concept.
5) Bilinear interpolation: This is a method suitable for organized stations that are equidistant, e.g., gridded input data are almost equidistant, hence the method of bilinear interpolation is less time consuming and most effective.

5.3.1 Temporal data

Rainfall measurements are prone to errors partly from the method of collection and largely due to human error. WaSiM in one of its steps of inputting the precipitation data, usually termed “precipitation correction” within the control file, automatically makes corrections to the precipitation data. These corrections are performed to counter the

errors induced by wind measurement. However, for simulated climate inputs, this function is not required.

Radiation and temperature are usually topographically dependent and thus require some adjustment. These adjustments are to compensate for shading effects due to topography in mountainous regions. Sensible heat flux and temperature depend strongly on incoming radiation. With the use of the DEM, incorporating the influence of the topographical data using methods after Oke (1987) cited in Jung (2006), the needed modifications are performed on the temperature and radiation inputs within the model.

Due to the flatness of the topography of the Volta Basin, the IDW interpolation was used for the interpolation of the obtained station data in the calibration and validation runs. For the future model runs when data from simulated climate models were used, the bilinear interpolation method was satisfactory for the efficiency of computer resources.

5.3.2 Spatial data

Hydrogeology

The hydrogeological inputs were largely from Martin and van de Giesen (2005) and Jung (2006). Based on Jung (2006), parameterization of the geology of the basin was carried out using various hydrogeological maps with additional information collected from Ghana and Burkina Faso. Because data from other countries were not readily available, extrapolation to the regions outside the Ghana and Burkina Faso boundaries within the basin became necessary. Hydro-geological units, horizontal hydraulic conductivities, storage coefficient and aquifer thicknesses were acquired from previous research conducted by Jung (2006). Literature values were used for parameters that were not location specific.

DEM

The digital elevation model (DEM) derived from the Shuttle Radar Topography Mission (SRTM) subset at 90m resolution provided by the GVP (Figure 5.1) was used in the topographical analysis (TANALYS) to derive exposition, slope, flow net structure, flow directions, flow times, and sub-catchment boundaries based on gauging points.

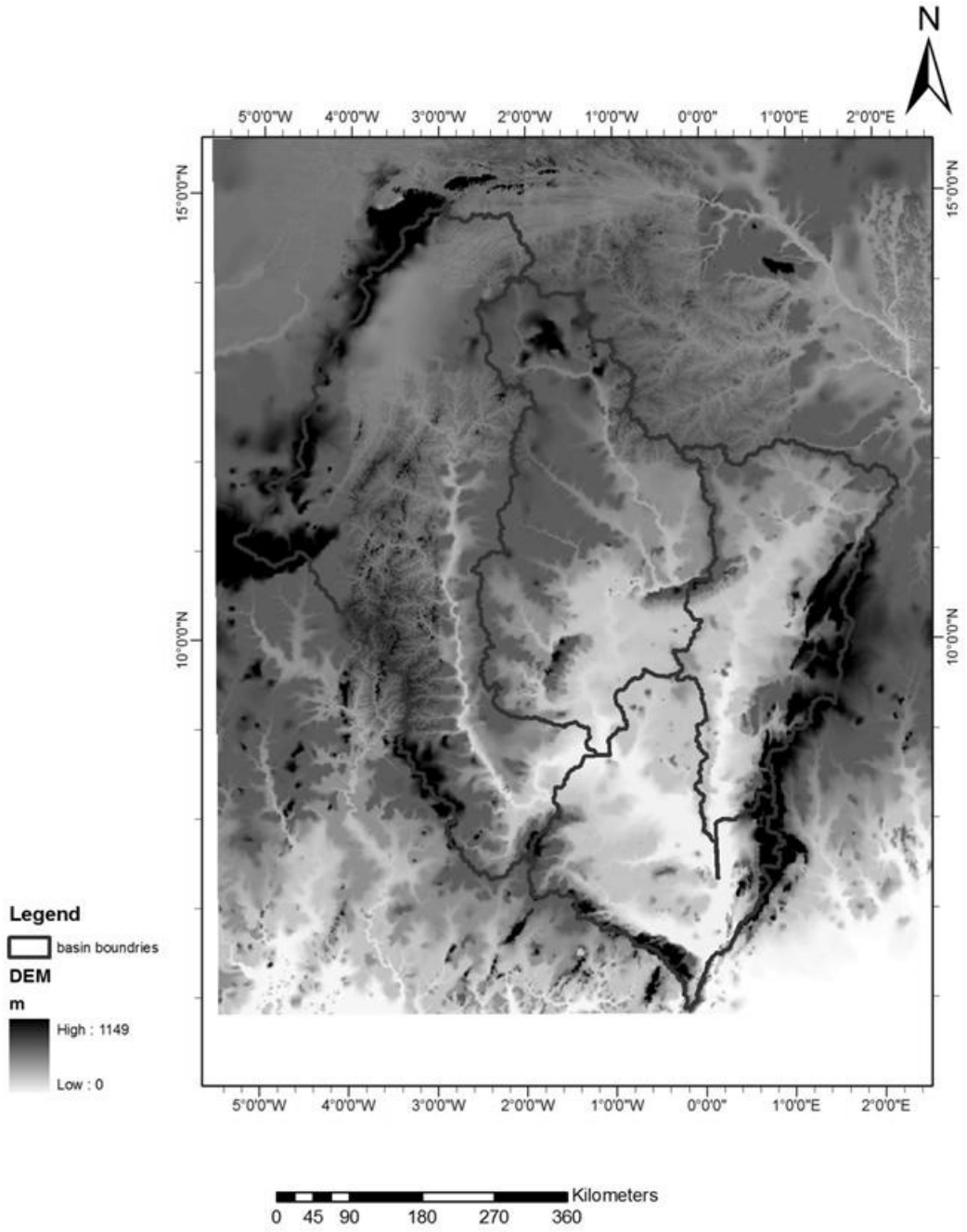

Figure 5.1 Digital elevation map of the Volta Basin (Data source: USGS EROS data centre)

Land-use/ land-cover data

The land-use representation of the Volta Basin for 1999/2000 (Figure 5.2) was derived from the GLOWA Volta project and compared with Jung (2006) for consistency. Default parameters for the various land-use classes were obtained from Schulla and Jasper (2000) and Grell et al. (1995).

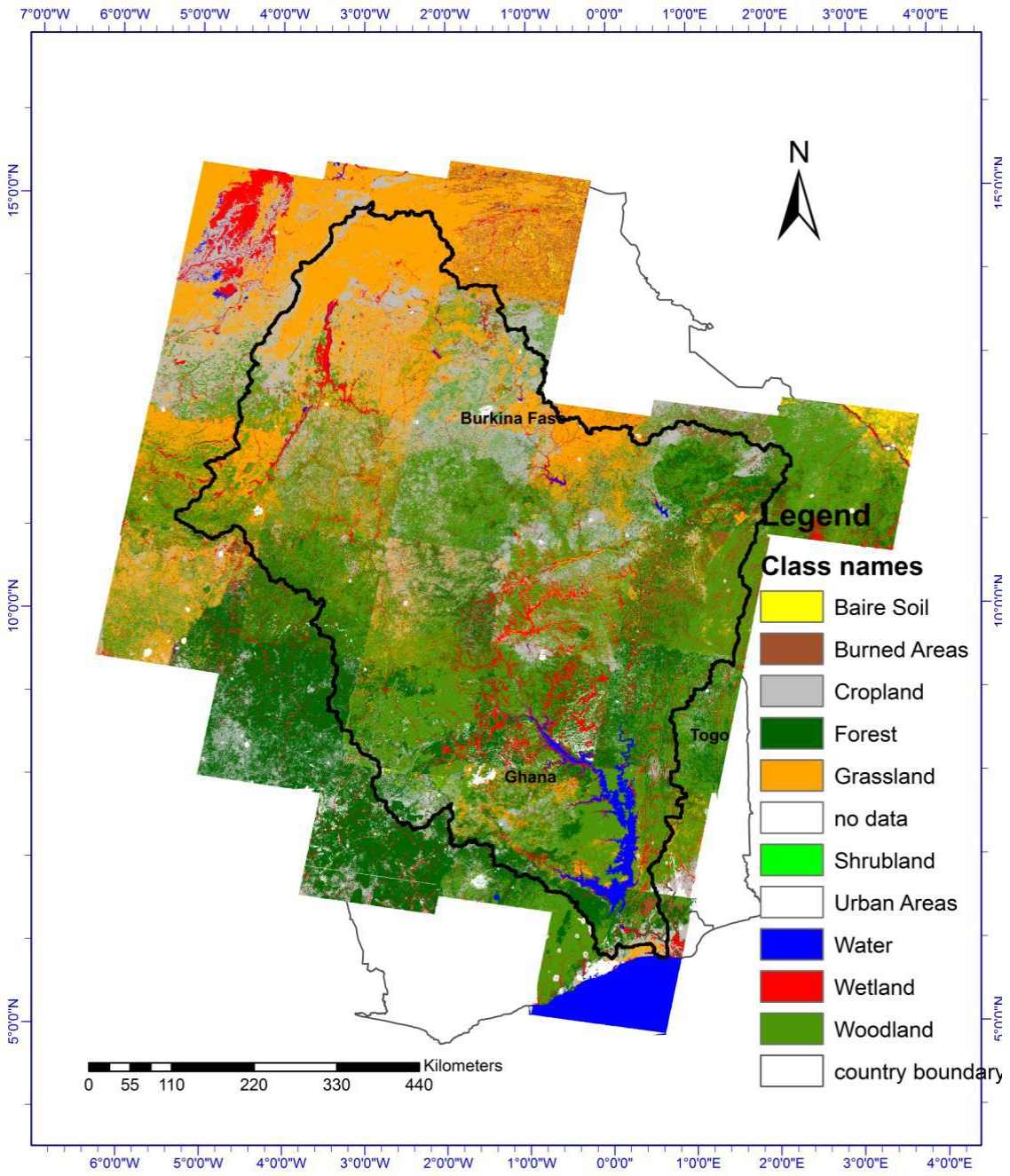

Figure 5.2 Land-cover/-use map of the Volta Basin (1990-2000) [Data source: Landcover change matrix derived from Landsat TM, Landsat ETM+ and MODIS data (1990 to 2000)]

Soil texture map

This was derived from the global FAO (United Nations Food and Agriculture Organization) soil map (FAO, 1995) and seen as updated from the soil map of FAO (1971-81). Soils were classified differently for Ghana and Burkina Faso (Figure 5.3).

The parameters required for the model, especially the van Genuchten parameters were obtained from Hodnett and Tomasella (2002). The other required parameters for the soils were from Jung (2006) and Schulla and Jasper (2002).

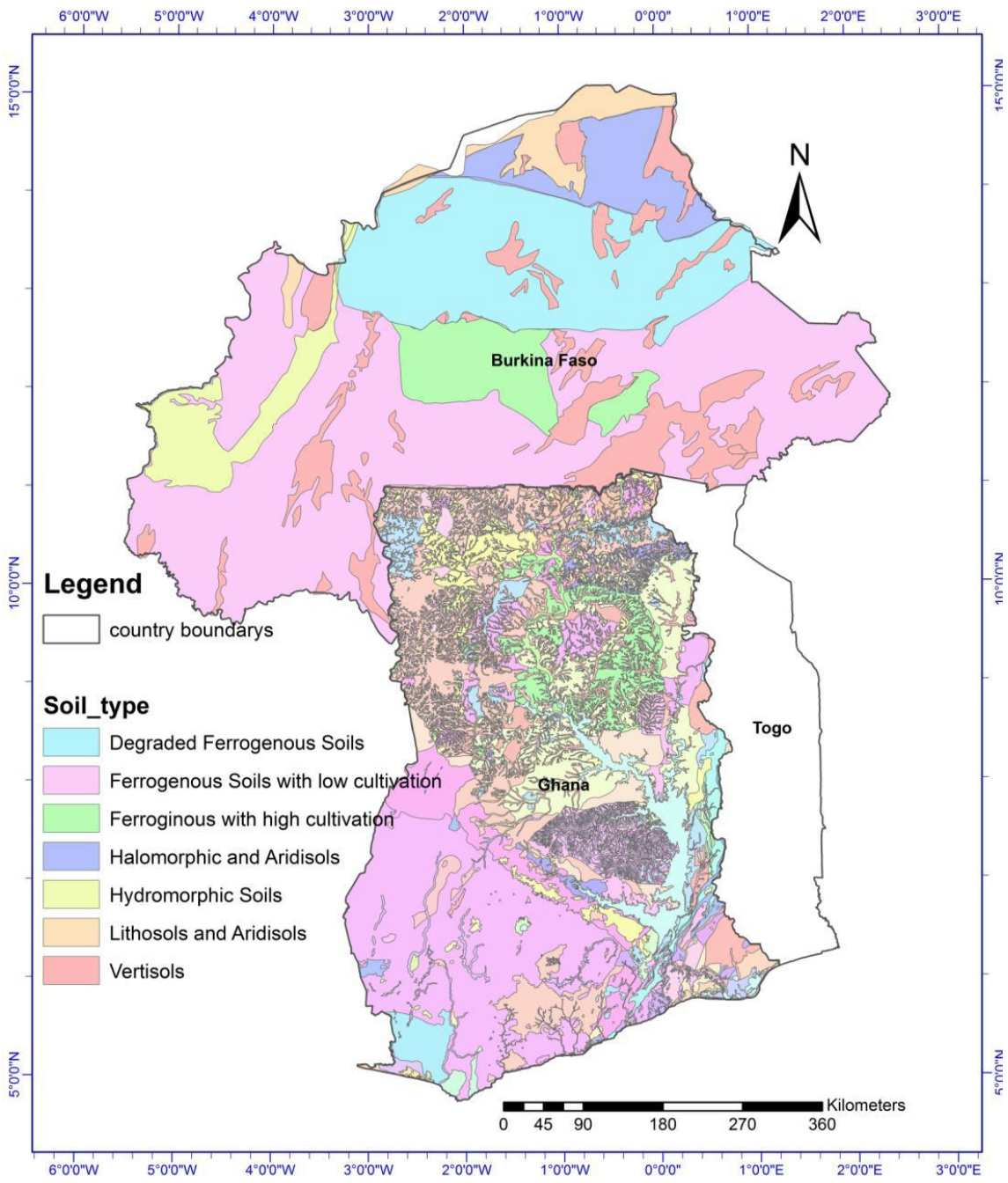

Figure 5.3: Soil texture map of Ghana and Burkina Faso (Data sources: FAO (1995) and the Ghana at a Glance database provided by the Soil Reseach Instite of Ghana)

5.4 WASIM-ETH modules

Schulla and Jasper (2000) give a detailed descriptions and explanations of the various modules of WaSiM with all the mathematical and empirical equations that each process entails. However, a brief description and basic equation relevant to this research is presented hereafter.

5.4.1 Potential and real evapotranspiration

Leemhuis (2005) describes evapotranspiration (ET) as the transfer of water vapour from land surfaces with or without vegetation to the atmosphere. Potential evapotranspiration (ETP) can be described as the maximum amount of water that will be evaporated and/or transpired assuming water availability to a referred surface and/or crop were not limited.

WaSiM uses the Penman-Monteith approach in the calculation of evaporation. This approach according to Monteith (1975) is most sensitive to the properties of the plants used for transpiration; these include the stomata resistance, effective height of the vegetation, distribution and depth of the root, LAI (Leaf Area Index), vegetation coverage, and the soil water content threshold below which transpiration starts to decrease. In the computation of real evapotranspiration, potential evaporation is first reduced by the amount of water equal to the interception storage of the plant canopy and then followed by a reduction of potential evaporation based on the actual suction of the soil and the physiological properties of the plant (Brutsaert, 1982). Equation (5.1) is the Penman-Montheith formula used to calculate evapotranspiration within WaSiM:

$$\lambda E = \frac{3.6 \cdot \left(\frac{\Delta}{\gamma_p}\right) \cdot (R_N - G) + \frac{p.c_p}{\gamma_p \cdot r_a} \cdot (e_s - e) \cdot t_i}{\frac{\Delta}{\gamma_p} + 1 + \frac{r_s}{r_a}} \qquad (5.1)$$

Where Λ latent vaporization heat [KJ·Kg^{-1}]

λ = $(2500.8 - 2.372 \cdot T)$

T = temperature in °C

E latent heat flux (kg·m^{-2})

Δ tangent of the saturated vapor pressure curve [hPa·K^{-1}]

R_N net radiation, conversion from Wh.m^{-2} to KJ-m^{-2} by factor 3.6 [Wh·m^{-2}]

G	soil heat flux [Wh·m^{-2}]
p	density of dry air (kg·m³) p ($RL \cdot T$) (at 0°C and 1013.25 hPa: p =1.26)
c_p	specific heat capacity of dry air (KJ·(Kg·K)$^{-1}$) at constant pressure
$c\,p$ =	1.005
e_s	saturation vapor pressure at temperature T [hPa]
e	actual vapour pressure (observed) (hPa)
t_i	number of seconds within a time step
γ	psychrometric constant [hPa·K^{-1}]
r_s	bulk-surface resistance [s·m^{-1}]
r_a	bulk-aerodynamic resistance [s·m^{-1}]

5.4.2 Interception

Interception is that part of precipitation caught up by canopy formed by the vegetation above the ground. For WaSiM, the simple bucket approach is used for the computation of interception storage, which is dependent on the total leave coverage (a factor of LAI) and the maximum height of the water layer on the vegetation. The underlying equation (5.2) after Schulla (1997) has varied conditions for too dry or wet soil:

$$SI_{max} = v \cdot LAI \cdot h_{SI} + (1 - v) \cdot h_{SI} \qquad (5.2)$$

Where SI_{max}	maximum interception storage capacity	[mm]
v	degree of vegetation coverage	[m^2/m^{-2}]
LAI	leaf area index	[m^2/m^{-2}]
h_{SI}	maximum height of water	[mm]

According to the developers of the model, the extraction of water out of the interception storage by evaporation is assumed to be at a potential rate. If there is a sufficient amount of water in the storage, the storage content is reduced by the potential evaporation, and no evaporation water will be taken from the soil. If the storage content is smaller than the potential evaporation rate, the remaining rate will be taken from the soil on condition that the soil is not too dry or too wet. In that light, interception evaporation will be:

$$EI = ETP \quad (\text{for } SI \geq ETP \text{ in mm}), \quad ETR = 0$$
$$\text{and } EI = SI \quad (\text{for } SI < ETP \text{ in mm}), \quad ETR = ETP - SI$$

where EI	the interception evaporation [mm]
ETR	remaining evaporation from soil and vegetation
SI	content of the interception storage [mm]

5.4.3 Snow module

WaSiM also includes a snow module, which simulates melting and accumulation of snow and their contributions to the water balance. However, in this study this module was useless because of the geographical location of the Volta Basin in the tropics and therefore was disabled.

5.4.4 Infiltration and the unsaturated zone module

In the modified Green and Ampt approach (1911), excess infiltration feeds directly to runoff, and the amount of infiltrating water serves as an upper boundary condition in the unsaturated zone module. In WaSiM release-2 (version 7.10.3) used in this research, the downward movement of water through the soil after Green and Ampt (1911) stems from the principle that, when saturation is reached or in situations when precipitation intensity exceeds infiltration capacities, almost all the excess precipitation is channeled into direct runoff. This module is hampered when potential macro-pore fluxes are not considered. This restriction for the Volta Basin affected the performance of the calibration and validation of the model. One major handicap was the use of daily precipitation values for simulations, which assumes a mean value over 24 hrs. A better resolution of at least a3-hr time step is desirable. The following equation is for the calculation of infiltration:

If $PI > K_s$

$$t_s = \frac{l_s \cdot n_a}{PI} = \frac{\frac{\psi_f}{PI/K_S - 1}}{PI} \tag{5.3}$$

Where t_S	saturation deficit from the beginning of the time step	[h]
l_S	saturation depth	[mm]
n_a	fillable porosity ($n_a = \theta_S - \theta$)	[-]
ψ_f	suction of the wetting front ($a \approx 1000n$)	[mm]
PI	precipitation intensity	[mm·h^{-1}]
K_S	saturated hydraulic conductivity	[mm·h^{-1}]

The water infiltrated until time F_s is calculated as:

$$F_s = l_s \cdot n_a = t_s \cdot PI \tag{5.4}$$

Hence, using the formula after Peschke (1989), the accumulated infiltration after saturation has been reached due to peculation for one time step is determined as:

$$F = \frac{A}{2} + \sqrt{[\frac{A^2}{4} + AB + F_s^2]} \tag{5.5}$$

Where

$A = K_s(t - t_s)$

and

$B = F_s + 2.n_a.\psi_f$

Within the unsaturated zone, calculation of vertical movement of water in soil assumes this zone as one-dimensional so that no exchange of water between neighboring cells takes place.

Each cell is divided into layers of uniform thickness as specified in the soil module. Percolation and capillary rise according to the soil properties are simulated with corresponding vertical moisture profiles and fluxes. The van Genuchten equation is used to account for the hydraulic conductivity with decreasing water content (van Genuchten, 1980). The water release curve of soils is a function of the saturated (Θs) and residual (Θr) soil water content, the soil matrix potential ψ and the parameters α and n with the premise that hydraulic head and conductivities depend on the van Genuchten principles (1980).

$$\theta(\psi) = \theta_r + \frac{\theta_s - \theta_r}{(1+(\alpha|\psi)^n)^m} \tag{5.6}$$

Where	θ	actual water content	[-]
	ψ	suction	[hPa]
	θ_r	residual water content at $k(\theta) = 0$	[-]
	θ_s	saturation water content	[-]
	α, n	empirical parameter (m=1-1/n)	[-]

Due to flow retention, linear storage approaches are applied to interflow and direct runoff, which requires the calibration of the recession constants K_D and K_I. Similarily, the runoff at time t, (Q_t) is a result of the runoff component at the initial time t_0, (Q_{t0}) and the corresponding recession constants K as given in the relation:

$$Q_t = Q_{t_o} \cdot e^{-\frac{\Delta t}{k}} \tag{5.7}$$

with change in time $\Delta t = t - t_o$

Bare soils on top of the soil profiles of the unsaturated zones are responsible for evaporation, while plants are responsible for uptake of water from other soil layers for transpiration, depending on the properties of the plant and the availability of moisture.

Interflow is generated between soil layers and relies upon the suction and the drainage density of the soil. Groundwater recharge is also calculated as the balance of inflows and outflows to the total layers in which the groundwater table resides.

The van Genuchten equation (5.6) is often used to determine unsaturated hydraulic conductivities.

5.4.5 Run-off routing

The run-off is that component that includes direct run-off, interflow and base flows assuming the groundwater module was inactive. The generated runoff in each cell is directed to the outlet of a basin with respect to flow times that are calculated by the pre-processor TANALYS for the entire catchment considering the distances to specific routed outlets (Figure 5.4). The different flow velocities for the different water levels in the channels are calculated using the kinetic wave approach and a simple linear storage approach. Thereafter, direct runoff and interflow are simulated. These flow times are calculated using the Manning-Strickler equation (Maidment, 1993). It is possible to simulate other processes within the catchments such as irrigation, artificial abstractions and regulated reservoirs.

5.4.6 Reservoir

Detailed information necessary for required to incorporating reservoirs and ponds into the modeling were not readily available. For the model runs in this study, water bodies were classified under the unsaturated module of the model with special characteristics, e.g., the van Genuchten parameter and *alpha* and *n* of 1.0 and 1.01, respectively, to adequately represent the reservoirs and ponds within the Basin.

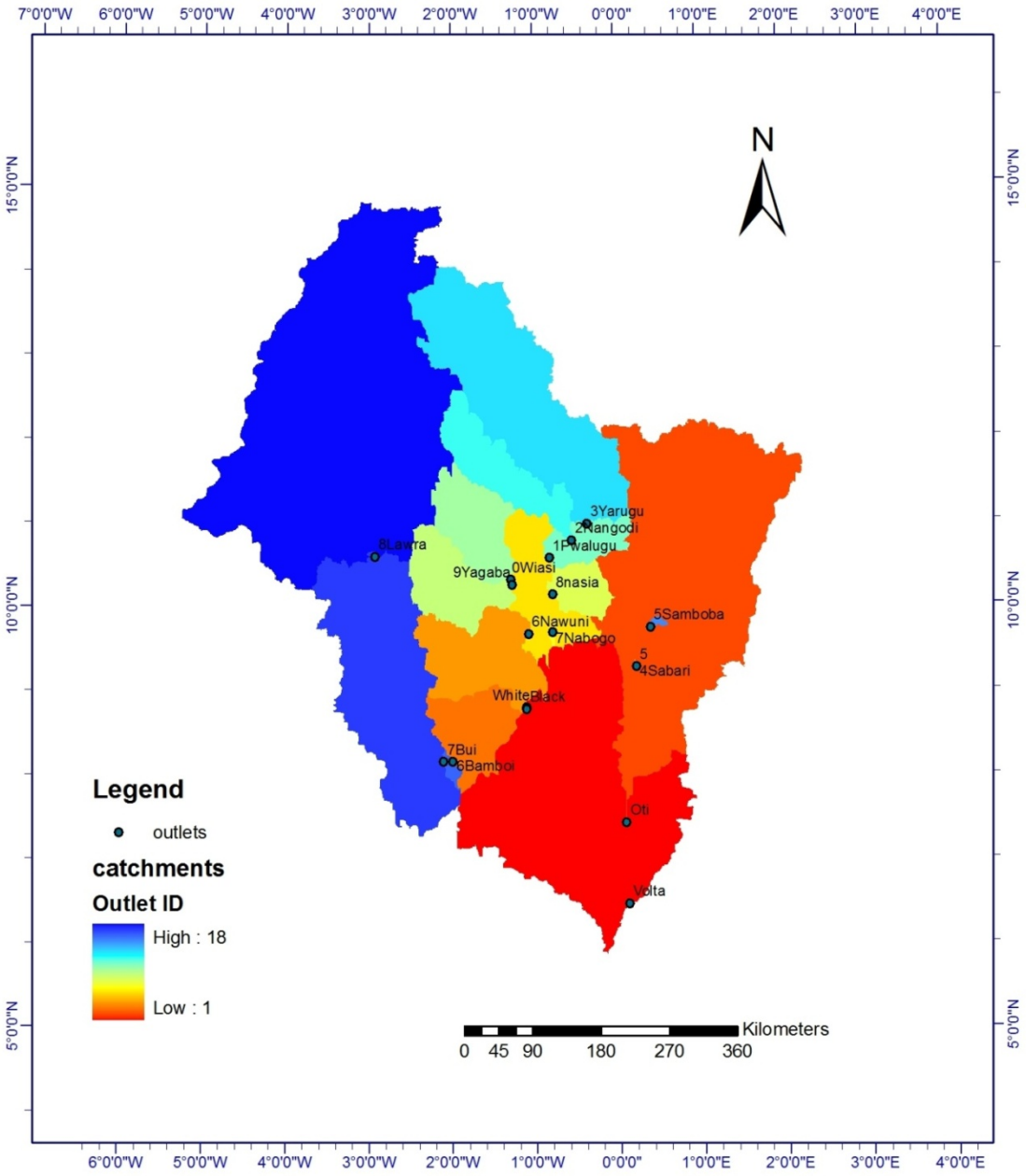

Figure 5.4: Discharge gauges within the Volta Basin

5.5 Calibration of WaSiM-ETH

Calibrating WaSiM for the Volta Basin requires adequate information in input parameters, especially climatic and hydrological (Table 5.1). This is essential for the Volta Basin according to Jung (2006), because this region lacks the necessary infrastructure, thus making this step the most important in the process of building up an efficient and reliable model. A short history of the basin and reports such as Jung (2006) and Wagner (2008) reveal that the natural flow regimes within the basin have been altered since the early 1970s due to the construction of dams and irrigation systems. Hence the periods before the 1970 were most suitable for the calibration. However, considering the availability of reliable data, the period 1968-1971 was selected as the calibration period. The selected period has meteorological and hydrological observation time series data with fewer gaps compared to other periods for the selected catchments. A rough sensitivity analysis showed that the drainage density *dr* (an empirical scaling parameter) responsible for linearly controlling the strength of interflow, and the calibration of the recession constant K_{rec}, the factor that controls the reduction of the saturated hydraulic conductivity with depth, were the main drivers in the water balance. The initialization condition of the groundwater level in a soil profile was set on default, setting the initial level at 40 % of the assigned profile column.

5.6 Main calibration parameters

WaSiM was calibrated for selected watersheds within the basin that had observed stream data available for the calibration periods and thereafter applied to other parts of the basin for various simulations (Table 5.2).

Table 5.1 summary of the most important parameters used in the running of the WaSiM model[4]

Input	ID	Parameter	Source
Meteorological			
Precipitation	Prec	Precipitation interpolation	Gauged
Temperature	Temp	Temperature Interpolation	Gauged
Sunshine Hours	Sun	Global radiation calculation	Gauged
Soil model	K_D	Storage coefficient for runoff	Calibrated
	K*I*	Storage coefficient for interflow	Calibrated
	d_r	Drainage density for interflow	Calibrated
Groundwater model	K_{sat}	Saturated hydraulic conductivity	Literature
Soil table	Θ_{sat}	Saturated soil moisture content	Literature
	Θ_{wp}	Wilting point of soil moisture content	Literature
	K_{sat}	Saturated hydraulic conductivity	Literature
	α	Van Genuchten parameter	Literature
	n	Van Genuchten parameter	Literature
	K_{rec}	Recessing constant for K_{sat} for depth z	Calibrated
	Cm_{sB}	Porosity to be filled	Literature
Land-use table	ρ	Root density	Literature
	α	Albedo	Literature
	zw	Root depth	Literature
	v	Degree of vegetation coverage	Literature
	LAI	Leaf area index	Literature
	rsc	Monthly minimum surface resistance	Literature
	φg	Minimum suction for total evaporation	Literature

Table 5.2: Main calibration parameters of WaSiM

ID	**Units**	**Description**
K_D	[h]	Recession constant for direct runoff
K_I	[h]	Recession constant for interflow
d_r	[m-1]	Drainage density
K_{rec}	[-]	Recession constant for saturated hydraulic conductivity with depth

[4] Parameter values are in the model control file, literature values and sources are available in APPENDIX II, the WaSiM manual

5.7 Calibration results

Calibrating WaSiM for the Volta Basin required credible meteorological and hydrological inputs. As already indicated, the basin is poorly gauged, which led to some bottlenecks in the calibration process. This is further complicated by uncertainties of the obtained data from national archives. Due to poor data quality and availability, manual model calibration was preferred and performed. In the evaluation of the model performance, an ensemble criterion of Pearson's statistics, Nash–Sutcliffe efficiency index (1970), Willmott's index of agreement (1981) were evaluated from the simulated discharge values and the available observed runoff for selected time periods.

The calibration results (Figure 5.5 through to Figure 5.10) for the Pwalugu and Bui gauging stations for daily, weekly and monthly time steps for the period January 1, 1968 to December 31, 1971 reveal that the simulated and observed hydrographs are similar with fairly good statistics (Table 5.3 and Table 5.4). Calibrations were done for total discharge as a composition of surface runoff, base flow and lateral flow estimated at the routed gauged stations to obtain the lowest mass balance error possible within a realistic water balance given the basin's properties. While the calibration process for discharge was done at daily, weekly and monthly scales, the validation was carried out for aggregated monthly scales due to data gaps within the gauged discharge data sets.

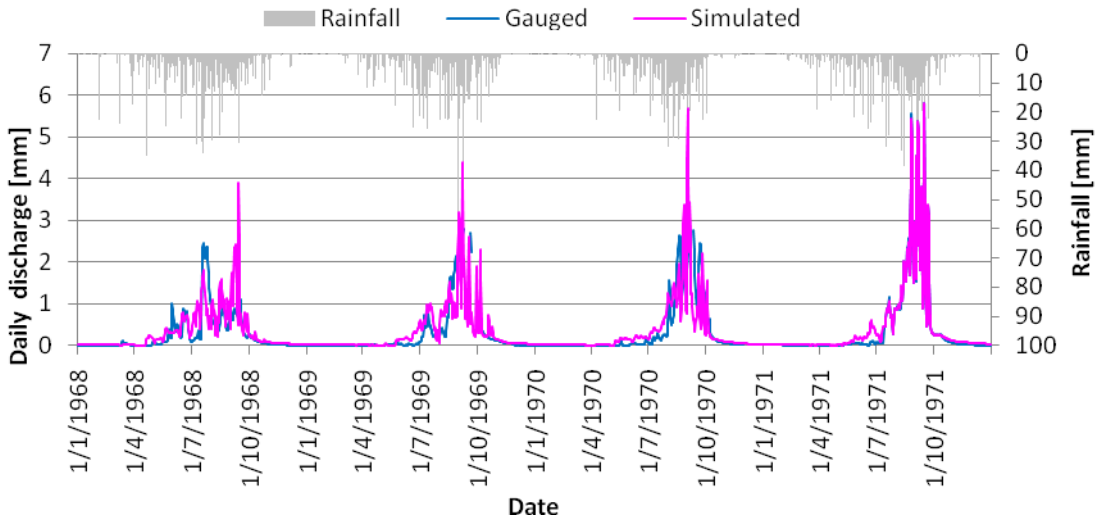

Figure 5.5: Calibration results for Pwalugu catchment of the Volta Basin (56,760 km2); daily gauged discharge plotted against daily rainfall for January 1968-December 1971

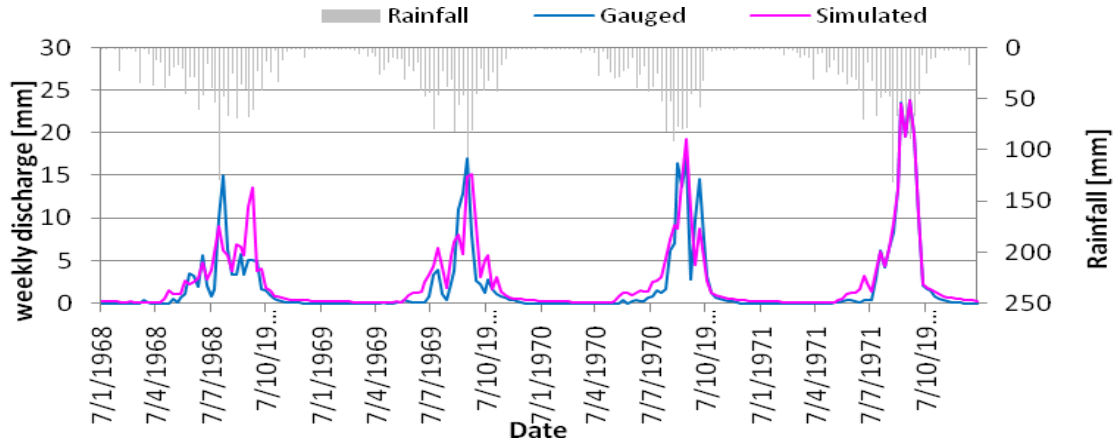

Figure 5.6: Calibration results for Pwalugu catchment of the Volta Basin (56,760 km^2); weekly gauged discharge plotted against total weekly rainfall for January 1968- December 1971

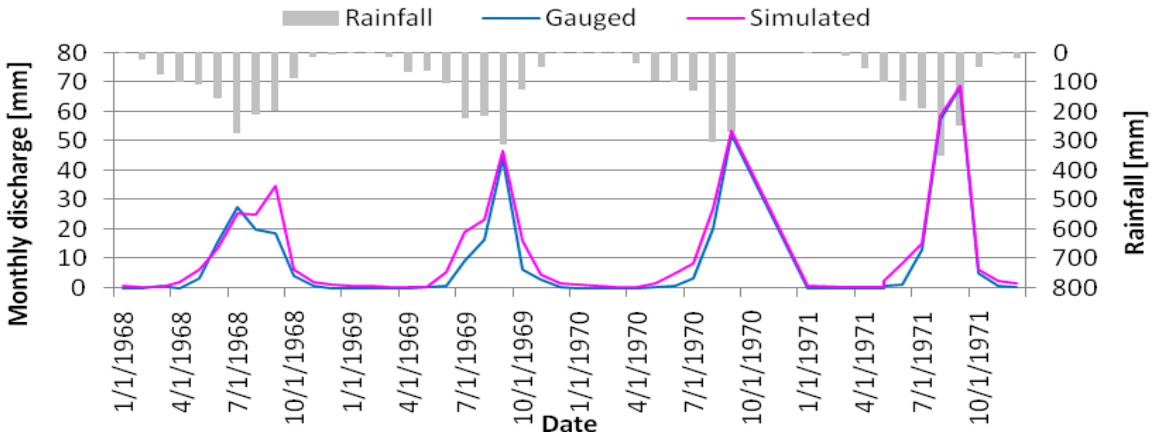

Figure 5.7: Calibration results for Pwalugu catchment of the Volta Basin (56,760 km^2); monthly gauged discharge plotted against total monthly rainfall for January 1968- December 1971

Table 5.3: Summary of model performance for the Pwalugu (north) catchment of the Volta Basin (56,760km^2) for daily, weekly and monthly gauged discharge against simulated discharge by WaSiM-ETH for the calibration period 1968-1971

	Criteria				
	Coefficient of correlation	r ²	Model efficiency	Index of agreement	Mass balance error [%]
Daily	0.87	0.75	0.74	0.93	-14
Weekly	0.92	0.84	0.83	0.96	
Monthly	0.98	0.96	0.94	0.99	

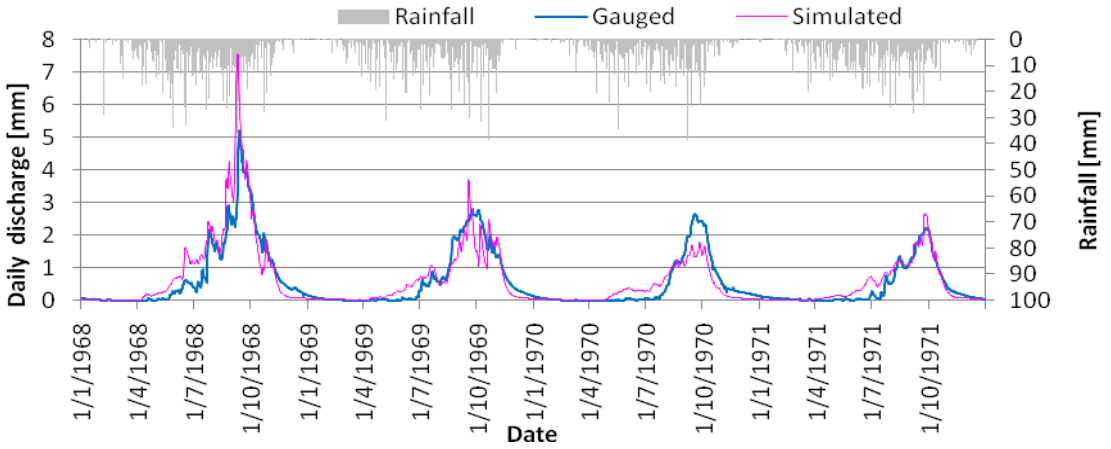

Figure 5.8: Calibration results for Bui catchment of the Volta Basin (99,360 km^2); daily gauged discharge plotted against daily rainfall for January 1968- December 1971

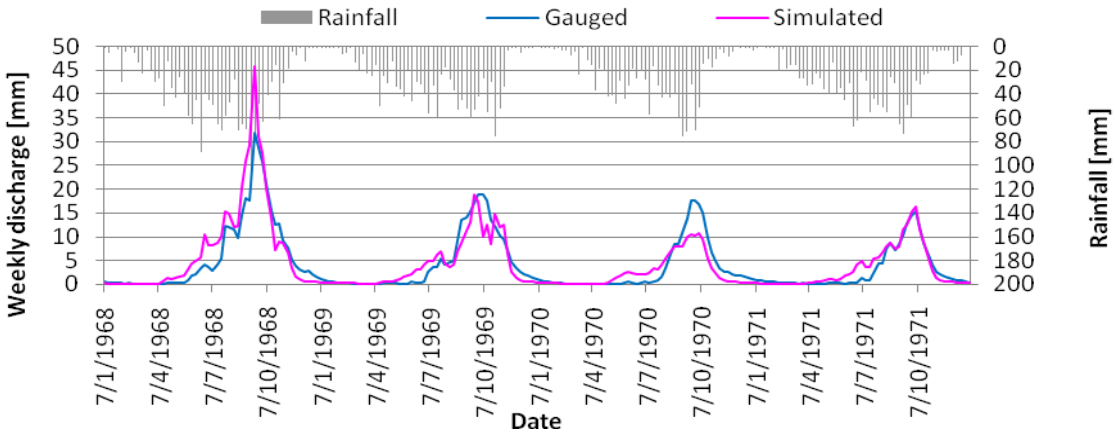

Figure 5.9: Calibration results for Bui catchment of the Volta Basin (99,360 km^2); weekly gauged discharge plotted against total weekly rainfall for January 1968- December 1971

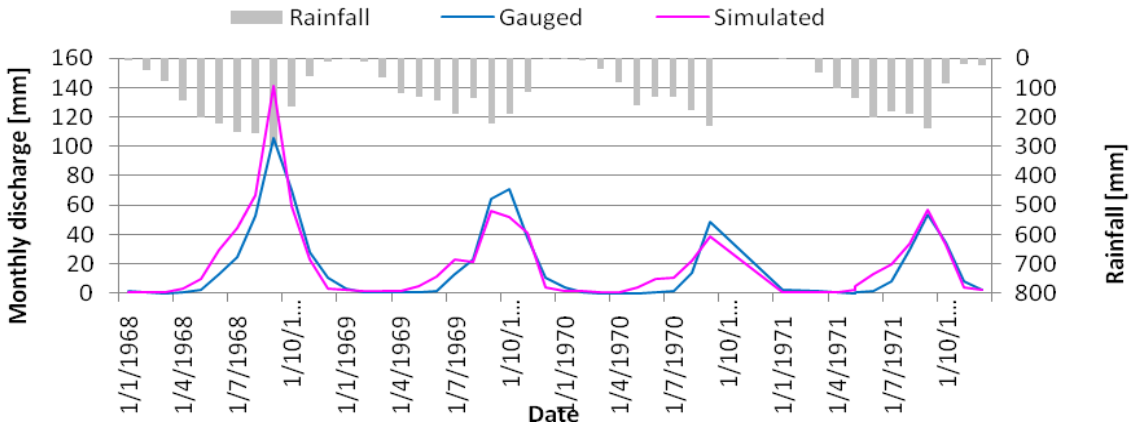

Figure 5.10: Calibration results for Bui catchment of the Volta Basin (99,360 km^2); weekly gauged discharge plotted against total weekly rainfall for January 1968- December 1971

Table 5.4: Summary of model performance for the Bui (South) catchment of the Volta Basin (99,360km^2) for daily, weekly and monthly gauged discharge against simulated discharge by WaSiM-ETH for the calibration period 1968-1971

	Criteria				
	Coefficient of correlation	r ²	Model efficiency	Index of agreement	Mass balance error [%]
Daily	0.90	0.81	0.78	0.95	-7
Weekly	0.92	0.84	0.82	0.96	
Monthly	0.94	0.89	0.86	0.97	

Table 5.5: Summary of simulated water balance for the Pwalugu (north) catchment (56,760km^2) and Bui (south) catchment of the Volta Basin (99,360km^2) for the calibration period 1968-1971

Catchment	Pwalugu (north)			Bui (South)		
Balance term	simulated [mm]	part of precn[5] (%)	average per year [mm]	simulated [mm]	part of precn (%)	average per year [mm]
Rainfall	4827	100	1207	5631	100	1408
Total discharge	525	11	131	909	16	227
Surface flow	106	2	26	274	5	69
Inter flow	358	7	89	545	10	136
Base flow	62	1	16	91	2	23
Potential evapotranspiration	11184	232	2796	10844	193	2711
Actual evapotranspiration	4081	85	1020	4585	81	1146
Balance change	221	5	55	137	2	34
Soil water content change	-224	-5	-56	-139	-3	-35
Balance error	-3	-0.1	-0.8	-3	-0.1	-0.7

[5] Precn = per centage

Results from the calibration show good agreements between simulated and observed discharge for all time steps (Figure 5.5 to 5.10), with coefficient of correlation (r) greater than 0.80 in both catchments, and r^2 of 0.75 for the smaller Pwalugu and 0.81 for the larger Bui catchment on the daily time steps. The Nash-Sutcliffe model efficiency (*Ef*) is higher than 0.7 for all time steps in both catchments. The indices of agreement for both catchments are above 90 %, with a 99 % agreement of monthly simulation to gauge for the Pwalugu catchment and 97 % agreement for the Bui.

For the calibration period, the model slightly overestimated against the gauged discharge with a mass balance of 14 % for the Pwalugu catchment and 7 % for the Bui.

5.8 Model performance

Based on the criteria mentioned in Chapter 4; with the goal of minimizing the mass balance error as much as possible, the outputs showed that the hydrograph reproduced by the model simulation in comparison to the observed runoff component of the water balance was satisfactory, although some discrepancies are observed between the peaks of the observed and simulated hydrographs. The overall difference was small. The discrepancies may be the result from the poor density of gauged stations within the watershed which led to an inadequately provision of inputs for the model simulations. The model performed slightly better for the smaller Pwalugu catchment (0.99), compared to the bigger Bui catchment (0.97) on a monthly scale.

The coefficient of correlation and index of agreement for both stations were fairly high indicating the mimicking ability of the model for the catchment. The mass balance error was noted to be higher for Pwalugu compared to Bui, but it still fell within satisfactory ranges. This was due to many more missing discharge data for the Pwalugu station compared to Bui, which had fewer missing data for the period.

In comparing sets of data such as observed and simulated values, many authors, for e.g., van Belle (2008), Aspden (2005), Bland and Altman (1995,1986) and Altman and Bland (1983) have cautioned the use of correlation or regression to assess the agreement between two methods when scale and location matter. If the two methods X and Y are estimating the same quantity from which the true value remains unknown According to Westgard and Hunt (1973) (cited in Altman and Bland, 1983), the correlation coefficient obtained from any such correlation or regression is of no

practical use in the statistical analysis of comparison in the estimated data. A plot of the difference against the mean of each data point is hence desirable. The model performs better in simulating low flows high or peak flows. The scatter plots are spread close and along the horizontal axis, especially with lower values of the x-axis, and do not show any pattern (Figures 5.11). It is important to note that calibrating simulated discharge against measured runoff of very low and peak flows (floods) is not ideal, as uncertainties are higher during these periods of the flow regimes. Appropriately, calibration is better during the middle part of the flow series when normal flow usually occurs. The performance of simulating low flows for the smaller Pwalugu site is much better than for the bigger Bui site. For this study, this output is satisfactory because reliable simulation of low flows, which are useful indicators of drought, is essential.

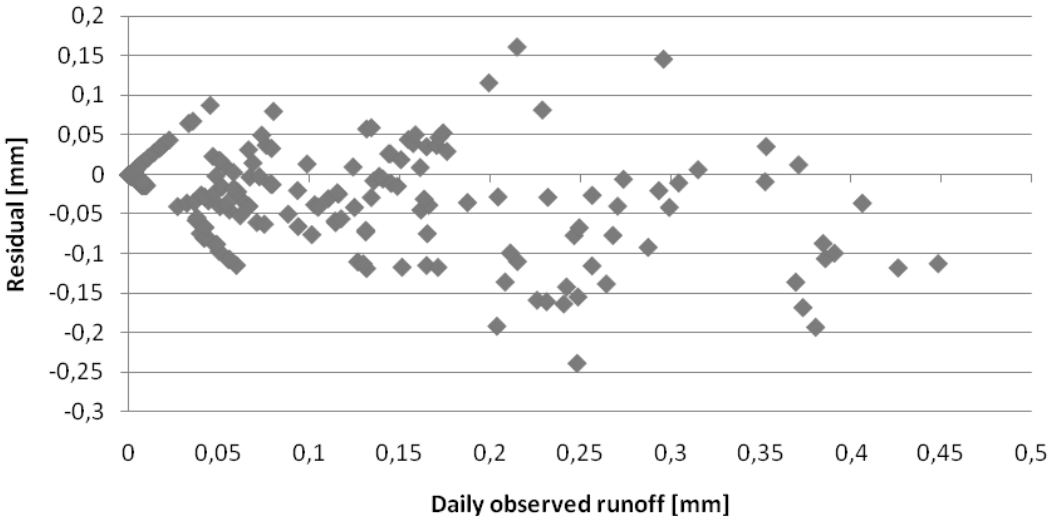

Figure 5.11: Residual vs. computed discharge for Pwalugu (56,760km^2) catchment (residual shows no trends and homoscedasticity for the period 1970-1973).

Assessing the water balance as simulated by the calibrated model showed good estimation of the real evapotranspiration of between 1,020 and1,148 mm per annum, i.e., between 81-85 % of total rainfall,most literature gives an estimate gradient of 789-1,490 mm for the basin. It must be noted that evapotranspiration is calculated by using the Penman-Monteith equation that is sensitive to temperature, relative humidity, and radiation. For this study, original average daily temperature values for some days were unusually low, and had to be corrected to simulate evapotranspiration correctly.

Over all, between 10-16 % of the total precipitation accounts for discharge, which consist of 2-5 % runoff, 7-10 % lateral flow, and 1-1.5 % base flow. The performance of WaSiM Volta in simulating dry and wet years is thus found to be satisfactory.

5.9 Validation results

The calibrated WaSiM-Volta was validated by using the method described in Chapter 4, with all input parameters from the calibration remaining unchanged. The model was validated for the period 1997-2001.

The goodness-of-fit statistics for the simulated and observed monthly discharge (Figure 5.12 and 5.13) give the coefficient of correlation, (r^2), model efficiency and index of agreement to be all above 0.75. The balance errors may be due to gaps in the archived observed data; for this reason an aggregation into monthly values was necessary.

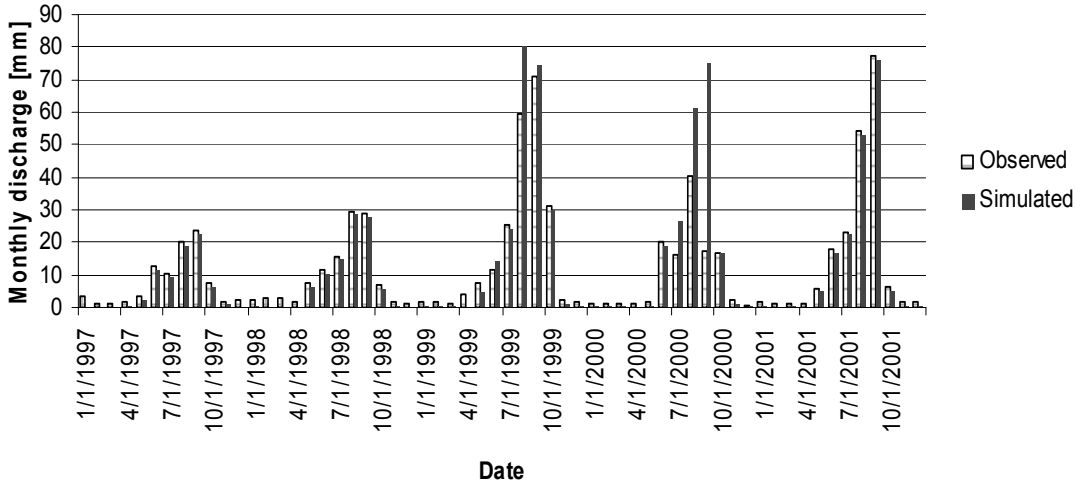

Figure 5.12: Validation results for Pwalugu (56760 km^2) monthly gauged for January 1997- December 2001

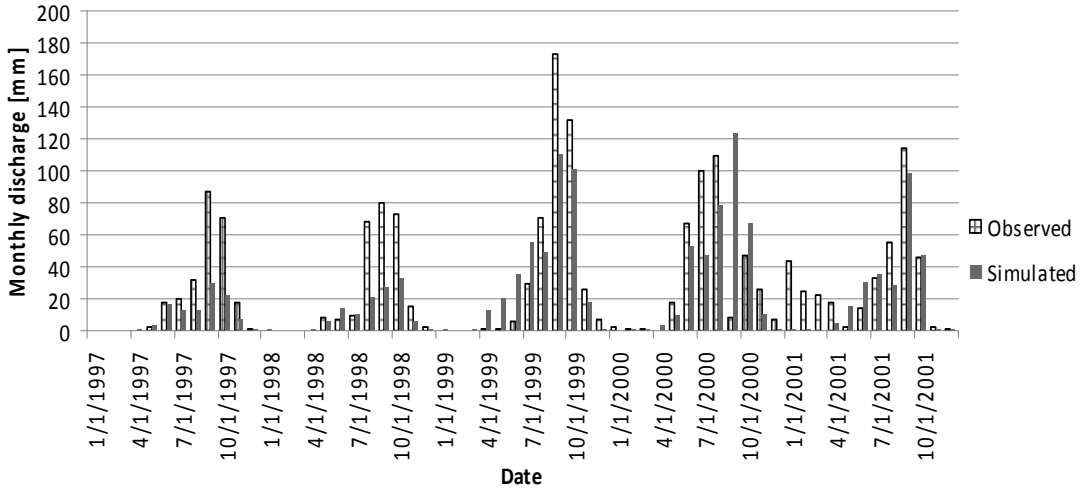

Figure 5.13: Validation results for Bui (99360 km^2) monthly gauged for January 1997-December 2001

Table 5.6: Summary of performance of the WaSiM model for the Calibration period January 1997-2001 for Pwalugu and Bui catchments of the Volta Basin

	Criteria				
Catchment	Coefficient of correlation	r ²	Model efficiency	Index of agreement	Mass balance error [%]
Pwalugu	0.92	0.85	0.75	0.95	-7
Bui	0.74	0.55	0.52	0.83	25

Table 5.7: Summary of simulated water balance for the Pwalugu (north) catchment (56,760km^2) of the Volta Basin for the validation period 1994-2001

Balance term	**Simulated [mm]**	**Percentage of precipitation (%)**	**Average per year [mm]**
Precipitation	8357	100	1045
Discharge	887	11	111
Potential evaporation	18179	218	2272
actual evaporation	6216	74	777
Soil water content change	-221	-3	-28
Balance error	-2	-0.02	0

The underestimation of the peak flows could be due to contributing lateral flows from neighboring networks that may not have been captured by the drainage density in the calibration of the model.

Results from the calibration and validation of WaSiM for the Volta show a very good performance in simulating the daily, weekly and monthly discharge for the calibration and validation periods of the selected routed stations. Therefore, the

hydrological parameters adopted for the catchments and hence for the basin adequately represent those of the basin and hence can mimic the hydrology of the Volta Basin for further analysis.

5.10 Water Balance

Comparison of wet (1931–1969) and dry (1970– 1995) periods of the Volta Basin, shows that on the whole, the ratio between direct runoff and base flow is 54 % to 46 %, with a maximum during the wet years at 66 % and a sharp decline to 6 % in dry years . According to Friesen et al. (2005), the decline of base flow is even more extreme when short dry spells of 2-4 years of constantly low rain occur. These findings conformed to results in the calibration and validation periods of this study (Table 5.6).

Table 5.8 Annual mean values of the water balance of the Pwalugu catchment of the Volta Basin of calibration (1967-1973) and validation (1994-2001)

Balance term	1967-1973 average per year	CV	1994-2001 average per year	CV	Literature range
Precipitation	1131	0.02	1045	0.09	910-1400[a-g]
Total discharge	184	0.93	111	0.73	8-22%[a-g]
Lateral flow	127		31		1-6%[f]
Surface runoff	39		73*		
Base flow	19		7*		3-5%*
Potential Evapotranspiration	1759	0.03	2272	0.25	1340-2275[b,e]
Actual Evapotranspiration	761	0.33	777	0.32	789-1490[b,e]
Soil water Content change	-17		-28		

* *Usually combined as reported as base flow or lateral flow.*

(a): Acheampong (1996); (b)Andreini et al. (2000); (c) Shahin (2002); (d): Martin (2005); (e): Friesen et al. (2005); (f): Darko and Krasn, (g) Obuobie, 2008

During the latter years of validation, evapotranspiration was 5 % higher (73 %) than in the calibration period . The annual discharge for the calibration period was estimated at 16 % of the annual precipitation against the 11 % during the validation period.

Base flow and lateral flow constituted 5 % during the calibration period and 3 % for the validation periods. The dynamics as simulated by WaSiM Volta are coherent with the general trend in most parts of the Volta Basin. As already stated in this study, over 80 % of the basin show a mono modal rainfall pattern, with a 6 to 7 months rainy season (Figure 5.14) starting in April-May and peaking in August.

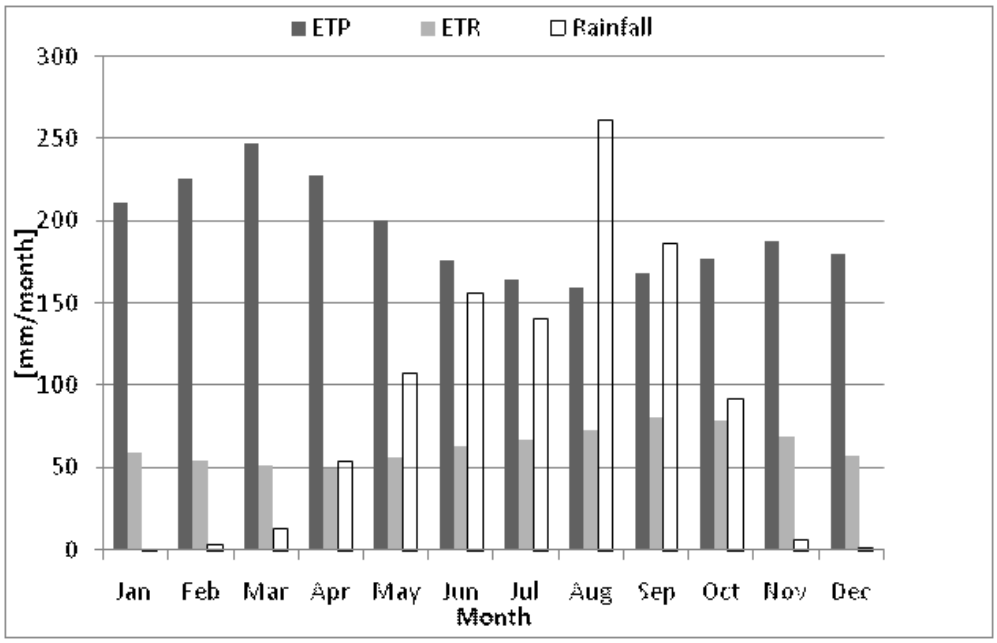

Figure 5.14: Dynamics of mean rainfall, potential evapotranspiration (ETP) and real evapotranspiration (ETR) in the Pwalugu catchment from WaSiM ETH (1994-2001)

The spatial dynamics and distribution of the period 1961-1970 was simulated for the Volta Basin using the calibrated and validated WaSiM Volta model (Figure 5.15). Maximum discharge was simulated for most of the southern parts of the basin correspondinging to the maximum rainfall within that area, with a large gradient. Daily mean evaporation is also high in the south compared to the dryer north driven by the higher availability of moisture in the south compared to the north. The soil water content is relatively lower in the north; this trend could be due to many factors such as rainfall and potential evapotranspiration, vegetation cover, soil properties, etc. The general gradient in the temporal and spatial distribution of the basin strongly influenced by the spatial distribution of rainfall, discharge and evapotranspiration, which vary widely between the north and south of the basin. Such a gradient however, is not visible between the east and west of the basin.

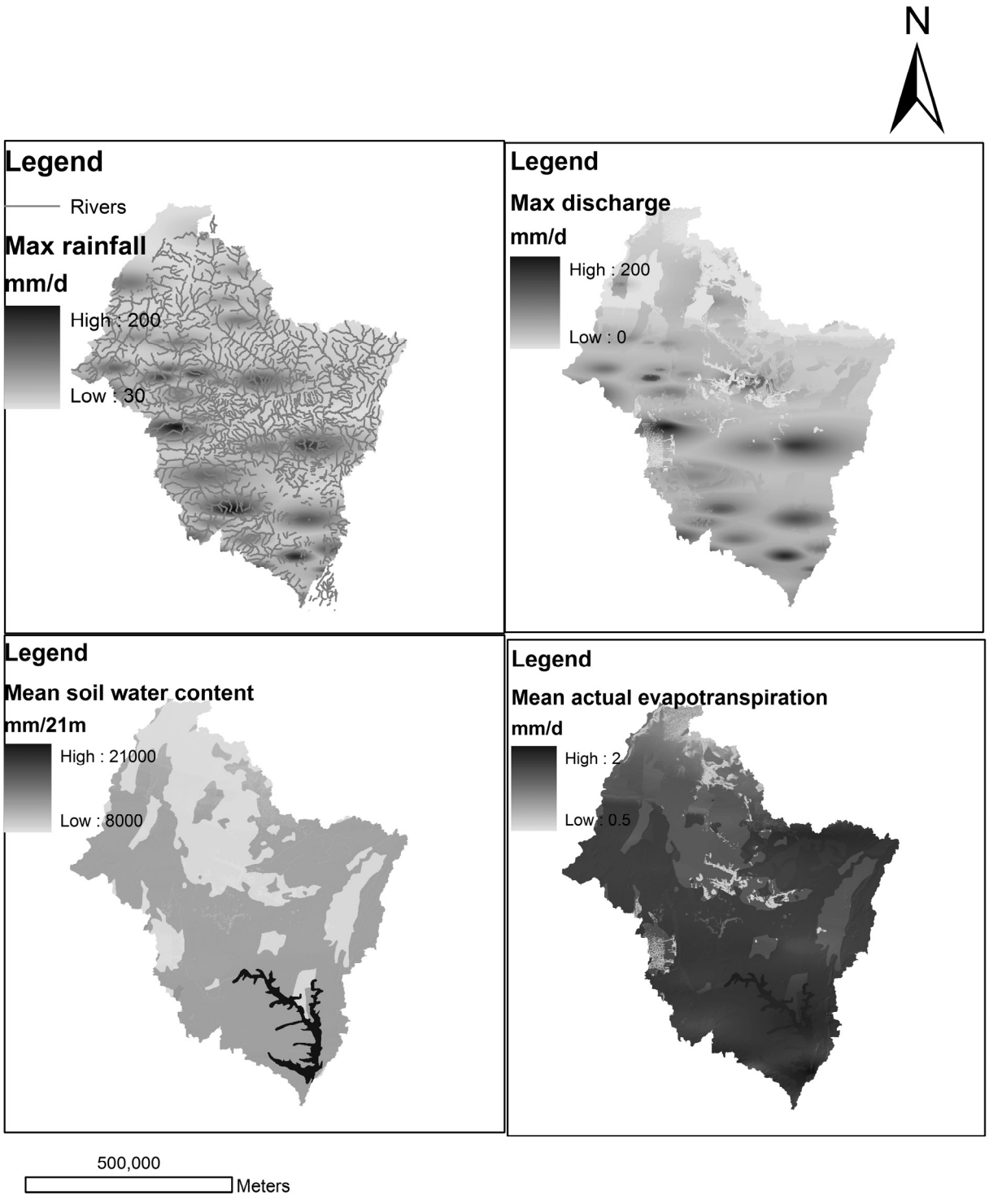

Figure 5.15: WaSiM Volta-simulated dynamics of the Volta Basin for the period 1961-1970.

6 DROUGHT IN THE VOLTA BASIN

6.1 Introduction

In most parts of West Africa, farmers practice shifting cultivation and traditional bush fallow systems under a unimodal or bimodal rainfed agriculture. High variability of rainfall patterns and distribution is the main factor causing fluctuations in food production in the Volta Basin especially the northern parts. The annual rainfall, which falls within one rainy season, is erratic both in onset and distribution; the rainy seasons are characterized by dry spells of varying duration (Kasei, 1995).

Various recent reports on the climate of the sub-region have suggested that there has been a recovery of the rainy season (Nicholson, 2005). The Intergovernmental Panel on Climate Change (IPCC) predicts that hot extremes, heat waves, and heavy precipitation are becoming more frequent in some regions in the world, and that subtropical regions are likely to receive less rainfall due to climate change (IPCC, 2007). Meteorological and hydrological data from the Volta Basin show a decline in rainfall amounts and duration of the length of the rainy season. The frequency of rainfall deficiency has increased since the early 1970s, and moderate to severe drought years have occurred at approximately 9-year intervals with a reoccurrence of severe droughts. Notable years of drought extending to 50 % of the basin area or more are 1961, 1970, 1983, 1992 and 2001.

In the early 1970s and mid 1980s, countries in the West African Sahel suffered from a series of drought years, which had devastating consequences for the inhabitants of the entire Volta Basin. Average rainfall for the 1982–1985 period was only 381 mm, less than nearly 60 % of the long-term average (Dugue, 1989).

The years of recurrent drought, high variability in the monsoon rains and variations in the start and end of the rains as well as their intensities greatly affected crop production, provoking structural food shortages and hunger. In the early 1980s, 14 out of 18 households studied by Broekhuyse (1983) in the village of Oualaga (Sanmatenga province, Burkina Faso) had a food deficit of more than 50 %. In Ghana, food production was below normal in the drought year of 1983 (PPMED 1987). In Senegal, rice yields decreased rapidly when rainfall was less than average over a 10-

year period (Elston, 1983). In the north of Ghana, inter-annual variation of rainfall is between 5 % and 45 % in areas across the zone (Kasei 1988).

6.2 Regional climate trends and global climate change

The mean climate of 1951-1980 showed a warmer period compared to the decades before this period, thus confirming the assumption that global surfaces temperatures have risen throughout the last century. The highest temperatures of this century have occurred within the last 10 years affecting the middle and higher latitudes. In poorly observed regions of Africa, the limited data also show warming temperatures throughout the 20th century. The Sahelian zone has recorded several decades of below normal rainfall, especially from the late 1960s to the 1990s, which consequently had a significant impact on economic development.

According to Henkins et al. (2002), scientists agree on anomalies in the decadal rainfall but differ on the causes. Some scientists are of the opinion that local processes (e.g., massive deforestation, desertification, etc.,) are to blame for the drying pattern observed within West Africa, while others hold external factors (e.g., Sea Surface Temperatures (SSTs) and global anthropogenic change) responsible.

Atlantic Multidecadal Oscillation (AMO) has recently been linked to the anomalies in the western and southern parts of Africa. However, a number of regional models suggest that there is a stronger link between the warming of the Indian Ocean SSTs to the drying of the Sahelian zone. A link is thereby suggested between the El Nino Southern Oscillation (ENSO) and climate change, which is thought to influence the intensity, duration and return periods of the AMO and the West African climate (Henkins et al. 2005). In general, ENSO is a disruption of the ocean-atmosphere system in the tropical Pacific and has an important impact on global weather, and is also known to cause SST anomalies in the tropical Pacific.

The IPCC reports that different climate models yield different trends and patterns of the West African climate (IPCC, 2001). Determining the character of the West African rainfall against a background of large natural variability supported by the use of imperfect climate models has become the major problem. However, most models agree that the African continent will experience a temperature increase of 1-3°C throughout the 21st century with some parts recording higher increases. In the face of

increasing temperatures, a further reduction in soil moisture as a result of increased evapotranspiration is expected (IPCC, 2001).

6.3 Drought in the Volta basin

The Volta Basin is regarded as one of the poorest regions in Africa, with over 80 % of the total surface area located in Burkina Faso and Ghana. Rainfed and irrigated agriculture are the principal basis of development for most of the people living in the basin. The growing population (3 % per annum) is increasing the pressure on land and water resources. Within the last decade, Burkina Faso (upstream) has improved its agricultural sector by developing more irrigation farms that depend largely on the availability of surface water resources. Ghana (downstream) on the other hand is suffering from the impact of the enhanced use of the water resources upstream by Burkina Faso, particularly at the Akosombo dam on which Ghana draws for over 80 % of its energy supply. Low flows resulting in low water levels behind the dam from 1998 and especially in the last 5years have led to a major energy crisis in Ghana in the last decades, often blamed on the recent development in Burkina Faso. Some also argue that the recent low flows recorded downstream may have been caused by unreliable rainfall variations and the poor understanding of these variations (Green Cross International, 2001).

The unreliable rainfall situation creates difficulties in meeting food production targets, and requires that more attention is paid to agricultural programmes to ensure food security. Nearly 90 % of the area is under rainfed farming. The onset of the monsoon determines the planting time, and the subsequent temporal distribution of rainfall greatly influences the growth and development of the crop. The sowing time in the north starts in May, and by June the monsoon activity covers the entire country. The length of the growing season in the north depends on the withdrawal of the monsoon rainfall activity sometime in October. Initial studies on drought using the probabilities of dry spell runs showed that the north of the basin as a whole is prone to drought conditions (Kasei et al. 1995). In the middle part of the basin (Tamale), a dry spell of 7 days can be expected to occur once a year in June and once in every four years in September at the peak of the rains (Kasei, 1993). Several trend analyses of precipitation were performed for West Africa. According to Le Barbé and Lebel (1997),

Servant et al. (1998), or Amani (2001) and Oguntunde et al. (2007), an overall tendency towards a decrease in rainfall has been observed since the discontinuity of the 1960s and 70s. The decrease in rainfall lies between 15 and 30 % (Nicholson, 1993) and the 1980s were the driest period of the 20th century in West Africa (Hulme et al. 2001). Thus, developing a method for predicting the probability of less than the minimum amount in rainfall would be useful. Such methods could be used as a basis for comparison of drought hazards during the rainy seasons in different areas. It is well known that consecutive spells of low rainfall, which result in drought conditions, often occur in the same areas. Simpler criteria close to those of Sastry (1976), which use the frequency and probability of the occurrence of a specified number of consecutive dry days based on the evapotranspiration parameter, could be developed for such analyses.

The need to analyze rainfall with regard to probable wet and dry periods in particularly important in areas characterized by high spatial and temporal variability. Oladipo, (1985) showed that when one is interested in meteorological applications, simple indices with rainfall as the only input perform as well as the more complicated drought indices such as those of Palmer (1965) and Bhalme and Mooley (1980).

Drought is a recurrent phenomenon that will continue to affect different parts of the Volta Basin at unexpected intervals. By virtue of its characteristics, manifestation and impacts on the society, drought is a complex natural hazard. Drought detection and monitoring is not an easy exercise for a number of reasons. What constitutes drought? Drought means different things to different people. Regardless of the divergence of views concerning drought definition, the simplest starting point to quantify and qualify drought is to regard it as a relative meteorological phenomenon that is generally nothing but a rainfall deficiency that tends to affect adversely water supplies, crop and livestock production, causing food shortages and disruption of economic activities. Hence, the aim of this part of the study is to characterize meteorological droughts in the Volta Basin to provide a guide for sustainable water resources management.

6.4 Rainfall anomalies in the Volta Basin

Climatic extremes that characterize this region are recurring drought, harmattan (a hot, dry, usually dusty wind that blows from the northeast or east in the southern Sahara,

mainly in winter), and sometimes torrential flooding. Highest precipitation levels occur in the south and can reach an annual 2,000 mm, while levels in the driest regions in the north can be as low as 200 mm annually (see section 2).

Around 80 % of annual rainfall occurs from July to September with most places experiencing monsoonal rains. Mean annual precipitation ranges from less than 300 mm up to more than 1500 mm, showing a strong north-south gradient, with higher rainfall amounts in the tropical south and smaller amounts in the semi-arid north of the basin. In addition, in the south-western corner of Ghana, which is actually not part of the Volta Basin, annual precipitation exceeds 2100 mm, whereas in south-eastern Ghana it is less than 800 mm (Jung 2006). This is a clear indication that not only a north-south gradient (Figure 6.2) exists, but also a quite strong west-east gradient (Figure 6.3) with regard to the transect (Figure 6.1) chosen.

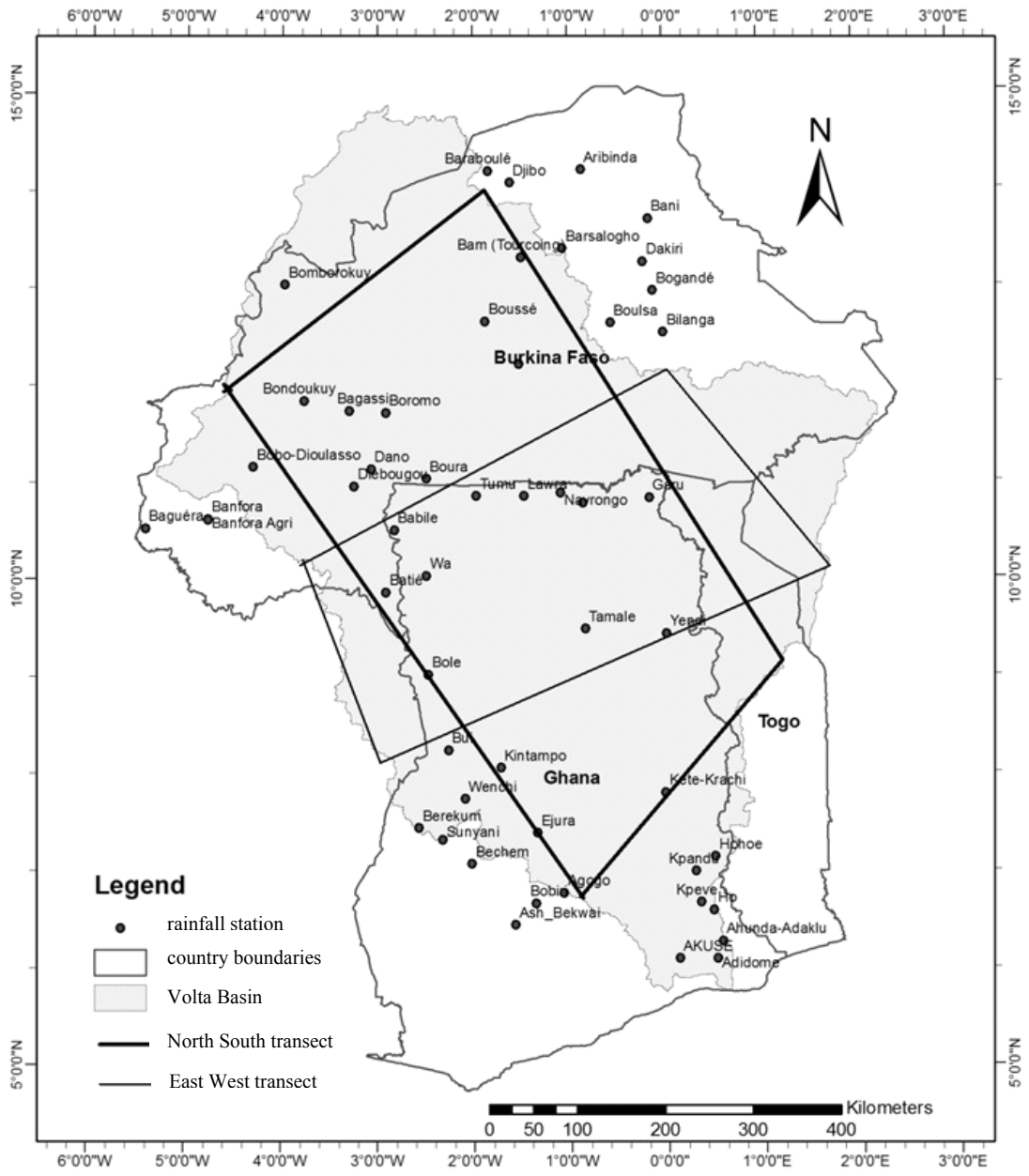

Figure 6.1: Map of West Africa showing the Volta Basin and transects

6.5 Standardized precipitation index (SPI)

The 44-year records of rainfall from 52 stations of the Volta Basin examined for temporal distribution show several prolonged drought periods according to the drought categorization by McKee et al. (1993). The Standardized Precipitation Index (SPI; McKee 1993) is the number of standard deviations that observed cumulative precipitation deviates from the climatological average. The meteorological data were obtained from the national meteorological organizations of Ghana and Burkina Faso.

Hydrological data were collected by the Hydrological Services Department of Ghana and the GLOWA Volta project. As indicated earlier, initial visualization of the data showed a 10-year reoccurrence of drought. Detailed analysis further demonstrates the strong relationship between rainfall in the Sahelian region and the position of the Inter-Tropical Convergence Zone (ITCZ).

The north-south and east-west gradients (Figures 5.2 and 5.3) also reveal that severely dry years occurred on the average at 9-years intervals.

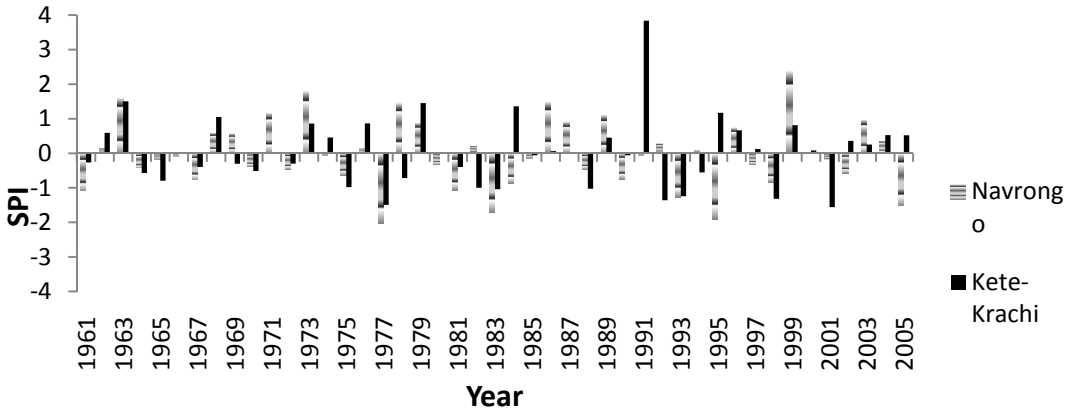

Figure 6.2: Standardized Precipitation Indices (SPI) for the north (Navrongo) - south (Kete-Krachi) gradient

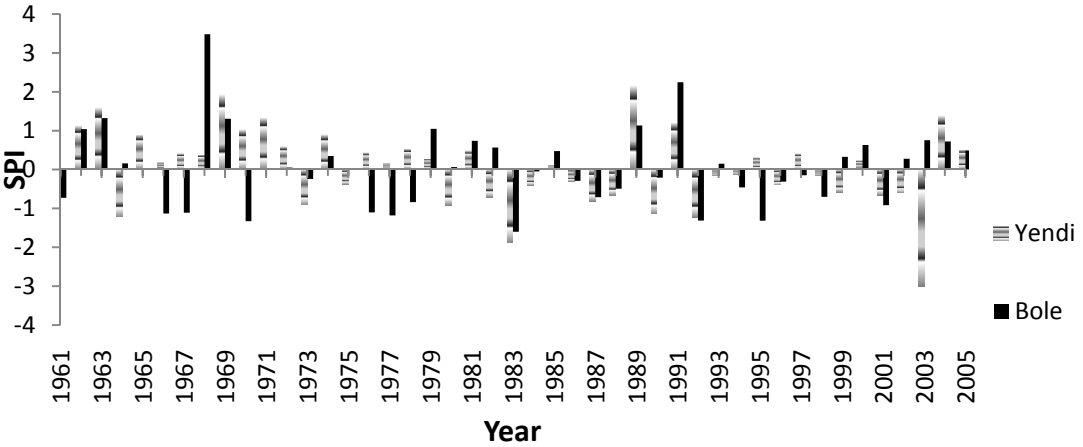

Figure 6.3: Standardized Precipitation Indices (SPI) for the north-west (Bole) – east (Yendi) gradient

Table 6.1: Correlation (Spearman's rho) of different rainfall stations in the Volta Basin For the exact position of the rainfall stations (see Figure 6.1) N = 45

		Navrongo	Tamale	Yendi	Ho	Wa
Tamale	Correlation Coefficient	.360*				
	Sig. (2-tailed)	.015				
Yendi	Correlation Coefficient	.154	.376*			
	Sig. (2-tailed)	.313	.011			
Ho	Correlation Coefficient	.450**	.455**	.344*		
	Sig. (2-tailed)	.002	.002	021		
Wa	Correlation Coefficient	.231	.555**	.306*	.467**	
	Sig. (2-tailed)	.127	000	.041	.001	.

* Correlation is significant at the 0.05 level (2-tailed).
** Correlation is significant at the 0.01 level (2-tailed).

6.6 Rainfall anomalies and impacts

There were years during which widespread below-normal rainfall occurred throughout most of the basin, which supports previous studies linking large-scale tropical circulation features to rainfall in the Sahel (Figure 2 and 3). A positive correlation of the north, south, east and west stations is evident (Table 6.1), where Tamale, Yendi, Wa and Ho are representative of the transect stations. At even 5 % level significance, Spearman's rho shows a strong correlation in the stations that are more than 100 km apart, exhibiting the extent to which an event affects the entire basin. Severe to extreme droughts generally affected most parts of the basin. In the gauged monthly mean volume and the monthly precipitation over the period 1965 to 2001 at the lower end of the basin at Akosombo the impact of the 1980's droughts was highest (figure 6.4)

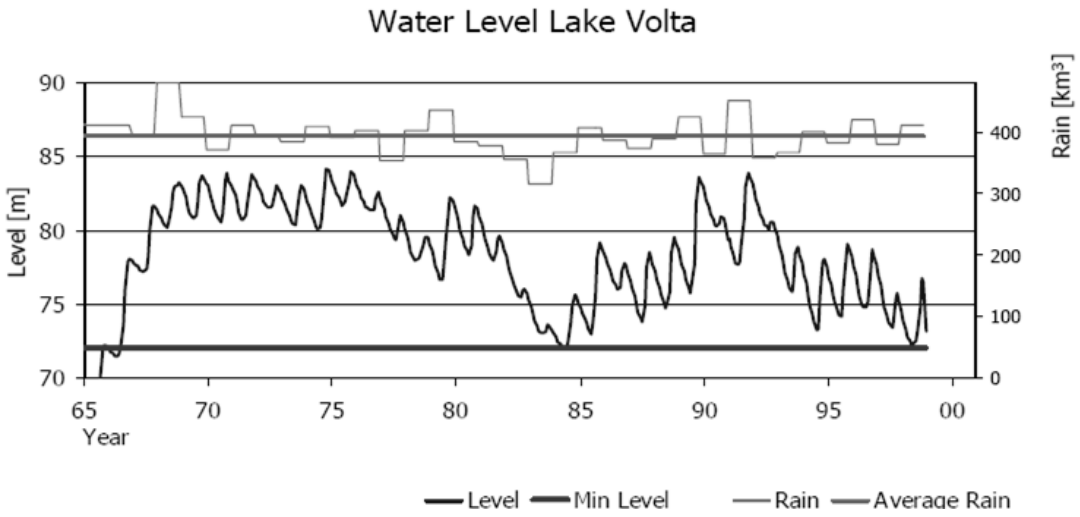

Figure 6.4 Long-term average volume of water in the Akosombo dam used for hydropower between 1965 and 2001 (Data from VRA)

There is a rippling of dry years at the Akosombo dam from the early 1980s when consecutive years of negative SPI were more frequent. It is evident that one year of good rains was not enough to offset years of subsequent droughts in the mid 1990s. The Akosombo dam was built in 1965, creating Lake Volta with an area of 8,502 km^2. The dam's maximum and minimum operating levels are 84.73m and 73.15m, respectively. The maximum annual inflow ever recorded was 3000m^3/s in 1963 and the lowest was 288m^3/s in 1983, which is classified as a severely dry year by the SPI. The volume of water in the dam has not significantly recovered to fill the dam for hydropower generation since the droughts of the early 1980s. The probability of reoccurrences of dry years (Figure 6.11) raises concern on availability of adequate water resources for the needs of the riparian states (Figures 6.5 – 6.8).

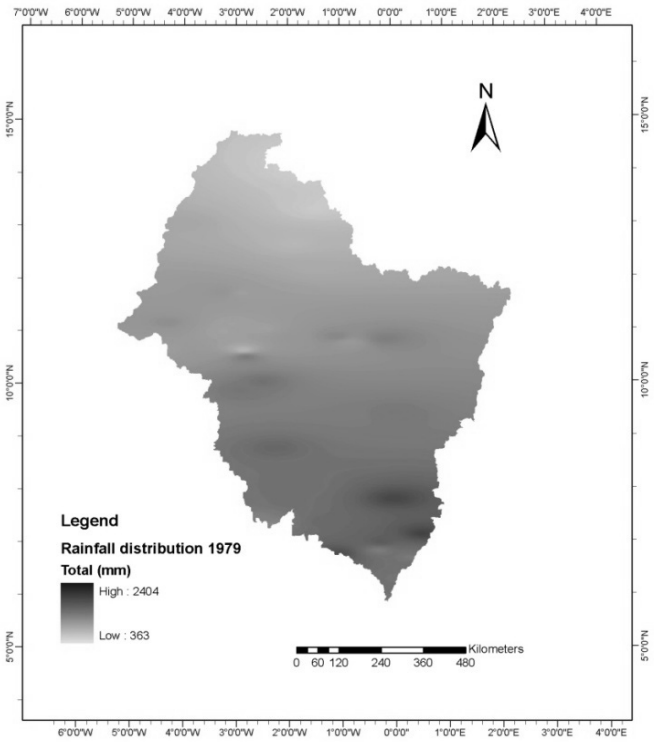

Figure 6.5 Total rainfall distribution (mm) for 1979 as a normal year

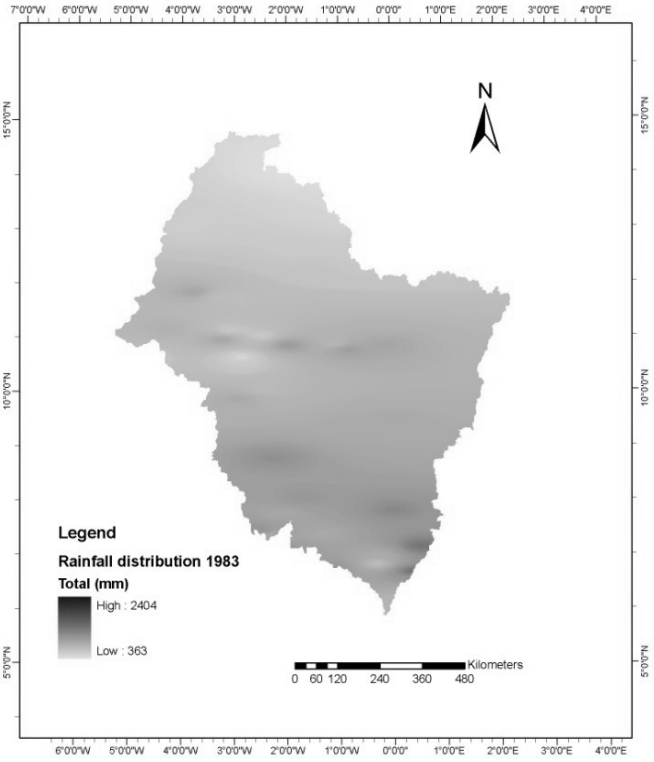

Figure 6.6: Total rainfall distribution for 1983 as a severely dry year

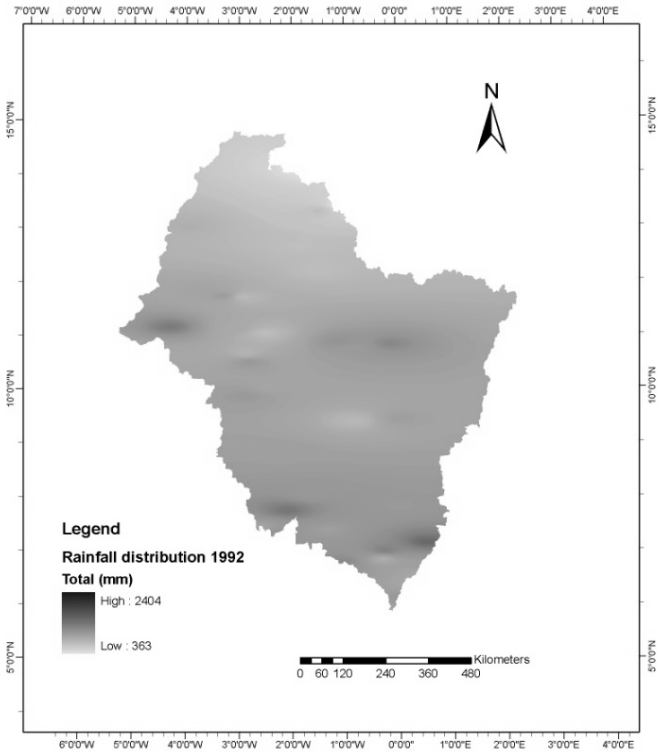

Figure 6.7: Total rainfall distribution for 1992 as a moderately dry year

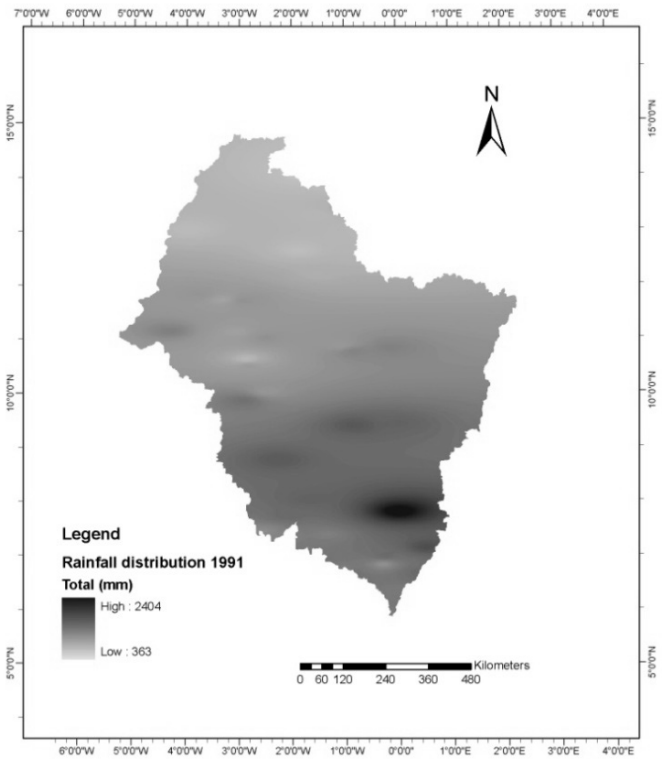

Figure 6.8: Total rainfall distribution for 1991 as a wet year

The selected gauged stations give a good representation of the basin, as a Jarque-Bera test (Jarque and Bera, 1980) based on skewness and excess kurtosis applied to the data could not reject the null hypothesis that the variable [rainfall] is normally distributed at even 10 % level of significance. Most parts of the basin in a wet year record an annual average of 900 mm of rainfall. The driest of all the years was 1983 (Figure 6.6), which saw over 90 % of the basin under extreme drought conditions. This was preceded by a moderate drought in 1982. The spatial distribution of rainfall over the entire basin, for a normal year (Figure 6.5) and moderate to severe drought years (Figures 6.6 and 6.7), gives an overview of basin area affected by some extreme events within the last decades. Over 50 % of the basin experienced rainfall of over 950 mm for 1991 (Figure 6.8), which is regarded at a wet year. When rainfall amounts fail to pick up from May through August (Figure 6.9) compared to the normal years 1989, 1991, and 1997, or, if cumulative rainfall below 800 mm by August is recorded, the year will be dry. Except for the years 1970 and 1989, the length of the rainy season seems not to vary between dry and normal years (Figure 6.10).

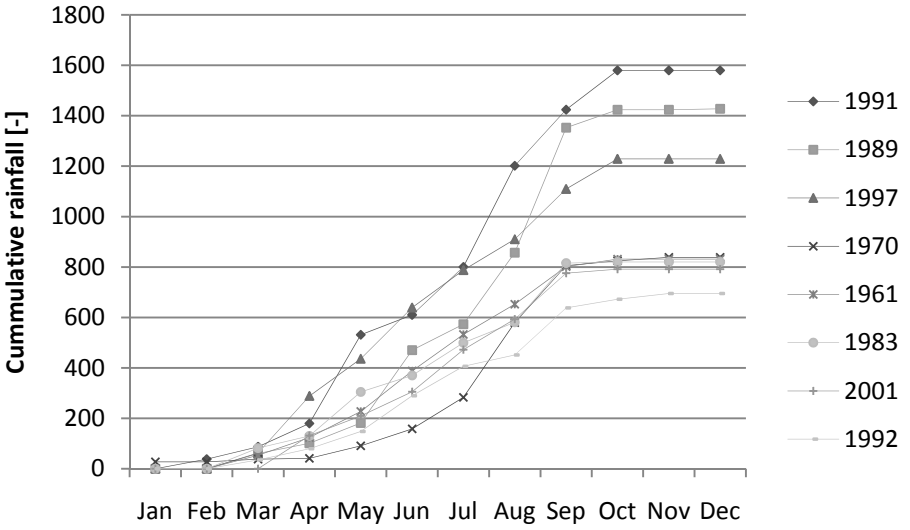

Figure 6.9: Cumulative monthly rainfall distribution of selected dry and wet years in Tamale.

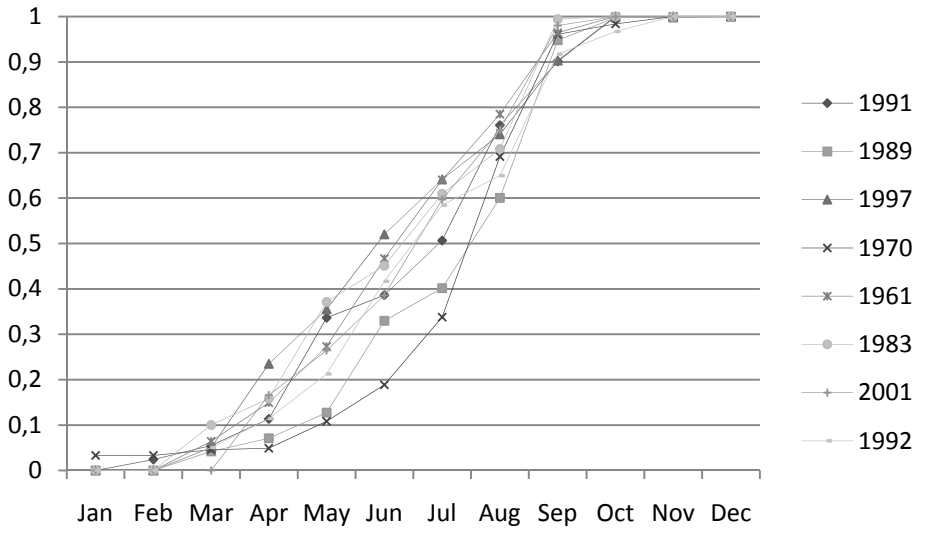

Figure 6.10: Distribution functions of relative rainfall. 1989, 1991, and 1997 are normal years, the others are dry years.

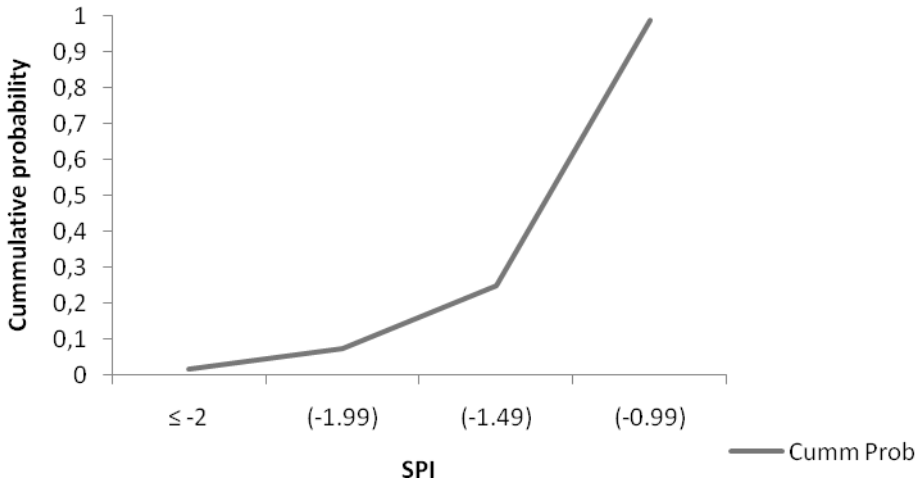

Figure 6.11: Relative drought frequency curve for the Volta Basin for 1961-2005

Typically, the rainy season, defined here as the period in which about 80 % of the rain falls, lasts 5 to 6 months. In 1970 (dry with a total rainfall of 838 mm) and 1989 (wet with a total rainfall of 1427 mm), the length of the rainy period was about 4 months.

Analyzing drought intensity and frequency for the Volta Basin reveals an average return period of 10 years for a moderate drought, which has a probability of 0.06 to 0.18 for the 44-year rainfall record (Figure 6.11). In the 1960s and 1970s, dry

years occurred at an interval of 3-4 years, but from the early 1980s till 2006, dry years occurred almost every other year, indicating an increase in the frequency of dry years in the basin with a probability of 0.7. The drought of 1983/84, which affected the whole region, had a much lower probability compared to other drought events. The drought intensity (Figure 6.2 and 6.3) with SPI lower than -2.0 usually affected nearly 75 % of the region. This would most often show that major parts of the region experience extreme drought conditions during these years. The droughts of 1961 and 1970 had a much higher probability of occurrence (0.7). The areal extent of extreme drought conditions was about 90 % during this drought period. The drought of 2001 seems to have had a relatively high probability of 0.17 compared to that of 1992, which had a probability of 0.06.

Dry years have become more frequent since the beginning of the 1980s and have occurred at shorter intervals. The areal extents of this dryness, though not severe, have been increasing over last 20 years. Between 1983 and 2001, the basin experienced at least 4 moderately dry years covering over 50 % of the area.

7 CHANGES IN HYDROLOGY AND RISKS FOR WATER RESOURCES IN THE VOLTA BASIN

7.1 Introduction

The International Union for Conservation of Nature (IUCN) used in their report "Reducing West Africa's Vulnerability to Climate Impacts on Water Resources, Wetlands and Desertification" in 2004 three main reasons why the changes in climate and hydrology need to be well understood and managed: (1) the significant contribution of rainfed agriculture to the region's economy, (2) the poor level of water control, and (3) the poor replenishment of reservoirs on which some countries depend heavily for the generation of hydropower and the electricity supply to industry and households. In general, the national economies of many West African states are directly affected by the variations in climate.

The climate of West Africa, particularly in the Sahelian zone of which much of the Volta is part, has been undergoing recurrent variations of significant magnitude, particularly since the early 1970's. According to the IUCN (2004), the region has experienced a marked decline in rainfall over the period 1961- 2000 and hydrometric series around 1968-1972, with 1970 as a transitional year. The IUCN also found a decline in average rainfall before and after 1970 ranging from 15 % to over 30 % depending on the area. This situation resulted in a 200-km southward shift in isohyets. Average discharge in the region's major rivers underwent concomitant and highly pronounced to average decline in the range of 40-60 % in discharge since the early 1970s.

Statistically, significant changes have been realized in the last century (Oguntunde et al., 2006). As the hydrological conditions in the Volta Basin have not been very favorable in the last decade, it has become necessary to pay attention to water management strategies, as problems may arise if this situation continues or shifts into more water-stressful conditions as predicted by some climate model ensembles used by IPCC (2007) for the region. If the general agreement that hydrological conditions across the world are changing, then concepts on water management need to fit the changing situations. The growing number of reservoirs in the Volta Basin would need to be improved, and flexible methods of operations are required.

Major sources of water in the Volta River system and riparian countries consist of natural and induced rainfall (from cloud seeding), rivers, streams, lakes, groundwater and artificial impounded water (dams, dug-outs and reservoirs). The estimation of direct discharge to the system is based on the assumption that discharge occurs when rainfall amounts and intensities surpass infiltration rates and subsurface saturation, balanced by actual evapotranspiration. Analyses of rainfall data from various stations within the Volta River system indicate that the months in which precipitation exceeds evapotranspiration are usually June, July, August, and September. The annual recharge for the river system ranges from 13 % to 16 % of the mean annual precipitation.

Throughout the Volta Basin, over the past decades, dams and reservoirs have been constructed to mobilize water for agricultural and hydroelectricity purposes. The number of large and small dams continues to increase as the population grows. Increasing use of water and uncertainty in precipitation in the basin threatens present sustainable programs focused on water management. Several large dams have been constructed (e.g. Akosombo and Bagri) and some are still being constructed (e.g., Bui) in the Volta River system with the primary purpose of generating electricity. The damming of the Volta River at Akosombo lake covering an area of approximately 8,500 km^2 is regarded as one of the largest man-made lakes in the world today . A smaller and shallower impoundment next to the Akosombo is the Kpong Head pond, covering an area of roughly 38 km^2 at Kpong, 20 km downstream of Akosombo. Bui, which is north-west of Akosombo, is under construction and due by 2011. The riparian states of the Volta (e.g., Benin) depend on hydropower from dams built on other tributaries of the Volta, while many more like the Pouya (Natitingou) on the Yéripao are planned. The Fresh water needs of the inhabitants of the basin come from within the basin, and hence a supply shortfall like that in 2002 and 2003 could mean catastrophic consequences for the city water supply, e.g., in Burkina Faso, and severe energy crises in Ghana.

In recent times, there has been immense pressure on Burkina Faso to increase the number of dams in the Volta Basin to meet the country's demand for fresh water. As a result, there are now an estimated 600 dams and 1,400 dugouts with a total storage potential of 4.7 km^3, and about 10,484 wells of which 8,020

are in good condition. The volume stored annually in these reservoirs is about 2.490 km^3, which is about 25 % of total discharge. With respect to hydropower generation, 13 locations have been identified in the country, and 10 are located within the Volta Basin. A total of 125.9 GWh/yr is expected to be generated from these hydro-power stations. A recent survey by Direction de l'inventaire des ressources hydrauliques (DIRH) indicates that several planned irrigation projects covering a total area of 1,045 ha will require about 65.3 million m^3 water *(*IUCN, 2004).

7.2 Climate change

Climate change may have a large impact on water resources, and that could ultimately affect fundamental drivers of the hydrological cycle. The use of hydrological models that depend largely on the outputs of the climate, offer platforms on which climate impacts could be studied. The climate models popularly used to derive or make projections into the future are the General Circulation Model (GCM). The GCM is basically a mathematical model based on the general circulation of the planetary atmosphere and ocean, which integrate the rotations of the sphere. According to Thorpe (2005), GCMs are among the best tools used for forecasting the weather, understanding the climate and projecting changes in climate.

Derived from the atmospheric global circulation models (AGCMs) and the atmosphere-ocean coupled GCMs (AOGCMs) are the HADCM, GFDL, CM2.X, ECHAM, among others, used for the study and simulation of the present climate and for the projections of the future climate. In the simulation of the hydrology of a watershed, credible input parameters of climate are essential for good results. Outputs of GCMs, however, have a spatial resolution of 250 km, offering only very coarse data for the study of small watersheds. According to Sintondji (2005) and Busche et al. (2005), GCMs have flaws for events of heavy rainfall in respect to their exceeding thresholds and frequencies. It is also evident that local or regional climates are influenced not only by the atmospheric processes, but are also greatly influenced by land-sea interaction, land use and the topography, which are poorly presented in GCMs due to their coarse spatial resolutions (Storch et al. 1993)

Regional Climate Models (RCMs) have been derived from the coarse GCMs to much higher resolutions. The process of downscaling of GCMs to meso-scales or

regional scales enables the downscaled regional climate model to adequately simulate the physical processes consistently with GCMs on a large scale (Mearns et al. 2004). Since parameters of land use and topography are crucial in the efficiency of the RCMs, the higher the resolution of the RCMs, the better the simulation of the climate and ultimately, a better hydrological simulation is achieved. Some of the RCMs that have been popular in West Africa are REMO, MM5 and PRECIS.

7.3 Regional climate scenarios – MM5

The regional climate model MM5 is a meso-scale model derived from the GCM-ECHAM4 recently developed for the assessments of the impacts of environmental and climate change on water resources on the Volta Basin of West Africa. The MM5 is a brain child of the cooperation of the Pennsylvania State University (PSU) and the National Center for Atmospheric Research (NCAR) of the USA. According to Grell et al. (1995), the MM5 non-hydrostatic or hydrostatic (available only in version 2) is designed with the initial and lateral boundary conditions of a region to simulate or predict meso-scale and regional-scale atmospheric circulation.

The GLOWA-Volta project (GVP) executed by the Center for Development Research (ZEF), Germany, ran MM5 with the initial and lateral boundary conditions derived from the ECHAM4 runs of the time slice 1860-2100, and based on IPCC's IS92a (assuming an annual increase in CO_2 of 1 %, and doubling of CO2 in 90 years (May and Rockner, 2001; cited in Jung, 2006). Using future climate scenario and girded monthly observational dataset from the East Anglia Climate Research Unit (CRU), UK, the model was calibrated to 0.5^o x 0.5^o resolution. GVP further down-scaled the MM5 model for the Volta Basin to finer resolutions of 9 km x9 km, and for some watersheds within the basin to 3 km x 3 km. Details of the setup, coupling and simulation are available in Kunstmann and Jung (2005) and Jung (2006).

A good agreement was reported between the ECHAM4-MM5 simulated climate and the CRU data sets for 1961-1990. According to Jung (2006), simulated temperature was slightly higher in the Sahara during the wet seasons and for the humid south during the dry season, while rainfall was generally comparable except for higher rainfall events that were underestimated. Between ECHAM4 and MM5, 1990-2000 simulations revealed that temperature was generally over estimated and rainfall under

estimated by the latter even though the spatial representation was relatively good. However, the future simulations of the models were almost the same. Generally, MM5-Volta estimated an increase in rainfall in the Sahel zone (10-30 %), an increase mean annual rainfall of 45 mm (5 %) between 1990-2000 and 2030-2039, and a 1.2^{o}C mean temperature rise (Jung, 2006).

GVP produced two 10-year simulated time slices of MM5 (1991-2000 and 2030-2039). For this section of the study, the 1991-2000 outputs were considered as the present climate and the time slice 2030-2039 as the future climate.

Changes in the hydrological cycle of a basin hinge largely on, among others, changes in climate. 10-year time slices were used to represent three windows of the past, present and future conditions. Climatic inputs for the past are data obtained from the meteorological agencies of Ghana and Burkina Faso through the GLOWA Volta project for the period 1961-1970. The present and future climate conditions are outputs of the MM5-Volta after Jung (2006) and Kunstmann and Jung (2005); these are 1991-2000 and 2030-2039, respectively. For these analyses, the Pwalugu watershed (Savannah) represents the north of the basin and the Bui watershed (transition zone) represents the south.

7.3.1 Highlights of MM5 on the Volta Basin

Rainfall

Results of the GLOWA-Volta climate studies showed some significant changes, most especially in rainfall over the entire basin across the periods (Figure 7.1). In general, average monthly rainfall decreased in the period 1991-2000 for the whole of the rainy season (May-September) compared to the previous climate years.

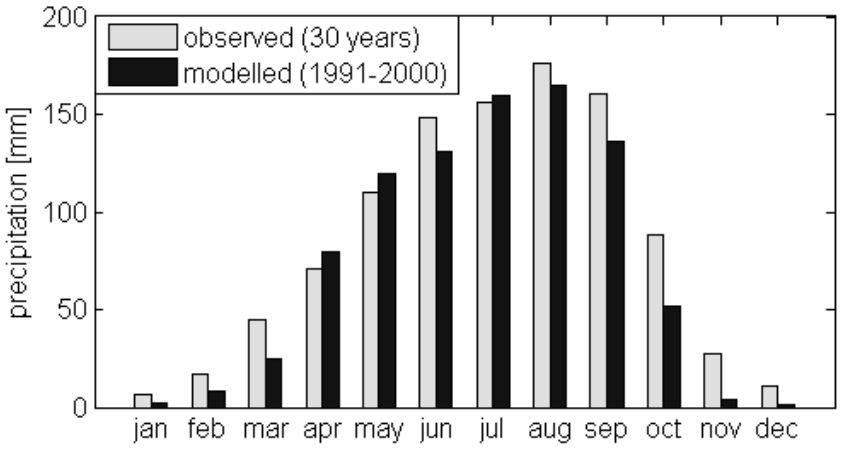

Figure 7.1 Spatially averaged, simulated mean monthly precipitation (1991-2000) versus observed long-term means [mm] for the Volta Basin area (Jung, 2006)

As shown in the example of Pwalugu and Bui (Figures 7.2 and 7.3 respectively), the Frequency Distribution Curves (FDCs) of 1991-2000 and 2030-2039 do not differ significantly except for the extremely high and low rainfall events. However, both simulated time slices differ considerably from those of the 1961-1970 data records. This accounts in particular for the high percentiles in the high rainfall range. For example, the extreme daily precipitation amounts of Pwalugu and Bui will nearly double from the past to the future (80 mm-160 mm) and (52 mm-78 mm), respectively. The frequency of the daily mean of 10 mm of rainfall, for example, is expected to reduce from 17 % to 8 % in the north, and from 14 % to 7 % in the south.

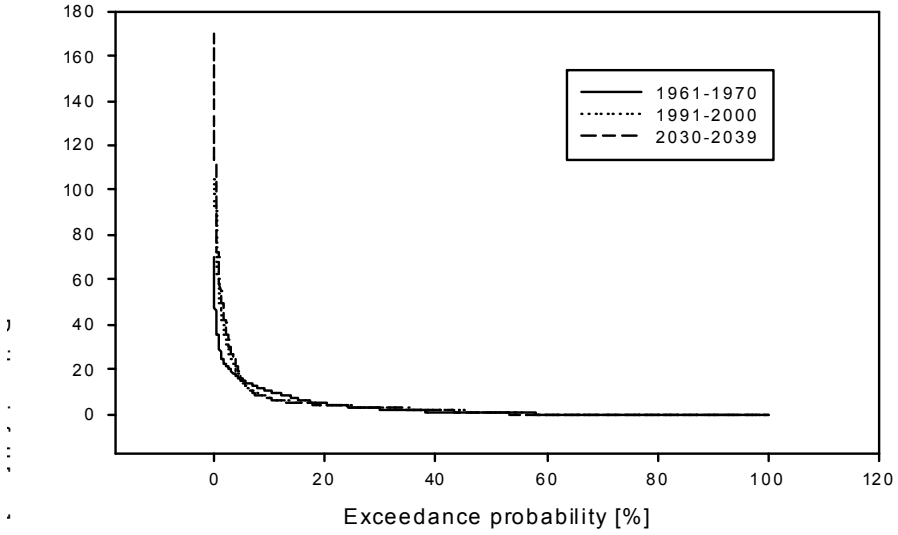

Figure 7.2: Frequency distribution curves of rainfall for the north of the Volta Basin at the Pwalugu (56,760 km^2) catchment for the time slices 1961-1970 (observed), 1991-2000 and 2030-2039 (both MM5 simulated)

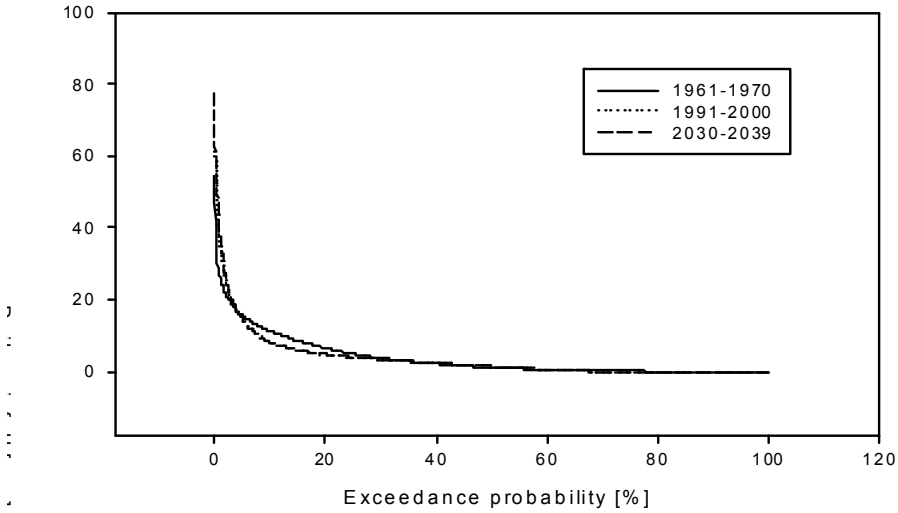

Figure 7.3: Frequency distribution curves of rainfall for the south of the Volta Basin at the Bui (99,360 km^2) catchment for the time slices 1961-1970 (observed), 1991-2000 and 2030-2039 (both MM5 simulated).

Evapotranspiration

Actual evapotranspiration and temperature are closely related in the basin. As predicted by almost all climatic models and the IPCC, increases in the global and the basin mean temperature are eminent. Jung (2006) reported that monthly mean

temperatures will increase in the Volta Basin by an average of 1.3°C by 2030-2039 compared to the present 1991-2000 data sets (Table 7.1) conforming to the assumptions of IPCC's IS92a of an annual increase in CO_2 of 1 %, and doubling of CO_2 in 90 years (May and Rockner, 2001).

Table 7.1: Mean monthly and annual temperatures (1991-2000 and 2030-2039) for the Volta Basin (after Jung, 2006)

	Average(1991-2000)°C	Average(2030-2039)°C	Temperature Change °C
January	28.10	28.90	0.80
February	30.10	31.30	1.20
March	32.40	33.60	1.20
April	32.20	34.30	2.10
May	30.10	32.20	2.00
June	28.80	30.10	1.30
July	28.40	29.60	1.20
August	28.20	29.30	1.10
September	29.10	29.80	0.70
October	30.90	31.90	1.00
November	30.40	32.00	1.60
December	27.90	29.60	1.60

Many reports on the Volta Basin estimated evapotranspiration between 70 % - 90 % of total rainfall (e.g., Andreini et al. 2000, Martin, 2005). According to Jung (2006), significant increases are expected based on the use of the MM5-Volta model for the 2030-2039 periods for nearly all the months of the rainy seasons except May. Increases range from an average 64 mm to 79 mm per month (Figure 7.4).

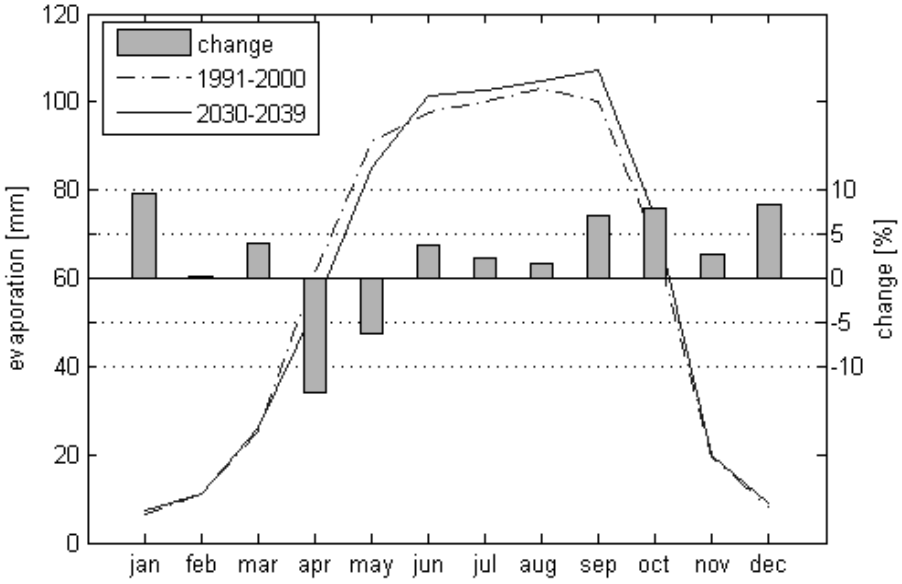

Figure 7.4: Spatially averaged monthly mean real evapotranspiration [mm], (1991-2000 and 2030-2039) and evapotranspiration change [%] for the Volta Basin (Jung, 2006))[6]

Calculating evapotranspiration using the Penman-Montheith method requires temperature, wind run, radiation and humidity data. The 1961-1970 plots (Figures 7.5 and 7.6) were produced based on archived data from the metrological agencies of Ghana and Burkina Faso, which were not adequately representative of the entire basin. Nevertheless, the trend and amounts of increase in evapotranspiration of the time slices is phenomenal. The dryer north is expected to experience much higher increases in evaporation and transpiration e.g., the probability of 3 mm of water lost to evapotranspiration per day is increased from 0.07 in 1961-1970 to 0.21 in 2030-2039. The transition zone (south) is expected to lose less water compared to the north but with similar trends, while the frequency of higher evapotranspiration days will increase. The spatial distribution of evapotranspiration shows a general increase over nearly the whole basin, with only the south showing little or no increase in evapotranspiration for the period from the 1990s to the 2030s.

[6] Actual evapotranspiration change for the Volta Basin using REMO simulation in APPENDIX

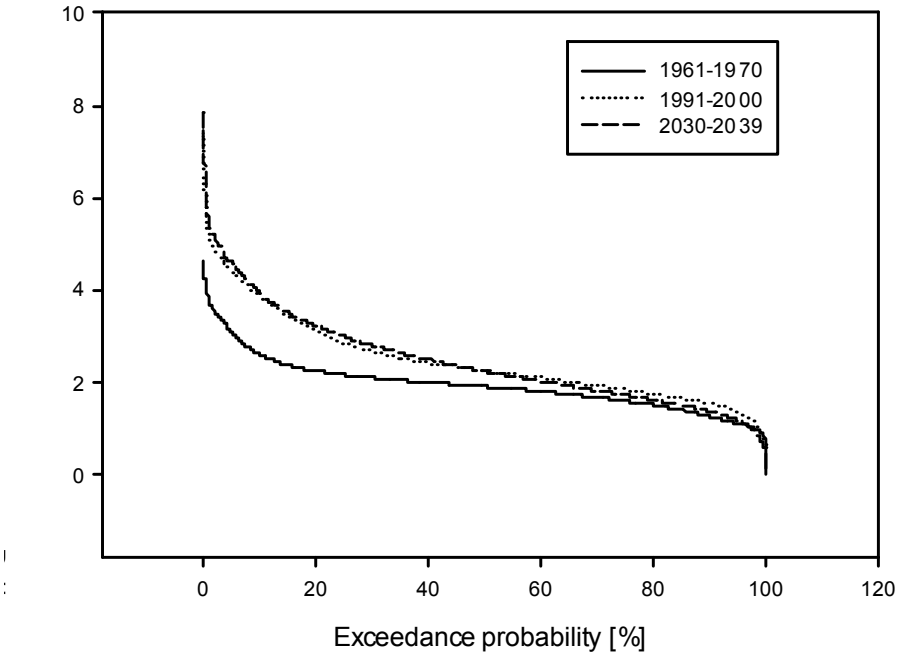

Figure 7.5: Frequency distribution curves of evapotranspiration for the north of the Volta Basin at the Pwalugu (56,760 km^2) catchment for the time slices 1961-1970 (gauged), 1991-2000 and 2030-2039 (both MM5 simulations).

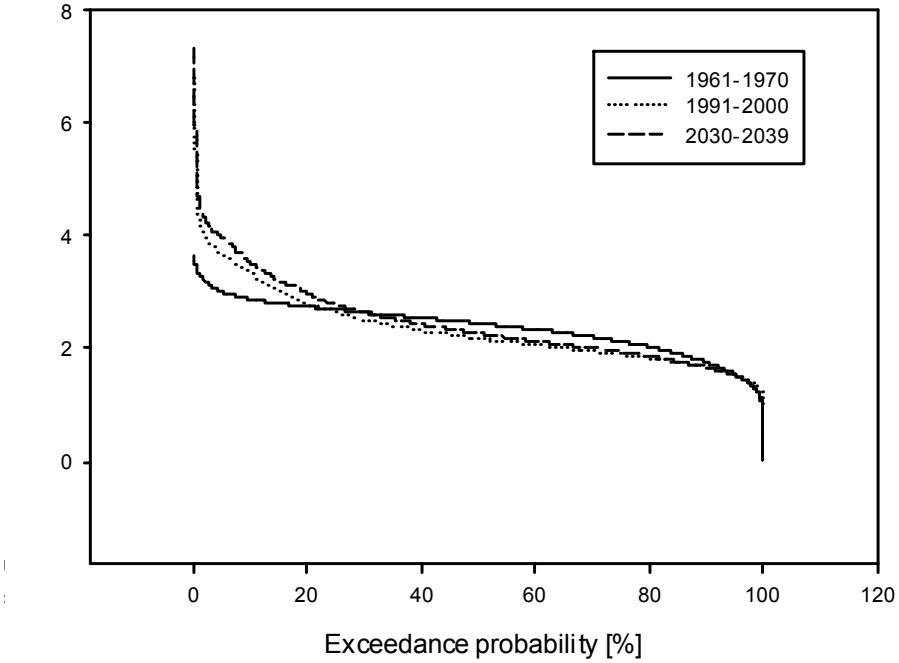

Figure 7.6: Frequency distribution curves of evapotranspiration for the south of the Volta Basin at the Bui (99,360 km^2) catchment for the time slices 1961-1970 (gauged), 1991-2000 and 2030-2039 (both MM5 simulations)

Runoff

Runoff in the Volta Basin is closely associated with the pattern of local precipitation, and changes in runoff frequency can reflect changes in climate, vegetation, or land use. An analysis of a stream in the Pwalugu catchment north of the basin (Figure 7.8) showed an increase in the frequency of extreme high flows, but more profound are the expected increase in low flow events that will ultimately have severe impacts on the water resources of the basin in terms of drought frequencies. Jung (2006) attributed the higher values in the future climate scenario run (Figure 7.7) to the increase in direct runoff especially in the rainfall-intense month of September. Discharge in the south of the basin shows a similar pattern (Figure 7.9), but differences are more pronounced between the past and future time slices. While the probability of daily discharge exceeding 15 mm increases in the future, there is also an equally significant increase in low flow events. For example, the probability of daily discharge exceeding 1 mm in south for the past time slice was 0.4, but is expected to rise sharply to 0.8 for the future time slice of 2030-2039.

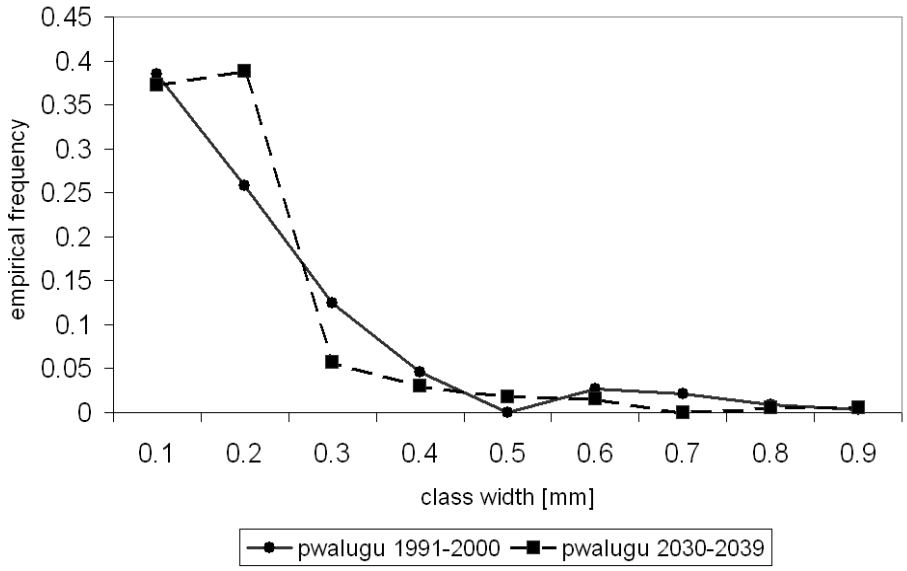

Figure 7.7: Normalized frequency distribution of daily runoff values [mm] (1991-2000 and (2030-2039), Pwalugu, Volta Basin (Jung, 2006)

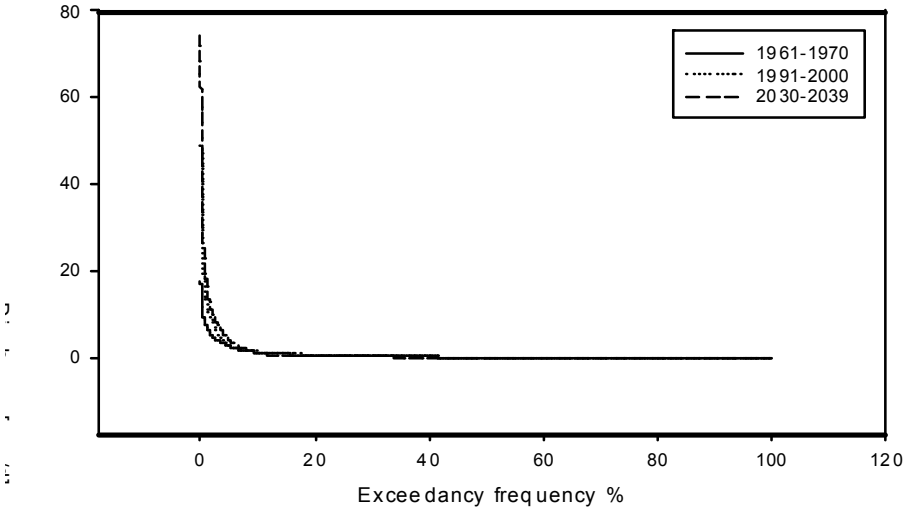

Figure 7.8: Frequency distribution curves of discharge for the north of the Volta Basin at the Pwalugu (56,760 km^2) catchment for the time slices 1961-1970 (observed), 1991-2000 and 2030-2039 (both MM5 simulations).

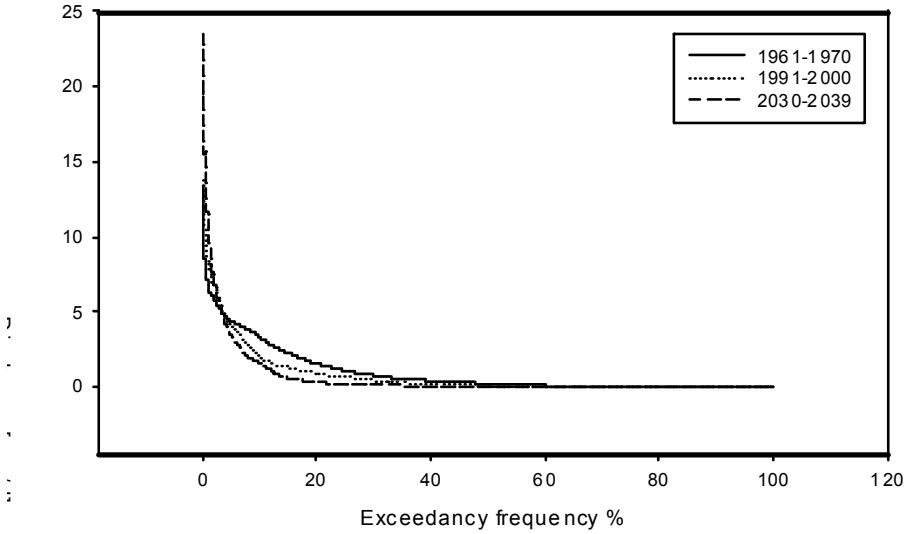

Figure 7.9: Frequency distribution curves of discharge for the south of the Volta Basin at the Bui (99,360 km^2) catchment for the time slices 1961-1970 (observed), 1991-2000 and 2030-2039 (both MM5 simulated).

7.4 Regional climate scenarios – REMO

REMO is a hydrostatic regional climate model, initially developed at the Max-Planck-Institute for Meteorology (MPI) in Hamburg, Germany, on the foundation of the operational weather forecast model Europa-Modell of the German Weather Service

(DWD) (Majewski 1991). According to Jacob et al. (2001) cited in Paeth (2005), the dynamical kernel is based on primitive equations with temperature, horizontal wind components, surface pressure, water vapor content and cloud water content as prognostic variables.

REMO simulations are driven according to Roeckner et al. (2003) by recent global coupled climate model simulations of ECHAM5/MPI-OM, which are known to be forced by enhanced greenhouse and sulphate aerosol conditions and are synonymous with the modeling approaches of the fourth assessment report of the Intergovernmental Panel on Climate Change (IPCC).

The simulation outputs used for this study are those produced and used in the GLOWA IMPETUS project whose focus was on western and northern Africa. The horizontal resolution is 0.5^{o}, equivalent to about 55-km grid spacing at the equator, and 20 hybrid vertical levels are resolved. These levels follow the orography near the surface and correspond to pressure levels in the upper troposphere (Paeth, 2005).

The global climate model ECHAM4 (Roeckner et al. 1996) was adjusted to the 0.5^{o} model grid scale of REMO to account for atmospheric processes like deep convection, cloud formation, convective rainfall, radiation and microphysics from the sub grid scale of ECHAM4. Similarly, land surface parameters such as soil characteristics, orography, vegetation, roughness length, and albedo are derived from the GTOPO30 and NOAA data sets (Hagemann et al. 1999) and partly modified according to the scenarios of land degradation. Underlying an idealized seasonal cycle over West Africa, the same daily interpolated surface parameters are prescribed each year using a model output statistics (MOS) system (Paeth, 2005).

The IMPETUS project made some changes to the default parameter of REMO to adapt to the tropical-subtropical West African region. The focus is on the key region of the West African monsoon system of which the Volta Basin is part. Some results of the adopted REMO correlated well with observed extreme climate year (Chapter 6). For example, the driest years derived from simulated rainfall were 1981, 1983, 1990, 1992 and 1998, whereas 1979, 1984, 1988, 1989, and 1991 were characterized by abundant monsoon rainfall. Parker and Alexander (2002) basically confirm that the CRU time series data set reveals almost the same composite years.

7.4.1 Highlights of REMO on Volta Basin area

Data on the West African region have large gaps, hence the CRU data set is deficient in regions with low data coverage. This problem applies to all available gridded rainfall data sets. REMO, in an attempt to resolve the handicap of data gaps, uses two statistical post processing steps:

(1) Monthly rainfall is adjusted to the observations by constructing a model output statistics (MOS) system.
(2) Daily rainfall intensity is corrected from grids by fitting Γ distributions to the simulated and observed time series, and then taking the ratios between both distributions as weighting factors in the combined correction algorithm. The MOS system is defined by von Storch and Zwiers (1999) as stepwise multiple linear regression analysis.

The MOS-corrected precipitation by the REMO model reveals a good performance according to Paeth et al. (2005) of the model in terms of the basic features of African climate, including the complex mid-tropospheric jet and wave dynamics and the climate seasonality of the Volta Basin area.

Available scenario runs of REMO (Jacob et al. 2001, 2007) in 0.5^{o} resolution over tropical Africa (Paeth et al. 2005) consider three scenarios of GHG (Figure 7.10) and emissions and land-cover changes in order to evaluate the range of options given by different achievements in mitigation policy and to quantify the relative contribution of land degradation in line with IPCC projections.

The 2007 report of the IPCC lacks new information on the African climate change but highlights model uncertainties, particularly over tropical Africa. The inconsistency of different model projections reflects in the low values of the regional climate change index in Giorgi (2006), which relies on regional temperature and precipitation changes in the IPCC multi-model ensemble framework. This model discrepancy clouds the interpretation of the results of uncertain model parameters, which may impact specifically on the simulation of African climate.

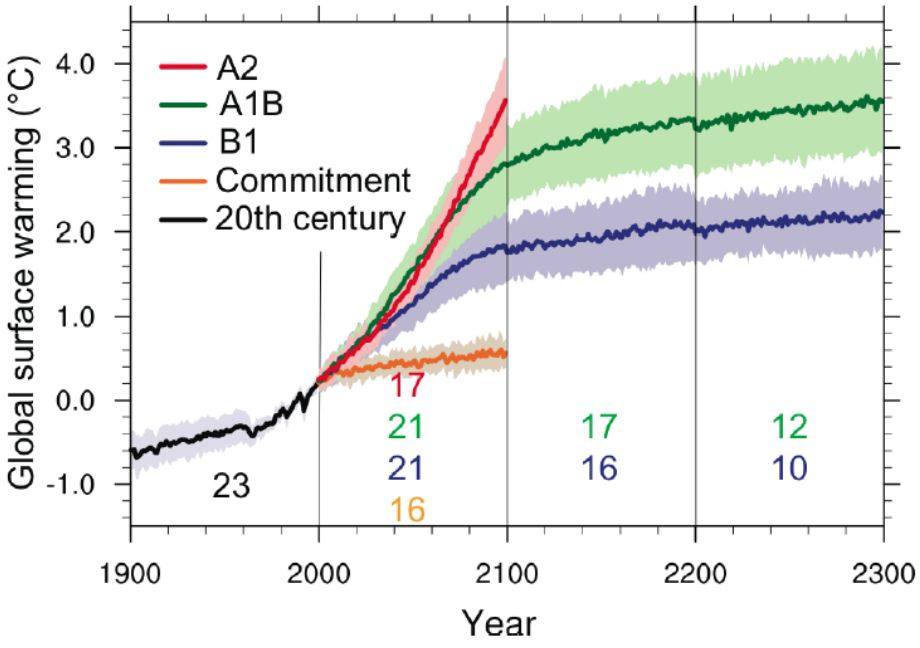

Figure 7.10: Multi-model means of surface warming for the scenarios A2, A1B and B1, shown as continuations of the 20th century simulation. Values beyond 2100 are for the stabilization scenarios. Linear trends from the corresponding control runs have been removed from these time series. Lines show the multi model means, shading denotes the plus minus one standard deviation range. (Source: http://ipcc-wg1.ucar.edu/wg1/wg1-report.html)

Within the adopted REMO, the spatial mean of the change of forest to agricultural land under the A2, B1 and A1B scenarios have been considered. For example, under the A1B (all)[7] scenario the estimate of the FAO (2006), assumes a decrease in forest coverage of about 30 % until 2050 for the entire Africa region. Associated albedo changes between 2000 and 2050 are in the order of 5-10 %. Forests transformation into grasslands and agricultural areas in the order of 10-15 % were incorporated. The B1 storyline and scenario family describes a convergent world with the same global population, that peaks in mid-century and declines thereafter, as in the A1 storyline, but with rapid change in economic structures toward a service and information economy, with reductions in material intensity and the introduction of clean and resource-efficient technologies. The emphasis is on global solutions to economic, social and environmental sustainability, including improved equity, but without additional climate initiatives, whereas the A2 storyline and scenario family describes a

[7] All ensemble scenarios of IPCC considered

very heterogeneous world. The underlying theme is self-reliance and preservation of local identities. Fertility patterns across regions converge very slowly, which results in continuously increasing population. Economic development is primarily regionally oriented and per capita economic growth and technological change more fragmented and slower than other storylines. The available REMO outputs from the IMPETUS project have three ensemble runs for the various scenarios and time slices. These are 901, 902, and 903 for the periods 1961-2000; the A1B scenarios with land-use changes are 911, 912, and 913 for 2001-2050 time periods; for the B1 scenarios are 921, 922 and 923 for 2001-2050 periods. Within the three ensemble runs of each scenario (Figure 7.11), no large differences were identified in annual totals between individual ensemble runs.

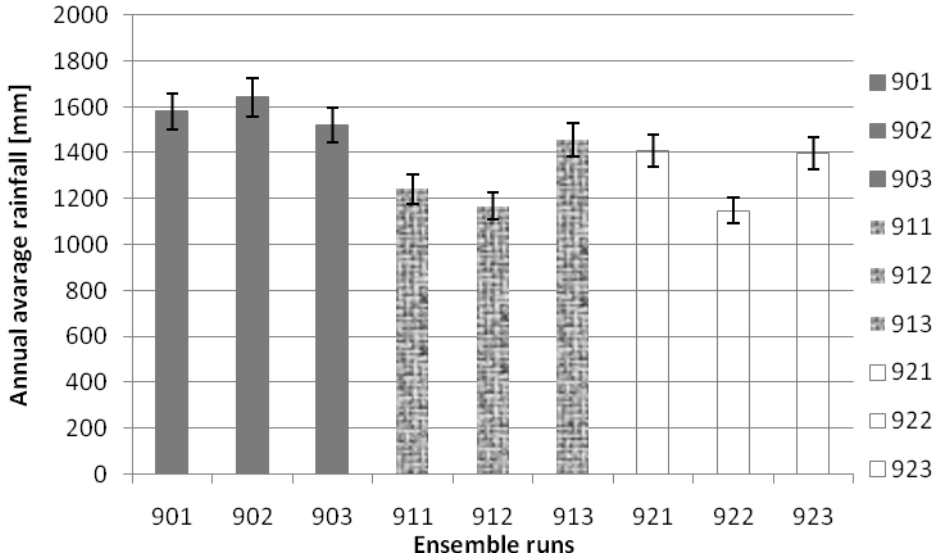

Figure 7.11: Annual rainfall average for three ensemble model runs of IPCC climate scenarios A2, A1B and B1 for present (1961-2000) and future (2001-2050) with standard deviations at 5^{o}N -2.5^{0}W south of the basin

7.5 Regional climate model performance of MM5 and REMO

Regional models share similar problems but differ in magnitude. Notable are MM5, MAR and REMO (Vizy and Cook, 2002; Gallée et al., (2004); Paeth et al., 2005). However, Schnitzler et al. (2001) suggest that integrating the interaction with vegetation cover and albedo considerably improves the simulation of rainfall over the Sahel in the global ECHAM4 model.

For the hydrological modeling for which these regional climate models are required, rainfall is a very important input parameter apart from temperature because it is the major driver of moisture input to the hydrological cycle. Hence it is important to ascertain that the annual, monthly and daily distributions of the data represent the amounts and the frequency statistics of the data, e.g., the exceedance of extremes are consistent with the long-term mean observed. To assess the reliability of the MM5 and REMO future climate scenario for the evaluation of the impacts of climate change on water resources in the Volta Basin, the REMO-simulated and MM5-simulated mean rainfall for the time slice 1991-1997 obtained for the basin weather stations are compared to the mean observed rainfall for the same area and periods (Figure 7.12). This time slice was selected because it contained certified gauged meteorological data with minimal gaps. The results of the comparison for the Pwalugu catchment station, for example, show a good correlation between the observed and MM5-simulated and REMO-simulated monthly rainfall (Figure 7.12). Pearson correlation of gauged 1991-1997 and REMO 1991-1997 = 0.823; P-Value = 0.001; for gauged 1991-1997 and MM5 1991-1997 = 0.957; P-Value < 0.0001 On average, MM5 and REMO overestimate rainfall for this selected time slice of 1,203 mm and 1,322 mm per annum, respectively, against the measured1,101 mm per annum. MM5 overestimates the rainfall from April through July and September and underestimates for August and October. REMO, on the other hand, overestimates rainfall for February through April, July, October and November and underestimates for August. The strongest overestimation for MM5 is for the month of July, while for REMO, this is March and April (Figure 7.13).

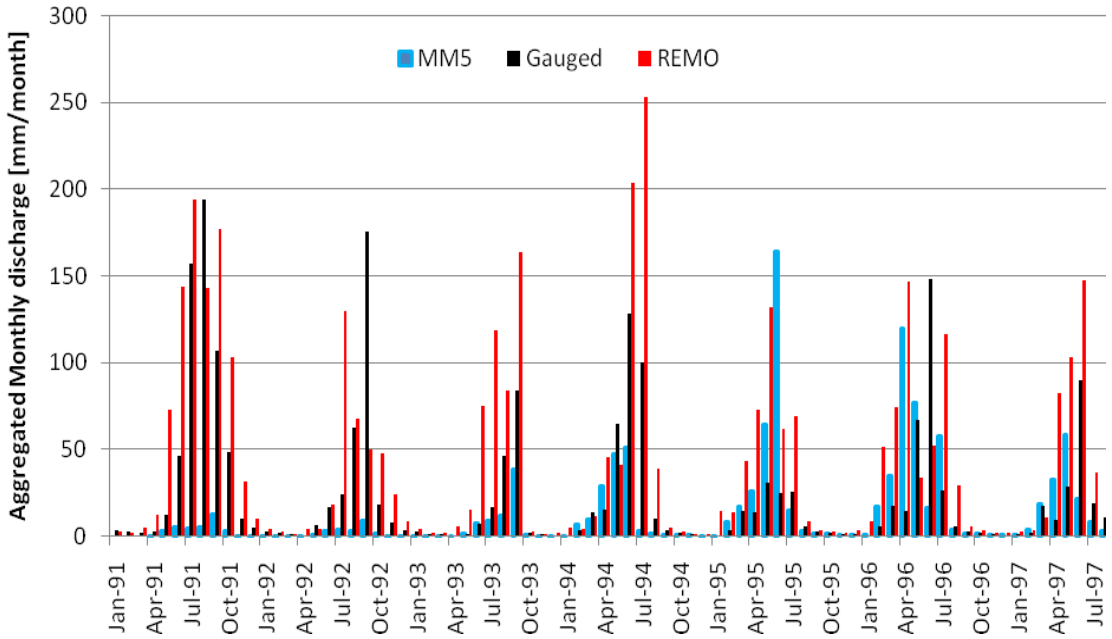

Figure 7.12: MM5-simulated and REMO-simulated compared to observed monthly rainfall at Pwalugu (56,760 km^2) catchment of the Volta Basin

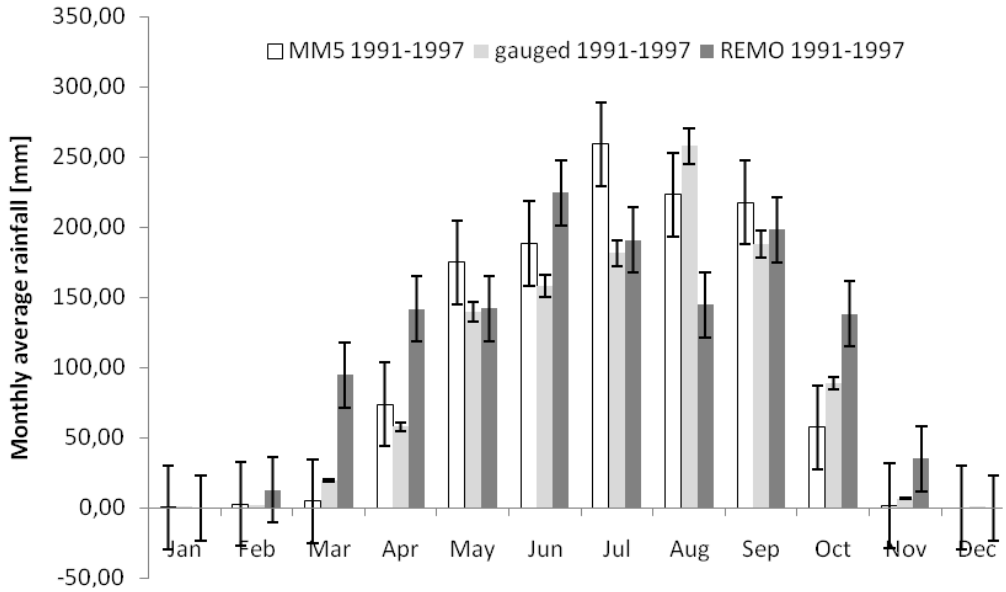

Figure 7.13: MM5-simulated (mean over 7 years) and REMO-simulated (mean over 7 years) compared to observed (mean over 7 years) rainfall including standard deviation (error bars) rainfall at Pwalugu (56,760 km^2) catchment of the Volta Basin

The resultant impacts on the hydrology are similar in most of the rainy seasons, apart from isolated extreme runoffs generated as a result of overestimations of some days and months of the season (Figures 7.14 and 7.15).

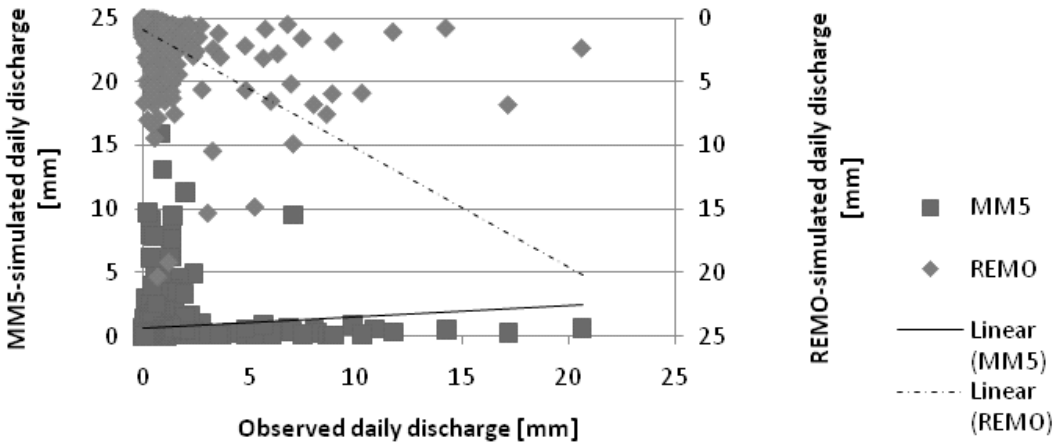

Figure 7.14: MM5-simulated (over 4 years) and REMO-simulated (over 4 years) compared to observed (over 4 years) discharge with trend lines at Pwalugu (56,760 km^2) catchment of the Volta Basin

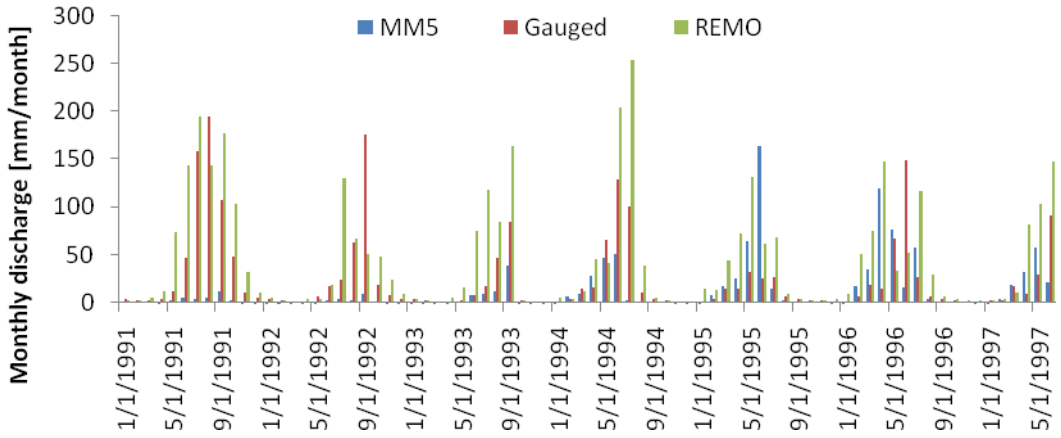

Figure 7.15: MM5-simulated and REMO-simulated compared to aggregated observed discharge at Pwalugu (56,760 km^2) catchment of the Volta Basin

Statistically, the Pearson correlation of MM5 and gauged = 0.181 with a P-Value = 0.108; Pearson correlation of REMO and gauged = 0.677 with a P-Value < 0.0001. The general trend for both MM5 and REMO for the period 1991-1997 is similar in pattern, and they simulate dry and wet years fairly well, with REMO better

for hydrological simulations. Available daily gauged runoff exist data for 1994-1997 (Figures 7.14 and 7.15).

7.6 Comparison of past, present and future hydrological dynamics of the Volta Basin

The 2001-2050 time slices representing the future period with increasing GHGs and changing land cover, according to the business-as-usual and a mitigation scenario from the IPCC SRES A1B and B1 scenarios (Nakicenovic and Swart 2000) are considered by REMO. The relative contribution of the land-use changes to total climate change in Africa was carried out using the A1B and B1 emission scenarios between 2001 and 2050. An annual growth rate of 2 %, land-use changes comprising of mainly prevailing cities and currently existing agricultural areas were some assumptions adopted (Paeth et al., 2005). MM5, on the other hand, did not consider land-use change scenarios and was based on IPCC's IS92a scenarios (May and Rockner, 2001), which are known to overestimate the CO_2 projections compared to the A1B and B1 emission scenarios.

A simulation by MM5 and REMO-B1 predicts high rainfall events compared to the scenarios of REMO-A1B (Figure 7.16). The resultant discharge in these scenario simulations shows a very high discharge for MM5 with a sharp gradient and larger amplitudes, closely followed by REMO-B1, and REMO-A1B (Figure 7.19). This is explained by the number of very low and rainy day event counts that are higher with MM5 than those of both scenarios of REMO (Figure 7.17).

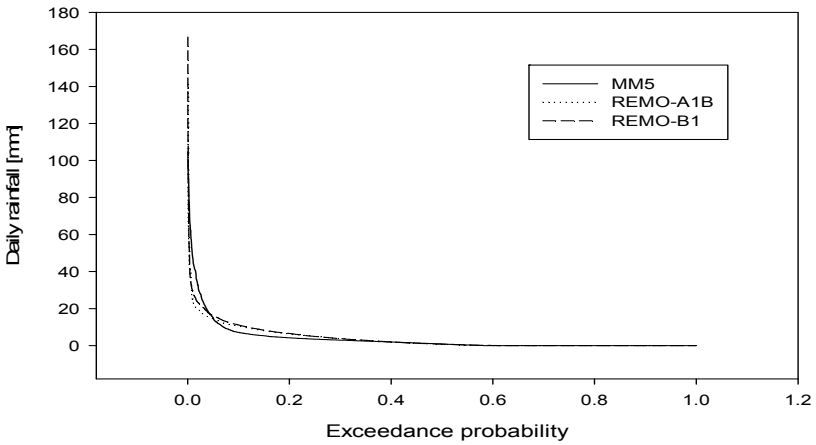

Figure 7.16: Exceedance probability of daily rainfall simulated by MM5, REMO-A1B and REMO-B1 with average total rainfall of 1,287 mm, 1291 mm, and 1,391 mm, respectively, for the Pwalugu catchment of the Volta Basin for 2030-2039.

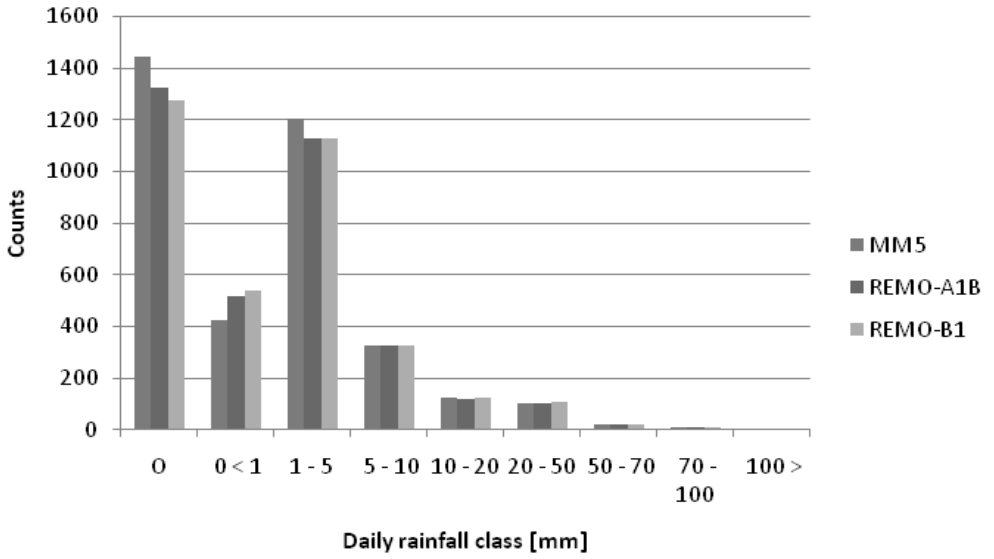

Figure 7.17: Rainfall distribution simulated by MM5, REMO-A1B and REMO-B1 with average total rainfall of 1,287 mm, 1291 mm, and 1,391 mm, respectively, for the Pwalugu catchment of the Volta Basin for 2030-2039.

7.7 Future projections

The regional climate models MM5 and REMO have demonstrated that they are able to simulate the observed main characteristics of African climate to some extent, with varied accuracy. For the resultant hydrological simulation with respect to discharge, the regional climate model REMO provides reliable and consistent high-resolution data for hydrological application of WaSiM-ETH for the Volta Basin (Figure 7.14). Nevertheless, both climate models have divergent projections for the future climate and hence the hydrology of the basin.

7.8 Water balance dynamics

The Volta Basin's water balance dynamics were simulated with the WaSiM-Volta model with daily climate inputs of historical data from the basin for the "past"; MM5-generated and REMO-generated climate series for the "present" and "future". The resultant outputs were compared.

Considering the basin's north-south transect in general, rainfall amounts have increased steadily from the past to the present and is projected to increase substantially in the north and marginally in the south by 2030-2039 according to MM5. A general decrease is projected by REMO under both IPCC's scenarios A1B and B1 (Tables 7.2 and 7.3). The projected increase in precipitation by MM5 is largely due to the abnormally high projected precipitation for the period 2035-2039 (Figure 7.18), for which precipitation exceeds the previous period of 2030-2034 by over 500 mm over the two periods. REMO's A1B and B1 scenarios also conflict on the sign of average annual precipitation for this period. While A1B projects a dryer period, B1 projects a relatively wetter period.

Table 7.2: Change in hydrology simulated using MM5 (1991-2000) and MM5 (2030-2039); REMO-A1B (1991-2000) and REMO-A1B (2001-2050); REMO-B1 (1991-2000) and REMO-B1 (2001-2050) for the north of the Volta Basin

	MM5		REMO-A1B		REMO-B1	
Balance term	Average amount change [mm]	% change	Average amount change [mm]	% change	Average amount change [mm]	% change
Precipitation	270	19	-83	-6	-58	-4
Total discharge	229	53	-93	-14	-59	-9
Interflow	228	76	-94	-19	-62	-13
Surface flow	-8	-9	27	58	26	55
Base flow	9	20	-26	-23	-23	-21
Potential ET	184	10	392	45	356	41
Actual ET	52	5	11	2	10	2
SWC change	-11		0.1		-9	
Balance error	-0.1		-0.3		-0.4	

Table 7.3: Change in hydrology simulated using MM5 (1991-2000) and MM5 (2030-2039); REMO-A1B (1991-2000) and REMO-A1B (2001-2050); REMO-B1 (1991-2000) and REMO-B1 (2001-2050) for the south of the Volta Basin

	MM5		REMO-A1B		REMO-B1	
Balance term	Average amount change [mm]	% change	Average amount change [mm]	% change	Average amount change [mm]	% change
Precipitation	154	11	-54	-4	-40	-3
Total discharge	116	30	-19	-3	13	2
Interflow	116	35	-6	-1	22	4
Surface flow	-0.1	-0.2	2	74	1	49
Base flow	-0.1	-0.1	-15	-14	-10	-10
Potential ET	-183	-10	-125	-15	-84	-10
Actual ET	-35	-4	-28	-4	-46	-7
SWC change	-3		-131		-7	
Balance error	0.1		-0.1		-0.0	

The change in hydrology as simulated by WaSiM based on MM5 and the two scenarios of REMO have conflicting results (Tables 7.2 and 7.3), whereas MM5 projects an increase in precipitation between 1991-2000 and 2030-2039 by 10 % to 19 % for the basin, both REMO simulations project a reduction of between 4 % and 6 % between 1991-2000 and 2001-2050 for the north and a decline of 3 % to 4 % for the south. Discharge is expected to increase under MM5 by nearly 53 %, whereas a decrease between 9 % and 14 % is expected under REMO for the north. The discrepancy in simulation between MM5 and REMO for the future may be due to extremely high projected precipitation of MM5 for the period 2036-2039 for which REMO does not project anything extraordinary (Figure 7.18). The only agreement between MM5 and REMO is in the area of soil water content change, where both scenarios show dry soils at the end of the seasons. These might be signs that drying soils maybe early warnings of drought events

Several authors have suggested that the prevailing droughts during the second half of the 20th century were at least partly caused by land-cover changes in tropical and subtropical Africa (Zeng and Neelin 2000; Pielke 2001; Semazzi and Song 2001; Zeng et al. 2002). Texier et al. (2000) have shown that the African monsoon system is much more sensitive to low frequency changes in vegetation cover (Paeth et al., 2005), and hence are evident in REMO simulations as they consider land-use changes.

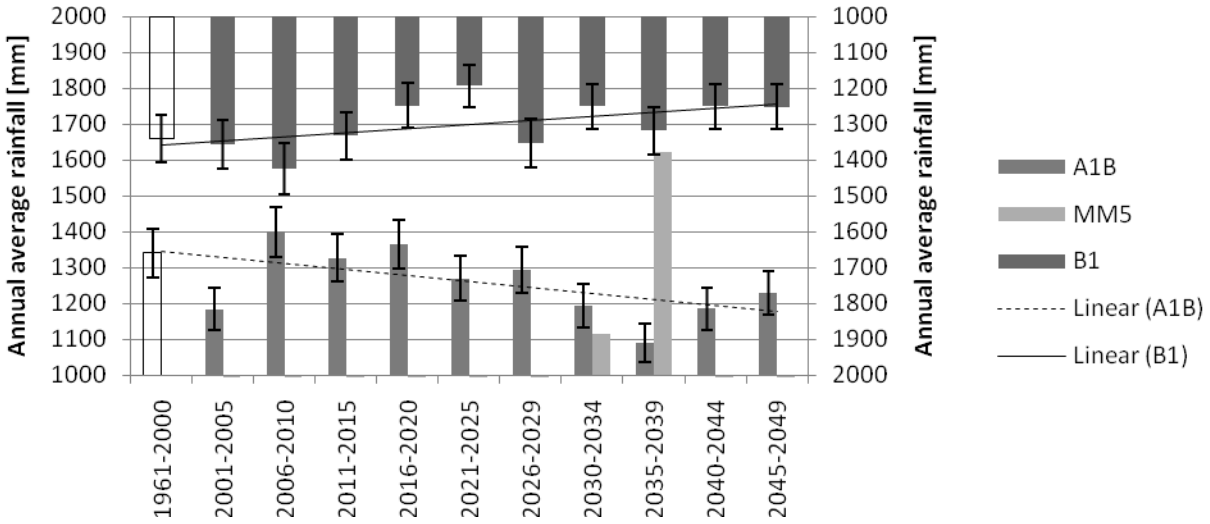

Figure 7.18: MM5-simulated and REMO-simulated compared to observe (mean over 4 years) rainfall including standard deviation (over the period) and trend lines of rainfall at Pwalugu (56,760 km^2) catchment of the Volta Basin

Under MM5 projections, total percentage discharge and surface flow are observed to increase at a steady rate in the north, which might be good for dugout and streams. The opposite is observed for the south even though the actual differences in amounts are not very large. This can be attributed to the wide variation of the increases in precipitation (Figure 7.19) within the highly heterogeneous basin. Projected changes in interflow differ in percentages between the past and the present, i.e. a significant increase from 6 % (present) to 76 % (future) is expected for the north, and from 8 % to 30 % for the southern parts of the basin. Interflow is closely related to the drainage density of the river system, and so a projected increase in interflow will mean an increase in the drainage density of the river network feeding into those catchments. Base flow is generally below 3 % of the total rainfall for both the past and the present, and will increase by nearly 20 % for the period of the future time slice. This phenomenon will further enhance the occurrence and frequency of saturated soils leading to high groundwater recharge and high flows of streams and may ultimately result in flooding of ecosystems.

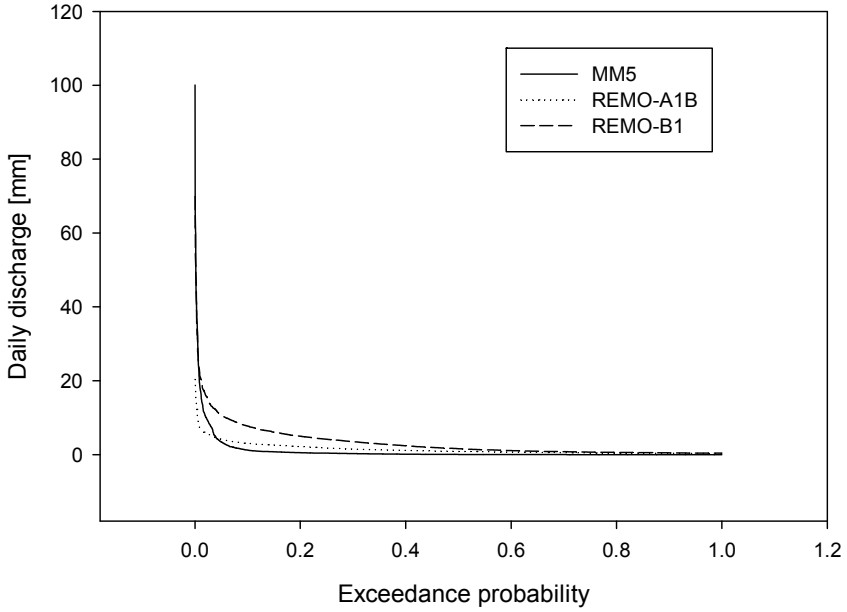

Figure 7.19: Exceedance probability of daily discharge simulated with MM5, REMO-A1B and REMO-B1 with annual average discharge of 338 mm, 523 mm and 1,200 mm, respectively, for the Pwalugu catchment of the Volta Basin for 2030-2039.

The combined transpiration from vegetation and evaporation from surfaces follows a decreasing trend as opposed to the rainfall, with slight decreases over time. Generally, annual mean evaporation in the north increases from 823 mm (past) to a little over 900 mm from the present to future. The south records a relatively low evapotranspiration compared to the north, mainly due to lower temperatures in the south, but it also shows a general increase in annual mean of 872 mm (past) to 893 mm (future).

The results presented by REMO show nearly the opposite of the projections of MM5. Total annual discharge is expected to reduce between 9 % and 14 % for the northern part of the basin, with an increase of between 40 % and 45 % of potential evapotranspiration and an increase of about 2 % in actual evapotranspiration (Table 7.2). For the south of the basin, REMO's A1B scenarios project a 3 % decrease in discharge whereas the B1 scenarios project a 2 % increase in discharge. Both scenarios, however, project between 4 % and 7 % decrease in evapotranspiration. Potential evapotranspiration is expected to decrease under both A1B and B1 scenarios by 10 % to 15 %.

By the estimations of MM5 outputs, average annual rainfall ranging from 1,133 mm (past) to 1,367 mm (future) representing 20 % increase in rainfall in the north results in 50 % increase in discharge, 9 % decrease in surface flow, and 76 % and 20 % increases in interflow and base flows, respectively. This scenario could be an indicator for extreme events of floods in the north. These projections seem to fit into the 2007-2009 rainfall patterns, when the basin experienced some extremes in rainfall accompanied with heavy floods. For the transition/south zones, a slight increase in the annual average of 1,239 mm (present) to 1,280 mm (future), results in 30 % increase in discharge with a slight decrease in surface runoff, 35 % increase in interflow, and 0.1 % decrease in base flows. It has already been established that with the use of MM5 projection many more days without rainfall are expected in the future compared to the past, which might result in low flow in streams. Rainfall amounts will generally increase across the basin, with the savannah zone generating a significant amount of the runoff of the basin (Figure 7.20) . This is however the opposite in the projection of REMO as discussed earlier.

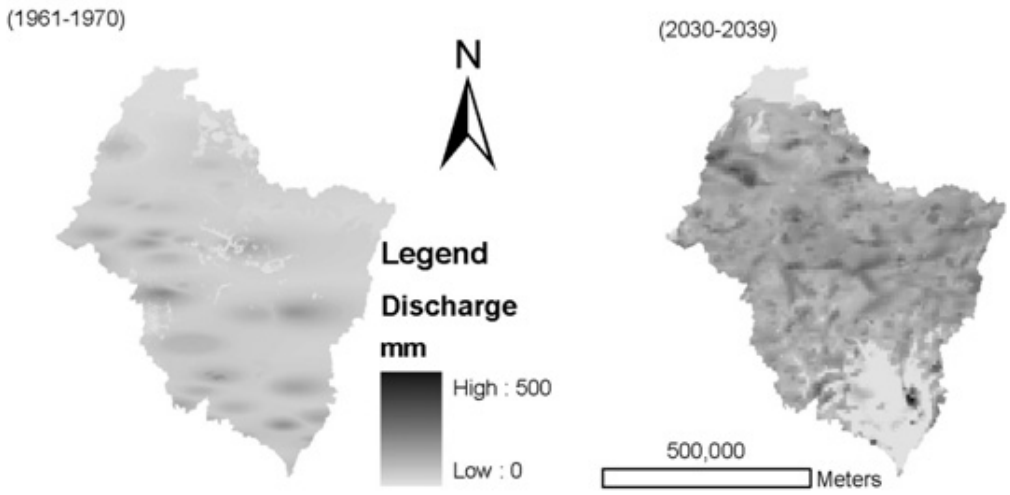

Figure 7.20: Spatial distribution of mean annual discharge [mm] for the 1961-1970 (gauged) and 2030-2039 (MM5 simulated) time-slices of the Volta Basin.

7.9 Soil moisture

Soil moisture data extracted from the Global Soil Moisture Archive follow patterns in agreement with climatic gradients of the watershed in correlation to water availability (Figure 7.21 and 7.22), as presented in this study (Scipal et al. 2002 cited in Friesen et al. (2007).

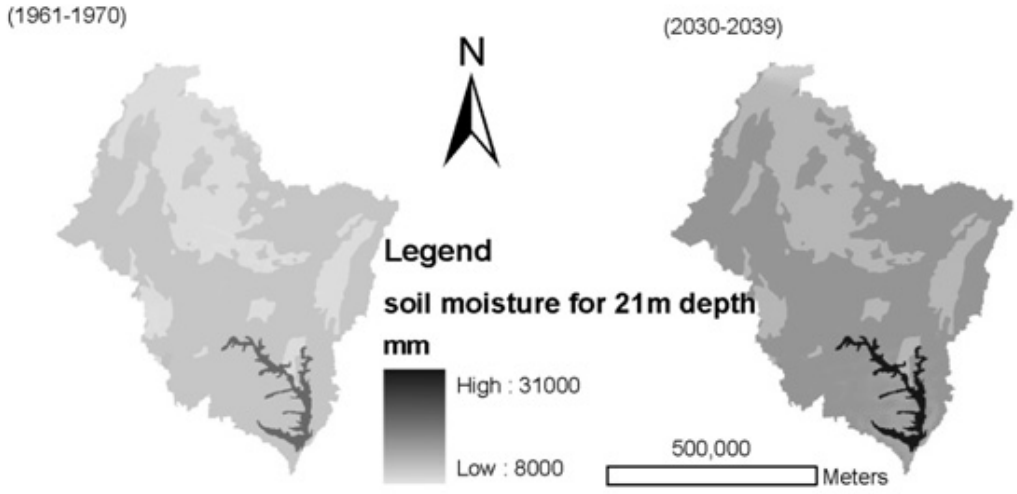

Figure 7.21 Spatial distribution of mean soil moisture for the 1961-1970 and 2030-2039 (MM5-simulated) time slices for soil profile of 21m of the Volta Basin.

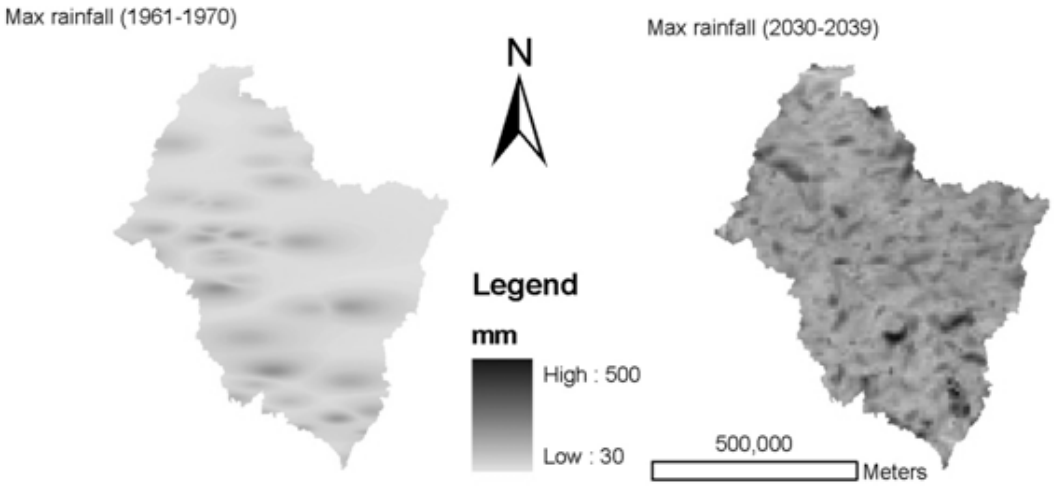

Figure 7.22 Spatial distribution of maximum daily rainfall for the 1961-1970 and 2030-2039 (MM5-simulated) time slices of the Volta Basin.

Simulations of soil moisture changes for the three time slices showed that the soil columns are adequately wet during the rainy season, but are becoming dryer at the end of the seasons over time. For example, the soil moisture content change will increase from 9 % from the 1991-2000 time-slice to 12 % of rainfall for the (2030-2039) time-slice using MM5 simulations. Relatively, soil moisture is higher during the rainy seasons for the future scenario than for the past (1961-1970). This is due to higher rainfall amounts attributed to the projected high rainfalls of the 2035-2039 periods. REMO-A1B projects 2 % decrease in soil water content for the north and 7 % increase for the south. In contrast, REMO-B1 projects a 9 % increase of soil water content for the north, and a 6 % increase for the south for the periods 1991-2000 and 2001-2050. This is mainly due to the temperature and rainfall projections of the scenarios.

7.10 Risk for water resources

The science of the future climate is plagued by uncertainties. For the region of West Africa, most climate change scenarios predict a decline in precipitation in the range of 0.5-40 % with an average of 10-20 % by 2025. Though other scenarios predict the contrary, many scenarios portray a more pronounced downtrend in flow regimes. As a result of the recent major droughts and a number floods with unusual magnitudes, climate specialists expect exacerbated extreme climate events in some parts of West Africa (IUCN, 2004). In the wake of all these predictions, it is important to point out that the climate change scenarios do not consist of definite predictions, but rather present plausible future conditions. According to Carter and La Rovere (2001), within climate change studies, high uncertainty requires the use of scenarios that are plausible but usually have no probability attached to them.

Considering the many possible future scenarios, what matters is the ability to manage the uncertainty. This includes reducing the current vulnerability of society and communities to climate variability and extreme events as well as improving and updating management options to deal with the worst-case scenarios and also take advantage of opportunities that may arise.

Assessing the risk of climate change, Page and Jones (2001) recommend that a knowledge of the likelihoods of both climate change and its consequences are necessary. For example, if greenhouse gas emission scenarios and climate change

scenarios are plausible with no further likelihood, then the consequences of those scenarios in terms of impacts have the same limitations. This leads to a growing cascade of uncertainties associated with a chain of consequences limited by the least predictable link. A Student's t-test according to Friesen (2008) on the mean rainfall in comparison of the periods 1930-1969 and 1970-1995 for the entire basin shows a significant decline of 28 km^3 of rainfall from the former to the latter period with a confidence interval of 99.9 %.

The water sectors of riparian states have postponed adaptation due to climate change uncertainty. Although there is wide acceptance that water resources are sensitive to climate change, managers have delayed accounting for climate change in their planning until the risks are better known. As generally accepted, the risk of climate change to a particular activity is a function of probability × hazard, and so, methods of managing the probabilities are required to go past this blind alley.

Risk is defined as "the objective (mathematical) or subjective (inductive) probability that the hazard will become an event. Factors (risk factor) can be identified that modify this probability. Such risk factors are constituted by personal behaviors, life-styles, cultures, environment factors, and the probability of loss to the elements at risk as the result of the occurrence, physical and societal consequences of a place in the community. Risk is the expected number of lives lost, persons injured, damage to property and disruption of economic activity due to a particular natural phenomenon, and consequently the product of specific risk and elements at risk" (Journal. of Prehospital and Disaster Medicine, 2004 cited in Thywisssen, 2006). By this definition, the basin's population can be regarded as being highly prone to the risk of frequent drought according to the projections of REMO and MM5 and some significant floods based on projected extreme precipitation in the future.

According to Garatwa and Bolli (2002), risk is conventionally expressed by the equation: Risk = Hazard X Vulnerability. However, the resilience of a society can help reduce the impact of risk; hence a modified expression as:

$$Risk = (Vulnerability\ X\ Hazards\ ) -\ Resilience$$

A hazard is defined as "A potentially damaging physical event, phenomenon or human activity that may cause the loss of life or injury, property damage, social and economic disruption or environmental degradation. Hazards can include latent conditions that may represent future threats and can have different origins: natural (geological, hydro-meteorological and biological) or induced by human processes (environmental degradation and technological hazards). Hazards can be single, sequential or combined in their origin and effects. Each hazard is characterized by its location, intensity, frequency and probability." (UN/ISDR, 2004).

The Volta Basin is prone to various environment-related hazards, most of which are regarded as natural hazards. Climate change is making the most common disasters of droughts and floods more likely, as the IPCC warns that global warming related climate change is likely to lead to more heat waves, droughts, floods and increased threats to human health. The IPCC Fourth Assessment Report (2007) elaborated future impacts of climate change on agriculture and many other sectors. In the Volta Basin region and most especially along the margins of the semi-arid and arid areas; the length of the growing season and yield potential are expected to decrease substantially, thus increasing the hazard levels of the basin in many sectors such as agriculture, food security, etc.

Although no coherent trends are found in the areas around the basin as reported by Peath et al. (2005), interannual rainfall variability is more pronounced in the northern Volta (Pwalugu) as revealed by the REMO protections (see Figure 7.23). The northern part of the basin is most vulnerable to these variations because it has a monomodal rainfall pattern compared to the south which has relatively higher rainfall amounts due to its bi-modal rainfall pattern. The SPI analysis conducted on projected precipitation based on REMO using IPCC's A1B and B1 scenarios against the base period of 1961-2000 (Figure 7.23) shows both scenarios agreeing to a general drying trend for the future. With the exception of B1-scenario-based extreme dry year projections for 2016 (-2.5) and 2049 (2.1), the A1B scenario generally projects higher negative SPI values than B1 spanning the entire projection period and more profound for the period 2019 to 2047.

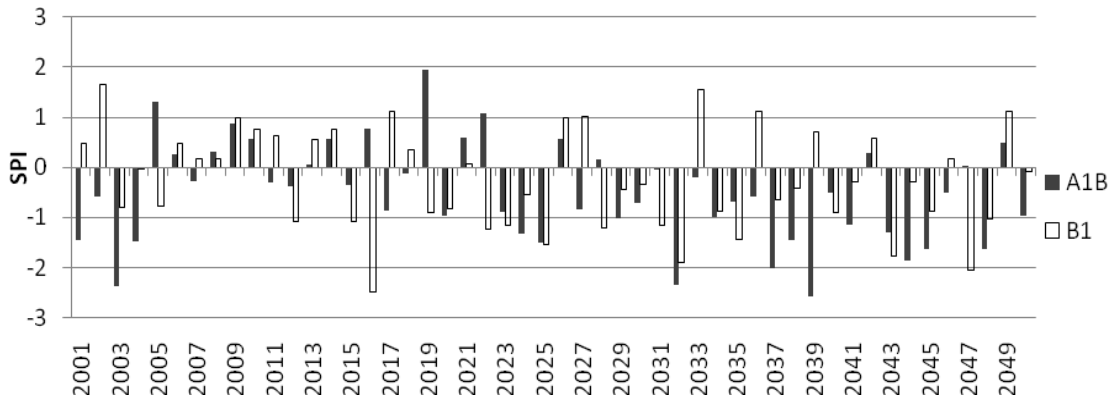

Figure 7.23: SPI characterization of REMO simulations for A1B and B1 scenarios for 2001-2050 for Pwalugu (north of Volta Basin) against base period of 1961-2000.

Table 7.4: Comparison of climate occurrences of past (1961-2005 gauged) with future (2006-2050 REMO's AIB-simulated) for the Volta Basin

	Past (gauged)	Future (REMO-simulated)
	1961-2005 No. of occurance	2006-2050 No. of occurances
Severely-extremely wet	5	5
Moderate wet	5	5
Normal year	16	10
Moderate dry	11	6
Severely dry	4	12
Severely-extremely dry	3	6

Both scenarios also agree on the few wet years that have been projected for the future. For instance, both REMO's A1B and B1 projections of 2008 and 2009 as very wet years have actually coincided with high rainfall and floods for the same years (official records). If these projections made in 2004 are anything to go by, then REMO's projections of a blend of moderate and extreme dry years for the future should be given close attention in policy formulation. The SPI also indicates an increase in frequency of moderate to severe drought for the future (Table 7.4). MM5 does not have simulated outputs for 2008 and 2009 of the Volta Basin for validation.

Vulnerability is defined by the IPCC as "the extent to which a natural or social system is susceptible to sustaining damage from [climate] change. Vulnerability is a function of the sensitivity of a system to changes in climate (the degree to which a system will respond to a given change in climate, including beneficial and harmful

effects), adaptive capacity (the degree to which adjustments in practices, processes, or structures can moderate or offset the potential for damage or take advantage of opportunities created by a given change in climate), and the degree of exposure of the system to climatic hazards" (IPCC, 2001). Rockström and Falkenmark (2000) and Friesen (2008) have noted that agricultural productivity within the basin is highly dependent on available soil moisture, also termed "blue water". In this light, the IUCN describes West Africa as among the most vulnerable regions with respect to climate change worldwide. The region is known not to be sensitized adequately to the predicted impacts of climate change so as to take actions in preparedness to cope with climate challenges. For example, the UNFCCC reports that in the Volta Basin region yields from rainfed agriculture could be reduced by up to 50 % by 2020. With agriculture being key to the development of the riparian states, losses of between 2 and 7 % of GDP are expected by the year 2100. In the area of water resources availability and management, the basin countries cannot be said to be doing any better. The Water Poverty Index (WPI) used to monitor development in water resources management credits most of the riparian states with a WPI of approximately 45 of 100 according to calculations over many years (Sullivan et al. 2001 cited in Eguavoen (2007)); this exacerbates the already gloomy situation.

The 2007 human development report of the UN Development Program (UNDP) described vulnerability in the context of climate change as "an inability to manage risk without being forced to make choices that compromise human well-being over time."

Resilience is also defined as "the capacity of a system, community or society potentially exposed to hazards to adapt by resisting or changing in order to reach and maintain an acceptable level of functioning and structure. This is determined by the degree to which the social system is capable of organizing itself to increase its capacity for learning from past disasters for better future protection and to improve risk reduction measures" (UN/ISDR, 2004). Resilience is one component that directly reduces risk. In the Volta Basin, building resilience to climate change through adaptive processes seem to be on the low priority end, as ad hoc relief measures are employed for addressing the effects of hazards without recourse to future occurrences.

In summary, the hazard factors regarding the risk of failing water resources are increasing in the basin, thus increasing the vulnerability of the population to climate shocks. With little or no resilience building, the risks for inhabitants of the Volta Basin threaten life and property, and thus need urgent attention.

7.11 Impacts of climate change on Volta Basin water resources

The impacts of climate-related factors on water resources and their management poses threats in many sectors of society. It is projected that though a general increase in rainfall is proposed by some regional models, the increases in low flow events in streams will eventually increase the occurrence of droughts which usually have severe consequences for most sectors, particularly agriculture, energy, and domestic water for most communities of the basin who depend on streams for their water needs.

On the other hand, according to the IPCC (2007), increases in the frequency and intensity of rainfall may increase the occurrence of flooding due to heavy rainfall events. Apart from the devastating consequences of flood to the vulnerable communities of the basin, groundwater recharge may also be affected, because more flash flows will be generated to the detriment of percolation; with such reductions, the availability of groundwater for drinking water and dry season irrigation could be at risk in some parts of the basin.

Water resources management has its own handicaps, but in addition to the typical problems of water management, climate change introduces another dimension and additional element of uncertainty about future water resource management, which need holistic approaches to overcome. In policies for water resources management, strategies will need to be developed to match continued evolution of the complex dynamics of water availability to address the issues. Implementation of adaptation measures, such as water conservation, reduction in water demand and use, new strategies for droughts and floods resistant farming, and the application of appropriate and pragmatic management practices will play a crucial role in the determination and reduction of the impacts of climate change on water resources of the Volta Basin.

Though regional models such as MM5 and REMO do not agree on the direction of changes within the Volta Basin, there is consensus that the impacts of

climate change on water resources could pose huge challenges to the uses and management of these resources.

7.12 Comparison of study results with previous studies

The contradicting future simulated annual discharge and changes in hydrology obtained with the use of the regional models MM5 and REMO in this study for the Volta Basin are similar to what has been obtained in other investigations. Jung (2006) coupled WaSiM version 1 with MM5 and reported that for the future of 2030-2039, an average of 5 % increase in rainfall was expected with a wide variation of 20 % - 50 % between the Sahel and the Guinea Coast. In her report, no changes are expected for interflow for the future in the entire basin. Surface runoff is projected to increase by 17 % resulting in an overall increase in discharge. Actual evapotranspiration will increase for the future Wagner (2008) agrees with results of Jung (2006).

Obuobie (2009) in an assessment of the impacts of climate changes on the hydrology of the White Volta of the Volta Basin using the soil-water assessment tool-SWAT with MM5 inputs and the climate generator LARS-WG for future scenarios, projected increases in total discharge and groundwater recharge for the periods 2030-2039 and 2070-2099. He reported 29 % increase in subsurface flow due to an increase in discharge and surface runoff. Rainfall is expected to increase by 6 % with MM5 projections and 3 % with LARS-WG, resulting in 3 % rise in discharge, 15 % increase in surface runoff and 4 % decrease in base flow. The discharge simulated with MM5 projections gives an increment of 33 % by 2030-2039.

It is worth noting that overland flow due to saturation excess is an important mechanism for runoff generation under natural vegetation, in particular at the bottom of slopes (see Hiepe, 2008). The lateral movement of water in the shallow subsurface that is usually termed interflow complicates the computation of surface runoff due to the interaction between surface and subsurface flows.

Most reports on climate and hydrology of the Volta Basin project increases in rainfall and discharge. However, reports of the IMPETUS project, which used the REMO model based on the IPCC's A1B and B1 second report emissions forcing scenarios incorporating land-use changes, forecast declines in rainfall and discharge for Benin, which is very similar in climate and hydrology to the Volta Basin and

shares the same micro-climate of West Africa. In the case of temperature, all projections of all studies for the basin agree on an increasing trend. For example, the results of the business as usual scenario, combined with IPCC Scenarios A1B and B2 through the year 2045 on plausible scenarios of future economic, demographic, and climate developments, effects of land-use and land-cover change, climate change, and demographic development on water availability and water demand for Benin (West Africa) reveal a significant decrease in water availability (surface water and groundwater) due to a decrease in rainfall and a significant increase in evapotranspiration. Although total water consumption increases strongly, it represents only about 0.5% of the yearly renewable water resources (Christoph et al., 2008). In the quantification of runoff processes and sheet and rill erosion in the Upper Ouémé River catchment in central Benin, Hiepe (2008) found that changes in climate variables led to decreases in sediment yield of 5 to 14 % in 2001-2025 and 17 to 24 % in 2026-2050, which could be attributed to increasing surface flow due to land-use changes and high rainfall events. Combined scenarios showed the dominance of land-use change leading to changes in mean sediment yield of -2 to +31 % in 2001-2025.

8 CONCLUSIONS AND OUTLOOK

8.1 Conclusions

The conclusions reached using WaSiM model agree with many in the natural science community that global warming is occurring as a result of anthropogenic activities which are causing climate change. It is therefore important to monitor the entire chain of water availability and use in order to understand and address the negative effects of climate change.

Implementing adaptation measures such as water conservation and reduction in water demand and use, new strategies for drought and flood-resistant farming, and the application of appropriate and pragmatic management practices will play a crucial role in the determination and reduction of the impacts of climate change on water resources of the Volta Basin.

The calibrated hydrological model WaSiM-Volta showed a good performance in the representation of the hydrology of the Volta Basin, and was thus suitable for the study of the hydrological dynamics of the basin. The calibration of WaSiM and the validation processes for the two sub-catchments of the basin at Pwalugu in the north and Bui in the south revealed that credible meteorological conditions, most especially rainfall and temperature, are critical in the realistic simulation of the resultant hydrological processes of the basin. The calibration period was 1968-1971 with a model warm-up period of 1961-1967 in daily, weekly and monthly aggregations. Validation was carried out for the period 1994-2001 for both catchments. The highest aggregation (monthly) exhibited the best calibration results with a coefficient of determination (R^2) of 0.98 between simulated and observed discharge and R^2=0.96 and R^2= 0.87 for the weekly and daily, respectively. The Willmott index of agreement was 0.93, 0.96, and 0.99 for the daily, weekly and monthly calibration, respectively, showing a good correlation between simulated and observed discharge. However, the model generally underestimated some peak flow that could be due to missing or inaccurate data, but simulated low and normal flow fairly well. The Nash-Sutcliffe efficiency index was 0.94, 0.83 and 0.74 for the monthly, weekly and daily discharge respectively**.**

The classification and evaluation of different SPI drought coverage according to WaSiM simulation resulted in percent areal distribution of drought intensities for

selected threshold levels and frequency analysis in percent areal distribution to determine return periods of drought intensities. From the 1980s, frequent dry periods of shorter intervals occurred between 1983 and 2001. The basin experienced at least four moderately dry years covering 50 % of the area. Simulations of changes in soil moisture for the three time slices showed that the soil profile is adequately wet during the wet season and dryer in the dry season. Simulations indicate changes in soil moisture declining from 9 % from the 1991-2000 periods to 12 % of rainfall for 2030- 2039. It also estimates higher soil moisture during the rainy season for the "future" scenario than for the "past" (1961 to 1970) due to "future" higher rainfall amounts.

The results from the comparison of the Volta Basin water balance dynamics, simulated with WaSiM-Volta model, using historical climate data from the basin for the "past", and MM5- generated climate series for the "present" and the "future" with even durations of 10 years show that in the basin in general, from the north to the south, rainfall has increased steadily from the past to the present, and it is projected to increase substantially in the north and marginally in the south from 2030 to 2039. The WaSiM simulation using REMO data show a different trend of decrease in rainfall, and consequently decreases in almost all the discharge components of the periods 1961-2000 and 2001-2050.

Analysis of climate data in the basin indicates that the months in which precipitation exceeds evapotranspiration are usually June, July, August and September. A comparison of wet and dry years shows that the ratio of direct runoff and base flow is at an average of 30 %, being high in the wet years with a sharp decline in the dry years. It is observed that total percentage discharge and surface flow have increased in the north, which might be good for dugouts and streams; the opposite is true for the south.

The probability of daily average discharge falling below 1 mm is expected to increase from 0.47 in the "past" to 0.75 for the "future" time slice of 2030 to 2039 in the south of the basin, thus increasing the frequency of low flow occurrences. The annual recharge for the Volta River System ranges from 13 % to 16 % of the mean annual precipitation, and annual rainfall amounts from the simulations show an increase of between 11 % and 20 % for the highly heterogeneous basin. It is important to note, however, that REMO gives exactly opposite outputs to the scenario outputs of MM5.

The calibration and validation results demonstrate that the model performed credibly in mimicking the daily, weekly and monthly discharge, surface runoff, interflow and base flow, soil moisture and evapotranspiration comparable to those of other numerous studies conducted within the basin at different times**.**

Modeling in general has many constraints, but is a good tool in understanding those underlying processes that are sometimes nearly impossible to measure. On the whole, the results from WaSiM-Volta show the capability of simulating and shedding light on impacts of climate variations on the hydrology of the Volta Basin.

Temperature has been rising over the years and causes increases in evapotranspiration, and hence annulling any surplus that might have been gained with the increase in rainfall amounts. With the increase in population and demand for food and increasing water use, coupled with poor water management practices and increasing risk of climate change, resultant impacts could reach undefined proportions for the inhabitants of the Volta Basin**.** The frequency of droughts has already been established to have increased over the last decades, and with the increase in high-intensity precipitation**,** flood occurrences are also eminent. The time has come to include the hazards with discovered trends into policy making for the riparian states of the Volta Basin to reduce the impacts of climate variability and increase the coping capacity of the communities. It is also now evident that, irrespective of the measures and policies aimed at mitigating the impacts of climate change, there is an urgent need to build capacity to reduce vulnerability to climate variability and change.

8.2 Outlook

Accurate estimation of the surface and subsurface hydrology is very important for sustainable management programs of water resources of any basin. However, this can only be achieved with equally accurate meteorological information. It is therefore advisable to verify as much as possible climatic data such as temperature, rainfall, humidity, wind speed, etc. It must be noted that gauged discharge is also estimated and suffer from some uncertainties. Care must be taken when simulations, which are estimates, are manipulated to fit observed measurements.

The hydrology of a basin is not only dependent on climate inputs, but also on spatial variables such as land use/land cover and topography among others. Future

scenarios were conducted with current land-use / land-cover maps, and this could lead to errors in projections. Projected simulations would be desirable if varied simulation of land use / land cover, and soil texture scenarios are modeled alongside the hydrology to access all possible scenarios to account for the feedback that might exist.

It is assumed that there are to some extent links between sea surface temperature and the rainfall distribution and pattern of the West African monsoon. Further studies concerning the influence of the sea surface temperatures on the rainfall of the Volta Basin are needed. The results fed into WaSiM simulations may give an improved view of the dynamics of the water of the Basin and increase the predictability of the hydrological impact on various scenarios.

9 REFERENCES

Acheampong SY (1996) Geochemical evolution of the shallow groundwater system in the Southern Voltaian Sedimentary Basin of Ghana. PhD dissertation, University of Nevada, Reno

Adger WN, Brooks N, Kelly M, Bentham G, Agnew M, and Eriksen S (2004) New indicators of vulnerability and adaptive capacity, Tyndall Final project Report P IT1.11: July 2001 TO June 2003

Agyare W (2004) Soil characterization and modelling of spatial distribution of saturated hydraulic conductivity at two sites in the Volta basin of Ghana. Doctoral thesis, University of Bonn, Bonn, http://www.zef.de/fileadmin/ webfiles/downloads/zefc_ecology_development/ecol_dev_17_text.pdf

Altman D (1991) Practical Statistics for Medical Research. Chapman & Hall, London.

Altman DG and Bland JM (1983) Measurement in medicine: the analysis of method comparison studies. Statistician. 32, pp. 307-317

Amani A (2001) Assessment of precipitation and resources variability across the Sahelian region, in: Gash, J.H.C., Odada, E.O., Oyebande, L. and Schulz, R.E.; Report of the International Workshop on Africa's Water Resources, Nairobi, 26-30 October 1999 (BAHC)

Amisigo BA (2005) Modelling riverflow in the Volta Basin of West Africa: A data-driven framework. PhD Thesis. Ecology and Development Series No. 34. ZEF Bonn. Cuvillier Verlag, Göttingen, http://www.glowa-volta.de/fileadmin/ template/ Glowa/ Downloads/Amisigo_doc_thesis _2006 .pdf

Anderson M P and Woessner WW (1992) Applied Groundwater Modelling. Academic Press, San Diego

Andreini M, van de Giesen N, van Edig A, Fosu M, and Andah W (2000) Volta Basin Water Balance. ZEF – Discussion Papers on Development Policy, No. 21, ZEF, Bonn

Arnold JG, Sirinivasan R, Muttiah RS, and William JR (1998) Large area hydrologic modelling and assessment, Part 1: Model development. Journal of the American water resources association, 34(1)

ASCE Task Committee on Definition of Criteria for Evaluation of Watershed Models of the Watershed Management, Irrigation, and Drainage Division (ASCE), (1993) Criteria for evaluation of watershed models. J. Irrig. Drain. Eng., 1193, 429–442

Aspden RM (2005) Agreement between two experimental measures or between experiment and theory. Journal of Biomechanics, 38, pp. 2136-2137.

Barry B, Obuobie E, Andreini M, Andah W, and Pluquet M (2005) The Volta river basin. Comprehensive assessment of water management in agriculture. Comparative study of river basin development and management. Draft http://www.iwmi.cgiar.org/assessment/research_projects/river_basin_develop ment_and_management/projects_locations/volta_river_burkina_faso_ghana.ht m

Beven K and Feyen J (2002) The future of distributed modelling. Hydrological Processes, 16, 169-172

Bevington P R and Robinson D K (1992) Data reduction and error analysis for the physical sciences. New York, McGraw-Hill

Bhalme H N and Mooley D A (1980) Large-scale drought flood and monsoon circulation. Mon. Weather Rev.: 108, 1197 - 1211

Birikundavyi S, Labib R, Trung H T, and Rousselle J (2002) Performance of neural networks in daily streamflow forecasting. J. Hydrol. Eng., 75, 392–398

Bland J M and Altman D G (1996) Transforming data. BMJ 312(7033): 770

Bland JM and Altman D G (1995. Comparing two methods of clinical measurement: a personal history. Int J Epidemiol 24 Suppl 1: S7-14

Bland JM and Altman DG (1986) Statistical methods for assessing agreement between two methods of clinical measurement. The Lancet

Blöschl,G. (1996): Scale and scaling in hydrology. Dissertation, TU Wien, 1-22.

Broekhuyse J (1983) Transformatie van Mossi land. Koninklijk Instituut voor de Tropen (Amsterdam): 168p

Brown JD and Heuvelink GBM (2005) Assessing Uncertainty Propagation Through Physically based Models of Soil Water Flow and Solute Transport. Anderson, M.G. & J.J. McDonnell (Eds) Encyclopaedia of Hydrological Sciences. Wiley Blackwell. 3456 p

Brutsaert W (1982) Evaporation into the atmosphere: theory, history and applications.

Reidel, Dordrecht.

Busche H, Hiepe C, Diekkrüger B (2005) Modelling the effects of land use and climate change on hydrology and soil erosion in a sub-humid African Catchment. Proceedings of the 3rd International SWAT Conference 2005, pp434-443Carter TR and La Rovere EL (2001) Developing and applying scenarios. In: McCarthy, J.J., Canziani, O.F., Leary, N.A., Dokken, D.J. and White, K.S. (eds.) Climate Change 2001: Impacts, Adaptation, and Vulnerability, Contribution of Working Group II to the Third Assessment Report of the Intergovernmental Panel on Climate Change, Cambridge University Press, Cambridge, 145–190

Castaing C, Billa M, Milesi JP, and Thieblemont D (2003) Notice explicative de la carte géologique et minière du Burkina Faso 1:1 000 000. Ministère des Mines, des Carrières et de l'Energie, Ouagadougou

Chekol DA (2006) Modelling of Hydrology and Soil Erosion of Upper Awash River Basin. PhD Thesis, University of Bonn: 233pp

Christoph M, Fink A, Diekkrüger B, Giertz S, Reichert B and Speth P (2008) Water SA Vol. 34 No. 4 (Special HELP edition) 2008

CLIVAR - Project (2004) National Research Council (U.S.). Committee to Review the U.S. Climate Variability and Predictability Review of the U.S. CLIVAR Project Office. Washington, DC, National Academies Press

Darko PK and Krasny J (2003) Regional transmissivity distribution and groundwater potential in hard rocks of Ghana, in Krasny, Hrkal, Bruthans (Edts): Groundwater in fractured rocks, 45-46, Prag

David S, Bowles P, and Enda O'Connell (1991) Recent advances in the modelling of hydrologic systems, North Atlantic Treaty Organization. Scientific Affairs Division, Springer, 667 pages

Diamond J (2005) Collapse: how societies choose to fail or succeed Viking: New York

Downer C W and Ogden F L (2004) “GSSHA: Model to simulate diverse stream flow producing processes.” J. Hydrol. Eng., 93,161–174

Dugue P (1989) Possibilités et limites de l’intensification des systemes de cultures vivriers en zone Soudano-Sahelienne: le cas du Yatenga (Burkina Faso). Collection Documents Systèmes Agraires No. 9(DSA/CIRAD, Montpellier, France)

Eguavoen I (2007) Now you have a new pump, you have to manage it. Household water management, water rights and institutional change in Northern Ghana. Doctoral thesis, Institute of Social Anthropology, Philosophical Faculty, Albert-Magnus Universität. Cologne/ Germany, http://www.glowa-volta.de/fileadmin/template/Glowa/Downloads/Eguavoen_phdThesis.pdf

Elston J (1983) "Climate." Potential productivity of field crops under different environments International Rice Research Institute (IRRI) Manila, Philippines: 3-14

Erpul G, Norton L D, and Gabriels D (2003) Sediment transport from interrill areas under wind-driven rain. J. Hydrol., 276, 184–197

FAO (1971-81) Soil Map of the World. United Nations Food and Agriculture Organization, UNESCO, Paris

FAO (1995) Digital soil map of the world and derived soil properties (CDROM) food and Agriculture Organization of the United Nations. FAO

FAO (2005) Irrigation in Africa in Figures. FAO Water Report No 29. Rome. 74pp

FAO (2006) Food and Africulture Organization, Global forest resources assessment 2005. Progress towards sustainable forest management. FAO Forestry Paper, 147, 348pp

Friesen J (2002) Spatio-temporal rainfall patterns in Northern Ghana. Diplom thesis, Geographic Institute, Rheinische Friedrich-Wilhelm-Universität, Bonn

Friesen J, Andreini M, Andah W, Amisigo B, and van de Giesen N (2005) Storage capacity and long term water balance of the Volta Basin, West Africa. p. 138-145. IAHS-AISH publication 296

Friesen J, Winsemius H C, Beck R, Scipal K, Wagner W, and van de Giesen N (2007) Spatial and seasonal patterns of diurnal differences in ERS Scatterometer soil moisture data in the Volta Basin, West Africa. p. 47-55. IAHS-AISH Publication 316

Friesen JC (2008) Regional vegetation water effects on satellite soil moisture estimations for West Africa. Doctoral thesis, Rheinische Friedrich Wilhelms Universität, Bonn/ Germany, http://www.glowa-volta.de/fileadmin/template/Glowa/Downloads/EDS_63__Jan_Friesen.pdf

Gallée H Moufouma-Okia W Bechtold P Brasseur O Dupays I Marbaix P Messager C Ramel R and Lebel T (2004) A high-resolution simulation of a West African rainy season using a regional climate mode. J. Geophys. Res. 109, 10.1029/2003JD004020

Garatwa W and Bollin C (2002) Disaster Risk Management Working Concept. Eschborn, Deutsche Gesellschaft für Technische Zusammenarbeit (GTZ), http://www2.gtz.de/dokumente/bib/02-5001.pdf>, last accessed 2/06/2009

Giertz S (2004) Analyse der hydrologischen Prozesse in den sub-humiden Tropen Westafrikas unter besonderer Berücksichtigung der Landnutzung am Beispiel des Aguima-Einzugsgebietes in Benin; PhD thesis; University Bonn, http://hss.ulb.uni-bonn.de/diss_online/ math_nat_fak/2004/giertz_simone/giertz.htm

Giorgi F (2006) Climate change hot-spots. Geophys. Res. Let., 33, doi:10.1029/2006GL025734

Green Cross International (2001) Trans-boundary Basin Sub-Projects: The Volta River Basin. Website: <www.gci.ch/Green- crossPrograms/ waterres/pdf/WFP_ Volta>

Green W H and Ampt G A (1911) Studies on soil physics: The flow of air and water through soils. Journal of agricultural science, 4, 1-24

Grell GA, Dudhia J, and Stauffer DR (1995) A description of the Fifth-Generation Penn State /NCAR Mesoscale Model (MM5). Tech. rept.

Gurtz J, Zappa M, Jasper K, Lang H, Verbunt M, Badoux A, and Vitvar T (2003) A comparative study in modelling runoff and its components in two mountainous catchment. Hydrological Processes, 17, 297-311

Hagemann S, Botzet M, Dümenil L and Machenhauer B (1999) Derivation of global GCM boundary conditions from 1 km land use satellite data. Max-Planck-Inst. f. Meteor., Report No. 289, Hamburg

Hayward D and Oguntoyinbo J (1987) Climatology of West Africa. Hutchindson.

Henriques AG and Santos MJJ (1999) Regional Drought Distribution Model. Phys. Chem. Earth (B) No.1-2:19-22

Herschy RW (1978) Hydrometry: principles and practices. Wiley & Sons, Chichester, 127-130

Herschy RW (1999) Hydrometry—Principles and Practices, Journal of Hydrology 222, 191–194

Hewitson BC and Crane RG (2006), Consensus between GCM climate change projections with empirical downscaling: Precipitation downscaling over South Africa, Int. J. Climatol. 26: 1315–1337 (2006)

Hiepe C (2008) Soil degradation by water erosion in a sub-humid West-African catchment: a modelling approach considering land use and climate change in Benin, Doctoral thesis, Rheinische Friedrich Wilhelms Universität, Bonn/ Germany, http://hss.ulb.uni-bonn.de/diss_online/math_nat_fak/2008/hiepe_ claudia/ index.htm

Hiepe C and Diekkrüger B (2007) Modelling soil erosion in a sub- humid tropical environment at the regional scale considering land use and climate change. Book of abstracts, 4th International SWAT conference, UNESCO-IHE Institute for Water Education, Delft, The Netherlands. July 4-6, 2007

Hisdal H and Tallaksen L M (2000) Assessment of the Regional Impact of Droughts in Europe. Drought Event Definition Technical Report to the ARIDE project No. 6

Hodnett M G and Tomasella J (2002) Marked differences between van Genuchten soil water-retention parameters for temperate and tropical soils: a new water retention pedo-transfer functions developed for tropical soils. Geoderma, 108, 155-180.

Hulme M, Doherty R, Ngara T, New M, and Lister D (2001) African climate IAHS Publ., No. 252: p. 307-314

International Institute of Environment and Development - IIED (1992) Annual report

IPCC 2007 Climate Change (2007) The Physical Science Basis. Contribution of working group I to the fourth Assessment Report of the Intergovernmental Panel on Climate Change [Solomon, S., D. Qin, M. Manning, Z. Chen, M. Marquis, K.B. Averyt

IPCC (2001) Climate Change (2001) Synthesis Report. A Contribution of Working Groups I, II, and III to the Third Assessment Report of the intergovernmental Panel on Climate Change. Watson, R.T. et al. (Eds.). Cambridge University Press, Cambridge, New York, p. 398

IPCC (2001) Climate Change -The Scientific Basis, J. T. Houghton et al., (Eds) Cambridge Univ. Press, Cambridge

IPCC (2007) IPCC Fourth Assessment Report: Climate Change 2007. Geneva, Switzerland

IPCC 2007 Climate Change 2007 Impacts, Adaptation, and Vulnerability. Contribution of Working Group II to the Fourth Assessment Report of the Intergovernmental Panel on Climate Change [Parry, Martin L., Canziani, Osvaldo F., Palutikof, Jean P., van der Linden, Paul J., and Hanson, Clair E. (eds.)]. Cambridge University Press, Cambridge, United Kingdom, 1000 pp

IPCC AR4 (2005) are available (https://esg.llnl.gov:8443/home/publicHomePage.do)

IUCN (2004) Reducing West Africa's Vulnerability to Climate Impacts on Water Resources, Wet lands and Desertification: Elements for a Regional Strategy for Preparedness and Adaptation. Niasse, Madiodio, Afouda, Abel, Amani, Abou.(Eds.) Gland, Switzerland and Cambridge, UK.xviii+66pp

Jacob D Van den Hurk BJJM Andrae U Elgered G Fortelius C Graham LP Jackson SD Karstens U Koepken C Lindau R Podzun R Rockel B Rubel F Sass BH Smith R and Yang X (2001) A comprehensive model intercomparison study investigating the water budget during the PIDCAP period. Meteorol. Atmos. Phys. 77, 19-44

Jacob D, Bärring L, Christensen OB, Christensen JH, de Castro M, Déqué M, Giorgi F, Hagemann S, Hirschi M, Jones R, Kjellström E, Lenderink G, Rockel B, Sánchez ES, Schär C, Seneviratne S, Somot S, van Ulden A, van den Hurk B (2007) An intercomparison of regional climate models for Europe: model performance in present-day climate. *Climatic Change*, 81:31-52

Jacob D Van den Hurk BJJM Andrae U Elgered G Fortelius C Graham LP Jackson SD Karstens U Koepken C Lindau R Podzun R Rockel B Rubel F Sass BH Smith R and Yang X (2001) A comprehensive model intercomparison study investigating the water budget during the PIDCAP period. Meteorol. Atmos. Phys. 77, 19-44

Jain S, Storm B, Bathurst J, Refsgaard J, and Singh R (1992) Application of the SHE to catchments in India Part 2. Field experiments and simulation studies with the SHE on the Kolar subcatchment of the Narmand river. Journal of Hydrology 140, 25–47

Jarque CM and Bera AK (1980) Efficient tests for normality, heteroskedasticity, and serial independence of regression residuals. Economic Letter 6, 255–259

Jasper K, Gurtz J, and Lang H (2002) Advances flood forecasting in Alpine watersheds by coupling meteorological observations and forecasts with a distributed hydrological model. Journal of Hydrology, 267, 40-52

Jenkins G S, Gaye A T, and Sylla B (2005) Late 20th century attribution of drying trends in the Sahel from the Regional Climate Model (RegCM3), Geophys. Res. Lett., 32, L22705, doi:10.1029/2005GL024225

Jenkins G S, Kamga A, Adamou G, Diedhiou A, Morris V, and Joseph E (2002) Summary of the Workshop on Modeling the West African Climate System with Global and Regional Scale Climate Models: Relevance to Understanding Climate Variability, Land-Use, and Climate Change, BAMS, 583-595, 2002

Johnson M S, Coon W, Mehta V, Steenhuis T, Brooke E, and Boll J (2003) Applications of two hydrologic models with different runoff mechanisms to a hillslope dominated watershed in the northeastern U.S.: A comparison of HSPF and SMR. J. Hydrol., 284, 57–76

Jung G (2006) Regional Climate Change and the Impact on Hydrology in the Volta Basin of West Africa. Dissertation Garmisch-Partenkirchen, Germany

Kalin L, Govindaraju R S, and Hantush M M (2003) Effect of geomorphological resolution on modelling of runoff hydrograph and sedimentograph over small watersheds. J. Hydrol., 276, 89–111

Kalin L, Govindaraju R S, and Hantush M M (2003) Effect of geomorphological resolution on modeling of runoff hydrograph and sedimentograph over small watersheds. J. Hydrol., 276, 89–111

Kasei C N (1988) The Physical environment of semi-arid Ghana. In: Challenges in Dryland Agriculture. A global perspective (ed). P. W. Unger. T. V. Sneed, W. R. Jordan and R. Jensen. : 350 – 354

Kasei C N and Sallah P Y K (1993) Drought evasion in crop production under a monomodal rainfall pattern. Paper presented at the third workshop on improving farming systems in the Savannah Zone of Ghana. April 17 - 29

Kasei C N, Mercer-Quarshie H, and Sallah P YK (1995) Identifying probable dry periods in maize production under a monomodal rainfall regime in Northern Ghana. 29 May - 2nd June 1995, IITA Proceedings of a Regional Maize Workshop A WECAMAN/IITA publication March, 1997

Kasei R (2006) Determination of Sensible Heat Flux from Large Aperture Scintillometer Measurements in the Volta Basin of Ghana. M.Phil Thesis. University of Cape Coast/ Wageningen University, Ghana, 119

Kilgore JL (1997) Development and evaluation of a GIS based spatially distributed unit hydrograph model. MSc. Thesis, Virginia Polytechnic Institute and State University

Krause J (2003) Inverse hydrologische Modellierung für das Einzugsgebiet der Ammer mittels WaSiM-ETH und PEST, University of Trier, master thesis (in german), 135 p

Krause P, Boyle DP, and Base F (2005) Comparison of different efficiency criteria for hydrological model assessment. Advances in Geosciences, 5,89–97

Kunstmann H and Jung G (2005) Impact of regional climate change on water availability in the Volta basin of West Africa. In: Regional Hydrological Impacts of Climatic Variability and Change. IAHS Publ. 295

LeBarbé L and Lebel T (1997) Rainfall climatology of the HAPEX-Sahel rgion during the years 1950-1990; Journal of Hydrology; Vol. 188-189: pp. 43–73

LeCompte FJ, Iannarilli MR, Hess GA, Freund DL, McMaster DB and Nichols JE (1994) Rice, Proceedings of the IRIS Specialty Group on Targets, Backgrounds, and Discrimination, Monterey, CA, February 1, 1994

Leemhuis C (2005) The Impact of El Niño Southern Oscillation Events on Water Resource Availability in Central Sulawesi, Indonesia: A hydrological modelling approach. Dissertation. Göttingen, Germany

Legates D R and McCabe G J (1999) Evaluating the use of goodness-of-fit measures in hydrologic and hydroclimatic model validation. Water Resources Research, 35, 233-241

Leube A and Hirdes W (1986) The Birimian Supergroup of Ghana: Depositional environment, Structural Development and Conceptual Model of an Early Proterozoic Suite. Hannover, Federal Ministry for Economic Cooperation, p. 259

M. Tignor and H.L. Miller (Eds.)]. Cambridge University Press, Cambridge, United Kingdom and New York, NY, USA, 996pp

Maidment DR (1992) Handbook of Hydrology. McGraw-Hill, Inc

Majewski D (1991) The Europa-Modell of the Deutscher Wetterdienst. Seminar Proceedings ECMWF 2, 147-191

Mamdouh S (2002) Hydrology and water resources of Africa, Springer, 659 Pages

Martin N (2005) Development of a water balance for the Atankwidi catchment, West Africa – A case study of groundwater recharge in a semi-arid climate. PhD

thesis; Georg- August-Universität Göttingen, Germany, http://www.glowa-volta.de/fileadmin/template/Glowa/Downloads/thesis_martin.pdf

Martin N and Giesen N van de (2005) Spatial distribution of groundwater production and development potential in the Volta river basin of Ghana and Burkina Faso. Water International, 30(2), 239–249,

May W and Röckner E (2001) A time-slice experiment with the ECHAM4 AGCM at high resolution: the impact of horizontal resolution on annual mean climate change; Climate Dynamics; Vol. 17: pp. 407–420

McKee T B, Doesken N J and Kleist J (1993) The Relationship of Drought Frequency and Duration to Time Scales. 8th Conference on Applied Climatology, Anaheim, CA, USA,: 179-184

Mearns LO, Giorgi F, Whetton P, Pabon D, Hulme M, and Lal M (2004) Guidelines for use of climate scenarios developed from regional climate model experiments, Tech. rep., Data Distribution Centre of the IPCC

Merz R and Bloschl G (2004) Regionalization of catchment model parameters. J. Hydrol., 287, 95–123

Monteith JL (1975) Vegetation and the atmosphere, vol.1:Principles Academic Press.

Moussa R (2008) Significance of the Nash-Sutcliffe efficiency measure for linear rise and exponential recession in event based flood modelling. Geophysical Research Abstracts, Vol. 10, EGU2008-A-08369, 2008 SRef-ID: 1607-7962/gra/EGU2008-A-08369 EGU General Assembly 2008 http://www.fao.org/DOCREP/005/Y3948F/y3948f00.htm#toc

Nakicenovic N and Swart R (Eds.) (2000) Emission Scenarios. 2000. Special Report of the Intergovernmental Panel on Climate Change. Cambridge University Press, U.K., 570pp

Nash J E and Sutcliffe J V (1970) River flow forecasting through conceptunal models. Journal of Hydrology, 10, 282-290

Nathan C (1970) Framework for River Basin Planning. Ghana Sector Studies. Interim Report for Ministry of Finance and Economic Planning

Nicholson S (1994) Recent rainfall fluctuations in Africa and their relationship to past conditions over the continent. The Holocene 4, 2, 121-131

Nicholson S (2005) On the question of the ‘‘recovery’’ of the rains in the West African Sahel. Journal of Arid Environments 63: 615-641

Nicholson SE (1979) Revised rainfall series for the West African subtropics. Monthly Weather Review, 107, 620-623

Nicholson SE (1983) Recent rainfall fluctuations in Africa and their relationship to past conditions over the continent. The Holocene 4, 2, 121-131

Nicholson SE (1983) Sub-Saharan Rainfall in the Years 1976-1980: Evidence of Continued Drought. Monthly Weather Review, 111, 8, 1646-1654

Nicholson SE (1985) Sub-Saharan rainfall 1981: - 1984:. Journal of Climate and Applied Meteorology, 24, 1388-1391

Nicholson SE (1993) An Overview of African Rainfall Fluctuations of the Last Decade. Journal of Climate, V6, 7. 1463-1466

Nicholson SE (1993) An Overview of African Rainfall Fluctuations of the Last Decade. Journal of Climate, V6, 7. 1463-1466

Nicholson SE (2007) A revised picture of the structure of the "monsoon" and land ITCZ over West Africa. Submitted to the Bulletin of the American Meteorological Society

Nicholson SE and Palao IM (1993) A Re-Evaluation of Rainfall Variability in the Sahel .Part I. Characteristics of Rainfall Fluctuations. Int. Journal of Climatology, 13, 371-389

Nicholson SE, Ba MB and Kim JY (1996) Rainfall in the Sahel during 1994 Journal of Climate, 9, July, 1673-1676

Nicholson SE, Marengo JA, Kim J, Lare AR, Galle S, Kerr YH. (1997) A daily resolution evapoclimatonomy model applied to surface water balance calculations at the HAPEX-Sahel supersites. Journal of Hydrology, 188-189 (1-4), pp. 946-964

Nicholson SE, Tchayi MGN and Bertrand JJ (1996) The Diurnal and Seasonal Cycles of Desert Dust over Africa North of the Equator . Journal of Applied Meteorology, 36, 868-882

Niehoff D (2001) Modellierung des Einflusses der Landnutzung auf die Hochwasserentstehung in der mesoskala. Dissertation, Universität Potsdam,

Obuobie E (2008) Estimation of groundwater recharge in the context of future climate change in the White Volta River Basin. Doctoral thesis, Rheinische Friedrich Wilhelms Universität, Bonn/ Germany, http://www.glowa-volta.de/fileadmin/template/Glowa/ Downloads/Obuobie_No_62_full.pdf

Oguntunde P G (2004) Evapotranspiration and complimentarity relations in the water balance of the Volta Basin: Field measurements and GIS-based regional estimates;. Ecology and Development Series No. 22, Cuvillier Verlag Göttingen, http://www.zef.de/fileadmin/webfiles/ downloads/zefc_ecology_ development/ecol_dev_22_text.pdf

Oguntunde PG, Friesen J, Giesen N van de, Hubert HG, and Savenije HHG (2006) Hydroclimatology of the Volta River Basin in West Africa: Trends and variability from 1901 to 2002 Physics and Chemistry of the Earth 31 (2006) 1180–1188

Oke TR (1987) Boundary Layer Climates. Routledge.

Oladipo E O (1985) A comparative performance analysis of three meteorological drought indices. 5, 655 - 664

Opoku-Ankomah Y (1998) Volta Basin System Surface Water Resources in Water Resources Management Study. Information Building Block. Part II, Vol. 2. Ministry of Works and Housing. Accra, Ghana

Opoku-Ankomah Y (2000) Impacts of Potential Climate Change on River Discharge in Climate Change Vulnerability and Adaptation Assessment on Water Resources of Ghana. Water Research Institute (CSIR), Accra, Ghana

Paeth H and Thamm HP (2007) Regional modelling of future African climate including greenhouse warming and land degradation. – In: Climatic Change 83, 401-427

Paeth H Born K Podzun R and Jacob D (2005) Regional dynamic downscaling over West Africa: Model evaluation and comparison of wet and dry years. Meteorol. Z., 14, 349-367

Page CM and Jones RN (2001) Coupling a climate scenario generator with impact models using OzClim. In: Proceedings of the MODSIM Congress, Canberra

Palmer W C (1965) Meteorological drought.U. S. Weather Bureau Res. paper No. 45

Parker DE and Alexander LV (2002) Global and regional climate in 2001. Weather 57,328-340

Pearson K (1900) On the criterion that a given system of deviations from the probable in the case of a correlated system of variables is such that it can be reasonably supposed to have arisen from random sampling. Philosophical Magazine Series 5, 50:157-175, 1900

Peschke G (1989) Localizing groups with action, Publicacions Matemátiques, Vol 33 (1989), 227-234

Pielke RA (2001) Influence of the spatial distribution of vegetation and soils on the prediction of cumulus convective rainfall. Rev. Geophysics 39, 151-177

Pierce DA and Schafer DW (1986) Residuals in Generalized Linear Models, Journal of the American Statistical Association, 81, 977-986

PPMED (1987) Ministry of Finance and Economic Planning (Accra, Ghana)

Rassmusson EM, Dickinson RE, Kutzbach JE and Cleaveland MK (1993) Climatology. In: Maidment, D.R. ed. Handbook of Hydrology. McGraw-Hill, Inc., New York, NY, 2.1-2.44

Refsgaard A and Storm B (1996) Distributed physically-based modelling of the entire land phase of the hydrological cycle. In: Abbott, M. B. and Refsgaard, J. C. (Eds.): Distributed hydrological modelling. Kluwer Academic Publisher, Dordrecht, 55-69

Rockström J and Falkenmark M (2000) Semiarid crop production from a hydrological perspective: gap between potential and actual yields. Critical Reviews in Plant Sciences, 19: 319–346

Rodier J (1964) Régimes Hydrologiques de l'Afrique Noire à Ouest du Congo. ORSTOM, Paris

Roeckner E Arpe K Bengtsson L Christoph M Claussen M Dümenil L Esch M Giorgetta M Schlese U and Schulzweida U (1996) The atmospheric general circulation model ECHAM-4: Model description and simulation of present-day climate. Max-Planck-Inst. f. Meteor., Report No. 218. Hamburg

Roeckner E et al. (2003) The atmospheric general circulation model ECHAM 5. PARTI: Model description. MPI Report, 349, 127pp

Sastry PSN (1976) Climate and crop planning with particular reference to rainfall. In: Climate and Rice, Proceedings of the Symposium, International Rice Research Institute, 1976, pp. 5163

Schellekens J (2000) Hydrological processes in a humid tropical rainforest: a combined experimental and modelling approach. Dissertation, Vrije Universiteit Amsterdam, 7-9

Schnitzler K-G Knorr W Latif M Bader J and Zeng N (2001) Vegetation feedback on Sahelian rainfall variability in a coupled climate land-vegetation model. Max-Planck-Inst. f. Meteor., Report No. 329, Hambrug

Schulla J (1997) Hydrologische Modellierung von Fliessgebieten zur Abschatzung der Folgen van Klimaandenmgen. Dissertation ETH 12018, Verlag Geographisches Institut ETH Zurich

Schulla J and Jasper K (1999) Model description WaSiM-ETH, ETH, Zürich, http://www.igm.uni-hohenheim.de/cms/fileadmin/documents/Project Docs/ OtherDocuments/wasim00english.pdf".

Schulla J and Jasper K (2000) Model Description WASIM-ETH (Water Balance Simulation Model ETH), ETH-Zurich, Zurich.

Scipal K, Wagner W, Trommler M, and Naumann K (2002) The global soil moisture archive 1992-2000 from ERS scatterometer data: First results. p. 1399-1401. International Geoscience and Remote Sensing Symposium (IGARSS)

Semazzi HF M and Sun L (1995) On the modulation of the Sahelian summer rainfall by bottom topography. AMS 75th anniversary. Global Climate Change Conference. Houston Texas January 1995

Semazzi FHM and Song Y (2001) A GCM study of climate change induced by deforestation in Africa. Climate Res. 17, 169-182

Servant E, Patureel I, Kouamé B, Ouédraogo T, Boyer JF, Lubés-Neil H, Fritsch JM, Masson JM and Marieu B (1998) Identification, characterization and consequences of a hydrological variability in West and Central Africa; In: Proc. Int. Conf. at Abidjan on the variability of water resources in Africa in the 20th century, IAHS Publ., No. 252: p. 307-314

Shahin M (2002) Hydrology and water resources of Africa. Water Science and Technology library. Kluwer academic publisher, Dordrecht, Netherlands. 659p

Singh V P and Woolhiser DA (2002) Mathematical modelling of watershed hydrology. Journal of Hydrologic Engineering 7:270-292

Stadler C (2002) Anwendung des hydrologischen flächendifferenzierten Wasserhaushaltmodell WaSIM-ETH im Einzugsgebiet der Mangfall. Diplom thesis, Universität Augsburg, Augsburg

Sintondji L (2005) Modelling of process rainfall-runoff in the Upper Quémé catchmentarea (Terou) in a context of climate change: extrapolation from the local scale to a regional scale. PhD Thesis. Shaker Verlag, Aachen, Germany

Storch H and Stehr N (2006) Anthropogenic climate change - a reason for concern since the 18th century and earlier. Geogr. Ann., 88 A (2): 107–113

Sullivan CA (2001) The potential for calculating a meaniful water poverty index. Water Int 26: 471-480

Texier D de Noblet N and Braconnot P (2000) Sensitivity of the African and Asian monsoons to mid-holocene insolation and data-inferred surface changes. J. Cimate 13, 164-181

Thorpe AJ (2005) Climate change prediction. A challenging scientific problem. A paper produced on behalf of the Institute of Physics, London, UK

Thywissen K (2006), Components of Risk-A comparative glossary. UNU Institute for Environment and Human Security (UNU-EHS), Germany

Troch PA, Paniconi C, and McLaughlin (2003) catchment-scale hydrological modelling and data assimilation, Preface/Advances in Water Resources 26:131-135

UN/ISDR (2004) Living with Risk: A global review of disaster reduction initiatives. 2004 Version, Volume II Annexes. Geneva

UNEP- United Nations Environment Programme (2008) UNEP Year Book: an overview of our changing environment 2008

UNEP -United Nations Environmental Protection (2001) Proposal for a Project Development and Preparation Facility (PDF) Block B Grant: Benin, Burkina Faso, Côte d'Ivoire, Ghana, Mali, Togo. Integrated Management of the Volta River Basin. Available at http://www.gefweb.org/COUNCIL/GEF_C15/GEF_C15_Inf.13/ PDFBVOLTAFINALSENT GEFSEC.pdf. Accessed in November 2004

UNESCO (1978) Some Suggestions on Teachings about Human Rights, UNESCO, Paris

Van Belle G (2008) Statistical rules of thumb, second edition, Jon Wiley & sons, Inc. Hoboken, New Jersey

van Edig A, van de Giesen N, Andreini M, and Laube W (2001) Institutional and legal aspects of the (transboundary) Water Resources Commission in Ghana. Wasserkonflikte in der Dritten Welt, 18

Van Genuchten M TH (1980) A closed form equation for predicting the hydraulic condictivity of unsaturated soils. Soil Science Society, 44, 892-898

Verbunt M, Gurtz J, Jasper K, Lang H, Warmerdam P, and Zappa M (2003) The hydrological role of snow and glaciers in alpine river basins and the distributed modelling. Journal of Hydrology, 282, 36-55

Vizy EK and Cook KH (2002) Development and application of a meso-scale climate model for the tropics: Influence of sea surface temperature anomalies on the West African monsoon. J.Geophys. Res. 107, 10.1029/2001JD000686

von Storch H and FW Zwiers (1999) Statistical analysis in climate research. Cambridge University Press, Cambridge, UK, 484pp

Wagner S (2008) Water Balance in a Poorly Gauged Basin in West Africa Using Atmospheric Modelling and Remote Sensing Information. Doctoral Thesis, Intitut für Wasserbau, Universität Stuttgart, Germany

Westgard JO and Hunt .R (1973) Use and interpretation of common statistical tests in method-comparison studies. Clinical Chemistry, 19, 49-57

Willmott CJ (1981) On the validation of models. Physical Geography 2, 184-194.

Willmott CJ (1984) On the evaluation of model performance in physical geography. in Spatial Statistics and Models, G.L. Gaile, and C.J. Willmott (Editors). D. Reidel, Dordrecht, 443-460

World Bank (1992) World Development Report 1992: Development and the Environment. Oxford University Press, Oxford, for World Bank, Washington DC. 308 pp

Xu C (1999) Operational testing of a water balance model for predicting climate change impacts, Jou Agricultural and Forest Meteorology, 98-99, 295-304

Yildiz O (2007) Investigating frequency and spatial characteristics of drought in the central anatolian region, Turkey. International Congress on River Basin Management.http://www.dsi.gov.tr/english/congress2007/chapter_3/91.pdf

Zeng N and Neelin JD (2000) The role of vegetation-climate interaction and interannual variability in shaping the African Savanna. J. Climate, 13, 2665-2670

Zeng N Hales K and Neelin JD (2002) Nonlinear dynamics in a coupled vegetation atmosphere system and implications for desert-forest gradient. J. Climate 15, 3474-3487

10 APPENDIX

APPENDIX I Data Inventory			UTM coordinates		Climate data used				
#	Station ID	Elevation [m]	Easting	Northing	Rainfall [mm]	Temperature[°C]	Rel. Humidity [%]	Windspeed[ms-1]	Sunshine Duration[1/1]
1	ABENASI	166	715872	663892	-	1965-2004	1965-2004	1965-2004	1965-2004
2	ACCRA	69	813938	620054	-	1966-1968	1965-2004	1966-1968	1965-2004
3	ADA	7	904572	640105	-	1967-1969	1966-1968	1966-1968	1967-1969
4	ADEISO	67	778741	640177	-	1965-2004	1965-2004	1965-2004	1965-2004
5	Adidome	8.8	889381	671838	1964-1966,1968-1982,1984-1985,1991-2000,2002-2006	1965-2004	1965-2004	1965-2004	1965-2004
6	Agogo	426.5	711833	750216	1961-1993,2003	1965-2004	1963-1971	1965-2004	1965-2004
7	Ahunda-Adaklu	76.2	892903	697704	1963-1985,1989-1994,2003	1965-2004	1965-2004	1965-2004	1965-2004

8	AIY	50	559143	556686	-	1967-1968	1965-2004	1965-2004	1965-2004
9	AKA	285	878559	822784	-	1965-2004	1965-2004	1965-2004	1965-2004
10	Akatsi School	45.7	920757	677590	1961-2005	1965-2004	1965-2004	1965-2004	1965-2004
11	AKUMADAN	316	615902	818393	-	1965-2004	1965-2004	1965-2004	1965-2004
12	AKUSE	17.4	845024	675257	1961-2006	1965-2004	1966-1968	1966-1968	1966-1969
13	AMEDIKA	59	898997	677004	-	1965-2004	1965-2004	1965-2004	1965-2004
14	ANUM	215	850694	719662	-	1965-2004	1965-2004	1965-2004	1965-2004
15	ANYINAM	183	771052	706523	-	1965-2004	1965-2004	1965-2004	1965-2004
16	Aribinda	370	729837	1574214	1961-2006	1965-2004	1965-2004	1965-2004	1965-2004
17	ASAMANKESE	87	758387	649308	-	1965-2004	1965-2004	1965-2004	1965-2004
18	ASSIN	200	242938	121689	-	1966-1968	1965-2004	1965-2004	1965-2004
19	Ash_Bekwai	228.6	845024	675257	1963-1986,1988-1994,2003	1965-2004	1964-1969	1965-2004	1965-2004
20	Ashanti-Mampong	457.2	676719	781422	-	1965-2004	1963-1970	1965-2004	1965-2004
21	ASU	100	786044	658650	-	1965-2004	1965-2004	1965-2004	1965-2004
22	ASUANSI	50	695807	586415	-	1965-2004	1965-2004	1965-2004	1965-2004
23	Atebubu	121.9	722413	857188.1	-	1965-2004	1961-1969	1965-2004	1965-2004
24	Aveyime	6.1	872776	668041.5	-	1965-2004	1963-1969	1965-2004	1965-2004

25	AWASO	200	579304	689353	-	1965-2004	1965-2004	1965-2004	1965-2004
26	AXIM	40	585031	538289	-	1966-1968	1966-1968	1966-1968	1965-2004
27	Babile	304.7	520060	1162544	1961-1963,1969-2006	1965-2004	1965-2004	1965-2004	1965-2004
28	Bagassi	280	467312	1298927	1961-2004	1965-2004	1965-2004	1965-2004	1965-2004
29	Baguéra	315	235146	1165035	1961-2006	1965-2004	1965-2004	1965-2004	1965-2004
30	Bam (Tourcoing)	264	662461	1474120	1961-2006	1965-2004	1965-2004	1965-2004	1965-2004
31	Banfora	284	306372	1175621	1961-1998	1965-2004	1965-2004	1965-2004	1965-2004
32	Banfora Agri	270	306366	1174515	1961-2005	1965-2004	1965-2004	1965-2004	1965-2004
33	Bani	310	806092	1518554	1961-2006	1965-2004	1965-2004	1965-2004	1965-2004
34	Baraboulé	308	805431	1573911	1965-2006	1965-2004	1965-2004	1965-2004	1965-2004
35	Barekese	-999.9	872776	668041.5	-	1965-2004	1969-1971	1965-2004	1965-2004
36	Barsalogho	330	708970	1484400	1961-2006	1965-2004	1965-2004	1965-2004	1965-2004
37	BATIE	298	509116	1092632	-	1965-2004	1965-2004	1965-2004	1965-2004
38	Batié	298	508771	1092146	1961-2006	1965-2004	1965-2004	1965-2004	1965-2004
39	Bechem	289.4	606755	783072	1961-1994,2003	1965-2004	1965-2004	1965-2004	1965-2004
40	Berekum	304.7	545976	823517	1961-2006	1965-2004	1961-1971	1965-2004	1965-2004

41	BIBIANI	233	571896	715136	-	1966-1968	1965-2004	1965-2004	1965-2004
42	Bilanga	281	823861	1389204	1970-2006	1965-2004	1965-2004	1965-2004	1965-2004
43	BOB	247	682414	739345	-	1965-2004	1965-2004	1965-2004	1965-2004
44	Bobiri	213.3	682389	739048	1961-1994,2003	1965-2004	1965-2004	1965-2004	1965-2004
45	Bobo-Dioulasso	432	358054	1235089	1961-2006	1961-1985	1966-1969	1967-1969	1966-1969
46	BODWESANGO	257	675181	695090	-	1965-2004	1965-2004	1965-2004	1965-2004
47	Bogandé	250	811369	1436677	1961-2006	1965-2004	1965-2004	1965-2004	1965-2004
48	Bole	299.5	556784	-999.958	1961-1964, 1966-2006	1961-2004	1999-2003	1961-2004	1961-2004
49	Bolgatanga	213	735096	1192848	1975-1985,1988-1994,2002	1965-2004	1965-2004	1965-2004	1965-2004
50	Bomborokuy	279	393744	1442870	1961-2006	1965-2004	1965-2004	1965-2004	1965-2004
51	Bondoukuy	359	416130	1310083	1963-2006	1965-2004	1965-2004	1965-2004	1965-2004
52	Boromo	264	508717	1296699	1961-2006	1961-1985	1966-1969	1966-1969	1966-1969
53	BOSOSO	420	785848	699219	-	1965-2004	1965-2004	1965-2004	1965-2004
54	Boulbi	315	659902	1352421	1961-2006	1965-2004	1965-2004	1965-2004	1965-2004
55	Boulsa	313	763949	1399657	1961-2006	1965-2004	1965-2004	1965-2004	1965-2004
56	Boura	281	554613	1221554	1961-2006	1965-2004	1965-2004	1965-2004	1965-2004

57	BOURZANGA	329	656796	1513254	-	1965-2004	1965-2004	1965-2004	1965-2004
58	BUNSO	210	333338	178849	-	1966-1968	1965-2004	1965-2004	1965-2004
59	station missings	-999.9	-999.9	-999.9	-	1966-1968	1965-2004	1965-2004	1965-2004
60	Boussé	345	621620	1400903	1961-2006	1965-2004	1965-2004	1965-2004	1965-2004
61	BUAKA	230	547944	707741	-	1965-2004	1965-2004	1965-2004	1965-2004
62	Bui	106.6	580653	970977	1961-1983,1985-2006	1965-2004	1961-1970	1965-2004	1965-2004
63	Dakiri	280	800148	1469768	1962-2006	1965-2004	1965-2004	1965-2004	1965-2004
64	Dano	290	492357	1232566	1961-2006	1965-2004	1965-2004	1965-2004	1965-2004
65	DEDOUGOU	299	447455	1378297	-	1961-1985	1965-2004	1965-2004	1966-1969
66	DIEBOUGOU	294	472665	1212411	-	1965-2004	1965-2004	1965-2004	1965-2004
67	Diébougou	294	472686	1212674	1961-2006	1965-2004	1965-2004	1965-2004	1965-2004
68	DIONKELE	342	312928	1303266	-	1965-2004	1965-2004	1965-2004	1965-2004
69	DISSIN	310	507265	1208715	-	1965-2004	1965-2004	1965-2004	1965-2004
70	Djibo	274	648975	1559223	1961-2006	1965-2004	1965-2004	1965-2004	1965-2004
71	DORI	276	378744	1036271	-	1961-1985	1966-1969	1966-1969	1966-1969
72	DODOWA	129	819324	651437	-	1965-2004	1965-2004	1965-2004	1965-2004
73	EFI	311	676825	757756	-	1965-2004	1965-2004	1965-2004	1965-2004

74	Ejura	228.5	680276	816456	1961-2006	1966-1968	1961-1970	1965-2004	1965-2004
75	ESSIAMA	4	572087	545644	-	1965-2004	1965-2004	1965-2004	1965-2004
76	FADA N'GOURMA	292	863803	1335417	-	1961-1985	1966-1969	1966-1969	1966-1969
77	Forifori	152.5	794743	756141	1972-1997	1965-2004	1965-2004	1965-2004	1965-2004
78	FRANKADUA	75	852551	701208	-	1965-2004	1965-2004	1965-2004	1965-2004
79	GAOUA	333	479908	1142386	-	1966-1969	1966-1969	1966-1969	1966-1969
80	Garu	237.7	809798	1200837	1976-1986,1988-1994,2005-2006	1965-2004	1965-2004	1965-2004	1965-2004
81	GOASO	213	553431	751961	-	1965-2004	1965-2004	1965-2004	1965-2004
82	GOURCY	332	570412	1459428	-	1965-2004	1965-2004	1965-2004	1965-2004
83	Ho	158	883443	730865	1961-2006,	1961-2004	1966-1968	1961-2004	1961-2004
84	Hohoe	169.1	884845	791788	1961-1998,2001	1963-1994	1965-2004	1965-2004	1965-2004
85	HOUNDE	324	443630	1269574	-	1965-2004	1965-2004	1965-2004	1965-2004
86	INC	50	645999	551281	-	1966-1968	1965-2004	1965-2004	1965-2004
87	INSU	30	618165	617560	-	1965-2004	1965-2004	1965-2004	1965-2004
88	KADE	137	739822	675043	-	1965-2004	1965-2004	1965-2004	1965-2004
89	KANAYER	229	132291	175305	-	1966-1968	1965-2004	1965-2004	1965-2004
90	KAMBOINCE	300	657567	1378679	-	1965-2004	1965-2004	1965-2004	1965-2004

91	KAMPTI	340	448855	1120305	-	1965-2004	1965-2004	1965-2004	1965-2004
92	KAYA	313	707781	1449067	-	1965-2004	1965-2004	1965-2004	1965-2004
93	Kete-Krachi	122	827210	865183	1961-2006,	1961-2004	1961-1969	1961-2004	1961-2004
94	Kintampo	372.6	641416	890047	1961-2006	1965-2004	1965-2004	1965-2004	1965-2004
95	KOFORIDUA	167	804436	673494	-	1976-2000	1965-2004	1965-2004	1965-2004
96	KOMBISSIRI	275	681393	1334572	-	1965-2004	1965-2004	1965-2004	1965-2004
97	KONONGO	235	697184	732024	-	1966-1968	1965-2004	1965-2004	1965-2004
98	KOSSOUDOUGOU	295	800191	1431473	-	1965-2004	1965-2004	1965-2004	1965-2004
99	KOUDOUGOU	250	568858	1356215	-	1965-2004	1965-2004	1965-2004	1965-2004
100	KOUPELA	275	788359	1348329	-	1965-2004	1965-2004	1965-2004	1965-2004
101	Kpandu	213.3	800169	774617	1961-2006	1966-1968	1965-2004	1965-2004	1965-2004
102	Kpeve	130.7	868616	739992	1961-2001	1961-2000	1965-2004	1965-2004	1965-2004
103	KPONG	85	841407	680979	-	1966-1968	1965-2004	1965-2004	1965-2004
104	KUKUOM	157	560810	740915	-	1965-2004	1965-2004	1965-2004	1965-2004
105	KUMASI	293	654762	742945	-	1966-1968	1961-2003	1966-1968	1965-2004
106	Lawra	4.8	514583	1177283	1961-1983,1988-1997,1999-2002	1965-2004	1965-2004	1965-2004	1965-2004
107	LEGMOIN	345	510935	1122113	-	1965-2004	1965-2004	1965-2004	1965-2004

108	LEO	347	598271	1227290	-	1965-2004	1965-2004	1965-2004	1965-2004
109	LOUMANA	320	242831	1170988	-	1965-2004	1965-2004	1965-2004	1965-2004
110	MAN	226	798715	1219436	-	1965-2004	1965-2004	1965-2004	1965-2004
111	MANGA	286	710736	1290513	-	1965-2004	1965-2004	1965-2004	1965-2004
112	MANGODARA	260	351966	1094773	-	1965-2004	1965-2004	1965-2004	1965-2004
113	MOGTEDO	272	735647	1358962	-	1965-2004	1965-2004	1965-2004	1965-2004
114	NANORO	312	588655	1402345	-	1965-2004	1965-2004	1965-2004	1965-2004
115	NASSO	339	343486	1238578	-	1965-2004	1965-2004	1965-2004	1965-2004
116	Navrongo	201.3	707669	1205574	1961-2006,	1961-2004	1987-2003	1966-2004	1961-2004
117	NIANGOLOKO	320	290055	1135635	-	1965-2004	1965-2004	1965-2004	1965-2004
118	NIAOGHO	240	743366	1301818	-	1965-2004	1965-2004	1965-2004	1965-2004
119	NOMOUNOU	274	358393	1312238	-	1965-2004	1965-2004	1965-2004	1965-2004
120	NSAWAM	47	793500	643932	-	1965-2004	1965-2004	1965-2004	1965-2004
121	NUNGUA	50	823188	618254	-	1965-2004	1965-2004	1965-2004	1965-2004
122	ODA	200	723288	654702	-	1965-2004	1965-2004	1965-2004	1965-2004
123	ORODARA	523	290544	1214910	-	1965-2004	1965-2004	1965-2004	1965-2004
124	OUAGADOUGOU	303	661262	1365795	-	1966-1969	1966-1969	1966-1969	1966-1969
125	OUAHIGOUYA	329	561285	1501797	-	1966-1969	1966-1969	1966-1969	1966-1969
126	OUARKOYE	315	427427	1335952	-	1965-2004	1965-2004	1965-2004	1965-2004

127	PABRE	295	655725	1384200	-	1965-2004	1965-2004	1965-2004	1965-2004
128	PAMA	230	912006	1244710	-	1965-2004	1965-2004	1965-2004	1965-2004
129	PO	326	702002	1235144	-	1965-2004	1965-2004	1965-2004	1965-2004
130	Pokoase	50.3	800932	628907	1966-2001	1961-2001	1965-2004	1965-2004	1965-2004
131	PUSIGA	224	815048	1226970	-	1965-2004	1965-2004	1965-2004	1965-2004
132	REO	228	568845	1361744	-	1965-2004	1965-2004	1965-2004	1965-2004
133	SABA	300	672126	1367701	-	1965-2004	1965-2004	1965-2004	1965-2004
134	SALTPOND	47	714318	575411	-	1967-1968	1966-1968	1966-1968	1965-2004
135	SAPONE	356	652371	1332567	-	1965-2004	1965-2004	1965-2004	1965-2004
136	SAPOUY	330	634470	1277184	-	1965-2004	1965-2004	1965-2004	1965-2004
137	SARIA	300	592423	1356280	-	1965-2004	1965-2004	1965-2004	1965-2004
138	SEGUENEGA	307	611846	1485373	-	1965-2004	1965-2004	1965-2004	1965-2004
139	SEI	281	553323	853291	-	1965-2004	1965-2004	1965-2004	1965-2004
140	SIDERADOUGOU	319	363269	1181351	-	1965-2004	1965-2004	1965-2004	1965-2004
141	SOGAKOFE	50	767139	664090	-	1965-2004	1965-2004	1965-2004	1965-2004
142	SOLENSO	314	382121	1347156	-	1965-2004	1965-2004	1965-2004	1965-2004
143	Sunyani	308.8	573582	810653	1974, 1976-2006	1976-2000	1986-2003	1976-2004	1976-2004
144	TAFO	198	791440	688182	-	1966-1968	1965-2004	1965-2004	1965-2004
145	Tamale	183.3	736091	1041643	1961-2006,	1961-1999	1966-1968	1966-1968	1965-2004

146	TEMA	314	633709	1443076	-	1965-2004	1965-2004	1965-2004	1965-2004
147	TENKODOGO	302	785166	1302179	-	1965-2004	1965-2004	1965-2004	1965-2004
148	TIEBELE	268	722081	1227900	-	1965-2004	1965-2004	1965-2004	1965-2004
149	TIKARE	400	637194	1468901	-	1965-2004	1965-2004	1965-2004	1965-2004
150	TITAO	319	600878	1522195	-	1965-2004	1965-2004	1965-2004	1965-2004
151	TOUGAN	305	492753	1446437	-	1965-2004	1965-2004	1965-2004	1965-2004
152	Tumu	313.2	611120	1201423	1961-1964 ,1970-1990	1965-2004	1965-2004	1965-2004	1965-2004
153	Wa	322.7	554790	1110982	1961-1984,1986-2006	1966-1968	1986-2003	1966-1968	1965-2004
154	Wenchi	338.9	599243	856765	1961-2006,	1976-2000	1965-2004	1965-2004	1967-1969
155	WINNEBA	15	764167	590332	-	1965-2004	1965-2004	1965-2004	1965-2004
156	WUR	219	796841	795164	-	1965-2004	1965-2004	1965-2004	1965-2004
157	Yendi	195.2	827636	1046005	1961-2006,	1976-1999	1966-1968	1966-1968	1967-1969
158	ZABRE	296	762092	1235576	-	1965-2004	1965-2004	1965-2004	1965-2004
159	ZORGHO	315	759258	1355436	-	1965-2004	1965-2004	1965-2004	1965-2004
160	ZUARUNGU	213	740591	1193141	-	1965-2004	1965-2004	1965-2004	1965-2004

APPENDIX II: Model control file and parameters

```
[model_time]
12              # start hour
1               # start day
1               # start month
1961            # start year
12              # end hour
31              # end day
12              # end month
2050            # end year

$set $year          = 1961-2050

$set $outpath       = /share/gridexp1/wasim-work/test1/outputc/
$set $inpath        = /share/gridexp1/wasim-work/test1/input/
$set $time          = 1440
$set $readgrids     =       0

$set $grid          = volta1km
$set $stack         = s1
$set $suffix        = grd
$set $code          = s

# variables for standardgrids
$set $zone_grid           = $grid//.zon
$set $subcatchments       = $grid//.ezg
$set $flow_time_grid      = $grid//.fzs
$set $river_links_grid    = $grid//.lnk
$set $regio_grid          = $grid//.reg

#second section: grids. which doesn't depend on subdivision (only pixel-values are of interest)
$set $elevation_model     = $grid//.dhm
$set $RelCellArea_grid    = $grid//.rca
$set $CellSizeX_grid      = $grid//.csx
$set $CellSizeY_grid      = $grid//.csy
$set $slope_grid          = $grid//.slp
$set $aspect_grid         = $grid//.exp
$set $land_use_grid       = $grid//.use
$set $ice_firn_grid       = $grid//.ice
$set $field_capacity_grid = $grid//.nfk
$set $ATBgrid             = $grid//.atb
$set $hydr_cond_grid      = $grid//.k
$set $soil_types          = $grid//.art
$set $sky_view_factor_grid = $grid//.hor
$set $drain_depth_grid    = $grid//.drn
$set $drain_distance_grid = $grid//.dis
$set $irrigationcodes     = $grid//.irr
$set $max_pond_grid       = $grid//.pnd
```

```
$set $clay_depth_grid      = $grid//.cly
$set $river_depth_grid     = $grid//.dep
$set $river_width_grid     = $grid//.wit
$set $kolmationsgrid       = $grid//.kol
$set $gw_kx_1_grid         = $grid//.kx1
$set $gw_kx_2_grid         = $grid//.kx2
$set $gw_kx_3_grid         = $grid//.kx3
$set $gw_ky_1_grid         = $grid//.ky1
$set $gw_ky_2_grid         = $grid//.ky2
$set $gw_ky_3_grid         = $grid//.ky3
$set $gw_bound_h_1_grid    = $grid//.bh1
$set $gw_bound_h_2_grid    = $grid//.bh2
$set $gw_bound_h_3_grid    = $grid//.bh3
$set $gw_bound_q_1_grid    = $grid//.bq1
$set $gw_bound_q_2_grid    = $grid//.bq2
$set $gw_bound_q_3_grid    = $grid//.bq3
$set $aquiferthick1        = $grid//.aq1
$set $aquiferthick2        = $grid//.aq2
$set $aquiferthick3        = $grid//.aq3
$set $gw_storage_coeff_1   = $grid//.s01
$set $gw_storage_coeff_2   = $grid//.s02
$set $gw_storage_coeff_3   = $grid//.s03
$set $gw_kolmation_1       = $grid//.gk1
$set $gw_kolmation_2       = $grid//.gk2
$set $gw_kolmation_3       = $grid//.gk3


# grids for surface hydrolgy modules
$set $albedo               = albe//$grid//.//$suffix
$set $soilstoragegrid      = sb__//$grid//.//$suffix
$set $throughfall          = qi__//$grid//.//$suffix
$set $snowcover_outflow    = qsno//$grid//.//$suffix
$set $melt_from_snowcover  = qsme//$grid//.//$suffix
$set $days_snow            = sday//$grid//.//$suffix
$set $snow_age             = sage//$grid//.//$suffix
$set $snow_rate            = snow//$grid//.//$suffix
$set $rain_rate            = rain//$grid//.//$suffix
$set $firn_melt            = qfir//$grid//.//$suffix
$set $ice_melt             = qice//$grid//.//$suffix
$set $preci_grid           = prec//$grid//.//$suffix
$set $irrig_grid           = irri//$grid//.//$suffix
$set $tempegrid            = temp//$grid//.//$suffix
$set $windgrid             = wind//$grid//.//$suffix
$set $sunshinegrid         = ssd_//$grid//.//$suffix
$set $radiationgrid        = rad_//$grid//.//$suffix
$set $humiditygrid         = humi//$grid//.//$suffix
$set $vaporgrid            = vapo//$grid//.//$suffix
$set $ETPgrid              = etp_//$grid//.//$suffix
```

```
$set $EIPgrid              = eip_//$grid//.//$suffix
$set $ETRgrid              = etr_//$grid//.//$suffix
$set $EVAPgrid             = evap//$grid//.//$suffix
$set $EVARgrid             = evar//$grid//.//$suffix
$set $ETRSgrid             = etrs//$grid//.//$suffix
$set $SSNOgrid             = ssno//$grid//.//$suffix
$set $SLIQgrid             = sliq//$grid//.//$suffix
$set $SSTOgrid             = ssto//$grid//.//$suffix
$set $sat_def_grid         = sd__//$grid//.//$suffix
$set $SUZgrid              = suz_//$grid//.//$suffix
$set $SIFgrid              = sif_//$grid//.//$suffix
$set $EIgrid               = ei__//$grid//.//$suffix
$set $SIgrid               = si__//$grid//.//$suffix
$set $ExpoCorrgrid         = exco//$grid//.//$suffix
$set $Tcorrgrid            = tcor//$grid//.//$suffix
$set $Shapegrid            = shap//$grid//.//$suffix
$set $INFEXgrid            = infx//$grid//.//$suffix
$set $SATTgrid             = satt//$grid//.//$suffix
$set $Nagrid               = na__//$grid//.//$suffix
$set $SSPgrid              = ssp_//$grid//.//$suffix
$set $Peakgrid             = peak//$grid//.//$suffix
$set $SBiagrid             = sbia//$grid//.//$suffix
$set $fcia_grid            = nfki//$grid//.//$suffix


# now variables for unsaturated zone model
$set $SB_1_grid     = sb05//$grid//.//$suffix
$set $SB_2_grid     = sb1_//$grid//.//$suffix
$set $ROOTgrid      = wurz//$grid//.//$suffix
$set $QDgrid        = qd__//$grid//.//$suffix
$set $QIgrid        = qifl//$grid//.//$suffix
$set $GWdepthgrid   = gwst//$grid//.//$suffix
$set $GWthetagrid   = gwth//$grid//.//$suffix
$set $GWNgrid       = gwn_//$grid//.//$suffix
$set $UPRISEgrid    = uprs//$grid//.//$suffix
$set $PERCOLgrid    = perc//$grid//.//$suffix
$set $GWLEVELgrid   = gwlv//$grid//.//$suffix
$set $QDRAINgrid    = qdrn//$grid//.//$suffix
$set $QBgrid        = qb__//$grid//.//$suffix
$set $GWINgrid      = gwin//$grid//.//$suffix
$set $GWEXgrid      = gwex//$grid//.//$suffix
$set $act_pond_grid = pond//$grid//.//$suffix
$set $MACROINFgrid  = macr//$grid//.//$suffix
$set $SUBSTEPSgrid  = step//$grid//.//$suffix

# variables for groundwater modeling
$set $flowx1grid    = gwx1//$grid//.//$suffix
$set $flowx2grid    = gwx2//$grid//.//$suffix
```

```
$set $flowx3grid    =  gwx3//$grid//.//$suffix
$set $flowy1grid    =  gwy1//$grid//.//$suffix
$set $flowy2grid    =  gwy2//$grid//.//$suffix
$set $flowy3grid    =  gwy3//$grid//.//$suffix
$set $head1grid     =  gwh1//$grid//.//$suffix
$set $head2grid     =  gwh2//$grid//.//$suffix
$set $head3grid     =  gwh3//$grid//.//$suffix

# Ergebnis-stacks for Unsatzonmodel
$set $Thetastack             = teth//$stack//.//$suffix
$set $hydraulic_heads_stack  = hhyd//$stack//.//$suffix
$set $geodetic_altitude_stack = hgeo//$stack//.//$suffix
$set $flowstack              = qu__//$stack//.//$suffix
$set $concstack              = conc//$stack//.//$suffix

# parameters for interpolation of meteorological input data
$set $SzenUse       =  0
$set $IDWmaxdist    =  900000
$set $IDWweight     =  2
$set $Anisoslope    =  0.0
$set $Anisotropie   =  0.35

# explanation of writegrid and outputcode some lines below
$set $Writegrid     =  353
$set $Writestack    =  353
$set $outputcode    =  2001
$set $output_meteo  =  2001
$set $day_sum       =  2001
$set $day_mean      =  2001
$set $hour_sum      =  2001
$set $hour_mean     =  2001
$set $routing_code  =  2001


#
#  Wrigegrid : max. 3 digits (nnn)
#
#    only if writegrid >= 100: 1. digit (1nn. or 2nn or 3nn)
#     0 = no minimum or maximum grid is written
#      1 = minimum grid is written (minimum value for each of the grid cells over the
entire model period)
#      2 = maximum grid is written (maximum value for each of the grid cells over the
entire model period)
#     3 = both grids are written (minimum and maximum value for each of the grid cells
over the entire model period)
#    only if Writegrid >=  10: 2nd digit: sums or means (n1n ... n8n)
#      0 = no sum grid will be written
#      1 = one sum grid will be written at the end of the model run
```

```
#       2 = one sum grid per model year
#       3 = one sum grid per model month
#       4 = one sum grid per day (only. if timestep < 1 day)
#       5 = one mean value grid at the end of the model run
#       6 = one mean value grid per model year
#       7 = one mean value grid per month
#       8 = one mean value grid per day
#     last digit (nn1 .. nn5) (for actual values. not for Sums or means)
#          1 = (over)write each timestep into the same grid (for security in case of model
crashs)
#       2 = write grids each timestep to new files. the name is build from the first 4 letters
#             of the regular grid name and then from the number of month. day and hour
(hoer as file extension)
#           example: tempm500.grd will become prec0114.07 for 14.January. 7:00
#       3 = only the last grid of the model run will be stored
#       4 = the grid from the last hour of each day (24:00) will be stored (for each day the
same file will be overwritten)
#       5 = like 4. but each day a new grid file is created (like for code 2)
#
# outputcode (for statistic files for zones or subcatchments)
#
# the Codes behind the names of the statistic files have the meaning of:
# <1000   : no output
# 1<nnn>  : spatial mean values for the entire basin. averaged in time over <nnn>
intervals (timesteps)
# 2<nnn>  : spatial mean values for all zones (subbasin) and for the entire basin.
averaged in time over <nnn> intervals (timesteps)
# 3<nnn>  : spatial means for the entire basin. added up in time over <nnn> intervals
(timesteps)
# 4<nnn>  : spatial means for all zones (subbasin) and for the entire basin. added up in
time over <nnn> intervals (timesteps)
# 5<nnn>  : spatial means for the entire basin and for those subbasins which are spcified
in the output-list. averaged in time over <nnn> intervals
# 6<nnn>  : spatial means for the entire basin and for those subbasins which are spcified
in the output-list. added up in time over <nnn> intervals
#
# example:
#  2001 = per timestep for all subcatchments (and for the entire basin) one (spatially
averaged) value.
#  2004 = each 4 time steps one averaged value over the last 4 time steps for all
subcatchments and for the entire basin.
#  4024 = Sums of the mean subcatchment/entire basin values of the timesteps over 24
timesteps (e.g. daily rain sums for subcatchments).
#  3120 = averaged values (over 120 time steps!) only for the entire basin (spatially
averaged)
#  5012 = averaged values (over 12 timesteps) as spatial averages for the entire basin
and for each of the subbasins specified in the output-list
```

```
[output_list]
1       # only of interest,when subbasins > 5000 Else 1
18      # Codes For the subbasins

[output_interval]
1             # increment of time steps until an output to the screen is done (24 = each day one output. if time steo = 1h)
1             # warning level for interpolation (no station within search radius)
1             # output of runoff results in 0=mm/time step. 1=m3/s
0             # minutes from the hour-entry in the input data files until the end

[coordinates]
10.0          # geogr. latitude (center of the basin -> for radiation calculations)
-1.5          # geogr. longitude (center of the basin)
0.0           # meridian according to the official time (middle europe: 15)(east: 0 ... +180 degree. west: 0 ... -180 (or 360 ... 180)
0             # time shift of Meteo-data-time with respect to the true local time (mean sun time)

[region_transition_distance]
10000000 # in m

[elevation_model]
$inpath//$elevation_model    # grid with the digital elevation data

[zone_grid]
$inpath//$zone_grid       # grid with Zone codes

[standard_grids]
9  # number of standard grids
# path                          # identification              # fillcode 0=no. 1=yes (fill missing values with values of nearest neighbor)
$inpath//$land_use_grid         landuse                 1    # grid with land use data
$inpath//$slope_grid            slope_angle             1    # grid with slope angle data
$inpath//$aspect_grid           slope_aspect            1    # grid with slope aspect data
$inpath//$subcatchments         zonegrid_soilmodel      1    # zone grid for the runoff generation model (and unstaurated zone model)
$inpath//$soil_types            soil_types              1    # soil types as codes for the soil table
$inpath//$flow_time_grid        flow_times              1    # grid with flow times for surface runoff to the subbasin outlet
$inpath//$river_depth_grid      river_depth             0    # grid with the depth of all streams in the stream network in m
$inpath//$river_width_grid      river_width             0    # grid with the witdh of all streams in m
$inpath//$river_links_grid      river_links             0    # grid with codes of tributaries. from which a channel was routed (only for real routing channels!!!)
```

```
[variable_grids]
1                                   # Number of variable grids to read
$outpath//$albedo          albedo      1 0     # albedo; for time without snow derived from land use data
$Writegrid                          # Writegrid for $albedo
$readgrids                          # 0. if albedo is derived from land use at model start time. 1. if albedo is read from file

[meteo_data_count]
5

[meteo_names]
temperature
precipitation
air_humidity
wind_speed
# sunshine_duration
global_radiation

[temperature]
1                   # Methode 1=idw. 2=regress. 3=idw+regress. 4=Thiessen
$inpath//temp.ext3.dat AdditionalColumns=0 # file name with station data (if method = 1. 3 or 4. else ignored)
$inpath//temp//$year//.out      # file name with regression data (if method = 2 or 3)
$outpath//$tempegrid        # name of the output grid (is also used for deriving names of daily. monthly. yearly sums or averages)
$Writegrid              # 0. if no grid-output is needed. else one of the codes described above
1                   # correction faktor for results
$outpath//temp//$grid//.//$code//$year $hour_sum # file name for the statistic output (statially averaged values per time step and subcatchment...)
998                 # error value: all data in the input file greater than this values or lesser the negative value are nodata
$IDWweight              # weighting of the reciprocal distance for IDW
0.1                 #  for interpolation method 3: relative weight of IDW-interpolation in the result
$IDWmaxdist             #  max. distance of stations to the actual interpolation cell
$Anisoslope             #  slope of the mean axis of the anisotropy-ellipsis (-90 ... +90 degree. mathem. positive)
$Anisotropie            #  ratio of the short to the long axis of the anisotropy-ellipsis
-40                 #  lower limit of interpolation results
-40                 #  replace value for results below the lower limit
60                  #  upper limit for interpolation results
60                  #  replace value for results with larger values than the upper limit
$SzenUse                # 1=use scenario data for correction. 0=dont use scenarios
1                   # 1=add scenarios. 2=multiply scenarios. 3=percentual change
0
```

```
[precipitation]
1                          # method: 1=idw 2=regress 3=idw+regress 4=thiessen 5=bilinear
6=bilinear gradients and residuals linarly combined
$inpath//prec.ext3.dat AdditionalColumns=0   # file name with station data (if method =
1. 3 or 4. else ignored)
$inpath//prec.out   # file name with regression data (if method = 2 or 3)
$outpath//$preci_grid         # name of the output grid (is also used for deriving names of
daily. monthly. yearly sums or averages)
$Writegrid                 # 0. if no grid-output is needed. else one of the codes described
above
1                       # correction faktor for results
$outpath//prec//$grid//.//$code//$year $hour_sum  # file name for the statistic output
(statially averaged values per time step and subcatchment...)
998                        # error value: all data in the input file greater than this values or
lesser the negative value are nodata
$IDWweight                 # weighting of the reciprocal distance for IDW
0.9                      # for interpolation method 3: relative weight of IDW-interpolation
in the result
$IDWmaxdist                # max. distance of stations to the actual interpolation cell
$Anisoslope                #  slope of the mean axis of the anisotropy-ellipsis (-90 ... +90
degree. mathem. positive)
$Anisotropie               #  ratio of the short to the long axis of the anisotropy-ellipsis
0.                       # lower limit of interpolation results
0                        # replace value for results below the lower limit
900                       # upper limit for interpolation results
900                       # replace value for results with larger values than the upper limit
$SzenUse                        # 1=use scenario data for correction. 0=dont use scenarios
5                        # 1=add scenarios. 2=multiply scenarios. 3=percentual change
0


[air_humidity]
1                       # method: 1=idw 2=regress 3=idw+regress 4=thiessen
$inpath//hum.ext3.dat AdditionalColumns=0  # file name with station data (if method =
1. 3 or 4. else ignored)
$inpath//hum//$year//.out     # file name with regression data (if method = 2 or 3)
$outpath//$humiditygrid        # name of the output grid (is also used for deriving names
of daily. monthly. yearly sums or averages)
$Writegrid                 # 0. if no grid-output is needed. else one of the codes described
above
0.01                     # correction faktor for results
$outpath//humi//$grid//.//$code//$year $hour_sum # file name for the statistic output
(statially averaged values per time step and subcatchment...)
998                        # error value: all data in the input file greater than this values or
lesser the negative value are nodata
$IDWweight                 # weighting of the reciprocal distance for IDW
```

```
0.5                    # for interpolation method 3: relative weight of IDW-interpolation
in the result
$IDWmaxdist            # max. distance of stations to the actual interpolation cell
$Anisoslope            # slope of the mean axis of the anisotropy-ellipsis (-90 ... +90
degree. mathem. positive)
$Anisotropie           # ratio of the short to the long axis of the anisotropy-ellipsis
0.01                   # lower limit of interpolation results
0.01                   # replace value for results below the lower limit
1.0                    # upper limit for interpolation results
1.0                    # replace value for results with larger values than the upper limit
$SzenUse               # 1=use scenario data for correction. 0=dont use scenarios
3                      # 1 = Szenarien add. 2 = Szenarien multiplizieren. 3 = prozentuale
Aenderung
1                      # Anzahl an Szenariozellen (0.5 Grad - Zellen hier)

[wind_speed]
1                      # method: 1=idw 2=regress 3=idw+regress 4=thiessen
$inpath//wind.ext2b.dat AdditionalColumns=0  # file name with station data (if method
= 1. 3 or 4. else ignored)
$inpath//wind//$year//.out    # file name with regression data (if method = 2 or 3)
$outpath//$windgrid           # name of the output grid (is also used for deriving names of
daily. monthly. yearly sums or averages)
$Writegrid             # 0. if no grid-output is needed. else one of the codes described
above
1                      # correction faktor for results
$outpath//wind//$grid//.//$code//$year $hour_sum  # file name for the statistic output
(statially averaged values per time step and subcatchment...)
998                    # error value: all data in the input file greater than this values or
lesser the negative value are nodata
$IDWweight             # weighting of the reciprocal distance for IDW
0.3                    # for interpolation method 3: relative weight of IDW-interpolation
in the result
$IDWmaxdist            # max. distance of stations to the actual interpolation cell
$Anisoslope            # slope of the mean axis of the anisotropy-ellipsis (-90 ... +90
degree. mathem. positive)
$Anisotropie           # ratio of the short to the long axis of the anisotropy-ellipsis
0                      # lower limit of interpolation results
0                      # replace value for results below the lower limit
90                     # upper limit for interpolation results
90                     # replace value for results with larger values than the upper limit
$SzenUse               # 1=use scenario data for correction. 0=dont use scenarios
3                      # 1 = add scenario data. 2 = multiply scenario data. 3 = prozentuale
Aenderung/ change by percentage
4                      # Anzahl an Szenariozellen (0.5 Grad - Zellen hier) number of
scnario cells (here: 0.5 degrees)

# [sunshine_duration]
1                      # method: 1=idw 2=regress 3=idw+regress 4=thiessen
```

```
$inpath//sun.ext2.dat AdditionalColumns=0  # file name with station data (if method = 1. 3 or 4. else ignored)
$inpath//sun//$year//.out   # file name with regression data (if method = 2 or 3)
$outpath//$sunshinegrid       # name of the output grid (is also used for deriving names of daily. monthly. yearly sums or averages)
$Writegrid                    # 0. if no grid-output is needed. else one of the codes described above
1                     # correction faktor for results
$outpath//ssd_//$grid//.//$code//$year  $hour_sum  # file name for the statistic output (statially averaged values per time step and subcatchment...)
998                           # error value: all data in the input file greater than this values or lesser the negative value are nodata
$IDWweight                    # weighting of the reciprocal distance for IDW
0.5                         # for interpolation method 3: relative weight of IDW-interpolation in the result
$IDWmaxdist                   # max. distance of stations to the actual interpolation cell
$Anisoslope                   # slope of the mean axis of the anisotropy-ellipsis (-90 ... +90 degree. mathem. positive)
$Anisotropie                  # ratio of the short to the long axis of the anisotropy-ellipsis
0                         # lower limit of interpolation results
0                         # replace value for results below the lower limit
1.0                        # upper limit for interpolation results
1.0                        # replace value for results with larger values than the upper limit
$SzenUse                      # 1=use scenario data for correction. 0=dont use scenarios
3                                   # 1 = add scenario data. 2 = multiply scenario data. 3 = prozentuale Aenderung/change by percentage
1                             # Anzahl an Szenariozellen/number o f scenario cells (here: 0.5 Grad/degree – Zellen/cells hier)

[global_radiation]
1                     # method: 1=idw 2=regress 3=idw+regress 4=thiessen
$inpath//rad.ext3.dat  # file name with station data (if method = 1, 3 or 4, else ignored)
$inpath//global//$year//.out  # file name with regression data (if method = 2 or 3)
$outpath//$radiationgrid      # name of the output grid (is also used for deriving names of daily, monthly, yearly sums or averages)
$Writegrid                    # 0, if no grid-output is needed, else one of the codes described above
1.0                        # correction faktor for results
$outpath//radiation_//$grid//.//$code//$year $hour_mean  # file name for the statistic output (statially averaged values per time step and subcatchment...)
9998                          # error value: all data in the input file greater than this values or lesser the negative value are nodata
$IDWweight                    # weighting of the reciprocal distance for IDW
0.5                         # for interpolation method 3: relative weight of IDW-interpolation in the result
$IDWmaxdist                   # max. distance of stations to the actual interpolation cell
$Anisoslope                   #  slope of the mean axis of the anisotropy-ellipsis (-90 ... +90 degree, mathem. positive)
```

```
$Anisotropie              #  ratio of the short to the long axis of the anisotropy-ellipsis
0                      # lower limit of interpolation results
0                      # replace value for results below the lower limit
10000                     # upper limit for interpolation results
10000                     # replace value for results with larger values than the upper limit
$SzenUse                  # 1=use scenario data for correction, 0=dont use scenarios

# ----------  parameter for model components  -----------------
#

[precipitation_correction]
1               # 0=ignore this module. 1 = run the module
0.5               # Snow-rain-temperature
1.05              # liquid:   b in:  y = p(ax + b)
0.05              # liquid:   a in:  y = p(ax + b) = 1% more per m/s + 0.5% constant
1.10              # Snow:     b in:  y = p(ax + b)
0.13              # Snow:     a in:  y = p(ax + b) = 15% more per m/s + 45% constant

# corretion factors for direct radiation are calculated
# if the cell is in the shadow of another cell. or if a cell is not in the sun (slope angle!)
# then the factor is 0.
# control_parameter: 1 = radiation correction WITH  shadow WITHOUT temperature correction
#               2 = radiation correction WITH  shadow WITH  temperature correction
#                    3 = radiation correction WITHOUT shadow WITHOUT temperature correction.
#               4 = radiation correction WITHOUT shadow WITH  Temperatur

[radiation_correction]
1               # 0=ignore this module. 1 = run the module
$time             # duration of a time step in minutes
2               # control parameter for radiation correction (see above)
$outpath//$Tcorrgrid # name of the grids with the corrected temperatures
$Writegrid       # Writegrid for corrected temperatures
5               # factor x for temperature correction x * (-1.6 .... +1.6)
$outpath//$ExpoCorrgrid   # name of the grids with the correction factors for the direct radiation
$Writegrid          # Writegrid
$outpath//$Shapegrid # name of the grids for codes 1 for theor. shadow. 0 for theor. no shadow (day; assumed: SSD=1.0)
$Writegrid          # Writegrid
1                # interval counter. after reaching this value. a new correction is calculated (3=all 3 hours a.s.o.)
1               # Spitting of the interval. usefull for time step=24 hours (then: split=24. -> each hour one correction calculation)


[evapotranspiration]
```

1 # 0=ignore this module. 1 = run the module
$time # duration of a time step in minutes
1 # Method: 1=Penman-Monteith. 2=Hamon (only daily). 3=Wendling (only daily) 4= Haude (only daily)
0.5 0.6 0.8 1.0 1.1 1.1 1.2 1.1 1.0 0.9 0.7 0.5 # PEC correction factor for HAMON-evapotranspiration
0.20 0.20 0.21 0.29 0.29 0.28 0.26 0.25 0.22 0.22 0.20 0.20 # fh (only for method 4: Haude) monthly values (Jan ... Dec) (here: for Grass)
0.5 # fk -> factor for Wendling-evapotranspiration (only for Method = 3)
$outpath//$ETPgrid # result grid for potential evapotranspiration in mm/dt
$Writegrid # 0. if no grid-output is needed. else one of the codes described above
$outpath//etp_//$grid//.//$code//$year $hour_sum # statisticfile for subcatchments (zones) of the potential evapotranspiration
$outpath//$ETRgrid # result grid for real evapotranspiration in mm/dt
$Writegrid # 0. if no grid-output is needed. else one of the codes described above
$outpath//etr_//$grid//.//$code//$year $hour_sum # statistic for subcatchments (zones) of the real evapotranspiration
$outpath//$EVAPgrid # result grid for real evapotranspiration in mm/dt
$Writegrid # 0. if no grid-output is needed. else one of the codes described above
$outpath//evap//$grid//.//$code//$year $hour_sum # statistic for subcatchments (zones) of the potential evaporation
$outpath//$EVARgrid # result grid for real evapotranspiration in mm/dt
$Writegrid # 0. if no grid-output is needed. else one of the codes described above
$outpath//evar//$grid//.//$code//$year $hour_sum # statistic for subcatchments (zones) of the real evaporation
$outpath//$ETRSgrid # result grid for real snow evapotranspiration in mm/dt
$Writegrid # 0. if no grid-output is needed. else one of the codes described above
$outpath//etrs//$grid//.//$code//$year $hour_sum # statistic for subcatchments (zones) of the real snow evaporation
$outpath//$EIPgrid # result grid for pot. interception evaporation in mm/dt
$Writegrid # 0. if no grid-output is needed. else one of the codes described above
$outpath//eip_//$grid//.//$code//$year $hour_sum # statisticfile for zones of pot. interception evaporation
$outpath//rgex//$grid//.//$code//$year $hour_sum # statistic for subcatchments (zones) of the corrected radiation
+0.23 +1.77 -2.28 +1.28 # coefficients c for Polynom of order 3 RG = c1 + c2*SSD + c3*SSD^2 + c4*SSD^3
+0.072 -0.808 +2.112 -0.239 # coefficients x for Polynom of order 3 SSD = x1 + x2*RG + x3*RG^2 + x4*RG^3
0.88 0.05 # Extinktion coefficient for RG-modeling (Phi and dPhi) (summer phi = phi-dphi. winter phi=phi+dphi)
1654.0 # recession constant (e-function for recession of the daily temperature amplitude with altitude [m]

3.3 4.4 6.1 7.9 9.4 10.0 9.9 9.0 7.8 6.0 4.2 3.2 # monthly values of the max. daily T-amplitudes (for 0 m.a.s.l)
0.62 0.1 # part of the temperature amplitude (dt). that is added to the mean day-temperature
(followed by the range of changing within a year ddt) to get the mean temperature of light day
in the night: mean night temperature is mean day temperature minus (1-dt)*(temp. amplitude)

[snow_model]
0 # 0=ignore this module. 1 = run the module
$time # duration of a time step in minutes
1 # method 1=T-index. 2=t-u-index. 3=Anderson comb.. 4=extended com.
1 # transient zone for rain-snow (T0R +- this range)
0.5 # T0R temperature limit for rain (Grad Celsius)
-0.5 # T0 temperature limit snow melt
0.1 # CWH storage capacity of the snow for water (relative part)
1.0 # CRFR coefficient for refreezing
2.0 # C0 degree-day-factor mm/d/C
1.8 # C1 degree-day-factor without wind consideration mm/(d*C)
0.8 # C2 degree-day-factor considering wind mm/(d*C*m/s)
0.07 # z0 roughness length cm for energy bilance methods (not used)
1.5 # RMFMIN minimum radiation melt factor mm/d/C comb. method
2.5 # RMFMAX maximum radiation melt factor mm/d/C comb. method
0.40 # Albedo for snow (Min)
0.85 # Albedo for snow (Max)
$outpath//$rain_rate # rain rate
$Writegrid # 0. if no grid-output is needed. else one of the codes described above
$outpath//rain//$grid//.//$code//$year $hour_sum # rain rate
$outpath//$snow_rate # snow rate
$Writegrid # 0. if no grid-output is needed. else one of the codes described above
$outpath//snow//$grid//.//$code//$year $hour_sum # snow rate
$outpath//$days_snow # number of days with snow (SWE > 5mm)
$Writegrid # 0. if no grid-output is needed. else one of the codes described above
$outpath//sday//$grid//.//$code//$year $hour_sum # number of days with snow (SWE > 5mm)
$outpath//$snow_age # snow age (days without new snow)
$Writegrid # 0. if no grid-output is needed. else one of the codes described above
$outpath//sage//$grid//.//$code//$year $hour_sum # days since last snowfall
$outpath//albe//$grid//.//$code//$year $hour_sum # Albedo
$outpath//$snowcover_outflow # discharge from snow. input (precipitation) for following modules

```
$Writegrid                  # 0. if no grid-output is needed. else one of the codes described above
$outpath//qsch//$grid//.//$code//$year $hour_sum  # melt flow (or rain. if there is no snow cover) in mm/dt
$outpath//$melt_from_snowcover # discharge from snow. input (precipitation) for following modules
$Writegrid                  # 0. if no grid-output is needed. else one of the codes described above
$outpath//qsme//$grid//.//$code//$year $hour_sum  # melt flow in mm/dt
$outpath//$SSNOgrid          # name of the grids with the snow storage solid in mm
$Writegrid                  # 0. if no grid-output is needed. else one of the codes described above
$outpath//$SLIQgrid          # name of the grids with the snow storage liquid in mm
$Writegrid                  # 0. if no grid-output is needed. else one of the codes described above
$outpath//ssto//$grid//.//$code//$year $hour_sum  # total snow storage. in mm. (liquid and solid fraction)
$outpath//$SSTOgrid          # name of the grids with the total snow storage solid AND liquid in mm
$Writegrid                  # 0. if no grid-output is needed. else one of the codes described above
$readgrids                  # 1=read snow storage solid. liquid grids from disk. 0=generate new grids


[ice_firn]
2   # method for glacier melt: 1=classical t-index. 2=t-index with correction by radiation
5   # t-index factor for ice
4   # t-index factor for firn
3   # t-index factor for snow
2   # melt factor
0.0001   # radiation coefficient for ice_min  (for method 2)
0.0007   # radiation coefficient for ice_max  (for method 2)
0.0001   # radiation coefficient for snow_min (for method 2)
0.00055  # radiation coefficient for snow_max (for method 2)
40       # els-konstante for ice
350      # els-konstante for firn
120      # els-konstante for snow
0.0006    # initial reservoir content for ice discharge (single linear storage approach)
0.0006    # initial reservoir content for firn discharge (single linear storage approach)
0.0006    # initial reservoir content for snow discharge (single linear storage approach)
$outpath//$firn_melt # melt from firn
$Writegrid          # 0, if no grid-output is needed, else one of the codes described above
$outpath//qfir//$grid//.//$code//$year $hour_mean # melt from firn as statistic file
$outpath//$ice_melt  # melt from ice
$Writegrid          # 0, if no grid-output is needed, else one of the codes described above
$outpath//qice//$grid//.//$code//$year $hour_mean # melt from ice as statistic file
```

$outpath//qglc//$grid//.//$code//$year $hour_mean # discharge from snow, ice and firn as statistic file

[interception_model]
1 # 0=ignore this module. 1 = run the module
$time # duration of a time step in minutes
2 # method: 1 = use ETP for calculating EI; 2 = use EIP for calculating EI (only effective for method 1 in evapotranspiration model -> for other methods. ETP = EIP)
$outpath//$throughfall # result grid : = outflow from the interception storage
$Writegrid # 0. if no grid-output is needed. else one of the codes described above
$outpath//qi__//$grid//.//$code//$year $hour_sum # statistic file interception storage outflow
$outpath//$EIgrid # Interzeption evaporation. grid
$Writegrid # 0. if no grid-output is needed. else one of the codes described above
$outpath//ei__//$grid//.//$code//$year $hour_sum # zonal statistic
$outpath//$SIgrid # storage content of the interception storage
$Writegrid # 0. if no grid-output is needed. else one of the codes described above
$outpath//si__//$grid//.//$code//$year $hour_sum # zonal statistic For interception storage content
0.35 # layer thickness of the waters on the leaves (multiplied with LAI -> storage capacity)
$readgrids # 1=read grids from disk. else generate internal

[infiltration_model]
0 # 0=ignore this module. 1 = run the module
$time # duration of a time step in minutes

[unsatzon_model]
1 # 0=ignore this module. 1 = run the module
$time # duration of a time step in minutes
3 # method, 1=simple method (will not work anymore from version 7.x), 2 = FDM-Method 3 = FDM-Method with dynamic time step down to 1 secound
2 # controlling interaction with surface water: 0 = no interaction. 1 = exfiltration possible 2 = infiltration and exfiltration possible
0 # controlling surface storage in ponds: 0 = no ponds. 1 = using ponds for surface storage (pond depth as standard grid needed -> height of dams oround fields)
0 # controlling artificial drainage: 0 = no artificial drainage 1 = using drainage (drainage depth and horizontal pipe distances as standard grids needed!)
0 # controlling clay layer: 0 = no clay layer. 1 = assuming a clay layer in a depth. specified within a clay-grid (declared as a standard grid)

5e-8 # permeability of the clay layer (is used for the clay layer only)
4 # parameter for the initialization of the gw_level (range between 1..levels (standard: 4))
$outpath//qdra//$grid//.//$code//$year $hour_sum # results drainage discharge in mm per zone
$outpath//gwst//$grid//.//$code//$year $hour_sum # results groundwater depth
$outpath//gwn_//$grid//.//$code//$year $hour_sum # results mean groundwater recharge per zone
$outpath//sb05//$grid//.//$code//$year $hour_sum # results rel. soil moisture within the root zone per zone
$outpath//sb1_//$grid//.//$code//$year $hour_sum # results rel. soil moisture within the unsat. zone (0m..GW table) per zone
$outpath//wurz//$grid//.//$code//$year $hour_sum # results statistic of the root depth per zone
$outpath//infx//$grid//.//$code//$year $hour_sum # results statistic of the infiltration excess
$outpath//pond//$grid//.//$code//$year $hour_sum # results statistic of the ponding water storage content
$outpath//qdir//$grid//.//$code//$year $hour_sum # results statistic of the direct discharge
$outpath//qifl//$grid//.//$code//$year $hour_sum # results statistic of the interflow
$outpath//qbas//$grid//.//$code//$year $hour_sum # results statistic of the baseflow
$outpath//qges//$grid//.//$code//$year $hour_sum # results statistic of the total discharge
$outpath//gwin//$grid//.//$code//$year $hour_sum # statistic of the infiltration from surface water into groundwater (from rivers and lakes)
$outpath//gwex//$grid//.//$code//$year $hour_sum # statistic of the exfiltration from groundwater into surface water (into rivers and lakes)
$outpath//macr//$grid//.//$code//$year $hour_sum # statistic of infiltration into macropores
$outpath//qinf//$grid//.//$code//$year $hour_sum # statistic of total infiltration into the first soil layer
$outpath//$SB_1_grid # grid with actual soil water content for the root zone
$Writegrid # writegrid for this grid
$outpath//$SB_2_grid # grid with actual soil water content for the root zone
$Writegrid # writegrid for this grid
$outpath//$ROOTgrid # grid with root depth
$Writegrid # writegrid for this grid
$outpath//$Thetastack # stack. actual soil water content for all soil levels
$Writestack # Writecode for this stack
$outpath//$hydraulic_heads_stack # stack. contaiing hydraulic heads
$Writestack # Writecode for this stack
$outpath//$geodetic_altitude_stack # stack. containig geodaetic altitudes of the soil levels (lower boudaries)
$Writestack # Writecode for this stack
$outpath//$flowstack # stack. containing the outflows from the soil levels
$Writestack # Writecode for this stack
$outpath//$GWdepthgrid # grid with groudwaterdepth
$Writegrid # writegrid for this grid

$outpath//$GWthetagrid # grid with theta in GWLEVEL
$Writegrid # writegrid for this grid
$outpath//$GWNgrid # grid with groundwater recharge
$Writegrid # writegrid for this grid
$outpath//$GWLEVELgrid # grid with level index of groundwater surface (Index der Schicht)
$Writegrid # writegrid for this grid
$outpath//$QDRAINgrid # grid with the drainage flows
$Writegrid # writegrid for this grid
$outpath//$SATTgrid # grid with code 1=saturation at interval start. 0 no sat.
$Writegrid # writegrid for this grid
$outpath//$INFEXgrid # grid with infiltration excess in mm (surface discharge)
$Writegrid # writegrid for this grid
$outpath//$QDgrid # grid with direct discharge
$Writegrid # writegrid for this grid
$outpath//$QIgrid # grid with Interflow
$Writegrid # writegrid for this grid
$outpath//$QBgrid # grid with baseflow
$Writegrid # writegrid for this grid
$outpath//$GWINgrid # grid with infiltration from rivers into the soil (groundwater)
$Writegrid # writegrid for re-infiltration
$outpath//$GWEXgrid # grid with exfiltration (baseflow) from groundwater (is only generated. if groundwater module is active. else baseflow is in QBgrid)
$Writegrid # writegrid for exfiltration
$outpath//$act_pond_grid # grid with content of ponding storge
$Writegrid # writegrid for this grid
$outpath//$UPRISEgrid # grid with amount of capillary uprise (mm)
$Writegrid # writegrid for this grid
$outpath//$PERCOLgrid # grid with amount of percolation (mm)
$Writegrid # writegrid for this grid
$outpath//$MACROINFgrid # grid with amount of infiltration into macropores (mm)
$Writegrid # writegrid for this grid
500 500 # coordinates of control plot. all theta and qu-values are written to files (qu.dat. theta.dat in the directory. from which the model is started)
$outpath//qbot//$grid//.//$code//$year # name of a file containing the flows between the layers of the control point
$outpath//thet//$grid//.//$code//$year # name of a file containing the soil moisture as theta values of the layers of the control point
$outpath//hhyd//$grid//.//$code//$year # name of a file containing the hydraulic head of the layers of the control point
$outpath//otherdata//$grid//.//$code//$year # name of a file containing some other water balance data of the control point (non layer data)
$outpath//etrd//$grid//.//$code//$year # name of a file containing the water withdrawal by evaporation and transpiration for each layer of the control point
$outpath//intd//$grid//.//$code//$year # name of a file containing the interflow rate for each layer of the control point
1 6 11 15 16 18 # range for subbasin codes

```
500    350    10     100    150    10    # kelsqd
600    300    20     200    200    20    # kelsqi
2      50     12     200    20     3    # drainage density
0.4    0.4    0.4    0.4    0.4    0.4    # k in qb = Q0 * exp(-k/z) with z = depth to groundwater
0.65   0.65   0.65   0.65   0.65   0.65   # Q0 in the above formula
0.1    0.1    0.1    0.1    0.1    0.1   # fraction of surface runoff on snow melt
$readgrids            # meanings are extended now! read the follwing comments
$outpath//storage.ftz   # if readgrids = 1. then this file contains the contents of the flow travel time zones for interflow and surface flow and for the tracers
60                                    # minimum dynamic time step in secounds. the smaller this number, the longer the model runs but the results will be more accurate due to a maintained Courant condition
$outpath//step//$grid//.//$code//$year $hour_mean # results statistic of the number of substeps
$outpath//$SUBSTEPSgrid                    # grid with number of substeps --> a good idea is to use writecode 5x (e.g. 53) to get the average number of substeps per cell for the model run
5//$Writegrid                              # for substeps, the areal distribution is of interest for the annual average value. This is code 6 as first digit in 2-digit codes. Or use 5 for the entire model run


[irrigation]
0                    # 0=ignore this module. 1 = run the module
$time                  # duration of a time step in minutes

[groundwater_flow]
0                  # 0=ignore the module. 1 = run the module
$time                  # duration of a time step in minutes; doen't change the value unless you have strong reasons to do so!!

[soil_model]
1                  # 0=ignore this module. 1 = run the module
$time                # duration of a time step in minutes


[routing_model]
1                    # 0=ignore this module. 1 = run the module. 2=run the module with observed inflows into the routing channels (from discharge files)
$time              # duration of a time step in minutes
0.01 100 90 24          # minimum/maximum specific discharge (l/s/km^2). number of log. fractions of the range. splitting of the timeintervall (24= 1 hour-intervalls are splitted into 24 Intervalls each of 2.5 min. duration)
$outpath//qgko//$grid//.//$code//$year $routing_code  # name of the statistic file with routed discharges
$inpath//spend.dat  # name of the file with observed discharges (mm/Timestep or m^3/s)
```

1 # number of following column descripotr (which column in the spec. disch. file corresponds to which subbasin
1 1 # first number: subbasin. second: column index
720 # timeoffset (for r-square calculation. intervals up to this parameter are not evaluated in r-square calculation. e.g. 12: first 12 intervals are neglected)
TG 2 (AE=75415.000, AErel=1.0)
from OL 15 (kh=0.1, kv=0.4, Bh=19.0, Bv= 75.9, Th= 1.90, Mh=30.0, Mv=12.0, I=0.0010, L=314082.8, AE=232.000)
and OL 5 (kh=0.1, kv=0.4, Bh= 6.6, Bv= 26.5, Th= 0.66, Mh=30.0, Mv=12.0, I=0.0010, L=243112.4, AE=14.000)
TG 11 (AE=56760.000, AErel=1.0)
from OL 13 (kh=0.1, kv=0.4, Bh=131.2, Bv=524.6, Th=13.12, Mh=30.0, Mv=12.0, I=0.0010, L=128183.4, AE=40180.000)
and OL 12 (kh=0.1, kv=0.4, Bh=82.1, Bv=328.4, Th= 8.21, Mh=30.0, Mv=12.0, I=0.0010, L=78627.2, AE=11522.000)
TG 6 (AE=94040.000, AErel=1.0)
from OL 10 (kh=0.1, kv=0.4, Bh=79.8, Bv=319.0, Th= 7.98, Mh=30.0, Mv=12.0, I=0.0010, L=138810.6, AE=10667.000)
and OL 11 (kh=0.1, kv=0.4, Bh=149.3, Bv=597.2, Th=14.93, Mh=30.0, Mv=12.0, I=0.0010, L=158739.6, AE=56760.000)
and OL 9 (kh=0.1, kv=0.4, Bh=80.0, Bv=319.8, Th= 8.00, Mh=30.0, Mv=12.0, I=0.0010, L=135982.2, AE=10737.000)
and OL 8 (kh=0.1, kv=0.4, Bh=58.2, Bv=232.7, Th= 5.82, Mh=30.0, Mv=12.0, I=0.0010, L=92284.0, AE=4598.000)
and OL 7 (kh=0.1, kv=0.4, Bh=13.6, Bv= 54.3, Th= 1.36, Mh=30.0, Mv=12.0, I=0.0010, L=53142.0, AE=95.000)
TG 4 (AE=109142.000, AErel=1.0)
from OL 6 (kh=0.1, kv=0.4, Bh=180.4, Bv=721.7, Th=18.04, Mh=30.0, Mv=12.0, I=0.0010, L=154396.4, AE=94040.000)
TG 17 (AE=143233.000, AErel=1.0)
from OL 18 (kh=0.1, kv=0.4, Bh=188.2, Bv=752.9, Th=18.82, Mh=30.0, Mv=12.0, I=0.0010, L=351260.2, AE=105259.000)
TG 16 (AE=143850.000, AErel=1.0)
from OL 17 (kh=0.1, kv=0.4, Bh=211.3, Bv=845.0, Th=21.13, Mh=30.0, Mv=12.0, I=0.0010, L=13656.8, AE=143233.000)
TG 3 (AE=153914.000, AErel=1.0)
from OL 16 (kh=0.1, kv=0.4, Bh=211.6, Bv=846.4, Th=21.16, Mh=30.0, Mv=12.0, I=0.0010, L=206005.8, AE=143850.000)
TG 1 (AE=402990.000, AErel=1.0)
from OL 2 (kh=0.1, kv=0.4, Bh=166.1, Bv=664.4, Th=16.61, Mh=30.0, Mv=12.0, I=0.0010, L=123798.8, AE=75415.000)
and OL 4 (kh=0.1, kv=0.4, Bh=190.8, Bv=763.1, Th=19.08, Mh=30.0, Mv=12.0, I=0.0010, L=329059.0, AE=109142.000)
and OL 3 (kh=0.1, kv=0.4, Bh=217.0, Bv=868.1, Th=21.70, Mh=30.0, Mv=12.0, I=0.0010, L=329059.0, AE=153914.000)

[abstraction_rule_reservoir_1]

```
0

[multilayer_landuse]
1 # count of multilayer landuses
1  grass_variable   { Landuse_Layers = 7, -9999, -9999;    k_extinct = 0.3; LAI_scale =
20;}


[landuse_table]
9            # number of following land use codes
6  crop.wood.mos_variable      {method      = VariableDayCount; # valid methods:
"VariableDayCount" with variable number of fix points (other methods will follow) -->
old method: if the table is structured like the old ones, they are still valid
                RootDistr       = 1.0;          # parameter for root density distribution
                TReduWet        = 0.95;      # relative Theta value for beginning water stress
(under wet conditions -> set >= 1 for crop which doesn't depend on an aeral zone
                LimitReduWet    = 0.5;              # minimum relative reduction factor of
real transpiration when water content reaches saturation. The reduction factor value will
go down linearly starting at 1.0 when relative Theta equals TReduWet (e.g. 0.95) to
LimitReduWet when the soil is saturated (Theta rel = 1.0)
                HReduDry        = 3.45;      # hydraulic head (suction) for beginning dryness
stress (for water content resulting in higher suctions, ETR will be reduced down to 0 at
suction=150m)
                IntercepCap     = 0.2;          # optional: specific thickness of the water layer
on the leafes in mm. if omitted here, the dedfault parameter from interception_model is
used
                JulDays         = 120 304;   # Julian days for all following rows. Each
parameter must match the number of julian days given here! The count of days doesn't
matter.
                Albedo          = 0.16  0.16;  # Albedo (snow free)
                rsc             = 80    80    70    70    50    50    50    55    55    70    80    80;
# leaf surface resistance in s/m
                rs_interception  = 80    80    70    70    50    50    50    55    55    70    80
80;    # INTERCEPTION surface resistance in s/m
                rs_evaporation   = 250   250   250   250   250   250   250   250   250   250
250    250;   # SOIL surface resistance in s/m (for evaporation only)
                LAI             = 3     5;     # Leaf Area Index (1/1)
                Z0              = 1.5   2.5;  # Roughness length in m
                VCF                             = 0.9     0.95;    # Vegetation covered fraction
("Vegetationsbedeckungsgrad")
                RootDepth       = 0.5    0.5;   # Root depth in m
                AltDep          = 0.025 0.025 0.025 0.025 0.025 0.025 -0.025 -0.025 -0.025 -
0.025 -0.025 -0.025; # Verschiebung des Juldays pro Meter (positiv: wird nach hinten
geschoben, negativ: wird nach vorne geschoben -> Limit: Wenn zwei Punkte
aufeinandertreffen, dann wird nicht weiter verschoben) Julian day shift per meter
(positive: backward shift, negative: forward shift,  limit: no further shift with two
converging values.
                }
```

7 grass_variable {method = VariableDayCount; # valid methods: "VariableDayCount" with variable number of fix points (other methods will follow) --> old method: if the table is structured like the old ones, they are still valid
RootDistr = 1.0; # parameter for root density distribution
TReduWet = 0.95; # relative Theta value for beginning water stress (under wet conditions -> set >= 1 for crop which doesn't depend on an aeral zone
LimitReduWet = 0.5; # minimum relative reduction factor of real transpiration when water content reaches saturation. The reduction factor value will go down linearly starting at 1.0 when relative Theta equals TReduWet (e.g. 0.95) to LimitReduWet when the soil is saturated (Theta rel = 1.0)
HReduDry = 3.45; # hydraulic head (suction) for beginning dryness stress (for water content resulting in higher suctions, ETR will be reduced down to 0 at suction=150m)
IntercepCap = 0.2; # optional: specific thickness of the water layer on the leafes in mm. if omitted here, the dedfault parameter from interception_model is used
JulDays = 120 304; # Julian days for all following rows. Each parameter must match the number of julian days given here! The count of days doesn't matter.
Albedo = 0.19 0.19; # Albedo (snow free)
rsc = 90 90 75 65 50 55 55 55 60 70 90 90; # leaf surface resistance in s/m
rs_interception = 90 90 75 65 50 55 55 55 60 70 90 90; # INTERCEPTION surface resistance in s/m
rs_evaporation = 250 250 250 250 250 250 250 250 250 250 250 250; # SOIL surface resistance in s/m (for evaporation only)
LAI = 2 4; # Leaf Area Index (1/1)
Z0 = 0.15 0.4; # Roughness length in m
VCF = 0.95 0.95; # Vegetation covered fraction ("Vegetationsbedeckungsgrad")
RootDepth = 0.4 0.4; # Root depth in m
AltDep = 0.025 0.025 0.025 0.025 0.025 0.025 -0.025 -0.025 -0.025 -0.025 -0.025 -0.025; # Verschiebung des Juldays pro Meter (positiv: wird nach hinten geschoben, negativ: wird nach vorne geschoben -> Limit: Wenn zwei Punkte aufeinandertreffen, dann wird nicht weiter verschoben) Julian day shift per meter (positive: backward shift, negative: forward shift, limit: no further shift with two converging values.)
}
8 shrubland_variable {method = VariableDayCount; # valid methods: "VariableDayCount" with variable number of fix points (other methods will follow) --> old method: if the table is structured like the old ones, they are still valid
RootDistr = 1.0; # parameter for root density distribution
TReduWet = 0.95; # relative Theta value for beginning water stress (under wet conditions -> set >= 1 for crop which doesn't depend on an aeral zone
LimitReduWet = 0.5; # minimum relative reduction factor of real transpiration when water content reaches saturation. The reduction factor value will go down linearly starting at 1.0 when relative Theta equals TReduWet (e.g. 0.95) to LimitReduWet when the soil is saturated (Theta rel = 1.0)

HReduDry = 3.45; # hydraulic head (suction) for beginning dryness stress (for water content resulting in higher suctions, ETR will be reduced down to 0 at suction=150m)
IntercepCap = 0.2; # optional: specific thickness of the water layer on the leafes in mm. if omitted here, the dedfault parameter from interception_model is used
JulDays = 120 304; # Julian days for all following rows. Each parameter must match the number of julian days given here! The count of days doesn't matter.
Albedo = 0.22 0.22; # Albedo (snow free)
rsc = 80 80 70 70 50 50 50 55 55 70 80 80; # leaf surface resistance in s/m
rs_interception = 80 80 70 70 50 50 50 55 55 70 80 80; # INTERCEPTION surface resistance in s/m
rs_evaporation = 250 250 250 250 250 250 250 250 250 250 250 250; # SOIL surface resistance in s/m (for evaporation only)
LAI = 3 5; # Leaf Area Index (1/1)
Z0 = 1.5 2.5; # Roughness length in m
VCF = 0.9 0.95; # Vegetation covered fraction ("Vegetationsbedeckungsgrad")
RootDepth = 0.5 0.5; # Root depth in m
AltDep = 0.025 0.025 0.025 0.025 0.025 0.025 -0.025 -0.025 -0.025 -0.025 -0.025 -0.025; # Verschiebung des Juldays pro Meter (positiv: wird nach hinten geschoben, negativ: wird nach vorne geschoben -> Limit: Wenn zwei Punkte aufeinandertreffen, dann wird nicht weiter verschoben) Julian day shift per meter (positive: backward shift, negative: forward shift, limit: no further shift with two converging values.)
}
10 savanna_variable {method = VariableDayCount; # valid methods: "VariableDayCount" with variable number of fix points (other methods will follow) --> old method: if the table is structured like the old ones, they are still valid
RootDistr = 1.0; # parameter for root density distribution
TReduWet = 0.95; # relative Theta value for beginning water stress (under wet conditions -> set >= 1 for crop which doesn't depend on an aeral zone
LimitReduWet = 0.5; # minimum relative reduction factor of real transpiration when water content reaches saturation. The reduction factor value will go down linearly starting at 1.0 when relative Theta equals TReduWet (e.g. 0.95) to LimitReduWet when the soil is saturated (Theta rel = 1.0)
HReduDry = 3.45; # hydraulic head (suction) for beginning dryness stress (for water content resulting in higher suctions, ETR will be reduced down to 0 at suction=150m)
IntercepCap = 0.2; # optional: specific thickness of the water layer on the leafes in mm. if omitted here, the dedfault parameter from interception_model is used
JulDays = 120 304; # Julian days for all following rows. Each parameter must match the number of julian days given here! The count of days doesn't matter.
Albedo = 0.2 0.2; # Albedo (snow free)

rsc = 80 80 70 70 50 50 50 55 55 70 80 80; # leaf surface resistance in s/m
rs_interception = 80 80 70 70 50 50 50 55 55 70 80 80; # INTERCEPTION surface resistance in s/m
rs_evaporation = 250 250 250 250 250 250 250 250 250 250 250 250; # SOIL surface resistance in s/m (for evaporation only)
LAI = 3 5; # Leaf Area Index (1/1)
Z0 = 1.5 2.5; # Roughness length in m
VCF = 0.9 0.95; # Vegetation covered fraction ("Vegetationsbedeckungsgrad")
RootDepth = 0.5 0.5; # Root depth in m
AltDep = 0.025 0.025 0.025 0.025 0.025 0.025 -0.025 -0.025 -0.025 -0.025 -0.025 -0.025; # Verschiebung des Juldays pro Meter (positiv: wird nach hinten geschoben, negativ: wird nach vorne geschoben -> Limit: Wenn zwei Punkte aufeinandertreffen, dann wird nicht weiter verschoben) Julian day shift per meter (positive: backward shift, negative: forward shift, limit: no further shift with two converging values.)
}
11 decids.Broadl_variable {method = VariableDayCount; # valid methods: "VariableDayCount" with variable number of fix points (other methods will follow) --> old method: if the table is structured like the old ones, they are still valid
RootDistr = 1.0; # parameter for root density distribution
TReduWet = 0.95; # relative Theta value for beginning water stress (under wet conditions -> set >= 1 for crop which doesn't depend on an aeral zone
LimitReduWet = 0.5; # minimum relative reduction factor of real transpiration when water content reaches saturation. The reduction factor value will go down linearly starting at 1.0 when relative Theta equals TReduWet (e.g. 0.95) to LimitReduWet when the soil is saturated (Theta rel = 1.0)
HReduDry = 3.45; # hydraulic head (suction) for beginning dryness stress (for water content resulting in higher suctions, ETR will be reduced down to 0 at suction=150m)
IntercepCap = 0.2; # optional: specific thickness of the water layer on the leafes in mm. if omitted here, the dedfault parameter from interception_model is used
JulDays = 120 304; # Julian days for all following rows. Each parameter must match the number of julian days given here! The count of days doesn't matter.
Albedo = 0.16 0.16; # Albedo (snow free)
rsc = 100 100 95 75 65 65 65 65 65 85 100 100; # leaf surface resistance in s/m
rs_interception = 100 100 95 75 65 65 65 65 65 85 100 100; # INTERCEPTION surface resistance in s/m
rs_evaporation = 250 250 250 250 250 250 250 250 250 250 250 250; # SOIL surface resistance in s/m (for evaporation only)
LAI = 0.5 8; # Leaf Area Index (1/1)
Z0 = 0.3 10; # Roughness length in m
VCF = 0.7 0.95; # Vegetation covered fraction ("Vegetationsbedeckungsgrad")

RootDepth = 1.4 1.4; # Root depth in m
AltDep = 0.025 0.025 0.025 0.025 0.025 0.025 -0.025 -0.025 -0.025 -0.025 -0.025 -0.025; # Verschiebung des Juldays pro Meter (positiv: wird nach hinten geschoben, negativ: wird nach vorne geschoben -> Limit: Wenn zwei Punkte aufeinandertreffen, dann wird nicht weiter verschoben) Julian day shift per meter (positive: backward shift, negative: forward shift, limit: no further shift with two converging values.)
}
13 evergreen.broadl_variable {method = VariableDayCount; # valid methods: "VariableDayCount" with variable number of fix points (other methods will follow) --> old method: if the table is structured like the old ones, they are still valid
RootDistr = 1.0; # parameter for root density distribution
TReduWet = 0.95; # relative Theta value for beginning water stress (under wet conditions -> set >= 1 for crop which doesn't depend on an aeral zone
LimitReduWet = 0.5; # minimum relative reduction factor of real transpiration when water content reaches saturation. The reduction factor value will go down linearly starting at 1.0 when relative Theta equals TReduWet (e.g. 0.95) to LimitReduWet when the soil is saturated (Theta rel = 1.0)
HReduDry = 3.45; # hydraulic head (suction) for beginning dryness stress (for water content resulting in higher suctions, ETR will be reduced down to 0 at suction=150m)
IntercepCap = 0.2; # optional: specific thickness of the water layer on the leafes in mm. if omitted here, the dedfault parameter from interception_model is used
JulDays = 120 304; # Julian days for all following rows. Each parameter must match the number of julian days given here! The count of days doesn't matter.
Albedo = 0.12 0.12; # Albedo (snow free)
rsc = 65 65 65 65 65 65 65 65 65 65 65 65; # leaf surface resistance in s/m
rs_interception = 65 65 65 65 65 65 65 65 65 65 65 65; # INTERCEPTION surface resistance in s/m
rs_evaporation = 250 250 250 250 250 250 250 250 250 250 250 250; # SOIL surface resistance in s/m (for evaporation only)
LAI = 8 8; # Leaf Area Index (1/1)
Z0 = 10 10; # Roughness length in m
VCF = 0.95 0.95; # Vegetation covered fraction ("Vegetationsbedeckungsgrad")
RootDepth = 1.4 1.4; # Root depth in m
AltDep = 0.025 0.025 0.025 0.025 0.025 0.025 -0.025 -0.025 -0.025 -0.025 -0.025 -0.025; # Verschiebung des Juldays pro Meter (positiv: wird nach hinten geschoben, negativ: wird nach vorne geschoben -> Limit: Wenn zwei Punkte aufeinandertreffen, dann wird nicht weiter verschoben) Julian day shift per meter (positive: backward shift, negative: forward shift, limit: no further shift with two converging values.)
}

15 mixed.forest_variable {method = VariableDayCount; # valid methods: "VariableDayCount" with variable number of fix points (other methods will follow) --> old method: if the table is structured like the old ones, they are still valid
RootDistr = 1.0; # parameter for root density distribution
TReduWet = 0.95; # relative Theta value for beginning water stress (under wet conditions -> set >= 1 for crop which doesn't depend on an aeral zone
LimitReduWet = 0.5; # minimum relative reduction factor of real transpiration when water content reaches saturation. The reduction factor value will go down linearly starting at 1.0 when relative Theta equals TReduWet (e.g. 0.95) to LimitReduWet when the soil is saturated (Theta rel = 1.0)
HReduDry = 3.45; # hydraulic head (suction) for beginning dryness stress (for water content resulting in higher suctions, ETR will be reduced down to 0 at suction=150m)
IntercepCap = 0.2; # optional: specific thickness of the water layer on the leafes in mm. if omitted here, the dedfault parameter from interception_model is used
JulDays = 120 304; # Julian days for all following rows. Each parameter must match the number of julian days given here! The count of days doesn't matter.
Albedo = 0.13 0.13; # Albedo (snow free)
rsc = 90 90 85 70 60 60 60 60 60 80 90 90; # leaf surface resistance in s/m
rs_interception = 90 90 85 70 60 60 60 60 60 80 90 90; # INTERCEPTION surface resistance in s/m
rs_evaporation = 250 250 250 250 250 250 250 250 250 250 250 250; # SOIL surface resistance in s/m (for evaporation only)
LAI = 2 10; # Leaf Area Index (1/1)
Z0 = 3 10; # Roughness length in m
VCF = 0.8 0.92; # Vegetation covered fraction ("Vegetationsbedeckungsgrad")
RootDepth = 1.3 1.3; # Root depth in m
AltDep = 0.025 0.025 0.025 0.025 0.025 0.025 -0.025 -0.025 -0.025 -0.025 -0.025 -0.025; # Verschiebung des Juldays pro Meter (positiv: wird nach hinten geschoben, negativ: wird nach vorne geschoben -> Limit: Wenn zwei Punkte aufeinandertreffen, dann wird nicht weiter verschoben) Julian day shift per meter (positive: backward shift, negative: forward shift, limit: no further shift with two converging values.)
}
16 water.bodies_variable {method = VariableDayCount; # valid methods: "VariableDayCount" with variable number of fix points (other methods will follow) --> old method: if the table is structured like the old ones, they are still valid
RootDistr = 1.0; # parameter for root density distribution
TReduWet = 0.95; # relative Theta value for beginning water stress (under wet conditions -> set >= 1 for crop which doesn't depend on an aeral zone
LimitReduWet = 0.5; # minimum relative reduction factor of real transpiration when water content reaches saturation. The reduction factor value will go down linearly starting at 1.0 when relative Theta equals TReduWet (e.g. 0.95) to LimitReduWet when the soil is saturated (Theta rel = 1.0)

HReduDry = 3.45; # hydraulic head (suction) for beginning dryness stress (for water content resulting in higher suctions, ETR will be reduced down to 0 at suction=150m)
IntercepCap = 0.2; # optional: specific thickness of the water layer on the leafes in mm. if omitted here, the dedfault parameter from interception_model is used
JulDays = 120 304; # Julian days for all following rows. Each parameter must match the number of julian days given here! The count of days doesn't matter.
Albedo = 0.08 0.08; # Albedo (snow free)
rsc = 20 20 20 20 20 20 20 20 20 20 20 20; # leaf surface resistance in s/m
rs_interception = 20 20 20 20 20 20 20 20 20 20 20 20; # INTERCEPTION surface resistance in s/m
rs_evaporation = 250 250 250 250 250 250 250 250 250 250 250 250; # SOIL surface resistance in s/m (for evaporation only)
LAI = 1 1; # Leaf Area Index (1/1)
Z0 = 0.01 0.01; # Roughness length in m
VCF = 1 1; # Vegetation covered fraction ("Vegetationsbedeckungsgrad")
RootDepth = 9 9; # Root depth in m
AltDep = 0.025 0.025 0.025 0.025 0.025 0.025 -0.025 -0.025 -0.025 -0.025 -0.025 -0.025; # Verschiebung des Juldays pro Meter (positiv: wird nach hinten geschoben, negativ: wird nach vorne geschoben -> Limit: Wenn zwei Punkte aufeinandertreffen, dann wird nicht weiter verschoben) Julian day shift per meter (positive: backward shift, negative: forward shift, limit: no further shift with two converging values.)
}
19 bar.Sparse.veg_variable {method = VariableDayCount; # valid methods: "VariableDayCount" with variable number of fix points (other methods will follow) --> old method: if the table is structured like the old ones, they are still valid
RootDistr = 1.0; # parameter for root density distribution
TReduWet = 0.95; # relative Theta value for beginning water stress (under wet conditions -> set >= 1 for crop which doesn't depend on an aeral zone
LimitReduWet = 0.5; # minimum relative reduction factor of real transpiration when water content reaches saturation. The reduction factor value will go down linearly starting at 1.0 when relative Theta equals TReduWet (e.g. 0.95) to LimitReduWet when the soil is saturated (Theta rel = 1.0)
HReduDry = 3.45; # hydraulic head (suction) for beginning dryness stress (for water content resulting in higher suctions, ETR will be reduced down to 0 at suction=150m)
IntercepCap = 0.2; # optional: specific thickness of the water layer on the leafes in mm. if omitted here, the dedfault parameter from interception_model is used
JulDays = 120 304; # Julian days for all following rows. Each parameter must match the number of julian days given here! The count of days doesn't matter.
Albedo = 0.25 0.25; # Albedo (snow free)

```
            rsc             = 250   250   250   200   100   80    60    60    80    100
200   250;   # leaf surface resistance in s/m
            rs_interception  = 250   250   250   200   100   80    60    60    80    100
200   250;   # INTERCEPTION surface resistance in s/m
            rs_evaporation   = 250   250   250   250   250   250   250   250   250   250
250   250;   # SOIL surface resistance in s/m (for evaporation only)
            LAI             = 1    3;    # Leaf Area Index (1/1)
            Z0              = 0.05  0.4;  # Roughness length in m
            VCF                         = 0.95    1;    # Vegetation covered fraction
("Vegetationsbedeckungsgrad")
            RootDepth       = 0.1   0.4;   # Root depth in m
            AltDep          = 0.025 0.025 0.025 0.025 0.025 0.025 -0.025 -0.025 -0.025 -
0.025 -0.025 -0.025; # Verschiebung des Juldays pro Meter (positiv: wird nach hinten
geschoben, negativ: wird nach vorne geschoben -> Limit: Wenn zwei Punkte
aufeinandertreffen, dann wird nicht weiter verschoben) Julian day shift per meter
(positive: backward shift, negative: forward shift,  limit: no further shift with two
converging values.)
            }
[soil_table]
6               # number of following entries
1 sandy_loam_(SL) {method = MultipleHorizons;
                    FCap = 6.21; mSB = 38.5; ksat_topmodel = 8.25E-5; suction = 385;
# optional parameters which are needed for Topmodel only
                    GrainSizeDist  = 0.4 0.4; # optional: when using silting up model,
the grain size fractions for sand, silt and clay must be given here
                    PMacroThresh   = 20     20;  # precipitation capacity thresholding
macropore runoff in mm per hour (not in m/s, because it's more convenient than to write
it down in m/s, e.g. 5mm/h = 1.38e-6)
                    MacroCapacity  = 3    3;  # capacity of the macropores in mm per
hour (not in m/s, because it's more convenient than to write it down in m/s, e.g. 5mm/h
= 1.38e-6)
                    CapacityRedu   = 0.5 0.5;  # reduction of the macropore capacity
with depth -> pores become less dense. This Factor describes the reduction ratio per
meter
                    MacroDepth     = 1.0 1.0;  # maximum depth of the macropores
                   horizon        = 1       2       ;  # ID of the horizon (must be ascendent)
it's recommended to name the horizons shortly in the following row
                    Name                = SL1m    SL2m    ;  # short descriptions
              ksat          = 8.25e-5 8.25e-5 ;  # saturated hydraulic conductivity in m/s
                    k_recession    = 0.98     0.98     ;  # k sat recession with depth (could
also be controlled by different layers if no k decrease is wanted (set this parameter to
1.0
                  theta_sat       = 0.41     0.41     ;  # saturated water content (fillable
porosity in 1/1)
                    theta_res      = 0.037   0.037   ;  # residual water content (in 1/1, water
content which cannot be poured by transpiration, only by evaporation)
                    alpha          = 3.8    3.8    ;  # van Genuchten Parameter Alpha
                    Par_n          = 2.474     2.474    ;  # van Genuchten Parameter n
```

Par_tau = 0.5 0.5 ; # sog. Mualem-Parameter tau in der van-Genuchten-Gleichung (dort normalerweise 0.5)
thickness = 1 1 ; # thickness of each single numerical layer in this horizon in m
layers = 20 1 ; # numerical number of layers in this horizon. The thickness of the layer is given by layers x thickness. All profiles must have an identical number of layers (for memory handling reasons only)
}
2 loamy_sandsand_(S) {method = MultipleHorizons;
FCap = 10.91; mSB = 37.3; ksat_topmodel = 4.05E-5; suction = 373; # optional parameters which are needed for Topmodel only
GrainSizeDist = 0.6 0.2; # optional: when using silting up model, the grain size fractions for sand, silt and clay must be given here
PMacroThresh = 15 15; # precipitation capacity thresholding macropore runoff in mm per hour (not in m/s, because it's more convenient than to write it down in m/s, e.g. 5mm/h = 1.38e-6)
MacroCapacity = 5 5; # capacity of the macropores in mm per hour (not in m/s, because it's more convenient than to write it down in m/s, e.g. 5mm/h = 1.38e-6)
CapacityRedu = 0.9 0.9; # reduction of the macropore capacity with depth -> pores become less dense. This Factor describes the reduction ratio per meter
MacroDepth = 1.5 1.5; # maximum depth of the macropores
horizon = 1 2 ; # ID of the horizon (must be ascendent) it's recommended to name the horizons shortly in the following row
Name = LS1m LS2m ; # short descriptions
ksat = 4.05E-5 4.05E-5 ; # saturated hydraulic conductivity in m/s
k_recession = 0.98 0.98 ; # k sat recession with depth (could also be controlled by different layers if no k decrease is wanted (set this parameter to 1.0
theta_sat = 0.438 0.438 ; # saturated water content (fillable porosity in 1/1)
theta_res = 0.062 0.062 ; # residual water content (in 1/1, water content which cannot be poured by transpiration, only by evaporation)
alpha = 8.37 8.37 ; # van Genuchten Parameter Alpha
Par_n = 1.672 1.672 ; # van Genuchten Parameter n
Par_tau = 0.5 0.5 ; # sog. Mualem-Parameter tau in der van-Genuchten-Gleichung (dort normalerweise 0.5)
thickness = 1 1 ; # thickness of each single numerical layer in this horizon in m
layers = 20 1 ; # numerical number of layers in this horizon. The thickness of the layer is given by layers x thickness. All profiles must have an identical number of layers (for memory handling reasons only)
}
6 loam_(L) {method = MultipleHorizons;
FCap = 12.9; mSB = 35.2; ksat_topmodel = 2.89E-6; suction = 352; # optional parameters which are needed for Topmodel only

GrainSizeDist = 0.2 0.4; # optional: when using silting up model, the grain size fractions for sand, silt and clay must be given here
PMacroThresh = 10 10; # precipitation capacity thresholding macropore runoff in mm per hour (not in m/s, because it's more convenient than to write it down in m/s, e.g. 5mm/h = 1.38e-6)
MacroCapacity = 4 4; # capacity of the macropores in mm per hour (not in m/s, because it's more convenient than to write it down in m/s, e.g. 5mm/h = 1.38e-6)
CapacityRedu = 1.0 1.0; # reduction of the macropore capacity with depth -> pores become less dense. This Factor describes the reduction ratio per meter
MacroDepth = 0.8 0.8; # maximum depth of the macropores
horizon = 1 2 ; # ID of the horizon (must be ascendent) it's recommended to name the horizons shortly in the following row
Name = L10m L10m ; # short descriptions
ksat = 2.89e-6 2.89e-6 ; # saturated hydraulic conductivity in m/s
k_recession = 0.98 0.98 ; # k sat recession with depth (could also be controlled by different layers if no k decrease is wanted (set this parameter to 1.0
theta_sat = 0.521 0.521 ; # saturated water content (fillable porosity in 1/1)
theta_res = 0.155 0.155 ; # residual water content (in 1/1, water content which cannot be poured by transpiration, only by evaporation)
alpha = 2.46 2.46 ; # van Genuchten Parameter Alpha
Par_n = 1.461 1.461 ; # van Genuchten Parameter n
Par_tau = 0.5 0.5 ; # sog. Mualem-Parameter tau in der van-Genuchten-Gleichung (dort normalerweise 0.5)
thickness = 1 1 ; # thickness of each single numerical layer in this horizon in m
layers = 20 1 ; # numerical number of layers in this horizon. The thickness of the layer is given by layers x thickness. All profiles must have an identical number of layers (for memory handling reasons only)
}
9 clay_(C) {method = MultipleHorizons;
FCap = 29.12; mSB = 31.2; ksat_topmodel = 5.56E-7; suction = 312; # optional parameters which are needed for Topmodel only
GrainSizeDist = 0.05 0.1; # optional: when using silting up model, the grain size fractions for sand, silt and clay must be given here
PMacroThresh = 8 8; # precipitation capacity thresholding macropore runoff in mm per hour (not in m/s, because it's more convenient than to write it down in m/s, e.g. 5mm/h = 1.38e-6)
MacroCapacity = 3 3; # capacity of the macropores in mm per hour (not in m/s, because it's more convenient than to write it down in m/s, e.g. 5mm/h = 1.38e-6)
CapacityRedu = 0.5 0.5; # reduction of the macropore capacity with depth -> pores become less dense. This Factor describes the reduction ratio per meter

MacroDepth = 0.7 0.7; # maximum depth of the macropores
horizon = 1 2 ; # ID of the horizon (must be ascendent) it's recommended to name the horizons shortly in the following row
Name = C10m C10m ; # short descriptions
ksat = 5.56e-7 5.56e-7 ; # saturated hydraulic conductivity in m/s
k_recession = 0.98 0.98 ; # k sat recession with depth (could also be controlled by different layers if no k decrease is wanted (set this parameter to 1.0
theta_sat = 0.546 0.546 ; # saturated water content (fillable porosity in 1/1)
theta_res = 0.267 0.267 ; # residual water content (in 1/1, water content which cannot be poured by transpiration, only by evaporation)
alpha = 4.63 4.63 ; # van Genuchten Parameter Alpha
Par_n = 1.514 1.514 ; # van Genuchten Parameter n
Par_tau = 0.5 0.5 ; # sog. Mualem-Parameter tau in der van-Genuchten-Gleichung (dort normalerweise 0.5)
thickness = 1 1 ; # thickness of each single numerical layer in this horizon in m
layers = 20 1 ; # numerical number of layers in this horizon. The thickness of the layer is given by layers x thickness. All profiles must have an identical number of layers (for memory handling reasons only)
}
12 clay_loam_(CL) {method = MultipleHorizons;
FCap = 21.24; mSB = 31.5; ksat_topmodel = 7.22E-7; suction = 315; # optional parameters which are needed for Topmodel only
GrainSizeDist = 0.1 0.4; # optional: when using silting up model, the grain size fractions for sand, silt and clay must be given here
PMacroThresh = 8 8; # precipitation capacity thresholding macropore runoff in mm per hour (not in m/s, because it's more convenient than to write it down in m/s, e.g. 5mm/h = 1.38e-6)
MacroCapacity = 2 2; # capacity of the macropores in mm per hour (not in m/s, because it's more convenient than to write it down in m/s, e.g. 5mm/h = 1.38e-6)
CapacityRedu = 0.4 0.4; # reduction of the macropore capacity with depth -> pores become less dense. This Factor describes the reduction ratio per meter
MacroDepth = 0.6 0.6; # maximum depth of the macropores
horizon = 1 2 ; # ID of the horizon (must be ascendent) it's recommended to name the horizons shortly in the following row
Name = SIC10m SIC10m ; # short descriptions
ksat = 7.22E-7 7.22E-7 ; # saturated hydraulic conductivity in m/s
k_recession = 0.98 0.98 ; # k sat recession with depth (could also be controlled by different layers if no k decrease is wanted (set this parameter to 1.0
theta_sat = 0.519 0.519 ; # saturated water content (fillable porosity in 1/1)

theta_res = 0.226 0.226 ; # residual water content (in 1/1, water content which cannot be poured by transpiration, only by evaporation)
alpha = 3.92 3.92 ; # van Genuchten Parameter Alpha
Par_n = 1.437 1.437 ; # van Genuchten Parameter n
Par_tau = 0.5 0.5 ; # sog. Mualem-Parameter tau in der van-Genuchten-Gleichung (dort normalerweise 0.5)
thickness = 1 1 ; # thickness of each single numerical layer in this horizon in m
layers = 20 1 ; # numerical number of layers in this horizon. The thickness of the layer is given by layers x thickness. All profiles must have an identical number of layers (for memory handling reasons only)
}
14 water {method = MultipleHorizons;
FCap = 89.0; mSB = 90.0; ksat_topmodel = 1.0E-3; suction = 1400; # optional parameters which are needed for Topmodel only
GrainSizeDist = 0.8 0.1; # optional: when using silting up model, the grain size fractions for sand, silt and clay must be given here
PMacroThresh = 38 38; # precipitation capacity thresholding macropore runoff in mm per hour (not in m/s, because it's more convenient than to write it down in m/s, e.g. 5mm/h = 1.38e-6)
MacroCapacity = 12 12; # capacity of the macropores in mm per hour (not in m/s, because it's more convenient than to write it down in m/s, e.g. 5mm/h = 1.38e-6)
CapacityRedu = 0.8 0.8; # reduction of the macropore capacity with depth -> pores become less dense. This Factor describes the reduction ratio per meter
MacroDepth = 1.6 1.6; # maximum depth of the macropores
horizon = 1 2 ; # ID of the horizon (must be ascendent) it's recommended to name the horizons shortly in the following row
Name = M10m M10m ; # short descriptions
ksat = 1.0E-3 1.0E-3 ; # saturated hydraulic conductivity in m/s
k_recession = 0.98 0.98 ; # k sat recession with depth (could also be controlled by different layers if no k decrease is wanted (set this parameter to 1.0
theta_sat = 0.99 0.99 ; # saturated water content (fillable porosity in 1/1)
theta_res = 0.010 0.010 ; # residual water content (in 1/1, water content which cannot be poured by transpiration, only by evaporation)
alpha = 1.00 1.00 ; # van Genuchten Parameter Alpha
Par_n = 1.01 1.01 ; # van Genuchten Parameter n
thickness = 1 1 ; # thickness of each single numerical layer in this horizon in m
layers = 20 1 ; # numerical number of layers in this horizon. The thickness of the layer is given by layers x thickness. All profiles must have an identical number of layers (for memory handling reasons only)
}
[substance_transport]

0 # number of tracers to be considered (max. 9)

[irrigation_table]
0 # number of following irrigation codes. per row one use

APPENDIX III

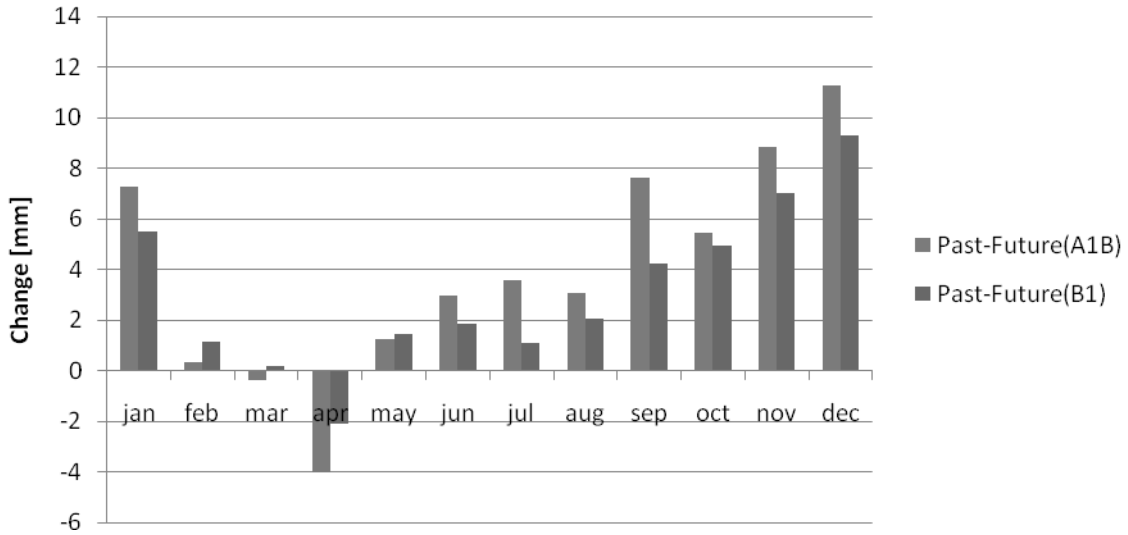

Figure 7.4b: Spatially averaged monthly mean actual evapotranspiration change [mm] (1961-2000 and 2001-2050) for the Volta Basin

ACKNOWLEDGEMENTS

To GOD be the glory, great things He has done.

I would like to express my heartfelt gratitude to my supervisor Prof. Dr. Bernd Diekkrueger, vice chair of the Department of Geography, University of Bonn, for his continuous scientific guidance, support and supervision throughout the entire course of this work. I have learned a lot from the fruitful discussions that we had, and have greatly benefited from his experience. I am specifically grateful for his extraordinary willingness to assist me whenever I needed help in every aspect of my work.

I would like also to thank my co-supervisor Prof. Dr. Paul Vlek, Director of the Center for Development Research (ZEF), for giving me the opportunity to do my PhD at ZEF. I very thankful to him for his useful comments and full support during my stay at ZEF.

I would like to thank the BMBF (Federal Ministry for Education and Research) for providing me with the financial support for my PhD study in Bonn. The ZEF-GLOWA Volta project deserves my special thanks for supporting my research expenses and also for creating the best environment for my study. I would like to extend my thanks to the entire staff members of ZEF, specifically to Dr. Günter Manske and Rosemarie Zabel. I would also like to express my sincere appreciation to Mrs. Zabel for her extraordinary assistance. I am really grateful for her readiness to help whenever I was in need. I would like to extend my thanks to Dr. Constanze Leemhius and Dr. Charles Rodgers (previous ZEF staff) for their constructive comments during this study and their valuable logistic support most especially after my field work. This work would not have been possible without the keen cooperation of the following people: Herwig Hölzel of the Department of Geography of University of Bonn, Dr. Serge Shumilov of the Computer Science Department of University of Bonn, Dr. Boubacar Barry of IWMI, Prof. Francis Allotey of Ghana Atomic Energy, Prof Haruna Yakubu, Pro Vice Chancellor of University of Cape Coast, Prof. Heiko Paeth of the GLOWA IMPETUS project and the meteorological departments of Ghana and Burkina Faso. I would also like to extend my deepest thanks to Daniel Ofori, Salisu Adams - of GLOWA Volta and now IWMI, not only for their immense professional assistance but also for being good friends. My drivers, Eli and Kwasi, deserve special thanks for assisting me during rough field work and data gathering and collection.

Acknoledgements

My special thanks go to my beloved parents who have given me their unconditional love in my entire life, and have been the source of my strength all along. I would like also to extend my gratitude to my dearest family Clara, Belinda, Martha, Gertrude, Raymond Jr. and Borisa for providing me with their love and support throughout my journey.